Palestine Polytechnic University

Deanship of Graduate Studies and Scientific Research

Master of Architecture - Sustainable Design

Chronological Evolution of Living Space in Palestinian Residential Units: Assessing Spatial Configuration, Social Dynamics, and Thermal Performance

Bara Awad Ahmad Obayat

Supervisor

Dr. Bader Alatawneh

Thesis submitted in partial fulfillment of the requirements of the degree
Master of Architecture – Sustainable Design

August, 2026

The undersigned hereby certify that they have read, examined, and recommended to the Deanship of Graduate Studies and Scientific Research at Palestine Polytechnic University:

Chronological Evolution of Living Space in Palestinian Residential Units: Assessing Spatial Configuration, Social Dynamics, and Thermal Performance

Bara Awad Ahmad Obayat

in partial fulfillment of the requirements for the degree of Master in Architecture – Sustainable Design.

Graduate Advisory Committee:

Dr. Bader Alatawneh ……,……..

(Supervisor), Palestine Polytechnic University.

Signature:_____ Date: 21/10/2026

Dr. Hussein Alragabi ……,……..

(Internal committee member), Palestine Polytechnic University.

Signature:_____ Date: 21/10/2026

Dr. Samar Alnazer ……,……..

(External committee member), Birzeit University

Signature:_____ Date: ٢١/١٠/٢٠٢٦

Thesis Approved by:

Dean of Graduate Studies & Scientific Research

Palestine Polytechnic University

Signature:……..……

Date:……..……

Chronological Evolution of Living Space in Palestinian Residential Units:
Assessing Spatial Configuration, Social Dynamics, and Thermal Performance

ABSTRACT

Palestinian residential architecture has changed substantially across the Ottoman, Jordanian, and contemporary periods, with traditional spatial elements such as the courtyard and mastaba (raised Platform) giving way to newer forms like the liwan (enclosed central hall) and enclosed kitchen. These shifts, driven by political, social, and constructional change, have tended to be documented descriptively, with little attempt to connect them to measurable thermal performance. This study addresses that gap by tracing how spatial configuration across the three periods has shaped indoor thermal comfort, and by testing whether design strategies drawn from historical precedent can improve contemporary housing performance.

The Ottoman envelope relied on thick walls and a low window-to-wall ratio, with the courtyard mediating between interior and exterior. In the Jordanian period, this gave way to the enclosed liwan, open on one side, which restored visual connection to the outside while retaining a buffering function. Contemporary housing has abandoned both in favour of fully enclosed, compartmentalized layouts suited to smaller households and modern construction.

Three case studies in Abu Dis were assessed through household questionnaires and field measurements, then modelled in DesignBuilder and EnergyPlus and calibrated to ASHRAE 14. The Ottoman house showed a summer diurnal swing of just 1.8°C, against 4.4°C in the contemporary case, which fell outside the Fanger comfort range for 69.5% of summer hours. Parametric testing identified an optimal window-to-wall ratio of 18.5–30.9%. Reintroducing a veranda as a transitional buffer cut solar heat gain by 43.9% in summer and 66.3% in winter, and reduced the Predicted Percentage of Dissatisfied to 19.2%, the strongest result among the strategies tested.

Selective reuse of historical spatial elements improves passive thermal comfort in contemporary Palestinian housing.

Keywords: Thermal comfort, passive design, courtyard, liwan, vernacular architecture, window-to-wall ratio, traditional spatial elements

التطور الزمني للفراغ المعيشي في الوحدات السكنية الفلسطينية:
تقييم التكوين الفراغي، و الديناميكيات الاجتماعية، والأداء البيئي

الملخص

شهدت العمارة السكنية في فلسطين تحولات ملحوظة عبر الفترات العثمانية والأردنية والمعاصرة نتيجة لتغير الظروف السياسية والاجتماعية وممارسات البناء، ما أدى إلى استبدال عناصر تقليدية كالفناء والمصطبة بعناصر أخرى مثل الليوان والمطبخ. ولم يكن نجاح البيت التقليدي قائمًا على تقنيات البناء فقط، بل على منظومة من الفراغات الاجتماعية كالفناء والساحة الأمامية، التي أدت وظائف بيئية واجتماعية متكاملة. ورغم أن الأدبيات وثّقت هذه التحولات، إلا أنها غالبًا تبقى وصفية ولا تربطها بنتائج حرارية قابلة للقياس ضمن إطار تحليلي موحد. تعالج هذه الدراسة هذه الفجوة من خلال تحليل أثر تطور التكوين الفراغي عبر الفترات الثلاث على الراحة الحرارية، واختبار استراتيجيات تصميمية مستمدة من السوابق التاريخية لتحسين أداء المساكن المعاصرة.

اتسم الغلاف المعماري في الطراز العثماني بسماكته التي ساعدت في ضبط انتقال الحرارة، وبنسبة فتحات منخفضة حدّت من الاتصال البصري مع الخارج، ليُعوَّض ذلك عبر الفناء والفراغات الانتقالية التي حافظت على اتصال فيزيائي ومناخي مع البيئة المحيطة. في الفترة الأردنية، استُبدل الفناء بالليوان المغلق، المحمي من ثلاث جهات والمفتوح من جهة واحدة بفتحات أكبر، ما أعاد الاتصال البصري مع الحفاظ على دور المنطقة العازلة شبه المغلقة. أما في الفترة المعاصرة، فقد تم التخلي عن الفناء والليوان لصالح مخططات مغلقة ومجزأة تتلاءم مع صِغر حجم الأسر وأنظمة البناء الحديثة، المعتمدة على جدران أخف ومواد مستحدثة، الأمر الذي أدى إلى تحولات جوهرية في الوظائف الاجتماعية والبيئية معًا.

تتبع هذه الدراسة أثر هذه التحولات على كفاءة الفراغ المعيشي اجتماعيًا وأدائه الحراري الداخلي. تم توثيق ثلاث حالات دراسية في أبو ديس عبر استبيانات وقياسات ميدانية، ثم نمذجتها باستخدام DesignBuilder وEnergyPlus ومعايرتها وفق ASHRAE 14. أظهرت النتائج أن البيت العثماني حافظ على تذبذب حراري صيفي محدود بلغ 1.8°م، مقابل 4.4°م في النموذج المعاصر، الذي قضى 69.5% من ساعات الصيف خارج نطاق الراحة وفق مؤشر فانغر. كما بيّنت الاختبارات البارامترية أن النسبة المثلى للفتحات إلى الجدران تتراوح بين 18.5% و30.9%، محققة توازنًا بين التهوية وزيادة طفيفة في ساعات عدم الراحة. وأسهمت إعادة تفعيل الشرفة كعنصر انتقالي في خفض الكسب الحراري الشمسي بنسبة 43.9% صيفًا و66.3% شتاءً، مع تقليل مؤشر عدم الرضا (PPD) إلى 19.2%، وهو أفضل أداء بين الاستراتيجيات المختبرة. تم تقييم الراحة الحرارية باستخدام مؤشري PMV/PPD ومعايير EN 16798-1، مما أتاح عزل آليات التأثير، بين التبريد بالتهوية في حالة الفتحات واعتراض الإشعاع في عناصر التظليل.

تخلص الدراسة إلى أن إعادة توظيف عناصر فراغية تاريخية بشكل انتقائي تحسّن الراحة الحرارية السلبية في المساكن الفلسطينية المعاصرة.

الكلمات المفتاحية: الراحة الحرارية، التصميم السلبي، الفناء، الليوان، العمارة المحلية، نسبة مساحة النوافذ الى مساحة الجدران، العناصر الفراغية التقليدية.

DECLARATION

I declare that the Master Thesis entitled “Chronological Evolution of Living Space in Palestinian Residential Units: Assessing Spatial Configuration, Social Dynamics, and Environmental Performance” is my own original work, and I hereby certify that unless stated, all work contained within this thesis is my own independent research and has not been submitted for the award of any other degree at any institution, except where due acknowledgement is made in the text.

Student Name…….

Signature: Date:

DEDICATION

To those who made this journey possible through their unwavering belief in me.

ACKNOWLEDGEMENT

To the companions of my journey — my parents, siblings, friends, and colleagues — whose presence, support, and belief in me gave meaning to every step along the way.

To my esteemed supervisor, Dr. Bader Alatawneh, for his guidance, wisdom, and continuous support that shaped this research.

To the Department of Architecture at Palestine Polytechnic University, my academic foundation and the place where my passion for architecture was nurtured.

To the Department of Architecture at Al-Quds University, the place I call home, for believing in me, embracing me, and supporting me throughout this chapter of my journey.

Table of Contents

Chapter 1 Introduction 1
1.1 Preface 1
1.2 Research Problem 2
1.3 Literature reviews 4
1.4 Research Gap 7
1.5 Research Question and Hypothesis 9
1.6 Objectives 9
1.7 Significance of the Study 10
1.8 Limit and Limitation 10
1.9 Research Structure 11

Chapter 2 The Palestinian House across Three Eras: A Historical Reading of Spatial Change 13
2.1 Preface 13
2.2 Spatial configuration of the Palestinian house architecture and urban attachment 13
2.2.1 Late Ottoman Period until 1917: First Period 14
2.2.2 British and Jordanian Period (1917-1967): Second Period 18
2.2.3 Third Period: Late Twentieth Century 21
2.3 Social Transformation of the Palestinian House Architecture 22
2.3.1 Ottoman Period (Until 1917): First Period 22
2.3.2 British and Jordanian Period (1917-1967): Second Period 26
2.3.3 Late 20th Century: Third Period 27
2.4 Environmental Elements in the Palestinian House Architecture 28
2.4.1 Environmental Performance as an Integrated System 28
2.4.2 The Ottoman-Period House: Courtyard, Mass and Opening as a Single Regulatory System 28
2.4.3 The British and Jordanian Period: Environmental impact of Spatial Reconfiguration (1917 to 1967) 31
2.4.4 Late 20th Century 34
2.5 Summery 36

Chapter 3 Research Methodology 38
3.1 Preface 38
3.2 Research Type 38

3.3 Conceptual Framework: From Historical Analysis to Design Application 39
3.4 Study Area Selection Criteria 41
3.5 Sample Selection Criteria 41
3.6 Data Collection Methods 43
3.7 Research Type 44
3.8 Study Area (Abu Dis) 45
3.9 Instrument Design and Analytical Structure of the Household Questionnaire 45
3.9.1 Theoretical operationalization of the four domains 45
3.9.2 Implications for sampling strategy 47
3.10 Creating and Validating Base Model 48
3.10.1 Strategy 1: Wall Thermal Mass and Time Lag 49
3.10.2 Strategy 2: Opening Ratio and Natural Ventilation 51
3.10.3 Scenario 3: From Veranda Concept to Simulation Logic 52
3.10.4 Scenario 4: Orientation as an Adaptive Environmental Strategy 53
3.10.5 Strategy 5: Spatial Configuration and Environmental Performance 55

Chapter 4 Case Study 57
4.1 Preface (Study Area Overview: Abu Dis) 57
4.2 Urban Morphological Analysis and Field Survey 58
4.3 Analysis of the survey work 61
4.3.1 Daily Dynamics of Living Space Usage: Behavior setting theory (Barker) and climate-responsive design 62
4.3.4 Comparative Analysis of Thermal Comfort by Building Era 66
4.3.5 Limitation 67
4.4 Analysis of the Selected Residential Case Studies 68
Case 1: Ottoman-style house (Beit Erekat – Abu Dis) 68
Case 2: Jordanian Style house 71
4.4.3 Case 3: Contemporary Style house 73
4.5 Climate Analysis 74
4.5.1 Annual Temperature Regime and Diurnal Behavior 74
4.5.2 Solar Geometry, Shading Exposure and Window Control 75
4.6 Summary 76

Chapter 5 Result and Discussion 78
5.1 Introduction 78

5.1.1 Analysis of Summer Measurement 78
5.1.2 Analysis of Winter Measurement 80
5.2 Validation of the Base Three Models 82
5.2.1 Late Ottoman Period: Case 1 82
5.2.2 Jordanian Period: Case 2 83
5.2.3 Contemporary Period: Case 3 85
5.3 Base case Thermal Performance Across the Three Cases 86
5.3.1 Case 1 Thermal Performance of the Ottoman house 86
5.3.2 Case 2 Indoor Thermal Performance of the Jordanian house 94
5.3.3 Case 3: Indoor Thermal Performance of the Contemporary house 99
5.4 Results of the Parametric Simulation Strategies 105
5.4.1 Strategy 1 — Wall Thermal Mass and Time Lag 105
5.4.2 Strategy 2 — Opening Ratio and Natural Ventilation 115
5.4.3 Strategy 3 — Veranda Shading concept as Thermal Buffer: base vs. enhanced shading conditions (Applied for case 2& 3) 130
5.4.4 Strategy 4 — Orientation: rotation-angle scenario results against solar exposure. 135
5.4.5 Strategy 5 — Room Geometry and Enclosure: results of the six ratio/enclosure scenarios on temperature gradient and ventilation decay. 163
5.6 Summary 172

Chapter 6 Conclusion and Recommendations 173
6.1 Synthesis of Findings 173
6.2 Contribution of the Study 176
6.3 Limitations of the Study 177
6.4 Recommendations for Future Research 178
6.5 Concluding Remarks 178

References

Appendix

List of Abbreviations

Abbreviation	Full Term
3D	Three-Dimensional
ACH	Air Changes per Hour
ANSI	American National Standards Institute
ARIJ	Applied Research Institute – Jerusalem
ASHRAE	American Society of Heating, Refrigerating and Air-Conditioning Engineers
CFD	Computational Fluid Dynamics
CIBSE	Chartered Institution of Building Services Engineers
COVID-19	Coronavirus Disease 2019
Csa	Köppen–Geiger Climate Classification Code (Mediterranean Hot-Summer Climate)
CTF(s)	Conduction Transfer Function(s)
CVRMSE	Coefficient of Variation of the Root Mean Square Error
DesignBuilder	Graphical simulation interface for EnergyPlus (building performance modelling software)
DOE-2	Department of Energy 2 (building energy simulation convection algorithm)
EN	European Norm / European Standard (e.g. EN 16798-1)
EnergyPlus	Whole-building energy simulation engine (software)
IES	Illuminating Engineering Society
ISO	International Organization for Standardization
NMBE	Mean Bias Error (as used in the thesis; commonly termed “Normalized Mean Bias Error” in the wider literature)
PCBS	Palestinian Central Bureau of Statistics
PMV	Predicted Mean Vote
PPD	Predicted Percentage Dissatisfied
RMSE	Root Mean Square Error
S1–S3	Scenario 1 – Scenario 3 (veranda shading configurations tested in Section 5.4.3)
TARP	Thermal Analysis Research Program
TM52	Technical Memorandum 52 (CIBSE: The Limits of Thermal Comfort – Avoiding Overheating in European Buildings)
U-value	Thermal Transmittance (Heat-Transfer Coefficient)
UNRWA	United Nations Relief and Works Agency for Palestine Refugees in the Near East
VOS viewer	Bibliometric Network Visualization Software
WWR	Window-to-Wall Ratio

List of Figures

Number	Caption	Page
Figure 1-1	Analytical Framework for the study	2
Figure 1-2	Comparative summary of Palestinian residential transformation across historical periods	4
Figure 1-3	VOS viewer analysis	8
Figure 1-4	Structure of the Thesis	11
Figure 2-1	Plans and section for Palestinian house in the Ottoman period (Amiry, S.1994)	16
Figure 2-2	Bethlehem street cross-section showing traditional courtyard-based spatial configuration (RehabiMed, 2015)	17
Figure 2-3	Schematic diagram for the house plan for Al-Jaar Palaca (1928) (RehabiMed, 2015)	19
Figure 2-4	Elevation analysis of buildings in the second period (Liwan house) (RehabiMed, 2015)	20
Figure 2-5	Extended family in Ramallah (Jubeh & Bshara, 2002)	23
Figure 2-6	Al-awneh (community participation) as a social value (Amiry and Tamari, 1989)	24
Figure 2-7	Mazra'a map, Association of Eretz Israel Authorized Surveyors, Haifa, prepared for the 1944 land dispute trial (detail). On right, from top to bottom: Badr mansion, Bahá'í mansion and Wakf structure, serf village	25
Figure 2-8	Khan near Mazra'a, circa 1950. Photography: Justus Mayer	26
Figure 2-9	The diurnal working mechanism of a courtyard (Freewan, 2019)	29
Figure 2-10	Schematic analysis of courtyard openings, Harizat house (RehabiMed, 2015)	30
Figure 2-11	Schematic analysis for opening of Harizat house courtyard (RehabiMed, 2015)	31
Figure 2-12	Comparative analysis of traditional and contemporary wall envelopes (RehabiMed, 2015)	33
Figure 2-13	Façade analysis of a house of the Jordanian period (Samman & Saifi, 2019)	34
Figure 2-14	Schematic diagrams of a) the uninsulated wall and b) the insulated wall (Aktemur, Bilgin, and Tunçkol, 2021)	34

Number	Caption	Page
Figure 2-15	Contemporary apartment housing typology, illustrative of the vertical, repetitive residential model that has become dominant in Palestinian cities since (1967)	36
Figure 3-1	Schematic representation of the research methodology	40
Figure 3-2	Site Selection Criteria	42
Figure 3-3	Instruments for measuring Environmental parameters	43
Figure 3-4	Type of Data	44
Figure 3-5	Site location map	45
Figure 3-6	Conceptual Framework of the constructed Questionnaire	47
Figure 3-7	creating & validating for the base model	49
Figure 3-8	Wall Thermal mass & Time Lag strategy	50
Figure 3-9	Opening Ratio & Natural Ventilation strategy	51
Figure 3-10	Impact of an External Transitional Space (Veranda) Connected to the Living Area	53
Figure 3-11	the environmental mechanism chain in strategy 3	53
Figure 3-12	Orientation as an Adaptive Environmental Strategy	54
Figure 3-13	Spatial Configuration and Environmental Performance	55
Figure 4-1	Abu Dis District map	57
Figure 4-2	Street Selection map	58
Figure 4-3	Master Map of Abu Dis with the surrounding	59
Figure 4-4	Master Map Showing the Boundaries from the Old Town to the Wall in Abu Dis	60
Figure 4-5	Historic Map of Abu Dis Village, Jerusalem Governorate, Survey of Palestine, 1946	60
Figure 4-6	Transformations in Urban Morphology in Abu Dis	61
Figure 4-7	Row-normalized percentage of respondents per period reporting each natural ventilation rating	62
Figure 4-8	Row-normalized percentage of respondents per period reporting each façade-opening configuration	64

Number	Caption	Page
Figure 4-9	Percentage of the whole sample (independent of period) reporting hot/very hot summer conditions or cold/very cold winter conditions, by façade-opening configuration.	64
Figure 4-10	Row-normalized percentage of respondents per period reporting each privacy rating	66
Figure 4-11	Row-normalized percentage of respondents per period reporting each thermal sensation, without air conditioning	67
Figure 4-12	selected Case Study	68
Figure 4-13	Architecture drawings & perspectives for Ottoman house sample	70
Figure 4-14	Exploded Axonometry for Ottoman house sample	71
Figure 4-15	Architecture drawings & perspectives for Ottoman house sample	72
Figure 4-16	Architecture drawings & perspectives for a contemporary house sample	73
Figure 4-17	Jerusalem Climate Analysis using Climate Consultant (UCLA Energy Design Tools Group)-A	75
Figure 4-18	Jerusalem Climate Analysis using Climate Consultant (UCLA Energy Design Tools Group)-B	76
Figure 5-1	Continuous weekly indoor air temperature variation across the three typologies, summer	78
Figure 5-2	Comparative diurnal indoor air temperature profile of the Ottoman, Jordanian, and Contemporary case buildings during the summer day monitoring period	79
Figure 5-3	Comparative diurnal indoor air temperature profile of the Ottoman, Jordanian, and Contemporary case buildings during the winter day monitoring period	81
Figure 5-4	Simulated versus field-measured indoor air temperature for Ottoman case study	83
Figure 5-5	Simulated versus field-measured indoor air temperature for Jordanian-period case study	85
Figure 5-6	Simulated versus field-measured indoor air temperature for Contemporary case study	85
Figure 5-7	Operative temperature profile- Typical summer week for Ottoman case	87
Figure 5-8	Discomfort Hours- Typical Summer Week (ASHRAE 55 Adaptive Comfort Model) for Ottoman base case	89

Number	Caption	Page
Figure 5-9	PPD & PMV Graphs, typical summer week, Ottoman case	90
Figure 5-10	Operative temperature profile- Typical winter week for Ottoman case	91
Figure 5-11	Discomfort Hours- Typical winter Week (ASHRAE 55 Adaptive Comfort Model) for Ottoman base case	93
Figure 5-12	Operative temperature profile (Typical summer week), Mean diurnal variation	94
Figure 5-13	Discomfort Hours- Typical summer Week (ASHRAE 55 Adaptive Comfort Model) for Jordanian period base case	95
Figure 5-14	Operative temperature Profile- Typical winter week, Mean diurnal variation across the simulated week	97
Figure 5-15	Discomfort Hours- Typical winter Week (ASHRAE 55 Adaptive Comfort Model) for Jordanian period base case	98
Figure 5-16	Operative temperature profile -Typical summer week, Mean diurnal variation across the simulated week	99
Figure 5-17	PPD Graph, case 3	101
Figure 5-18	Discomfort hour, Typical summer week, contemporary case	102
Figure 5-19	Operative Temperature Profile- Typical winter week, Mean diurnal variation across the simulated week	103
Figure 5-20	Discomfort hour, Typical winter week, contemporary case	105
Figure 5-21	Thermal Response of the Ottoman Case wall Assembly (External vs Internal Surface temperature, 1-7 Aug simulation Period)	107
Figure 5-22	Diurnal temperature response, Case 2 Wall, 7 August (peak summer design day)	110
Figure 5-23	Weekly indoor–outdoor temperature trend, Case 2 Wall, summer design week (1–7 August)	111
Figure 5-24	Thermal Response of the Contemporary Case wall Assembly (External vs Internal Surface temperature, 1-7 Aug simulation Period)	114
Figure 5-25	Indoor air temperature, mean diurnal profile, typical summer week, by WWR scenario.	117
Figure 5-26	Indoor air temperature, mean diurnal profile, typical winter week, by WWR scenario.	117
Figure 5-27	Operative temperature, mean diurnal profile, typical summer week, by WWR scenario.	118

Number	Caption	Page
Figure 5-28	Operative temperature, mean diurnal profile, typical winter week, by WWR scenario.	118
Figure 5-29	Discomfort hours (Fanger PPD \> 20%) by season and WWR scenario	119
Figure 5-30	Predicted Mean Vote (PMV), mean diurnal profile, typical winter week, by WWR scenario	120
Figure 5-31	Predicted Percentage Dissatisfied (PPD), mean diurnal profile, by WWR scenario.	121
Figure 5-32	Mean diurnal air temperature profile	124
Figure 5-33	Mean diurnal ACH profile, summer design week.	125
Figure 5-34	Weekly hourly operative temperature profile — summer (1–7 August)	128
Figure 5-35	Weekly hourly operative temperature profile — winter (15–21 January)	128
Figure 5-36	Operative Temperature Profile (Veranda scenarios)	132
Figure 5-37	Air temperature profile (three veranda scenario)	133
Figure 5-38	hours within thermal comfort range	134
Figure 5-39	Mean diurnal solar heat gain profile through the south-west glazing, for the unshaded reference, base shading, and enhanced veranda scenarios.	136
Figure 5-40	Mean diurnal operative temperature profile, compared with outdoor dry-bulb temperature, for the unshaded reference, base shading, and enhanced veranda scenarios.	138
Figure 5-41	Weekly air temperature & operative temperature comparison across the four orientations, summer week (1–7 August)	141
Figure 5-42	Weekly air temperature & operative temperature comparison across the four orientations, Winter week (15–21 Jan)	141
Figure 5-43	Weekly operative temperature plotted against the Category II adaptive comfort band (summer week)	142
Figure 5-44	Weekly PMV (a) and PPD (b) trends by orientation, summer week	144
Figure 5-45	Weekly PMV (a) and PPD (b) trends by orientation, winter week.	145
Figure 5-46	Diurnal PMV (a) and PPD (b) for peak summer day (7 August).	146
Figure 5-47	Weekly operative temperature by orientation, summer design week, natural ventilation enabled, with the EN 16798-1 Category II adaptive comfort band (shared across orientations, shaded)	147

Number	Caption	Page
Figure 5-48	Cumulative solar gain through exterior windows by orientation, summer design week	150
Figure 5-49	Weekly operative temperature by orientation, winter design week, against outdoor dry-bulb temperature	152
Figure 5-50	Diurnal PMV (a) and PPD (b) on the peak summer day (7 August), by orientation, natural ventilation enabled	153
Figure 5-51	Weekly operative temperature comparison across the four orientations, summer week (1–7 August).	155
Figure 5-52	Weekly air temperature comparison across the four orientations, summer week (1–7 August).	155
Figure 5-53	Weekly operative temperature comparison across the four orientations, winter week (15–21 January)	156
Figure 5-54	Weekly air temperature comparison across the four orientations, winter week (15–21 January)	157
Figure 5-55	Diurnal operative temperature profiles for the representative peak summer day, 7 August, with peak and minimum values annotated.	157
Figure 5-56	Weekly operative temperature against the EN 16798-1 Category II adaptive comfort band, summer week	158
Figure 5-57	Weekly PMV (a) and PPD (b) trends by orientation, summer week	159
Figure 5-58	Weekly PMV (a) and PPD (b) trends by orientation, winter week	159
Figure 5-59	Diurnal PMV (a) and PPD (b) profiles for the representative peak summer day, 7 August	159
Figure 5-60	Mean operative temperature by scenario	164
Figure 5-61	Weekly operative temperature profiles, summer week, by plan ratio	164
Figure 5-62	Weekly operative temperature profiles, winter week, by plan ratio	165
Figure 5-63	Mean ventilation rate by scenario	165
Figure 5-64	Diurnal operative temperature profile, peak summer day (1 Aug)	166
Figure 5-65	Diurnal operative temperature profile, peak winter day (15 Jan)	167
Figure 5-66	Operative temperature Profile across three proportion scenarios	170
Figure 5-67	Ventilation Rate Profile across three proportion scenarios	172

List of Tables

Number	Caption	Page
Table 2-1	Summary of the transformation of Palestinian housing across periods	37
Table 3-1	Research Methodology Structure: Phases, Inputs, and Outputs	38
Table 3-2	Wall Construction Characteristics and Time-Lag Behavior by Case Study	50
Table 5-1	Adaptive Comfort Performance: Comparison of 80% and 90% Acceptability Thresholds for Ottoman case (summer week)	89
Table 5-2	Adaptive Comfort Performance: Comparison of 80% and 90% Acceptability Thresholds for Ottoman case (winter) week)	92
Table 5-3	Comparison of Dynamic Thermal Properties between ISO 13786 Analytical Calculations and DesignBuilder Simulation Results	108
Table 5-4	Peak temperatures and their timing, Case 2 Wall, 7 August (peak summer design day)	111
Table 5-5	Time lag summary, Case 2 Jordanian Wall	112
Table 5-6	Parametric Window-to-Wall Ratio (WWR) Scenarios and Their Thermal Implications for case study 1	116
Table 5-7	Parametric Window-to-Wall Ratio (WWR) Scenarios and Their Thermal Implications for case study 2	123
Table 5-8	Summer and winter temperature statistics by scenario (°C)	123
Table 5-9	Adaptive comfort compliance, summer design week	125
Table 5-10	Fanger PMV/PPD summary and discomfort hours	126
Table 5-11	Operative temperature summary statistics by WWR scenario and season	127
Table 5-12	Fanger PMV/PPD summary by WWR scenario and season.	129
Table 5-13	Percentage of summer hours within each EN 16798-1 adaptive comfort category	129
Table 5-14	Summary of solar heat gain indicators, base shading vs. enhanced veranda scenarios	137
Table 5-15	Adaptive Thermal Comfort Performance of the Ottoman House under Different Orientation Scenarios	143
Table 5-16	Weekly mean PMV, mean PPD, and ISO 7730 comfort-band hours by orientation and season.	146

Number	Caption	Page
Table 5-17	Summer design-week adaptive comfort compliance by orientation and adaptive category, with and without natural ventilation (EN 16798-1, n = 161 occupied hours)	147
Table 5-18	Weekly summer operative temperature statistics and cumulative solar gain by orientation, (7-day design week, peak day 7 August).	149
Table 5-19	Weekly winter operative temperature statistics and cumulative solar gain by orientation.	151
Table 5-20	Mean Fanger PMV, mean PPD, and percentage of occupied hours within the ±0.5 PMV acceptable range, by orientation and simulation condition, typical summer week	152
Table 5-21	Mean Fanger PMV, mean PPD, and percentage of occupied hours within the ±0.5 PMV acceptable range, by orientation and simulation condition, typical winter week	152
Table 5-22	Weekly operative and air temperature statistics (°C) by orientation and season	156
Table 5-23	Summer overheating hours (of 168) under the fixed threshold versus EN 16798-1 adaptive comfort categories I–II. summer week	159
Table 5-24	Weekly mean PMV, mean PPD and comfort-band hours by orientation and season	161
Table 5-25	Room geometry scenarios, Ottoman case, floor area held constant	163
Table 5-26	Room geometry scenarios, Jordanian case, floor area held constant	166
Table 5-27	Combined mechanical, natural, and infiltration air change rate by scenario and season	167

Chapter 1
Introduction

1.1 Preface

The transformation of Palestinian residential space across the Ottoman, British-Jordanian, and post-1967 contemporary periods are understood in this study as a sequence of legally and regulatory induced spatial changes, in which successive frameworks directly reconfigured the conditions of land ownership, plot formation, and domestic organization. The Ottoman Land Code of 1858 initiated the decisive shift from communal musha' tenure in Ottoman Palestine in which shares of arable land were periodically allotted among shareholders, often by lottery, toward individual private title; paradoxically, this transition made shared spatial elements more formally articulated and visibly defined — the courtyard and the liwan emerged as deliberately designed collective thresholds, organizing household life around a central shared domain while simultaneously permitting spatial separation and privacy between family units within the dwelling (Gerber, 1987; Atran, 1986). Socially, this formalization sustained extended-family cohabitation and intergenerational interaction through these defined collective spaces, while environmentally, the courtyard and liwan together performed their most developed passive-climatic function — regulating ventilation, shading, and thermal mass in direct response to the region's semi-arid conditions.

The British-Jordanian period did not rupture this spatial logic but continued and gradually modified it. Planning legislation introduced under the Mandate and retained by Jordanian administration brought new plot standards and building regulations, yet the liwan persisted as the central organizing element of domestic space — a covered transitional zone around which rooms remained arranged, preserving the coexistence of collective gathering and spatial privacy that had characterized the Ottoman house (Khamaisi, 1997). Socially, the extended family remained the dominant household structure, and intergenerational spatial arrangements continued to shape domestic organization; environmentally, however, the gradual introduction of masonry construction and imported building typologies began to compromise the passive climatic performance that the courtyard-liwan configuration had sustained.

The post-1967 contemporary period marks a genuine spatial rupture, the convergence of shifting spatial standards, new construction materials, reduced unit sizes prescribed by emerging building regulations, and a fundamental change in building typology. The multi-story apartment block displaced the courtyard

house as the normative residential form, reinforced concrete replaced stone and earthen construction, and minimum area standards institutionalized the compact dwelling unit as the regulatory baseline. These changes eliminated the liwan and courtyard as organizing spatial elements, producing interiors in which kitchen and living areas merged into open-plan configurations as a direct consequence of reduced floor areas rather than spatial preference. Socially, this period marks the consolidation of the nuclear family as the dominant household unit, displacing the extended-family arrangements that both Ottoman and Jordanian spatial forms had accommodated; environmentally, sealed concrete construction with negligible passive performance has generated near-total dependence on mechanical conditioning, severing the thermal and spatial relationship between dwelling and outdoor environment that had defined Palestinian domestic space across earlier periods. Across all three periods, shifts in land law, planning regulation, and spatial standards preceded and determined shifts in housing form, with social and environmental transformations following as compounding downstream consequences of each successive regulatory condition.



Figure 1-1: Analytical Framework for the study

1.2 Research Problem

The Palestinian domestic living space has undergone a continuous process of spatial transformation across three historically distinct yet structurally interconnected phases, each of which has progressively reshaped the relationship between spatial configuration, social organization, and environmental performance.

In the Ottoman period, the residential spatial system was organized around the open courtyard (the hosh) — as its functional and social core. This configuration sustained a coherent logic in which spatial, social, and environmental performance were mutually reinforcing. The courtyard served simultaneously as the primary zone of family interaction, as a passively regulated semi-outdoor space that moderated indoor temperatures, and as a graduated threshold structuring the privacy sequence from street to the most intimate domestic zones. The surrounding rooms were oriented inward, maintaining direct connectivity to

the shared center and enabling continuous intergenerational interaction through the same architectural arrangement that also ensured climatic responsiveness.

The transitional period — represented in the West Bank by the Jordanian-period dwelling (1948–1967) — did not constitute a rupture with this spatial logic but a partial translation of it under new material and constructional conditions. The liwan, a covered central hall, emerged not as a straightforward replacement for the courtyard but as an intermediate spatial element that preserved the courtyard's essential functions within an enclosed form. It retained the inward orientation of the surrounding rooms, sustained the spatial conditions for family gatherings and guest receptions, and maintained partial climatic regulation through its position at the heart of the plan and its connection to cross-ventilation pathways. The liwan thus represented a transitional spatial intelligence — bridging the Ottoman spatial system and the pressures of modernization without fully abandoning the performance logic of either.

The shift to contemporary Palestinian housing represents a more decisive break. The corridor-based apartment eliminates the central shared space entirely, replacing it with a linear arrangement of functionally designated rooms. Socially, this removes the spatial precondition for collective domestic life — the intermediate zone in which family members could gather and guests could be received without penetrating the private domain. Environmentally, it eliminates the primary passive thermal mechanisms: the sky-connected central void, the thermal mass of the surrounding walls, and the graduated daylight diffusion that both the courtyard and the liwan had provided; these are replaced by a sealed envelope dependent on mechanical conditioning.

The critical analytical point is that these social and environmental consequences are not independent outcomes — they are the cumulative result of the same spatial transformation. The courtyard and the liwan performed socially and environmentally through the same architectural logic: inward orientation, shared central space, graduated privacy, and direct indoor–outdoor connectivity. When that arrangement was progressively dismantled, both dimensions of performance declined together. Understanding this interconnection across the full historical trajectory, rather than at isolated endpoints, is the analytical problem this study is designed to address.

As a result, the contemporary dwelling is no longer merely a place to live but a complex system that influences mental health, family relationships, energy consumption, and interactions with the surrounding environment. Understanding this historical transformation across spatial, social, and environmental

dimensions is therefore essential for developing sustainable design strategies that support social cohesion, environmental performance, and future resilience.

Dimension	Ottoman (pre-1917)	British–Jordanian (1917–67)	Contemporary (1967–present)
Legal Framework & Core Drivers	Ottoman Land Code 1858 — musha' → freehold	Mandate setback & planning ordinances, retained by Jordan	Military Order 418 (1971) — centralized planning authority
Spatial Configuration of the Living Environment	Hosh (courtyard) house — inward, unified organism	Liwan house — closed hall, setback-bound	Corridor-plan block /Open plan block: no shared core
Family structure	Extended hamula — intergenerational cohabitation	Transitional — nuclear units emerging post-1948	Nuclear family — individualized; reduced domestic interaction
Social Characteristics	Collective domestic life; 'awneh (cooperative labor)	Functional separation emerging; collective threshold retained	Privacy over collectivity; no intermediate social zone
Environmental Performance	Courtyard: stack-effect ventilation, radiative night cooling, diffuse daylight, 3–7°C indoor temperature reduction vs. enclosed buildings (Ratti et al., 2003). Stone walls 60–100 cm: thermal time lag 8–10 hrs, ΔT reduction 2–5°C (Givoni, 1998). No mechanical systems.	The liwan retained part of the Ottoman courtyard's environmental logic through thermal mass, cross-ventilation, and daylighting, though the loss of the open courtyard reduced stack-driven ventilation and nocturnal cooling. Clay tile (qarmīd) corbels above window openings provided informal shading for larger façades, reflecting an applied—though not systematized—environmental awareness.	Sealed RC envelope: negligible passive performance. External walls frequently lack climate-appropriate insulation, producing significant seasonal fluctuations. Window design not grounded in solar orientation or thermal gain control (Mallah et al., 2024; Nasereddin, 2022).
Key outcome	Thermal comfort without machines; strong social cohesion	Transitional decline — partial passivity, partial collectivity	High energy demand; social fragmentation; spatial rigidity

Figure 1-2: Comparative summary of Palestinian residential transformation across historical periods

1.3 Literature reviews

The literature documents a sustained and multi-dimensional process of transformation in residential living spaces, driven by the intersection of social, cultural, environmental, and technical forces. Spatial configurations originally designed for specific social and environmental conditions have been progressively restructured to accommodate shifting occupant needs and climatic demands — often at the cost of the spatial qualities that made earlier forms socially and environmentally effective.

A central concern of recent housing research is the capacity of residential spaces to accommodate diverse and evolving occupant needs without requiring extensive structural modification. Magdziak (2019) demonstrates that adaptability must address the full life-cycle of occupancy if it is to constitute a genuinely sustainable design approach rather than a superficial accommodation of short-term preference. Femenías and Geromel (2019), whose quantitative analysis of user-modified apartment layouts provides direct

evidence that residents actively reorganize their spatial environments when the original configuration fails to support their daily practices, reinforce the persistent gap between design intention and lived spatial experience. Pelsmakers and Warwick (2022) extend this analysis by demonstrating that buildings designed for spatial flexibility are better positioned to respond to changing climatic and social conditions over time, establishing adaptability as both a social and an environmental design requirement.

The relationship between spatial configuration and social life is constitutive rather than incidental. Sylejmani (2020) argues that lifestyle changes actively restructure spatial logic, altering the relative importance of different rooms and dissolving boundaries that earlier configurations had maintained as socially meaningful thresholds. Jóźwik (2024) develops this argument in the urban context, demonstrating that the social consequences of spatial change extend beyond functional inconvenience to affect residents' sense of identity and place attachment. Rochma (2023) contributes a further dimension by examining the role of collective memory and material culture in sustaining community identity within high-rise residential environments in which the shared spatial structures of earlier dwelling types have been eliminated — a finding directly relevant to understanding what is retained and what is lost as Palestinian domestic space evolves across historical periods. Nimlyat et al. (2021), in their study of residential satisfaction across different housing typologies, confirm that the availability of shared intermediate zones and the spatial management of privacy gradients are among the strongest predictors of occupant wellbeing and social interaction frequency, providing empirical grounding for the argument that spatial transformation carries measurable social consequences.

The environmental dimension of spatial transformation has received increasing scholarly attention as the gap between the passive performance of traditional configurations and the energy dependence of contemporary buildings has become empirically measurable. Saifudeen and Mani (2024) demonstrate that passive approaches — thermal mass, controlled natural ventilation, and shading — remain effective and implementable in contemporary construction but are consistently underutilized, reflecting a structural disconnection between environmental research and design practice. Al Tawayha, Bragança and Mateus (2019) establish the environmental logic of traditional Arab vernacular architecture in the Palestinian and regional context specifically, demonstrating how the spatial organization of the courtyard house — its inward orientation, shaded transitional zones, and exploitation of natural air movement — constituted an integrated passive environmental system whose climatic logic remains valid independently of its material and constructional basis. Freewan (2019) further documents the environmental effectiveness of passive

cooling strategies in Palestinian residential buildings, confirming that contemporary construction has moved away from these strategies in ways that are measurable in terms of energy consumption and indoor comfort. In the Palestinian context, Nasereddin (2022) and Mallah, Hussein, and Ardda (2024) have empirically confirmed that contemporary residential buildings exhibit inadequate thermal performance and high dependence on mechanical energy — deficiencies directly traceable to the spatial and material transformations examined in this study.

The COVID-19 pandemic revealed the spatial inadequacies of layouts that prioritize room count and functional separation over flexibility and access to semi-outdoor environments. Tokazhanov et al. (2020) document how the pandemic shifted sustainability priorities in residential design, elevating the importance of multifunctional spaces, improved indoor air quality, and direct connections to outdoor areas — spatial qualities that traditional courtyard and liwan-based configurations had provided structurally but that contemporary apartment layouts have largely eliminated. Yasmin and Nilufar (2023), in their analysis of public housing adaptability, demonstrate that residents subjected to spatially rigid layouts exhibit significantly lower capacity to reorganize their domestic environments in response to changed conditions — confirming the practical consequences of designing for a fixed program rather than for spatial adaptability.

The technical dimension of residential spatial transformation has been addressed through both design strategy research and systematic classification of transformation models. Shehata et al. (2022), in their analysis of residential transformation in affordable housing, demonstrate that sustainable spatial transformation requires design frameworks that address social, environmental, and functional drivers simultaneously rather than in isolation. Itma and Monna (2022) contribute directly to the Palestinian context by documenting the relationship between spatial reorganization in Palestinian housing and changes in patterns of social use, confirming that the technical decisions embedded in building layouts carry long-term social consequences that extend well beyond their immediate functional rationale. Carabelli (2021) further demonstrates that the vertical spatial reconfiguration characteristic of contemporary Palestinian residential buildings has produced measurable reductions in the availability of shared space and opportunities for social interaction — a finding that connects the technical dimension of spatial transformation directly to its social outcomes.

This body of literature establishes that the social and environmental performance of residential space is directly and measurably shaped by its spatial configuration, and that transformations in that configuration carry consequences across both dimensions simultaneously. Spatial arrangements integrating shared intermediate zones, passive environmental mechanisms, and adaptable room configurations consistently outperform those that prioritize functional separation and individual privacy — in terms of social, environmental, and occupant satisfaction alike. This convergence provides the analytical foundation for the present study's examination of how the spatial configurations of the Ottoman courtyard house, the Jordanian-period liwan dwelling, and the contemporary Palestinian apartment have each performed across these dimensions, and what design intelligence can be recovered from this historical trajectory for contemporary application.

1.4 Research Gap

Despite a growing body of international literature on residential adaptability and thermal performance, scholarship on the transformation of Palestinian domestic space remains fragmented across disciplinary boundaries and uneven in its analytical depth. Architectural historians have documented the morphology of the Ottoman courtyard house (Amiry and Tamari, 1989; Al-Rimmawi, 2003); political geographers have analyzed the macro-level spatial restructuring of the West Bank under successive administrative regimes (Weizman, 2007; Yiftachel, 2006); and anthropologists have examined the social meanings of home in the Palestinian experience (Taraki, 2006; Peteet, 2005). However, these disciplinary streams rarely converge: studies that simultaneously address spatial morphology, environmental performance, and patterns of social use across a continuous historical sequence from the Ottoman period to the present are effectively absent from the literature.

This fragmentation is most consequential at the level of historical continuity. The transformation of Palestinian domestic space unfolds across three structurally distinct yet analytically interconnected phases: the Ottoman courtyard house, grounded in collective domestic organization and passive climatic responsiveness; the Jordanian-period dwelling (1948–1967), representing a critical transitional moment in which traditional spatial logics were partially preserved while new materials, standardized construction systems, and evolving family structures progressively restructured the domestic interior; and contemporary Palestinian housing, which has descended directly from this transitional form while further compressing its spatial depth, eliminating intermediate social zones, and increasing its dependence on

mechanical environmental systems. Existing literature addresses each phase in isolation and primarily in descriptive terms, documenting formal change without measuring its environmental or social consequences, and without treating the three phases as a coherent analytical trajectory.

This gap is compounded by the near-total absence of empirical studies that link the reorganization of Palestinian domestic space across historical periods to measurable changes in environmental performance and daily social use — the two dimensions of residential quality most directly affected by spatial transformation, and the two dimensions most relevant to the development of evidence-based design guidance for contemporary West Bank housing. The present research addresses these intersecting gaps by treating the Ottoman, Jordanian, and contemporary dwelling types as successive spatial configurations of equal analytical weight, whose differences are measurable in environmental and social terms, and whose continuities carry design intelligence recoverable for contemporary application.

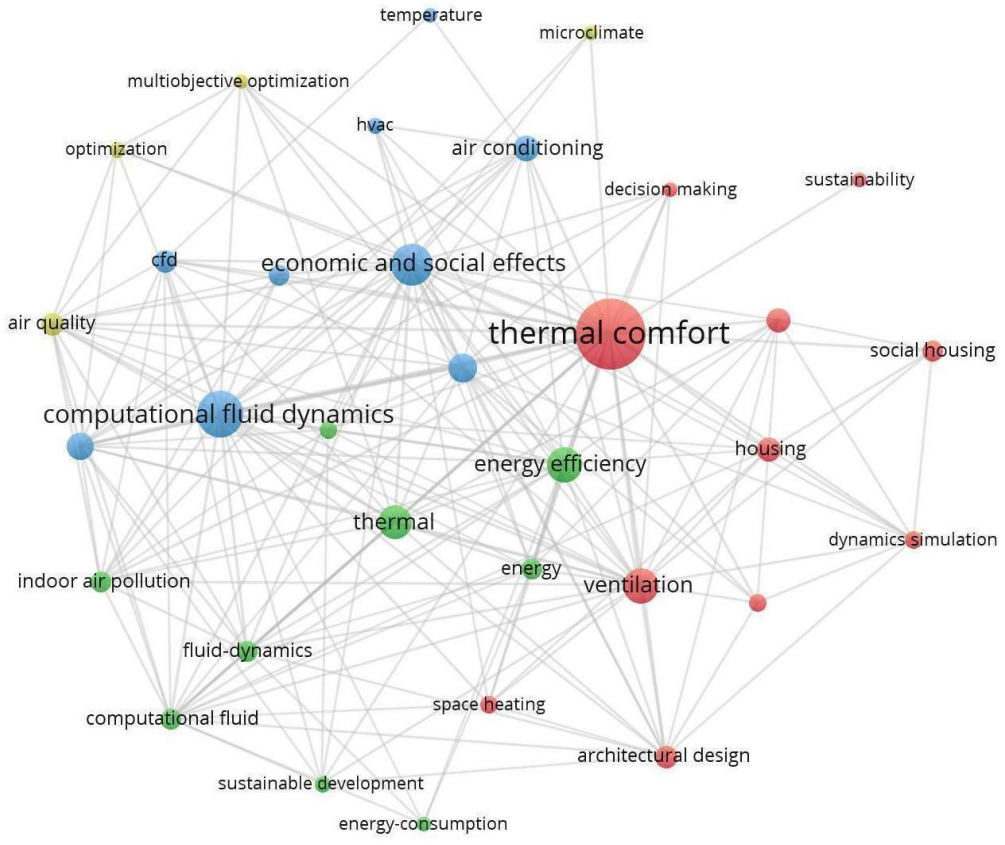


Figure 1-3: VOS viewer analysis

1.5 Research Question and Hypothesis

The study seeks to answer the following question: How have successive colonial and post-colonial governance regimes — Ottoman, British Mandate, Jordanian, and contemporary Israeli occupation — reconfigured the spatial organization of the Palestinian domestic living space, and what are the measurable implications of this reconfiguration for thermal comfort and social interaction in contemporary single-family houses within a Mediterranean semi-arid climate?

To address this overarching research question, the study is guided by the following specific questions:

1. How has the spatial configuration of the Palestinian domestic living space transformed across the Ottoman, Jordanian, and contemporary periods in terms of form, function, and social organization?

2. To what extent do changes in the spatial configuration of the lived space across historical periods affect indoor thermal performance and patterns of social interaction in contemporary single-family homes within a Mediterranean semi-arid climate?

The study assumes that the configuration and organization of living spaces significantly influence both social interactions and environmental comfort in contemporary single-family housing, suggesting that design strategies inspired by historical spatial patterns can improve residents' daily experience.

1.6 Objectives

This study aims to examine the transformation of the domestic living space across the Ottoman, Jordanian, and contemporary periods, analyzing the functional, social, and environmental dimensions of this transformation and their implications for contemporary residential design in a Mediterranean semi-arid climate. The study further aims to:

1. Document and analyze the spatial, social, and environmental characteristics of Palestinian domestic lived space across the Ottoman, Jordanian, and contemporary periods, identifying the causes and consequences of transformation in each phase.
2. Develop evidence-based design principles for contemporary residential living spaces that draw on the spatial and environmental intelligence of historical Palestinian dwelling types, addressing both environmental performance and social quality of life.

1.7 Significance of the Study

The findings of this study contribute to architectural knowledge across three analytically distinct dimensions:

1. Theoretical contribution: The study establishes a causal analytical framework — linking the drivers of spatial transformation across historical periods to their measurable consequences for environmental performance and social use — that existing scholarship on Palestinian domestic architecture has not systematically applied. This framework reframes the environmental and social deficiencies of contemporary Palestinian housing as the cumulative outcome of identifiable transformation processes, rather than isolated design failures.

2. Disciplinary contribution: By treating spatial morphology, environmental performance, and patterns of daily social use as interconnected dimensions of a single historical trajectory, the study bridges disciplinary boundaries that have kept architectural history, building performance research, and social analysis of the Palestinian home largely separate. The result is an integrated, evidence-based account of how Palestinian domestic space has changed across the Ottoman, Jordanian, and contemporary periods — and what those changes have cost in measurable terms.

3. Applied contribution: The study produces design principles derived from documented local spatial and environmental performance across all three historical periods, rather than from typological description or imported international benchmarks. These principles are grounded in the specific climatic, spatial, and social conditions of Palestinian residential life, making them directly applicable to the design of contemporary single-family houses within the Mediterranean semi-arid context of the region.

1.8 Limit and Limitation

This study takes the residential living space — rather than the building as a whole — as its primary unit of analysis. It examines the functional, social, and environmental dimensions of living spaces across historical periods, with particular reference to Palestinian and local housing contexts, the study limits are:

1. Context-Specific Findings. The findings are applicable to regions sharing comparable climatic and social conditions. This specificity may limit the broader generalizability of the results, though it ensures analytical precision within the defined context.

2. Building Typology Scope**.** The study is confined to single-story residential buildings, a deliberate boundary that enables focused and consistent analysis of living-space performance within this particular housing typology.
3. Cultural Context Scope. The study is intentionally grounded in Palestinian and local housing patterns, producing insights that reflect the region's distinct cultural and spatial characteristics. While the findings are primarily directed at comparable cultural settings, they offer a meaningful reference point for future comparative research in other contexts.

This scope and set of limitations provide a clear framework for the research, ensuring that the study remains focused while acknowledging potential constraints on its findings. The limitations of the study are:

1. Scope Limitation. The study does not engage with the full structural or architectural composition of entire buildings. The analysis is explicitly bounded by the living space as the core unit of investigation, and findings should be understood within that frame.
2. Simulation Constraints. Although simulation-based validation is incorporated into the research methodology, the reliability of simulation outputs depends on the assumptions, boundary conditions, and input parameters used in the modeling environment. Results should be interpreted accordingly.
3. Historical Data Limitation. The examination of historical living spaces draws on available documentation and case studies, which may not fully capture the range of variation across all historical periods under consideration.

1.9 Research Structure

(Figure 1-4) lays out the thesis's five-chapter structure. Chapter 1 introduces the research (problem, gap, question, objectives). Chapter 2 traces the chronological transformation of the Palestinian house (spatial, social, and environmental dimensions across the three periods). Chapter 3 sets out the methodology, including case-study/sample selection, data collection, and base-model creation and validation. Chapter 4 presents the case study of Abu Dis, covering the survey analysis and the three selected buildings (Ottoman, Jordanian, contemporary). Chapter 5 delivers the results and discussion — model validation, baseline thermal performance, the five parametric strategies (wall mass, WWR, veranda shading, orientation, room geometry), cross-strategy discussion, and a chapter summary.

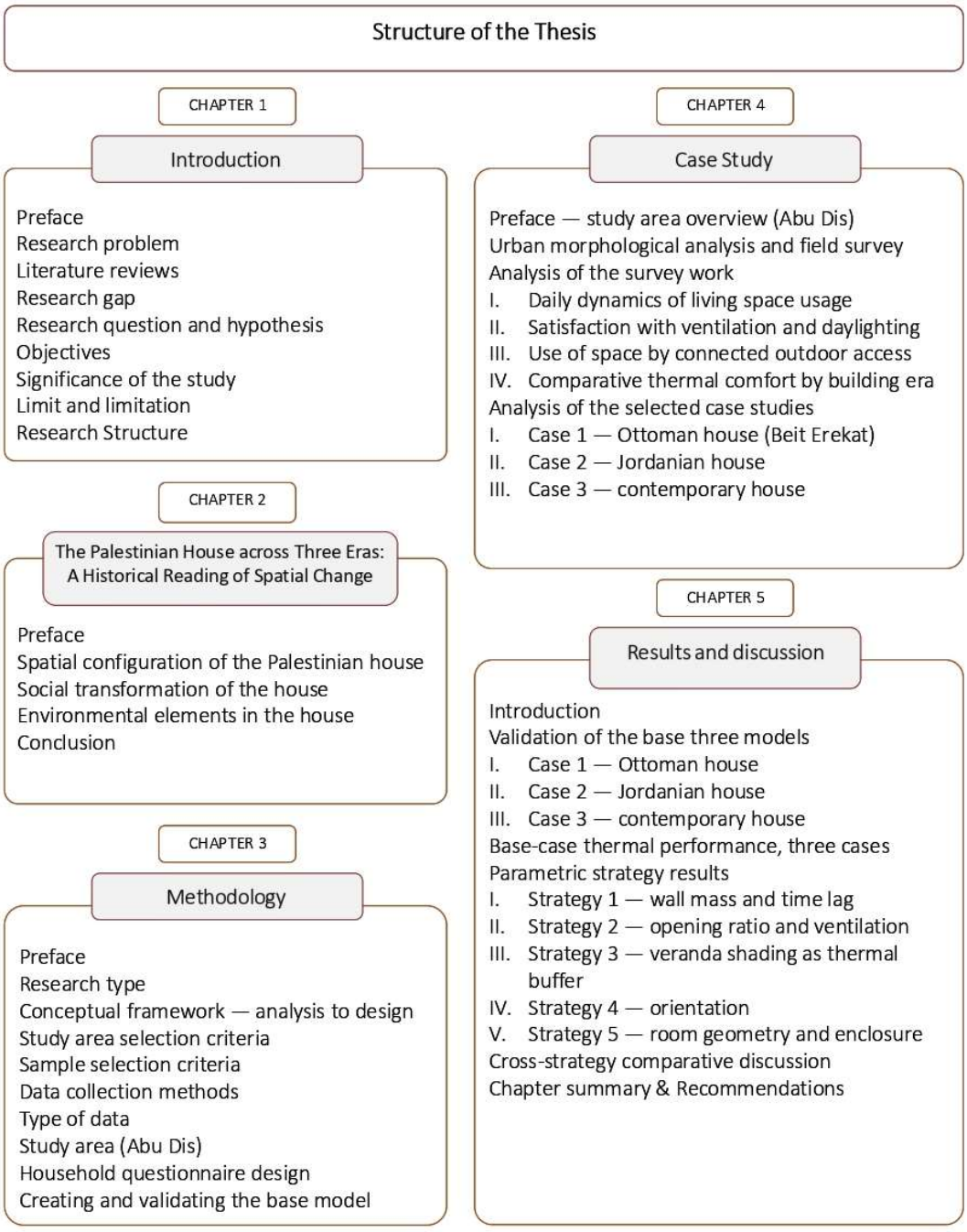


Figure 1-4: Structure of the Thesis

Chapter 2

The Palestinian House across Three Eras: A Historical Reading of Spatial Change

2.1. Preface

Palestinian residential architecture has undergone cumulative spatial and architectural transformations closely tied to the political, social, and economic conditions experienced by Palestinian society across successive historical periods. These transformations were not merely formal or stylistic; they represented fundamental shifts in the organization of domestic space, in the relationship between the house and its surroundings, and in how inhabitants inhabited architectural space. During the Ottoman period, the traditional Palestinian house was characterized by a cohesive, inward-oriented spatial system structured around the courtyard (hosh) as the principal living core.

This configuration gradually shifted during the British Mandate and Jordanian periods toward more functionally segmented layouts, a change driven by evolving lifestyles and increasing exposure to modern urban and architectural models. Following the Nakba, Palestinian housing entered a new phase shaped by forced displacement, spatial constraint, and political control, resulting in reduced spatial scale, fragmented living arrangements, and a diminished role for traditional open space. Contemporary Palestinian housing, in turn, has developed under conditions combining high population density, economic constraint, and the influence of globalized architectural typologies, conditions that have produced repetitive residential models prioritizing functional efficiency, frequently at the expense of environmental performance and spatial continuity.

Within this framework, the chapter traces the chronological transformation of the Palestinian house by examining its spatial configuration and its relationship to the surrounding context. This provides the analytical foundation for the subsequent discussion of the environmental and social transformations that have shaped the performance of contemporary Palestinian housing.

2.2. Spatial configuration of the Palestinian house architecture and urban attachment

This section examines how the internal spatial organization of the Palestinian house — the courtyard, liwan, and their successors — shaped and was shaped by the dwelling's relationship to the street, the

neighborhood, and the wider urban fabric. It traces how these spatial arrangements mediated privacy, social exchange, and a sense of belonging across the Ottoman, Jordanian, and contemporary periods.

2.2.1 Late Ottoman Period until 1917 :First Period

This period is characterized by an inward-oriented, unified spatial organization, in which the courtyard (hosh) and the multifunctional living space (al-bayt) structured daily life through continuity and adaptability rather than functional division. The following section examines how this spatial system was articulated at both the house and settlement scale, from the courtyard's mediating role down to the fine-grained differentiation achieved through elements such as the mastabeh (raised platform) and wall nīsh.

- Spatial Configuration at the House Scale in Late Ottoman Period

The spatial configuration of the Palestinian house during the Ottoman period was characterized by a unified, inward-oriented living structure in which domestic life was organized around a limited number of interconnected spaces rather than functionally specialized rooms (Badran, 2017). This produced a coherent architectural system in which spatial continuity and adaptability formed the basis of daily habitation (Itma & Monna, 2022).

Central to this system was the (hosh) courtyard, which functioned as the principal living space of the house, structuring movement, orientation, and adjacency between enclosed spaces and accommodating a wide range of daily activities (Shaded, 2023a). The courtyard served as the primary mediator between the house's component parts, reinforcing an internal spatial hierarchy that privileged inward relations over external exposure (Abdelkader & Park, 2018).

Directly connected to the courtyard, the main living space (al-bayt) functioned as a multifunctional interior domain rather than a single-purpose room, shifting between sitting, eating, and sleeping across the day, with flexibility generated by spatial configuration rather than fixed functional zoning (Shaded, 2023b; Itma & Monna, 2022). Architectural elements integrated into the building fabric (the nīsh (wall niche) for bedding and storage, and the mastabeh (raised platform)) supported this multi-functionality while keeping the room open and continuous (Shaded, 2023b).

Within the same spatial continuum, the mastabeh introduced a subtle vertical differentiation, accommodating sitting, sleeping, and the storage of food supplies in clay jars without dividing the room, so that hierarchy was articulated through level variation rather than partition walls. Above or behind the

mastabeh, the rawieh (or siddeh) served as an elevated grain-storage chamber, while at the lowest level the qā‘al-bayt (basement floor) accommodated animals, tools, and fodder, reflecting a continuous relationship between living and service functions (Shaded, 2023a).

The spatial configuration extended beyond the enclosed structure through the sīrah (external yard enclosed by stone walls, and through seasonal shaded structures such as the arīsheh/khus (which functioned as extensions of the domestic spatial network (Al Tawayha, Bragança and Mateus, 2019)). Structurally, load-bearing stone walls, vaults, and occasionally domes produced compact, continuous interiors that reinforced introversion.

In this configuration, the Ottoman-period Palestinian house operated as a single spatial organism in which living, storage, and service functions were layered within a unified architectural framework, and adaptability was achieved through architectural articulation rather than functional division (Figure 2-1).

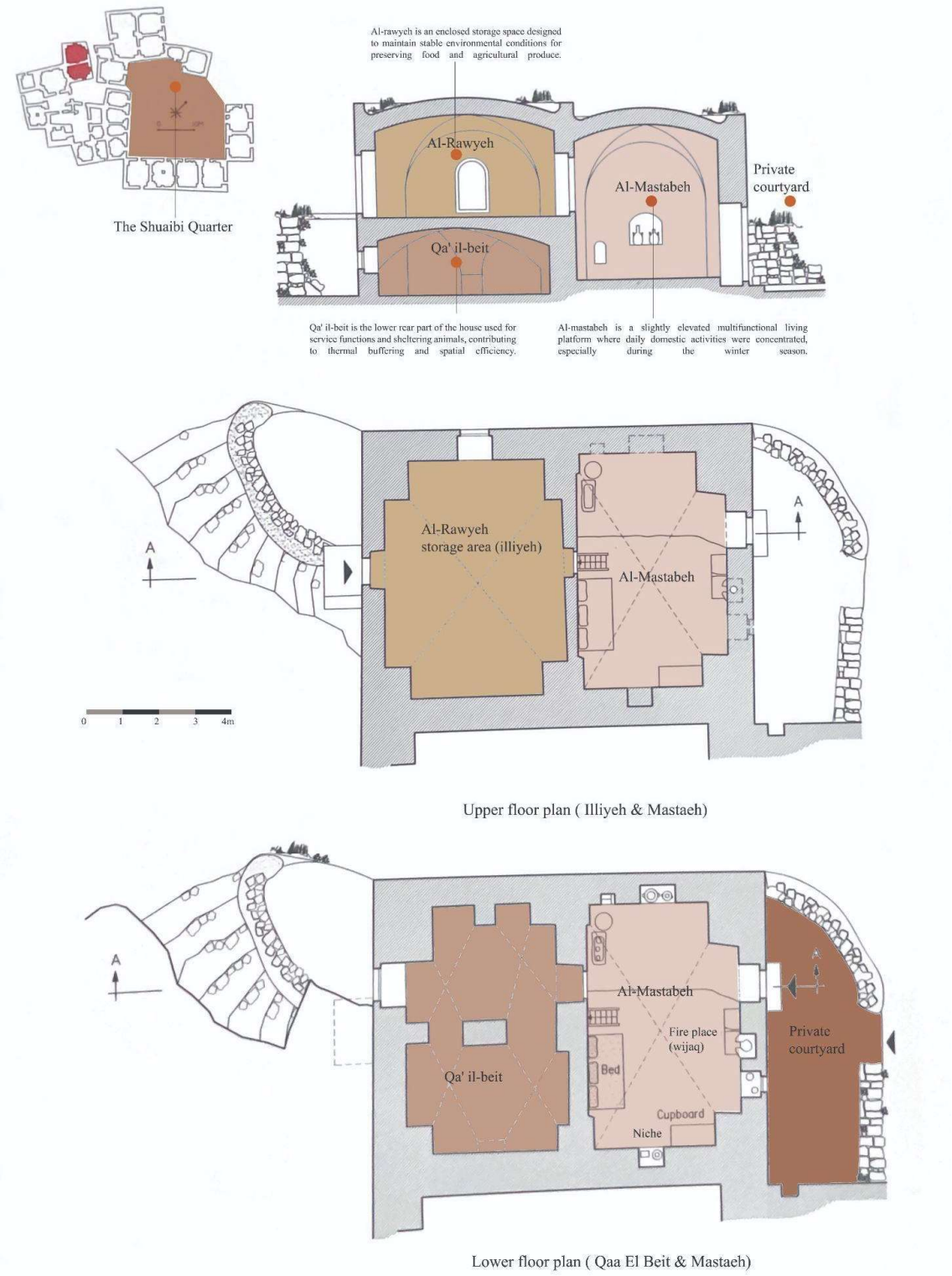


Figure 2-1: Plans and section for Palestinian house in the Ottoman period (Amiry, S.1994)

- Spatial Configuration of Traditional Urban Fabric in Late Ottoman Period

Historic Palestinian towns developed through a hierarchical socio-spatial structure in which the hosh (courtyard cluster) functioned as the fundamental unit of urban organization, rather than as merely an internal residential space. The hosh operated as an intermediate spatial entity linking the individual dwelling to the wider urban fabric, generating dense networks of spatial relations based on kinship, proximity, functional continuity, and regulated movement. The sequential accretion of courtyard clusters produced a compact urban fabric of high density and limited permeability, in which circulation, daylight access, and ventilation were regulated through a clear spatial gradient from private to semi-public to public realms. This logic is directly legible in the morphology of narrow, irregular streets and the absence of linear urban axes.

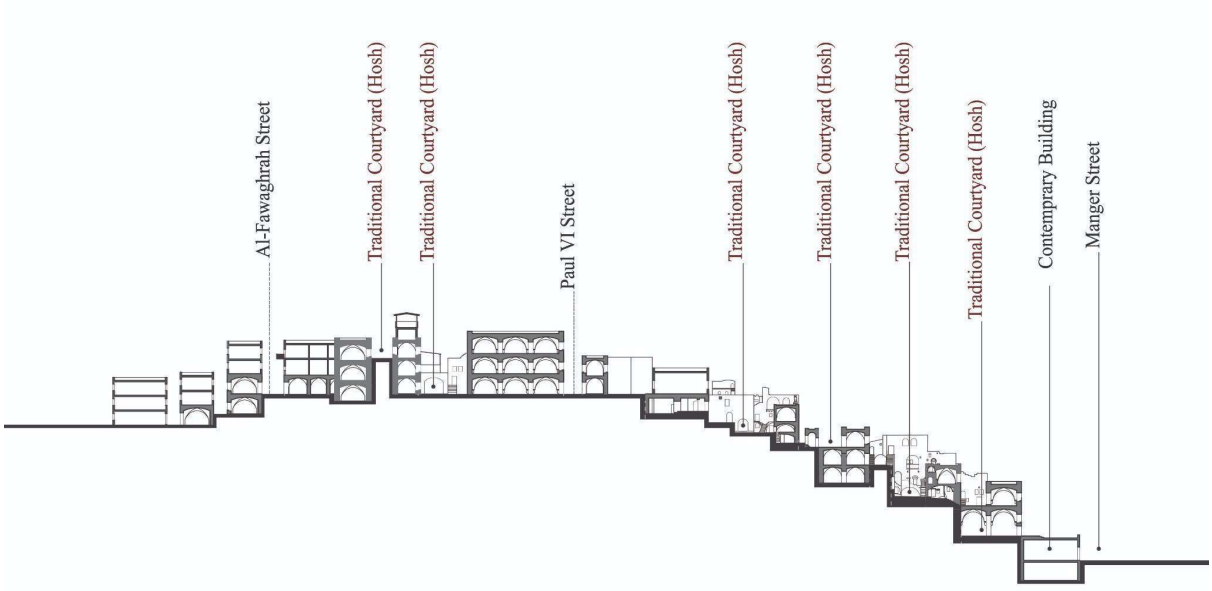


Figure 2-2: Bethlehem street cross-section showing traditional courtyard-based spatial configuration (RehabiMed, 2015)

Studies of Palestinian historic urbanism indicate that this system was neither incidental nor informal, but an effective mechanism of urban organization enabling both horizontal and vertical growth without undermining structural coherence or functional integration. Within this framework, the hosh remained critical to the long-term unity and stability of the urban fabric, ensuring adaptability while preserving its underlying spatial logic over time (Bianca, 2000; Amiry, 1994; Al-Houdalieh, 2010).

2.2.2 British and Jordanian Period (1917-1967) :Second Period

During the British and Jordanian period, the spatial configuration of the Palestinian house underwent a fundamental transformation, marked by the disappearance of the traditional open courtyard and the emergence of the (liwan) as the principal living space. This shift was closely associated with the adoption of reinforced concrete, which made it structurally possible to enclose the courtyard and to consolidate the interior into a more unified, standardized layout. The liwan became a central, multifunctional space mediating between domestic interior life and the surrounding urban context, reflecting the broader technological and spatial changes that redefined the relationship between house and environment during this period.

- Transformation from Courtyard to Liwan in British and Jordanian Period

During this period (1917–1967), the spatial configuration of the Palestinian house underwent a clear architectural transformation marked by the enclosure of the traditional open courtyard. This produced the central-hall type, in which the courtyard was converted from an open void into a covered internal space. As (Jawabrah, 2005) argues, this transformation represents an evolutionary development of the courtyard house rather than a complete departure from earlier spatial types, retaining the centrality of the internal void while altering its physical condition (Figure 2-3).

Within this configuration, the enclosed central hall (liwan) became the house's primary organizing element, functioning as a spatial core around which rooms were arranged. It preserved the courtyard's generative logic while redefining the internal spatial hierarchy. The shift from an open to a covered space altered the house's environmental relationship by internalizing what had previously been an open-air void, modifying patterns of light, ventilation, and enclosure without eliminating the central spatial role of the void. (Jawabrah, 2005)

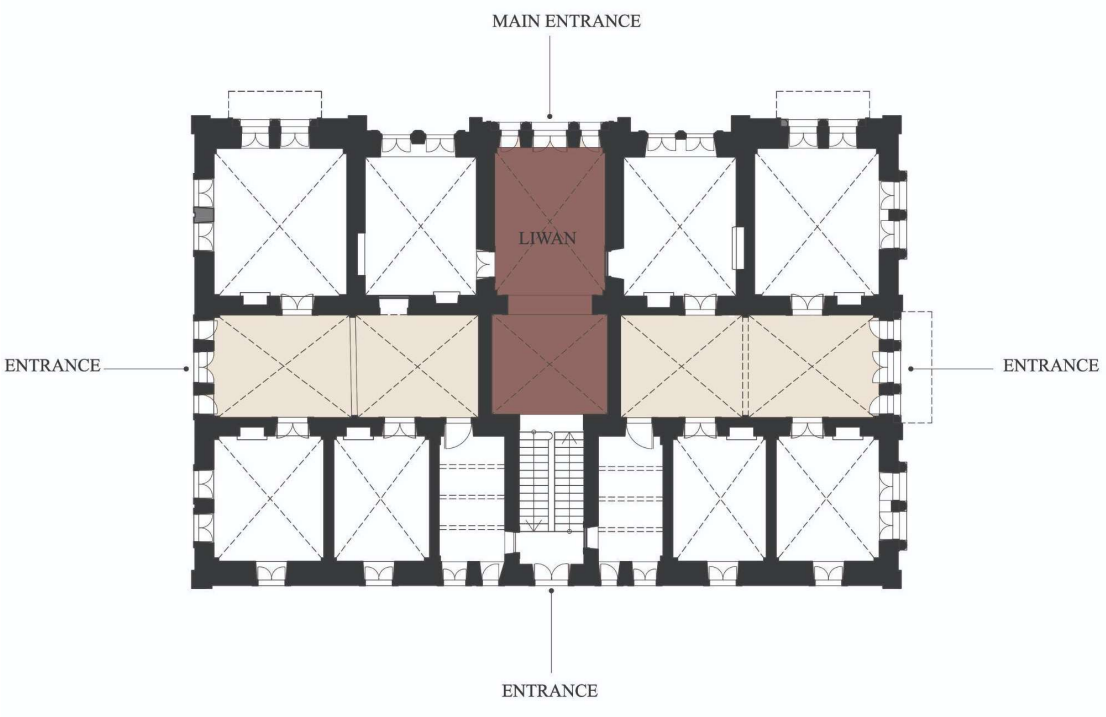


Figure 2-3: Schematic diagram for the house plan for Al-Jaar Palaca (1928) (RehabiMed, 2015)

- Transformation in the Construction System in British and Jordanian Period

Traditional Palestinian houses relied on load-bearing stone walls and vaulting systems, which structurally constrained spatial span and limited the possibility of covering large internal spaces. During the Jordanian period, the increasing use of reinforced concrete introduced new structural capacities, enabling the enclosure of the courtyard and the formation of larger, uninterrupted internal spaces (Samman and Saifi, 2021).

This shift from vaulting to concrete slabs and beams altered the house's internal organization by reducing structural constraints on spatial layout. Despite the absence of major change in planning regulation (Jordan largely retained inherited British Mandate planning law) these constructional shifts occurred through local building practice rather than formal architectural policy (Abuarkub & Al-Zwainy, 2018) Architectural transformation in this period was therefore material-driven, shaping spatial configuration through construction technique rather than through imposed design models.

- Transformation in Elevation Design, Material, and Style British and Jordanian Period

Changes in construction systems also affected the size and configuration of window openings. In traditional courtyard houses, openings were small and limited, reflecting the structural constraints of load-bearing walls and vaulting. These constraints reinforced an inward-oriented architectural composition, with minimal engagement between interior space and the external environment (Jawabrah,2005).

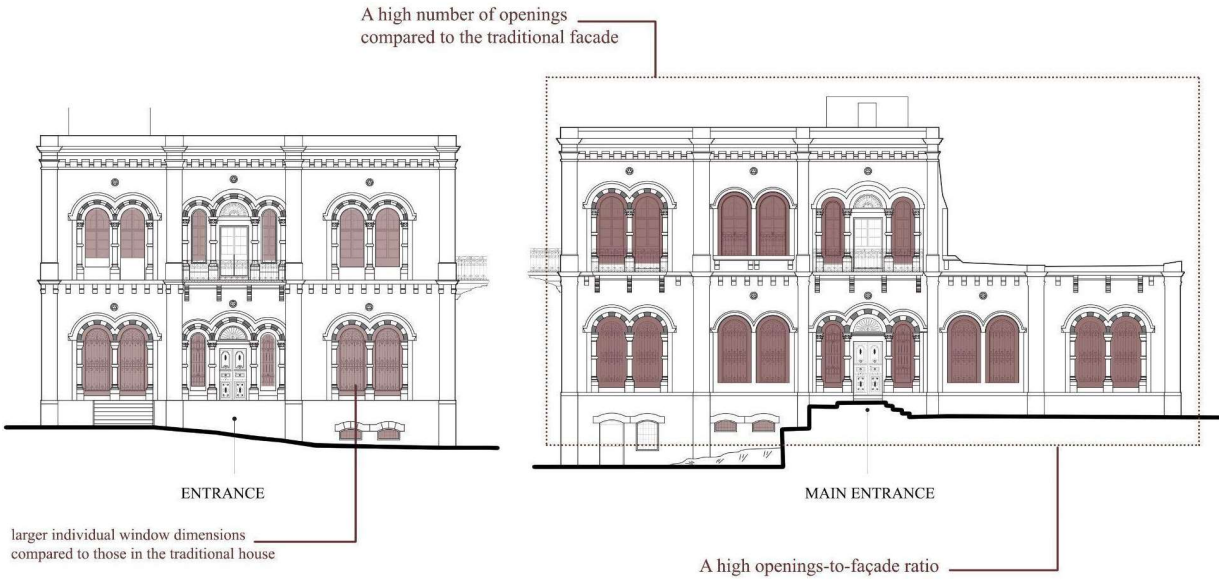


Figure 2-4: Elevation analysis of buildings in the second period (Liwan house) (RehabiMed, 2015)

The introduction of reinforced concrete and steel elements reduced these constraints, permitting larger façade openings. This structural flexibility increased the penetration of light and air and established a more direct architectural relationship between the house and its immediate surroundings (Samman & Saifi, 2021). The enlargement of openings did not eliminate the centrality of the internal spatial core, but it did reconfigure the building envelope, rendering façades more permeable and less structurally restrictive. These changes occurred incrementally and without a unified planning framework, reflecting the broader absence of coordinated architectural development strategy in the West Bank during the Jordanian period (Abuarkub & Al-Zwainy, 2018)

2.2.3 Third Period: Late Twentieth Century

The Palestinian dwelling in the modern period has undergone significant spatial transformation. Unlike earlier periods, there is no longer a single dominant residential type. Instead, a plurality of housing forms has emerged (single houses, villas, apartment buildings, and mixed-use multi-story buildings), particularly in cities and their peripheries. This diversification reflects economic and social pressures, notably rising land prices and increasing population density, which have shifted development from horizontal expansion toward vertical construction, redefining the relationship between the dwelling, the land, and the urban context (Carabelli, 2021).

At the scale of internal space, these typologies have reorganized spatial priorities within the residential unit. Living space has been reduced in favor of enclosed functional rooms, alongside growing reliance on open-plan arrangements that combine kitchen, living room, and dining area into a single multifunctional space. This integration responds not only to spatial limitation but also enhances functional efficiency, establishing the living area as the household's central hub (Carabelli, 2021)

In contrast, bedrooms have become more private and relatively spacious, reflecting a functional separation between day and night zones and emphasizing privacy in personal spaces compared to communal areas (Samman & Saifi, 2021). Moreover, modern housing layouts have transformed guest reception areas, with the traditional separate guest room often eliminated in favor of using space within the open living area. This indicates a cultural shift in hospitality and social interaction, in which guests now participate in daily activities in an open space rather than in a dedicated suite (Itma & Monna, 2022).

At the interface with the surroundings, these spatial transformations have redefined the connection between the interior and the exterior. Interaction with the street no longer occurs through expansive ground-level spaces, as in traditional homes, but is instead visually mediated through balconies, facades, and vertical openings on upper floors, reflecting a fundamental shift in the dwelling’s relationship with its immediate urban environment. This shift is significant in the modern context, as limited physical connection to the surroundings may affect the sense of place and social belonging. In contrast, balconies and facade openings provide visual connectivity, natural ventilation, and daylight, thereby improving the quality of life within the home.

The modern transformation of the Palestinian dwelling's spatial configuration is therefore not merely architectural; it constitutes a practical and cultural response to contemporary social and economic conditions, redistributing the balance between privacy and efficiency and reshaping the house's mode of engagement with the urban environment, and so establishing a residential model that negotiates limited space against the social and functional needs of its inhabitants.

2.3. Social Transformation of the Palestinian House Architecture

This section traces how the social values embedded in the Palestinian house — extended-family cohabitation, hospitality, and mutual cooperation (al-'awneh) — were reshaped, eroded, or newly generated as spatial arrangements responded to shifting political and economic conditions. It follows this trajectory across the Ottoman, British-Jordanian, and contemporary periods, showing how each phase left its own imprint on domestic social life and the architecture that housed it.

2.3.1 Ottoman Period (Until 1917): First Period

At the Village and Town Scale**,** Palestinian domestic architecture of the Ottoman period should be understood as a spatial system that both reflects and reproduces social structure: design decisions were not neutral but responded directly to prevailing modes of living, family organization, and social interaction (Amad, 2012; Abu Hilal, 2009).

The organization of space reveals privacy as an embedded social principle. Rather than relying on total isolation, builders employed a hierarchy of spaces to regulate movement, visibility, and interaction; recessed entrances and internal courtyards functioned as deliberate strategies for managing social exposure, demonstrating that privacy operated as a dynamic social practice rather than a fixed condition (Amad, 2012).

This spatial logic extended to the extended family (hamūla), which served as the central social unit. The courtyard functioned as a communal regulator, allowing multiple generations to coexist while distributing social roles within the household; surrounding rooms retained varying degrees of autonomy, mediating between collective living and individual independence (Abu Hilal, 2009) (Figure 2-5).

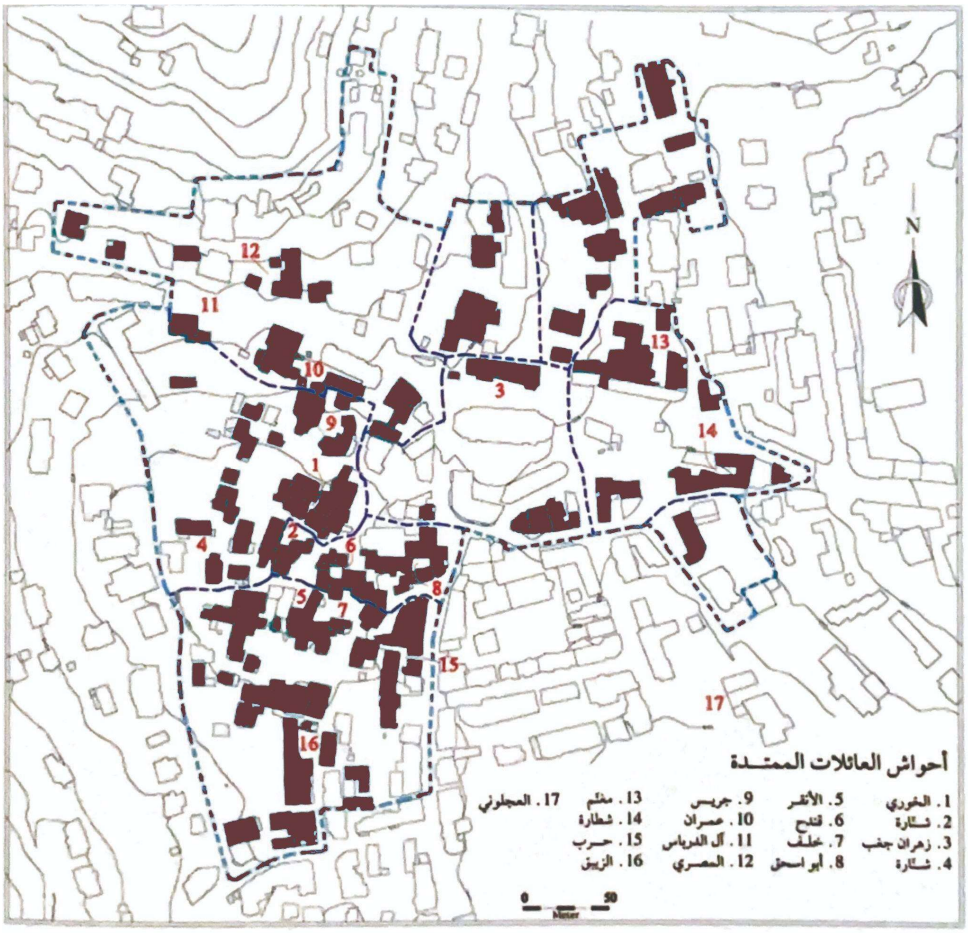


Figure 2-5: Extended family in Ramallah (Jubeh & Bshara, 2002)

The principle of hospitality further shaped spatial arrangement. Semi-independent reception areas marked the boundary between public and private spheres, reflecting both social convention and an architectural awareness of social boundary-making; in merchant households such spaces became visible markers of social status, illustrating the interplay between architecture, economic position, and social representation (Norris, 2020).

The social organization of Palestinian domestic architecture was further informed by the principle of al-‘awneh (mutual assistance and cooperation). The construction and maintenance of houses depended on family and neighborhood networks, reflecting a system of reciprocal obligation and social interdependence; this practice shaped spatial arrangement directly, as shared courtyards and adaptable work areas facilitated collaborative labor while reinforcing daily interaction and collective responsibility. Architecture thus materialized social norms, making the house a site in which cooperation, mutual support, and communal identity were continuously enacted and reproduced (Amari, 2001) (Figure 2-6).



Figure 2-6: Al-awneh (community participation) as a social value (Amiry and Tamari, 1989)

Read through this lens, the Ottoman-period Palestinian house emerges as a living structure in which spatial organization, social value, and daily practice are tightly interwoven, producing a dynamic and durable architectural expression of society.

- The Plantation as Reshaping Social and Spatial Relations

Plantation is a modern agricultural landscape organized around for-profit, monoculture production for a global market, owned by a single proprietor and worked by landless laborers who hold no rights to the soil they cultivate. This structure emerged from the 1858 Ottoman Land Code, which commodified and individualized land titles, severed ownership from cultivation, and allowed a small class of local and absentee owners to accumulate large estates while fellahin who had previously held land through customary cultivation rights lost that access. Unlike the traditional village, the plantation's labor settlements, called (saknat), provided housing without land rights attached to it, a break from earlier, communal forms of land-based belonging.

The Social impact for consequences of this restructuring was lived, not only legal. At Mazra'a (Farm) landlord's mansion stood about two kilometers from the serf village, so the class division built into the plantation system was part of daily spatial experience rather than an abstraction. The two households were built differently because they lived differently. Landlords put accumulated capital into multi-room mansions, such as the two-story residence with five ground-floor rooms and three upper rooms served by a gallery, roofed with imported materials and built by professional masons. Serfs kept building single-

room mud huts by hand, structures that had to be rebuilt every year and offered no real permanence. Older patterns of collective life did not survive this split either. The courtyard house's shared wall, once maintained jointly by the households living around it, had no equivalent on the plantation, where serf dwellings sat scattered and unconnected rather than enclosed in a shared, mutually sustained compound. The plantation did not merely reflect Palestine's new class structure; it produced it, and in doing so it underlies the two political horizons the article traces: a landed elite oriented toward territorial nationalism through capitalist land control, and plantation serfs oriented toward a village-based idea of homeland and land reform. (Allweil, 2016). (Figure 2-7)

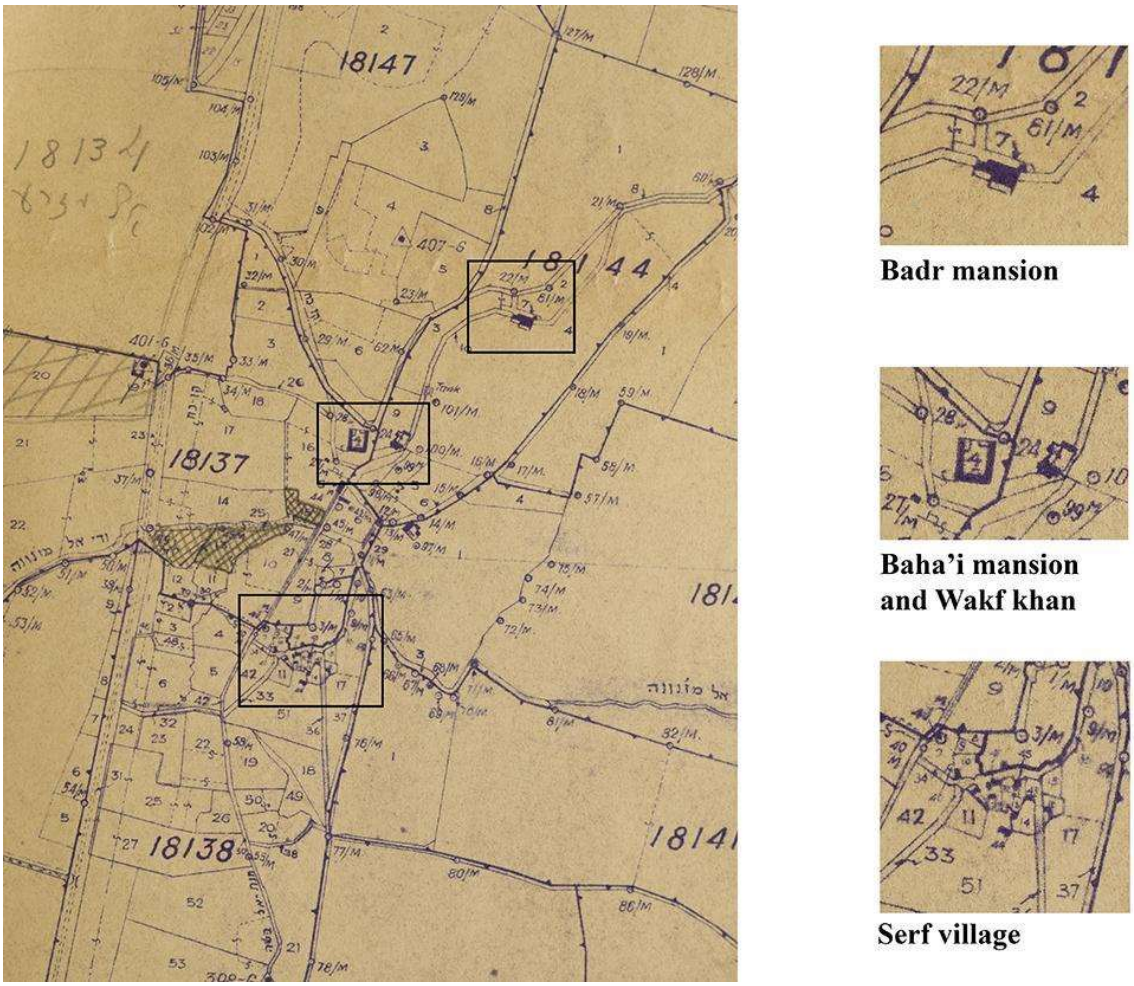


Figure 2-7: Mazra'a map, Association of Eretz Israel Authorized Surveyors, Haifa, prepared for the 1944 land dispute trial (detail). On right, from top to bottom: Badr mansion, Bahá'í mansion and Wakf structure, serf village



Figure 2-8: Khan near Mazra'a, circa 1950. Photography: Justus Mayer

2.3.2 British and Jordanian Period (1917-1967): Second Period

This period marks a decisive break from the extended-family household of the Ottoman era, as Nakba-induced displacement, camp life, and shifting economic conditions gave rise to smaller nuclear households and new domestic arrangements. It examines how these social changes drove the emergence of specialized spaces within the house, reshaping the spatial logic inherited from the preceding period.

- Transformation of Household Structure

Following the 1948 Nakba, the social structure of Palestinian households changed significantly under Jordanian rule. Traditional extended families, comprising several co-resident generations, gradually gave way to smaller nuclear households of parents and children alone (Shemesh, 2004; PCBS, 2010). This structural shift affected the organization of interior space, generating increasing demand for private areas, separate bedrooms distinct from the main living space. Demographic evidence indicates that nuclear households became increasingly common in refugee camps and newly established urban settlements, a pattern driven by the redistribution of families following land loss (PCBS, 2010).

- Changing Functions and Occupations after Displacement

Displacement and land loss also produced a substantial transformation in the population's economic and social functions. Many Palestinians who had previously relied on agricultural livelihoods in their villages

of origin shifted to a wider range of occupations in urban areas and refugee camps, including trade and manual labour (El Zein, 2017). This shift was reflected in the use of domestic space, with growing emphasis on rooms designated for specific functions, such as enclosed kitchens and storage rooms, replacing the courtyard's earlier accommodation of mixed domestic and agricultural activity.

- Demographic Transformation through Camps and Household Overlap

The influx of Palestinian refugees and the establishment of new camps in the West Bank produced substantial demographic pressure and led to the overlapping of households within single dwellings or neighborhoods (UNRWA, 2010; Badil Center, 2010). This necessitated the reorganization of internal space to accommodate multiple families or generations while maintaining privacy and social hierarchy; households adapted their internal layouts to manage these pressures, preserving functional separation and social order despite spatial constraint.

- Emergence of Specialized Spaces within the House

As a consequence of social and demographic change, Palestinian houses began to include specialized internal spaces previously absent from the typology. Bedrooms became separated from the main living hall, and kitchens were enclosed as independent rooms (Shemesh, 2004). This functional specialization allowed households to regulate daily life more efficiently, accommodate a wider range of domestic activities, and sustain continuity in social practice despite broader shifts in social and demographic conditions.

2.3.3 Late 20th Century: Third Period

The transformation of Palestinian housing in the modern period reflects not only architectural change but profound shifts in social routine and domestic life. One central aspect is the reduction of engagement with indoor living space: modern households spend considerably more time outside the home owing to work, education, and social commitments, resulting in reduced interaction with the domestic environment. This has diminished the priority placed on the quality and richness of indoor space, in contrast to traditional houses, where courtyard and living area were central to daily life and social interaction (Carabelli, 2021)

Consequently, the internal spatial hierarchy has shifted: living areas remain multifunctional but are less socially engaging, while private spaces such as bedrooms receive proportionally greater attention, emphasizing individual privacy over collective domestic interaction (Samman & Saifi, 2021). The courtyard, once central to family life and social interaction, has lost its role as the primary communal

space, reflecting the diminished importance of shared domestic activity (Itma & Monna, 2022). This transformation illustrates how social behavior (increased time spent outside the home and reduced household interaction) directly reshapes architectural priorities, producing interior spaces that remain functional but are more socially constrained.

2.4 Environmental Elements in the Palestinian House Architecture

This section examines how thermal mass, openings, orientation, and enclosed space worked together as an integrated environmental system in the Palestinian house, rather than as isolated components. It traces this system across the Ottoman, Jordanian, and contemporary periods, reading each material and spatial shift for its effect on heat and air movement.

2.4.1 Environmental Performance as an Integrated System

A house's environmental behavior is not the sum of its parts. It comes from how mass, opening, orientation and enclosed space work together across the day and the year, an argument developed in the foundational studies of vernacular hot-climate design (Fathy, 1986; Givoni, 1998) and confirmed in later comparative work on courtyard building form (Ratti, Raydan and Steemers, 2003). Taking the Palestinian house apart into courtyard, wall and window and assessing each in turn risks mistaking a component for the system it belongs to.

What follows instead asks two questions of each period: how did heat, air and light actually move through the house, and what social and economic pressures pushed the material and spatial choices that changed that movement? Both questions matter, because a decision made for social or economic reasons, enclosing the courtyard, switching to concrete, still has to be read for what it did to the building's physics.

2.4.2 The Ottoman-Period House: Courtyard, Mass and Opening as a Single Regulatory System

The Ottoman-era Palestinian house had to cope with high solar radiation, hot summers and a wide swing between day and night temperature, and it did so without mechanical assistance. It managed this because the courtyard, the stone envelope and the small courtyard-facing window did not operate independently. The courtyard governed shading and air movement, the wall stored and delayed heat, and the opening set the balance between light, air and solar gain. What matters is how tightly these pieces were coupled, not that each of them existed.

The courtyard does the organizing work in that loop. Accounts of courtyard houses often list its jobs separately: shading, ventilation, daylight, but in practice they are one mechanism. Shade over the walls and floor for part of the day sets up the stack effect: heated air rises and pulls in cooler air drawn from the shaded zones, which is also how the space feeds diffuse rather than direct daylight into the rooms around it (Almhafdy et al., 2013; Soflaei, Shokouhian and Mofidi Shemirani, 2016). Take the shading away and the air simply sits there, uncirculated. Keep the shading but block the airflow and the incoming air has already been heated by an exposed floor before it reaches the room. Modelling of courtyard geometry across different climates finds that height-to-width ratio, along with how much of the floor stays shaded through midday, governs this far more than courtyard size does (Muhaisen, 2006), which is one reason Palestinian hosh courtyards tend to be deep and narrow rather than wide and open: a taller, narrower proportion keeps more floor in shade relative to the sky-facing gap that lets heat escape at night. (figure 2-9)

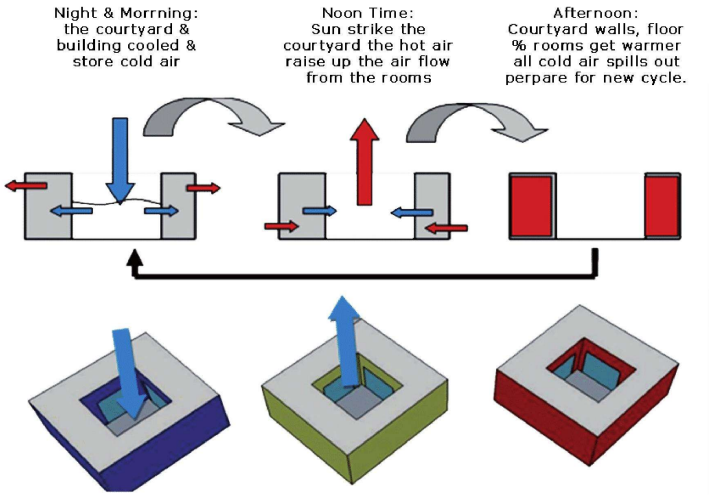


Figure 2-9: The diurnal working mechanism of a courtyard (Freewan, 2019)

At night, the same geometry works in reverse. The courtyard radiates stored heat upward into the sky, but only if its enclosing walls can retain heat long enough to release it slowly rather than all at once (Ratti, Raydan and Steemers, 2003). This is where courtyard and wall mass stop being separate topics. Ottoman-period stone walls, commonly well over half a meter thick, store enough heat and conduct it slowly enough that peak solar gain takes several hours to reach the inner face (Givoni, 1998; Fathy, 1986). So the hottest point indoors lags the hottest point outdoors: by the time stored heat reaches the inner wall, evening has already begun cooling the outside air, and where the courtyard allows night ventilation, that heat gets

flushed out rather than carried over into the next day. A thick wall on its own only stores heat. It takes an open, ventilated courtyard to get rid of it.

Window openings were the most constrained part of the system, because a single aperture had to do thermal, ventilation and privacy work at once rather than being optimized for any one of them. Windows stayed small and faced the courtyard rather than the street: this cut solar gain on habitable rooms, kept the household visually and acoustically private, and still let courtyard-cooled air enter at a height that reached the occupied part of the room rather than passing overhead (Al Tawayha, Bragança and Mateus, 2019). Because privacy and ventilation had to be satisfied by the same opening, glazing could not simply be enlarged to improve daylight without compromising privacy, which is why the window area remained modest relative to the wall area even where more light would have helped. Courtyard, wall and window were never really three separate strategies. They were three settings on the same dial, each one constrained by where the other two sat.

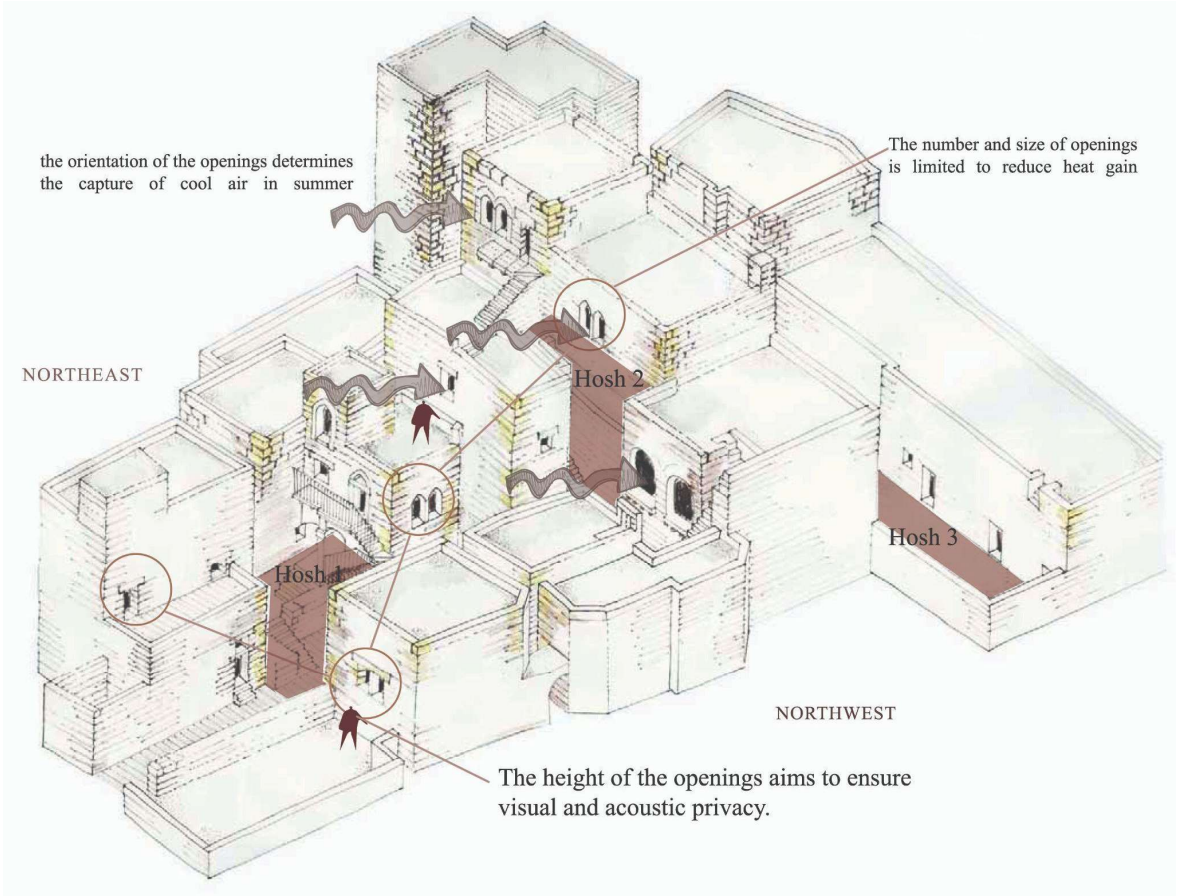


Figure 2-10: Schematic analysis of courtyard openings, Harizat house (RehabiMed, 2015)

Quantitative studies on stone used in Mediterranean vernacular architecture indicate that materials with high specific heat (≈0.84–0.92 kJ/kg·K) and moderate thermal conductivity (≈1.1–1.5 W/m·K) can reduce indoor temperature fluctuations by 2–5°C, depending on orientation, thickness, and solar exposure (Givoni, 1998; Ratti, Raydan and Steemers, 2003). The effectiveness of thermal mass is enhanced when integrated with courtyard ventilation. However, it may diminish under high humidity or insufficient night-time ventilation, highlighting the need to consider thermal mass as part of a holistic passive environmental system (Almhafdy et al., 2013).

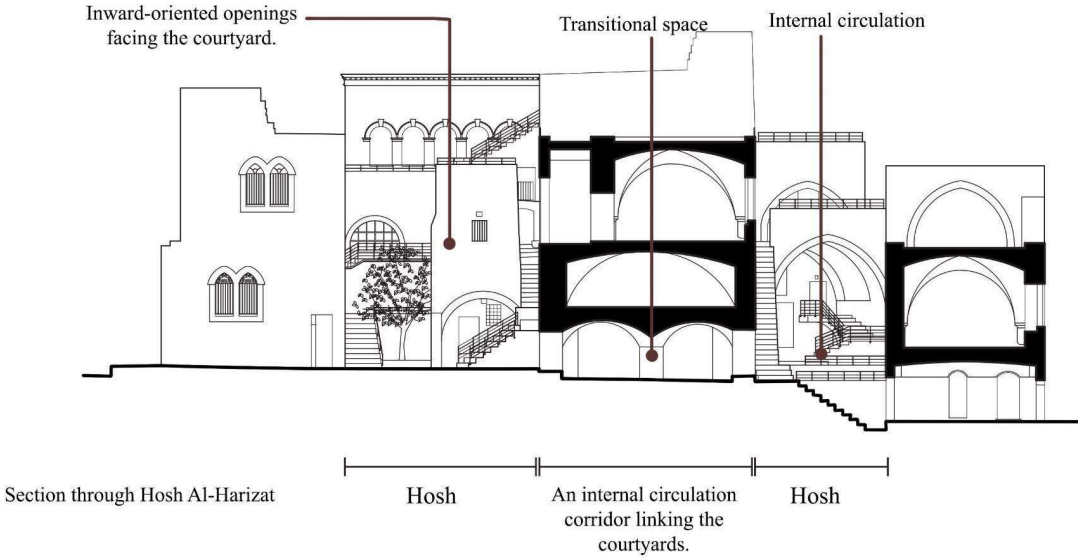


Figure 2-11: Schematic analysis for opening of Harizat house courtyard (RehabiMed, 2015)

2.4.3 The British and Jordanian Period: Environmental impact of Spatial Reconfiguration (1917 to 1967)

Nobody set out to redesign the Palestinian house's environmental performance in this period. British Mandate planning law carried over largely intact under Jordanian administration, and no comprehensive framework governed residential construction. What changed instead was construction material, urban land pressure, and the kind of space households wanted, and environmental performance shifted as a side effect (Al Tawayha, Bragança and Mateus, 2019). Stone had been the default structural material for Palestinian housing for centuries before this period, valued for its local availability and its suitability to the region's climate as much as for its structural role (Abuarkub and Al-Zwainy, n.d.), which is part of why the shift away from it marks a genuine break rather than a minor substitution. New building technology was central to that shift: The Mandate period brought the wide availability of reinforced concrete and metal beams, materials that freed house plans from the structural constraints of stone-arch construction and let the

central-hall, liwan-based house become the dominant urban form across Palestinian cities. Contemporary analysis of this house type treats its environmental logic as deliberate rather than incidental, arguing that the liwan was built into the plan specifically to help the house adapt to its surrounding climatic conditions, not simply to organize circulation between rooms (Abuarkub and Al-Zwainy, 2022). The question is what happened to courtyard, mass and opening, the settings that had been holding each other in balance, once the pressures that set them began to move.

- From open courtyard to liwan

The clearest structural change was the partial or full enclosure of the courtyard, which in many houses was replaced by the liwan, a covered, usually south-facing space inserted between the enclosed rooms and the exterior. This was not a break with the Ottoman house so much as an inheritance carried forward and reworked: documented village houses show the liwan already present as a covered space inside Ottoman-period stone construction, continuing into Mandate-period houses built with the new reinforced concrete roof, where it persisted as the household's main reception and living space even as the surrounding construction system changed (Kafr Malek village documentation, cited in Al Tawayha, Bragança and Mateus, 2019). Central-hall houses of this type were typically organized with rooms grouped on three sides of the liwan, so that the liwan mediated air and light exchange for the whole house rather than for a single room, a configuration read as evidence that environmental performance, not just circulation or status, shaped the room layout around it (Ragette, 1974, cited in Abuarkub and Al-Zwainy, 2022). Detailed field research on Jerusalem houses built in the decades leading up to 1967 shows that the liwan did not simply take over the courtyard's job. It did a related but seasonally reversed one. Deep enough to hold shade through summer, yet angled so that low winter sun could still reach in, it worked as a passive solar collector in winter rather than a cooling device in summer, and residents used it that way: as a second living room on sunny winter days (Saifi, 2023). What it could not replicate was the courtyard's role in driving stack-effect ventilation and night-sky radiative cooling, since a covered, partly enclosed liwan has no open sky-facing surface to radiate through. So the house kept a passive-solar strategy for winter and lost the summer night-cooling mechanism that had depended on an open courtyard working with high-mass walls. That is a substitution, not simply a loss, and reading it as decline misses how much environmental thinking survived the shift.

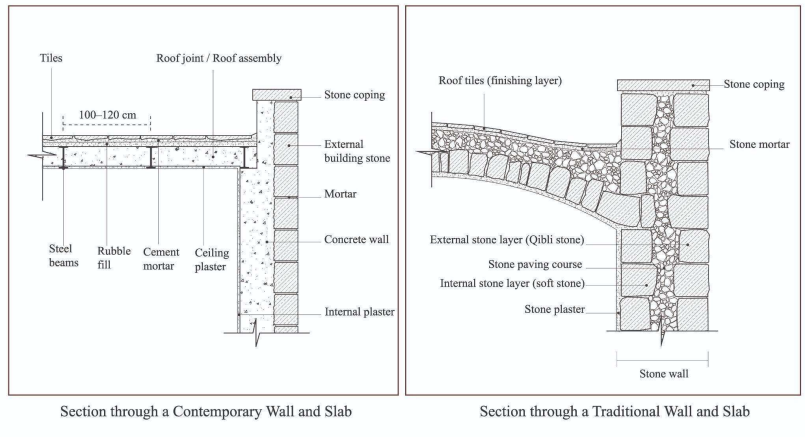


Figure 2-12: Comparative analysis of traditional and contemporary wall envelopes (RehabiMed, 2015)

- Construction material and the erosion of thermal mass

Alongside this spatial change came a shift in the construction system, from load-bearing stone to reinforced concrete framing with lighter infill. The Ottoman system depended on courtyard, mass and opening working together, so weakening the mass component had consequences beyond the wall itself. A concrete-framed envelope without comparable thickness or heat-storage capacity responds far more quickly to outdoor temperature swings, so even where a liwan still provided solar and shading control, the building's capacity to buffer daily temperature fluctuation was reduced (Givoni, 1998). Call this period transitional in a precise sense: it kept an adapted version of solar orientation and cross-ventilation through the liwan and paired window openings, but lost the high-mass buffering that had made the Ottoman house's whole envelope, not just its living rooms, thermally stable

- From controlled apertures to relative openness

Concrete and steel construction also allowed larger façade openings than load-bearing stone walls could easily carry, and window area grew accordingly. That improved daylighting and horizontal cross-ventilation, but it also let in more solar heat, on interior spaces that no longer had the mass to absorb the extra gain without a rise in indoor temperature. Clay roof tiles (Qarmid), set above openings or projecting from the façade, show up in houses of this period as a response to that added exposure. The practice was applied rather than codified, never standardized into a formal design rule, but it reflects an environmental sensibility carried over from earlier building tradition, one that used simple elements to moderate light and heat at exactly the point on the façade most exposed to the sun.

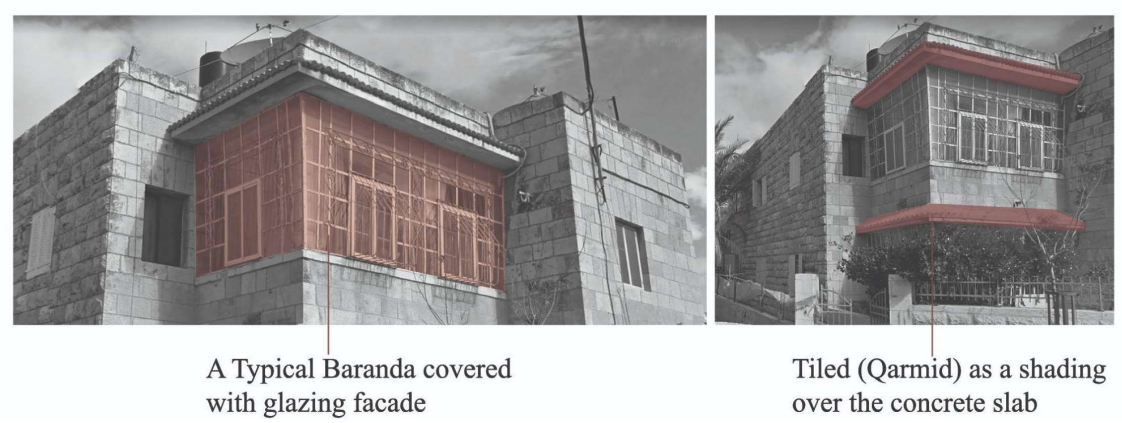


Figure 2-13: Façade analysis of a house of the Jordanian period (Samman & Saifi, 2019)

2.4.3 Late 20th Century

When examined against the dwelling's actual needs, the contemporary Palestinian house reveals a clear gap between what environmental performance requires and what its design delivers. Features nominally linked to environmental performance — larger windows and, increasingly, thermal insulation — have become common in practice, yet their use is seldom grounded in any integrated understanding of solar orientation, control of thermal gain, or daylighting requirements.

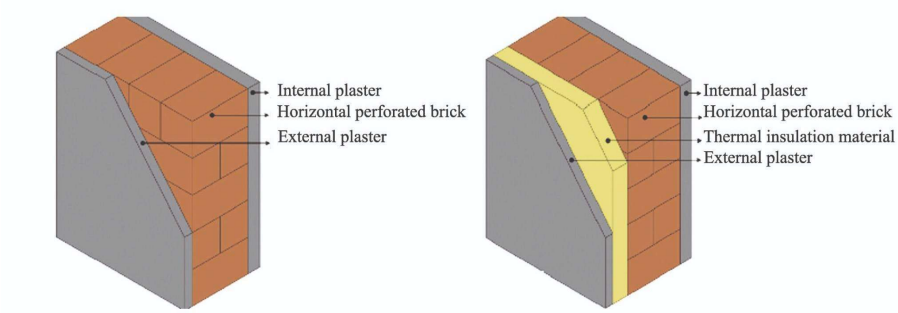


Figure 2-14: Schematic diagrams of a) the uninsulated wall and b) the insulated wall (Aktemur, Bilgin, and Tunçkol, 2021)

The scale of this gap has been measured directly for Palestinian housing stock. A DesignBuilder-based simulation study comparing the existing Palestinian building energy code, green building guidelines, ASHRAE envelope requirements and the Jordanian building energy code across representative two- and four-apartment typologies found that current common practice, building either without any energy code or under the existing Palestinian code, performs far below what internationally established codes would

achieve, and that applying adequate thermal insulation could reduce heating energy demand by between 43% and 83%, depending on building type, climatic zone and target U-value (Haj Hussein et al., 2022). A separate household-level survey in Hebron found that residents who heat any part of their home in winter consume, on average, approximately 27 kWh per square metre of heating energy annually, spend an estimated 3.5% to 21.6% of monthly income on winter heating, and heat, on a typical winter day, only around 9.2% of total dwelling floor area (Al Qadi, Sodagar and Elnokaly, 2018). Read together, these two studies show a building type in which most of the house is left thermally unaddressed rather than uniformly heated, inefficiently, a pattern with no equivalent in the whole-envelope buffering achieved passively by the Ottoman-period stone house.

The gap is not only a matter of envelope specification. Research into the relationship between vernacular and contemporary housing in Palestinian cities finds that new residential development is often produced with little reference to the environmental logic of the buildings it replaces, and that the courtyard concept, still recognized as an effective route to better indoor thermal quality, is rarely reintroduced when existing housing stock is retrofitted or redesigned, despite growing evidence for its relevance (Al Tawayha, Bragança and Mateus, 2019). Separate research into the social use of outdoor and semi-private space in contemporary Palestinian housing points to a behavioral side of the same mismatch: window operation and natural ventilation practices stay closely tied to inherited patterns of domestic use, so a dwelling's actual performance depends as much on whether its design fits how residents already live as on the specification of its parts in isolation (Haj Hussein, Barlet and Semidor, 2010). Put the performance modeling and the occupant-practice research side by side, and they point the same way: contemporary Palestinian housing has picked up the vocabulary of environmental design, larger windows, some insulation, without the integrated logic that let the traditional envelope perform as a system rather than a set of independent parts (Figure 2-15).



Figure 2-15: Contemporary apartment housing typology, illustrative of the vertical, repetitive residential model that has become dominant in Palestinian cities since (1967)

2.5. Summery

The transformation traced across this chapter is not one of steady, cumulative improvement. It is better described as a progressive uncoupling of the house from the integrated social and environmental system that once defined it. The Ottoman-period house achieved thermal comfort through the coordinated operation of courtyard, mass and opening, a system whose components could not be optimized in isolation because each depended on the others, and that same spatial order also structured the household's social life, its patterns of privacy, gathering and daily use. The Mandate and Jordanian period did not abandon this logic outright: the liwan preserved a related, seasonally adapted passive-solar function even as the courtyard's summer ventilation and night-cooling role was lost to enclosure and to the shift toward reinforced concrete. What the evidence does not support is a reading of this period as a simple decline; it is more accurately a substitution of one passive strategy for another, incomplete one, occurring without a framework capable of managing the trade-off deliberately.

It is in the contemporary period that the coupling breaks down most clearly, and this is also the period for which Palestinian-specific quantitative evidence is most extensive. Simulation-based code analysis shows that straightforward measures, principally insulation specified to an adequate U-value, could cut heating demand by close to half in typical cases (Haj Hussein et al., 2022), while household survey data shows that current practice leaves the majority of the dwelling unheated through winter rather than heated

inefficiently across its full area (Al Qadi, Sodagar and Elnokaly, 2018). Neither figure describes a technically difficult problem: both describe a building type that has adopted the isolated components once integrated in the historic house, larger windows, partial insulation, an enclosed volume, without recovering the systemic logic that made those components perform together. Research on the everyday use of contemporary Palestinian housing points to a parallel social uncoupling: as time spent outside the home increases and household structure changes, the living space has been redefined by design decisions that no longer track the social and environmental needs those spaces are meant to serve (Haj Hussein, Barlet and Semidor, 2010; Al Tawayha, Bragança and Mateus, 2019).

That matters for the framework this chapter is building toward. Closing the gap through isolated technical correction, adding insulation without reconsidering orientation, adding a window without reconsidering shading, is unlikely to work, because the Ottoman-period evidence shows exactly why isolated correction underperforms an integrated one. What the evidence points toward instead is a residential model that reconnects design decisions with environmental mechanism and lived social need at the same time: not applying passive strategy as a historical reference selectively borrowed from, but treating it as a coordinated system, courtyard or its contemporary equivalent working with mass and controlled opening, whose logic still holds under present climatic and material conditions. The remainder of this thesis develops a spatial performance framework for contemporary Palestinian housing on that basis.

Table 2-1: Summary of the transformation of Palestinian housing across periods

Period	**Social Organization**	**Spatial and Material Form**	**Environmental Consequence**
Traditional Palestinian house (pre-1917)	Extended family, collective and home-based daily life, strong social interaction	Courtyard house (hosh); inward-oriented, multifunctional rooms; spatial flexibility	Passive design as an integrated system: natural ventilation, thermal mass, climate-responsive envelope
Mandate and Jordanian period (1917 to 1967)	Displacement, spatial pressure, changing family structure, reduced social cohesion	Compact housing units; functional separation; loss of the courtyard; standardized layouts	Reduced environmental responsiveness; weaker thermal control; more limited natural ventilation
Contemporary Palestinian housing (post-1967)	Individualized lifestyle, more time spent outside the home, reduced use of living space	Apartment buildings; open-plan living; vertical, repetitive typologies	High energy dependency; inadequate insulation; poor daylight performance; user-dependent ventilation

Chapter 3
Research Methodology

3.1 Preface

This chapter outlines the methodological framework adopted in this study and clarifies the sequential research procedures implemented to ensure coherence between data collection, processing, and analysis. The methodology is structured as a multi-stage framework in which each phase builds systematically on the outcomes of the preceding stage. This structured approach enables controlled comparisons, integrated analysis, and consistent, evidence-based results. The chapter emphasizes the research design, case and study area selection strategies, data collection methods, data processing and analysis techniques, and the procedures for developing and refining the proposed design model.

3.2 Research Type

The study adopts a sequential, explanatory mixed-methods design in which qualitative historical-spatial analysis precedes and structures the quantitative measurement, survey, and simulation work. This sequencing reflects the argument advanced throughout the thesis that regulatory and spatial change precedes, and is causally prior to, the environmental and social outcomes observed in contemporary housing; the research design mirrors that causal order rather than treating history and simulation as parallel, unconnected tasks. This structure is consistent with methodological precedents in the environmental design literature that combine descriptive-analytical historical review with software-based simulation within a single qualitative-quantitative framework, and with studies of thermal comfort that proceed through discrete phases of fieldwork measurement, occupant survey, and simulation before comparing the three sources of evidence against one another.

Table 3-1: Research Methodology Structure: Phases, Inputs, and Outputs

Phase	Input	Output
1.Historical-environmental analysis	Chapter Two findings: hosh, liwan/iwan, courtyard typologies across the Ottoman, Jordanian, and contemporary periods	A defined set of passive design principles expressed as measurable spatial and geometric parameters
2. Field measurement and survey	Selected case houses in the study area; environmental monitoring equipment; questionnaire	Baseline indoor climate data and occupant perception data for each period
3. Simulation testing	Validated base models; three design scenarios derived from Phase 1	Quantified performance indicators referenced against ASHRAE 55, 90.1, and 62.1
4. Synthesis	Combined results of Phases 1 to 3	A conceptual design model reintroducing the historically-derived spatial principles into contemporary housing

3.3 Conceptual Framework: From Historical Analysis to Design Application

The methodology rests on a single directional sequence: historical spatial-environmental analysis leads to the extraction of passive design principles, which are then restated as testable design variables, verified through simulation, and finally folded back into a design model. Each step in this sequence is described below.

1. Historical spatial-environmental analysis (Chapter Two): documents how the hosh, the liwan, and the enclosed courtyard organized orientation, openings, and shading in Ottoman and Jordanian-period houses, and how the elimination of these elements after 1967 altered indoor thermal conditions.
2. Extraction of passive design principles: converts each documented feature into a parameter that can be varied in simulation, for example courtyard or liwan aspect ratio, opening proportion relative to wall area, and the presence of a shaded transitional zone between indoor and outdoor space.
3. Simulation-based verification: tests each variable against the validated base model using DesignBuilder/EnergyPlus, producing quantified outputs referenced against ASHRAE 90.1.
4. Design model refinement: synthesizes the verified interventions into a coherent design model that restores, in contemporary form, the spatial logic identified in the historical analysis.

This sequence also links to Lefebvre's theoretical framework: the historical analysis examines spatial practice and representational space as lived in the *hosh* and *liwan*, while the simulation-based strategies

operate on representations of space — the measurable, modellable geometric description of the house. The methodology treats the courtyard-liwan configuration's erosion as a shift in the dominant representation of space imposed by post-1967 planning regulation, and treats the proposed strategies as an attempt to reinsert the earlier periods' lived, climate-responsive logic into a representation of space that current regulation and construction practice can accommodate.

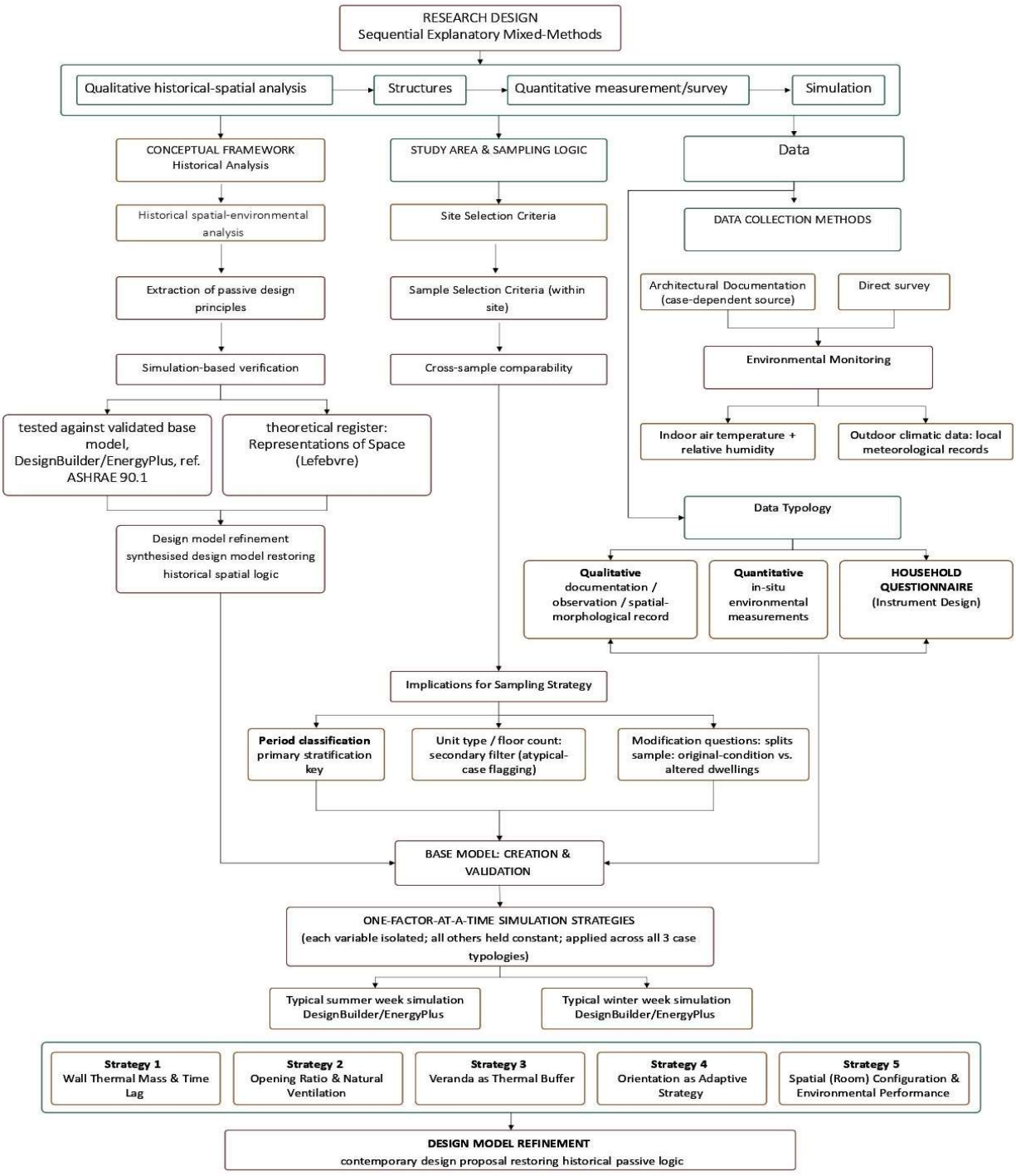


Figure 3-1: Schematic representation of the research methodology

3.4 Study Area Selection Criteria

The research aim, tracing how domestic spatial configuration has changed across three historical-legal periods and what that change has meant for thermal comfort and social interaction, sets the terms for both the site chosen and the individual houses studied within it.

A suitable site requires a traceable line of continuity between the periods under study, so that the argument connecting land tenure, planning regulation, and spatial form is visible in the built fabric rather than merely claimed in the text. Abu Dis and the surrounding Jerusalem periphery meet this because the area was never cleared and rebuilt as a single planned unit. Its housing accumulated gradually, through Ottoman-era construction, subsequent building under Jordanian administration, and the more recent wave of contemporary concrete housing, largely on the same or adjacent parcels of land. That continuity is the physical evidence the thesis's central claim depends on: that legal and administrative regimes shaped plot formation, plot formation shaped house typology, and house typology shaped how people live and how their homes perform thermally.

Climate is the second reason for choosing this site, and it is just as important. If the three case buildings came from separate locations, any difference in thermal comfort between them could be put down to altitude, exposure, or regional microclimate rather than to the buildings' form. Keeping the study within one settlement means all three houses experience roughly the same sun path, wind exposure, and seasonal temperature range, so any differences that show up in the simulation can be attributed to spatial typology rather than to where each house happens to sit on the map.

3.5 Sample Selection Criteria

Choosing a suitable site does not, by itself, produce a usable sample. Within a site that meets these conditions, the choice of which houses to study still has to be argued, along five lines that work together.

1. The first is typological clarity, weighed against typological memory. Each house had to show the spatial organization that defines its period clearly enough to read as representative: the yard and load bearing wall of the Ottoman house, the liwan arrangement, the more compartmentalized roomed layout of Jordanian-era construction, the largely courtyard-less, vertically stacked contemporary dwelling. But a house with no trace of the period before or after it was less useful than one carrying some visible layering, a later addition, an altered opening, a partially infilled veranda, because those traces are themselves

evidence of the transformation this thesis is trying to describe. The goal was never typological purity. It was legible.

2. The second is environmental exposure. Orientation, shading from neighboring structures, and the potential for natural ventilation needed to be broadly comparable across the three houses. A house sitting in a deeply shaded lane next to one standing fully exposed would make it impossible to tell whether any thermal difference came from built form or from accidental siting. Perfect matching on this front is unrealistic in a historic urban fabric, and where it could not be achieved.

3. The third is data richness: whether a house could actually be turned into a reliable simulation model and support a meaningful occupant survey. Wall construction, window dimensions, and overall geometry all had to be verifiable, either through direct measurement or through documentation that could be trusted, because the whole thermal analysis rests on an accurate baseline model.

4. The fourth is comparability across the sample as a whole. The three houses needed to be broadly similar in scale and, so a difference in simulated comfort could not simply be explained by one house being much larger or more densely occupied than another.

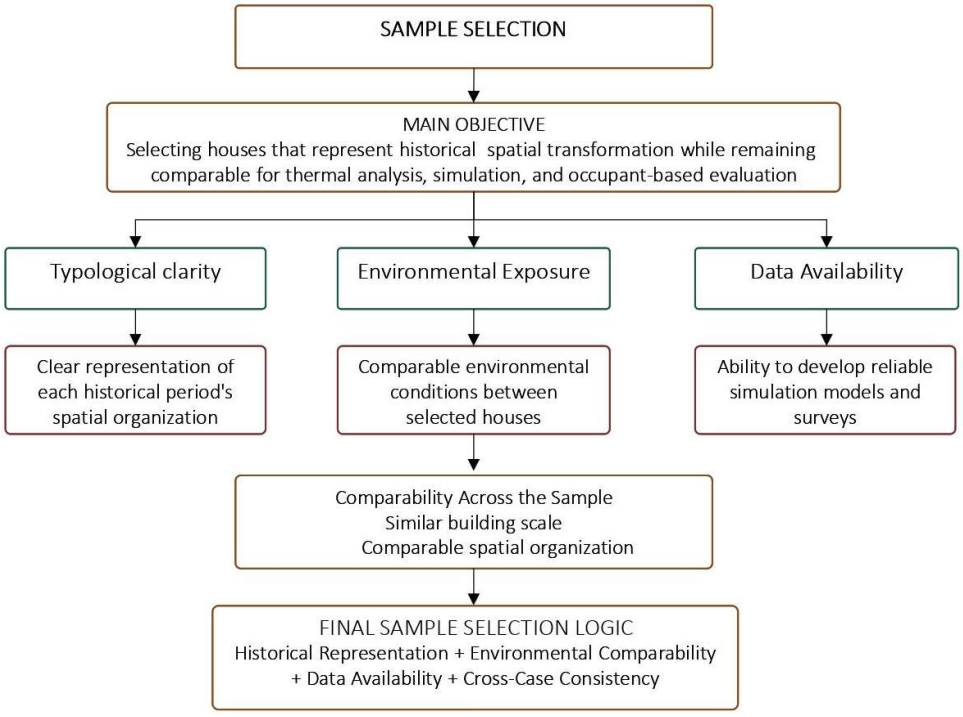


Figure 3-2: Site Selection Criteria

3.6 Data Collection Methods

Data for this study were collected from two different kinds of sources, depending on the historical case in question. For the Ottoman house, the architectural documentation was not produced directly by the researcher. It relies on an existing 3D laser-scanner survey conducted earlier by a group of students working under the (Taawon) Foundation. That survey produced detailed spatial and geometric data of the building, and this dataset forms the basis for understanding the Ottoman house's layout and for building its simulation model. Relying on an existing high-resolution survey rather than repeating fieldwork made sense in this case, since the building's condition and access made a fresh researcher-led survey impractical, and the scanned data already provided the level of geometric detail the simulation work required.

The Jordanian and contemporary cases, by contrast, were documented directly by the researcher. Each involved an on-site survey with hand and tape measurements taken to check and correct discrepancies against any available drawings, followed by the preparation of new architectural drawings where existing records were incomplete or outdated. Photographic documentation was collected throughout each site visit, covering both the overall building and specific construction and spatial details relevant to the study. Alongside the measured survey, the researcher also recorded the spatial narrative of each house, meaning how rooms are used, how the layout has changed over time, and how the building relates to its immediate social and historical setting, since this contextual understanding is part of what distinguishes the three typologies and cannot be captured through measurement alone.

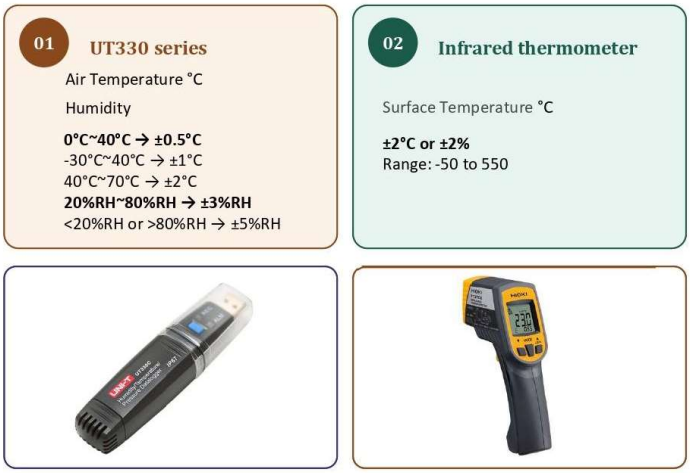


Figure 3-3: Instruments for measuring Environmental parameters

Alongside this architectural documentation, quantitative environmental data were collected across the residential cases to support the thermal and comfort analysis at the center of the study. Indoor air temperature and relative humidity were logged at set intervals using environmental data loggers placed in the selected habitable rooms for monitoring. Outdoor climatic data needed to define the boundary conditions for the simulation models were obtained from established local meteorological records rather than measured on site. Building physical parameters required for the DesignBuilder/EnergyPlus models, including geometry, orientation, envelope construction, and opening dimensions, were drawn from the architectural documentation described above: the laser scan survey for the Ottoman house, and the researcher's own measured drawings for the Jordanian and contemporary cases. Keeping these sources distinct matters here, since the Ottoman dataset was produced by a different team using different equipment, and treating all three cases as though they had been surveyed in the same way would misrepresent how the underlying data were actually obtained.

3.7 Research Type

This study draws on three types of data. Quantitative data consist of in-situ environmental measurements, namely indoor air temperature and relative humidity, recorded within the selected residential spaces. Qualitative data include architectural documentation, observations of how spaces are used, and recorded spatial and morphological characteristics of each case, drawn from the 3D laser scan survey of the Ottoman house and the researcher's own site surveys of the Jordanian and contemporary cases. Secondary data, mainly climatic records and other contextual information, were also drawn on to support the wider research framework.

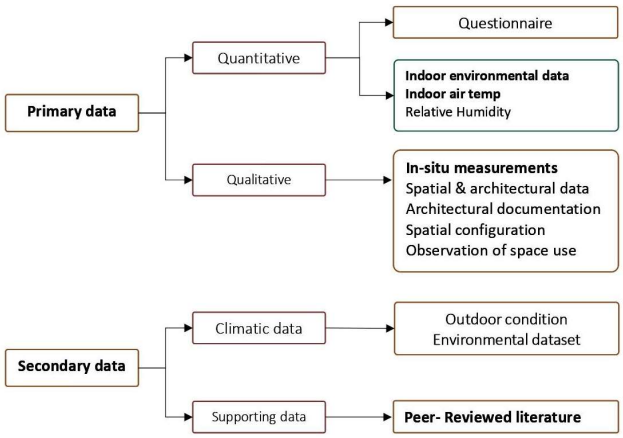


Figure 3-4: Type of Data

3.8 Study Area (Abu Dis)

Abu Dis, situated on the eastern urban belt of Jerusalem within the Csa (Köppen–Geiger) climate zone, is characterized by long, hot, dry summers and mild, wet winters, with its stepped topography producing varied microclimatic conditions across the town. Its urban fabric compounds these climatic pressures: rapid, largely unplanned growth since the 1990s has produced a heterogeneous mix of compact traditional dwellings and modern construction, expanding under geopolitical and regulatory constraints that leave little room for the passive design responses the older fabric once relied on.

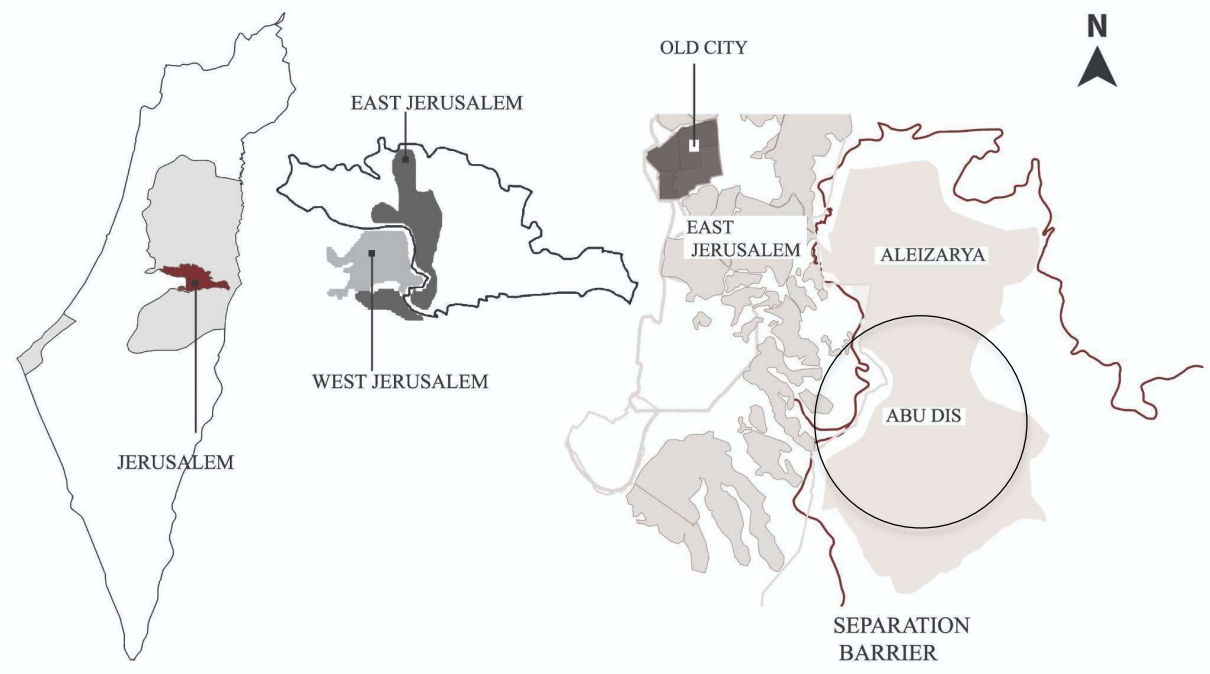


Figure 3-5: Site location map

3.9 Instrument Design and Analytical Structure of the Household Questionnaire

The 45-item household questionnaire is structured around four analytical domains — household and spatial configuration, lived experience and spatial practice, environmental affordances, and perceived environmental performance — moving progressively from the dwelling as a classifiable object to the occupant's adapted, lived response to it. This structure operationalizes Lefebvre's spatial triad alongside affordance and adaptive comfort theory, ensuring each question is anchored in an explicit theoretical rationale rather than treated as a free-standing survey item.

3.9.1 Theoretical operationalization of the four domains

Section 1, Household and Spatial Configuration, gathers every question that describes the dwelling as a designed, classifiable object: who occupies it, what type of unit it is, which historical period it belongs to, how its living space is laid out, whether a shaded transitional threshold precedes that living space, and whether the unit has since been extended or internally reconfigured. In Lefebvre's terms, this section corresponds to representations of space: the dwelling as it would be read off a plan, independent of how anyone actually lives in it. Placing the period-classification question and the transitional-space question inside this section, rather than treating one as background and the other as an environmental feature, follows directly from the thesis's argument that the presence of a forecourt-type threshold is a classificatory, typological fact about a dwelling, on the same footing as its layout or unit type, and not a downstream environmental outcome to be inferred later from other variables.

Section 2, Lived Experience and Spatial Practice, gathers questions describing how the dwelling is actually inhabited: how often and where daily life is concentrated, how private the space feels, why any modifications were undertaken, and how the occupant's own use of the space has changed since moving in. This section operationalizes Lefebvre's spatial practice and representational space, the gap between the plan and the life lived inside it. The modification-purpose question opens this section immediately after modification-type closes Section 1, marking the shift from asking what changed to asking why, which is the same shift from conceived to lived space that the section as a whole is built to capture.

Section 3, Environmental Affordances, gathers the architectural features that make particular environmental behaviors possible without yet describing whether those behaviors succeed: orientation, opening distribution, and shading device type. This follows Gibson's affordance theory and Barker's behavior-setting theory, in which a feature of the environment structures a range of possible action, a window affords ventilation, whether that ventilation is actually adequate is a separate matter, addressed in the next section.

Section 4, Perceived Environmental Performance, gathers the outcome variables: ventilation, daylight, and summer and winter thermal sensation. This section operationalizes adaptive thermal comfort theory, in which comfort is read as an occupant's adapted response to their environment and history of exposure rather than a fixed physiological threshold. Together, the four sections move from the dwelling as designed, through the dwelling as inhabited, to the building as an environmental system, and finally to that system's perceived outcome.

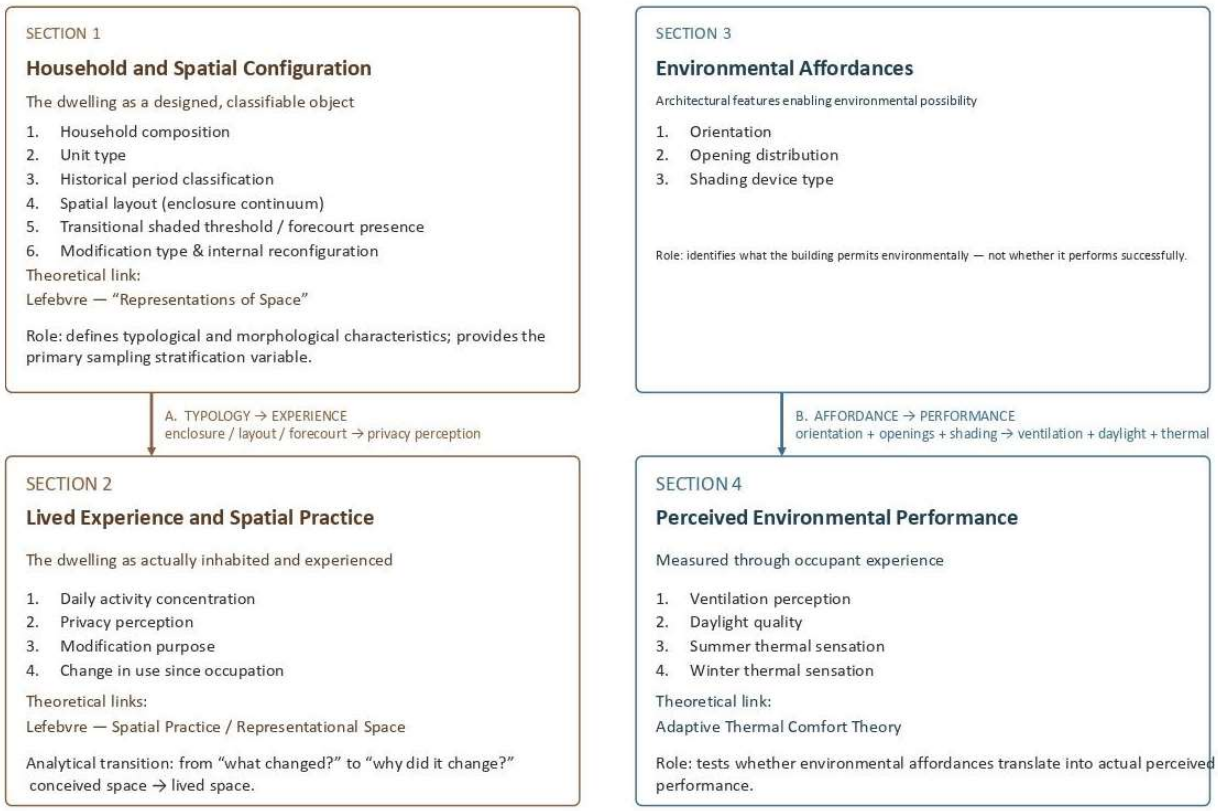


Figure 3-6: Conceptual Framework of the constructed Questionnaire

3.9.2 Implications for sampling strategy

Several questions in Section 1 function less as descriptive items than as filtering and stratification variables. Period classification is the primary stratification key, defining the three comparative groups around which the whole analysis is organized. Unit type and floor count provide a secondary filter for identifying structurally atypical cases, a high-rise apartment classified under an historical period it does not architecturally represent would need to be flagged rather than folded uncritically into that period's comparison. The modification questions in allow the sample to be split, after collection, into dwellings that remain close to their original condition and dwellings that have since diverged from it, which materially affects how confidently any single response can be read as evidence about the original typology. Read together, these variables mean that sampling adequacy is not simply a matter of collecting enough responses per period; it is a matter of collecting enough structurally representative, minimally altered responses per period, something the restructured instrument now allows to be checked directly rather than assumed.

3.10 Creating and Validating Base Model

The three DesignBuilder models — Ottoman, Jordanian, and contemporary — were checked against field measurements from two campaigns: 48 continuous hours in winter and seven continuous days in summer. For each model and period, the DesignBuilder run period was set to the exact calendar dates of the matching campaign, using an actual weather file rather than a typical one from the Meteoblue website (Meteoblue is a weather service that provides detailed climate data, forecasts, and environmental analysis based on meteorological models and observations.), so that the simulated hours aligned with the hours actually measured on site. The comparison covered the two variables recorded in the field, indoor air temperature and relative humidity, pulled from the simulation output at an hourly step to match the logger interval. That gives, for each model and season, a measured series and a simulated series side by side, one pair for temperature and one for humidity, so each hour can be checked against its counterpart.

Accuracy was assessed using statistical error indicators applied to these paired series, since only microclimatic variables were available, not energy data. RMSE and its normalized form, CVRMSE, measured how far the simulated values deviated from the measured values; NMBE captured any systematic bias; the Pearson correlation coefficient assessed whether the simulated curve followed the same daily rise and fall as the measured one. Winter and summer were kept separate rather than averaged into a single score, since the two periods differ in thermal behavior, ventilation, and exposure duration. A model counted as validated only once both seasons met the accepted error thresholds. Where a result fell outside those thresholds, parameters such as infiltration rate, envelope properties, and occupancy schedules were adjusted within plausible ranges and the simulation rerun until the agreement improved.

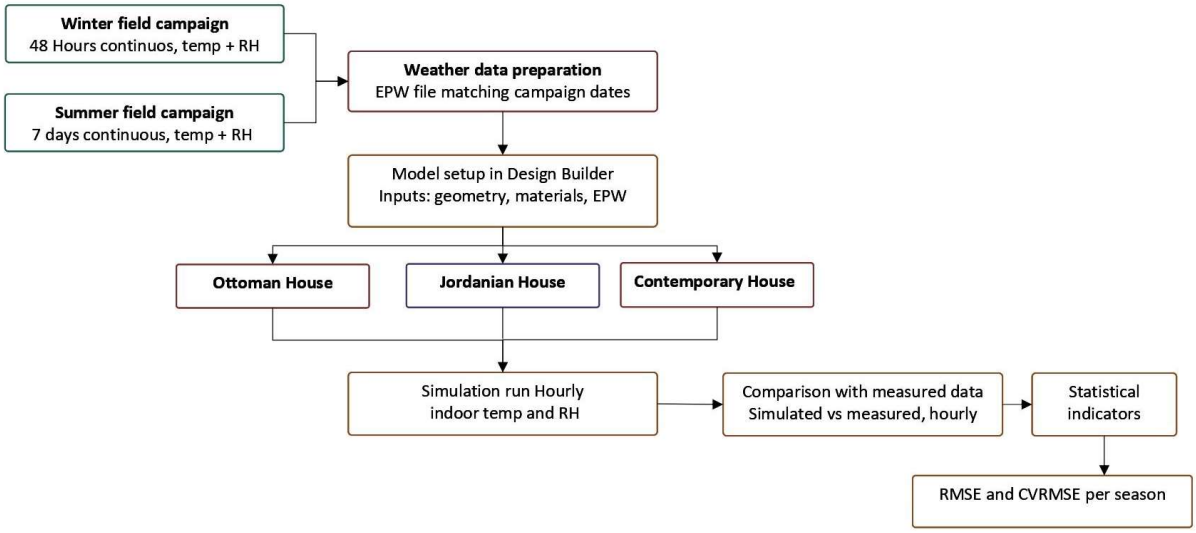


Figure 3-7: creating & validating for the base model

3.10.1 Strategy 1: Wall Thermal Mass and Time Lag

The three periods show a steady drop in wall mass. The Ottoman wall is a thick, single-leaf stone assembly. The Jordanian wall thins that down to a composite of stone and early concrete block. The contemporary wall goes further still, built from lightweight reinforced concrete or hollow block at a fraction of the mass of either predecessor. This is not simply a descriptive trend carried over from the preceding analysis. It is treated here as the main driver behind the differences in indoor thermal stability across the three periods, and it converts into a variable that can actually be tested: time lag, the delay between the peak outdoor temperature and the corresponding peak on the internal wall surface. Time lag rises with wall thickness and with the density and position of thermal mass within the wall section (Asan and Sancaktar, 1998; Asan, 2006).

Time lag and its companion metric, the decrement factor, are not abstractions. Both are standard outputs of one-dimensional transient heat conduction analysis, and EnergyPlus reproduces them directly through hourly wall surface and zone temperature reporting. Field and numerical work on masonry walls shows that thickness alone does not set the resulting time lag; material layering matters just as much, since the sequence of dense and lightweight layers within a wall section change where heat is stored and how quickly it reaches the interior (Quagraine et al., 2020). That gives the strategy four separately adjustable parameters rather than one: overall thickness, material density, layer sequence and Decrement factor.

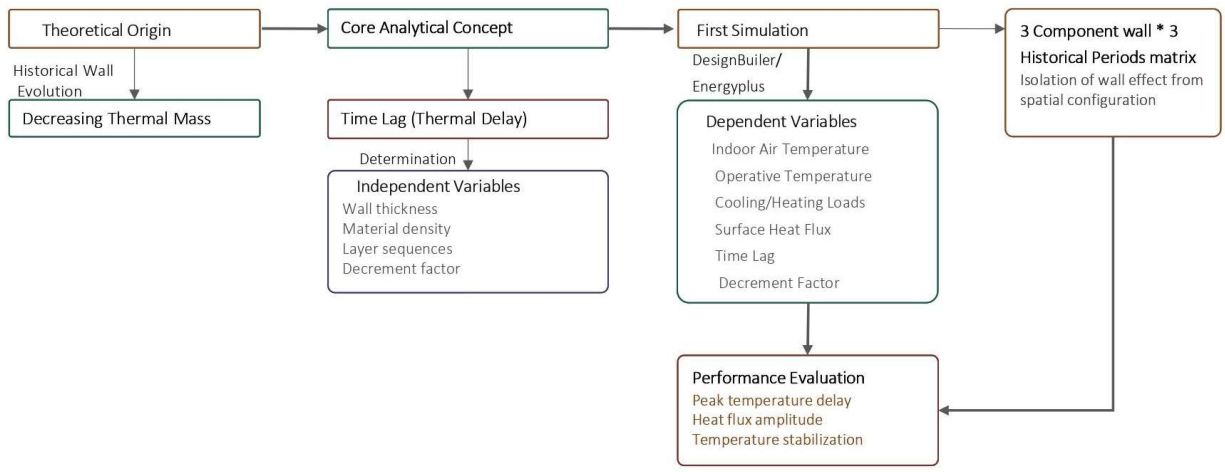


Figure 3-8: Wall Thermal mass & Time Lag strategy

The independent variable is wall construction, defined jointly by thickness, material density, and layer sequence. Three discrete configurations are entered into DesignBuilder, each matching the as-built envelope of one case: a thick single-leaf stone wall for the Ottoman case, a stone-and-block composite for the Jordanian case, and a thin reinforced concrete or hollow-block wall for the contemporary case.

Simulations run over two representative periods: a typical summer week, selected to capture peak cooling demand and maximum outdoor-to-indoor temperature swing, and a typical winter week, selected to capture peak heating demand under the opposite thermal direction. Running both seasons separately makes it possible to check whether a given wall's time lag behaves consistently in both directions of heat flow, rather than only under one set of boundary conditions.

Each of the three case models first runs with its own as-built wall, forming the base case. Every wall configuration is then cross-applied to the other two cases, with geometry, openings, and orientation held constant, so the wall used in the Ottoman case is also tested in the Jordanian and contemporary geometries and vice versa. This 3-by-3 cross-matrix separates the effect of wall composition from the effect of spatial configuration, something a same-case before-and-after comparison cannot do on its own.

Table 3-2: Wall Construction Characteristics and Time-Lag Behavior by Case Study

Case	As-built wall configuration	Expected time-lag behavior
Ottoman	Thick single-leaf stone, high density, no insulation layer	Long time lag, low decrement factor, slow indoor stabilization
Jordanian	Stone-and-block composite, moderate thickness	Intermediate time lag and decrement factor
Contemporary	Thin reinforced concrete or hollow block, low density	Short time lag, high decrement factor, rapid indoor response to outdoor swings

Time lag is judged on three fronts: peak temperature delay, the number of hours between the outdoor peak and the corresponding indoor surface peak; heat flux behavior, read through the amplitude and phase of the hourly heat flux through the wall section; and indoor temperature stabilization, the time the indoor operative temperature takes to settle within a defined band after a step change in outdoor conditions.

3.10.2 Strategy 2: Opening Ratio and Natural Ventilation

Wall mass is not the only thing that moves across the three periods. Opening ratio moves with it, and in the opposite direction: the small, deep-set openings of the Ottoman forecourt-facing rooms give way to the wider liwan openings of the Jordanian house, which in turn give way to the largely unregulated glazing ratios of the contemporary house. This strategy treats the opening ratio as a second, independent environmental variable. It is tested apart from wall mass so that its effect is not tangled up with the results from Strategy 1.

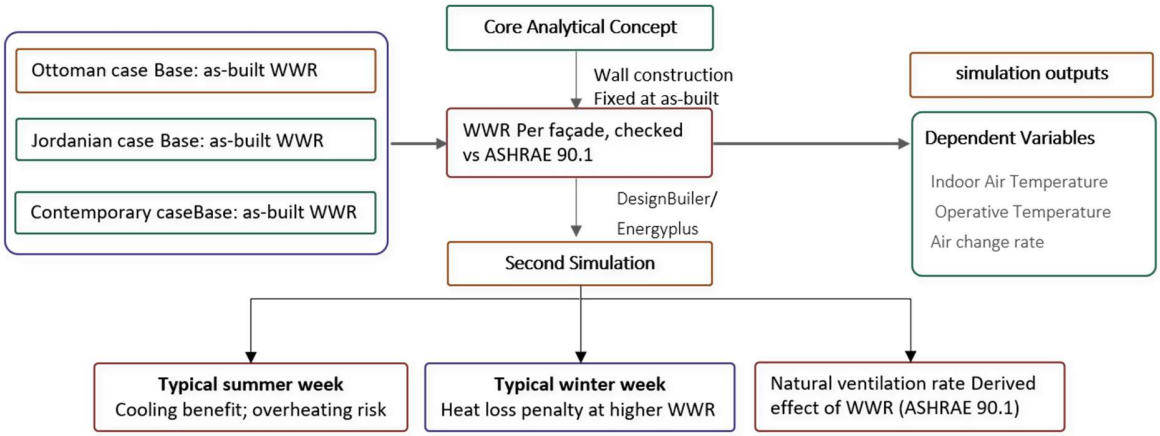


Figure 3-9: Opening Ratio & Natural Ventilation strategy

The independent variable is window-to-wall ratio (WWR) per façade, checked against the fenestration provisions of ASHRAE 90.1, together with the natural ventilation rate it produces, checked against ASHRAE 90.1.

As with Strategy 1, simulations are run over two representative periods rather than a full year: a typical summer week to capture natural ventilation's cooling contribution and the risk of overheating from larger openings, and a typical winter week to capture the heat-loss penalty associated with a higher WWR. Reading both seasons side by side shows whether a given opening ratio helps in one season but works against the building in the other.

The dependent variables are indoor air temperature, operative temperature, cooling and heating loads, and air change rate.

Each case's as-built WWR is recorded first, as its base case. A common set of WWR increments is then applied across all three case geometries, with wall construction held at each case's own as-built condition throughout. That keeps the effect of the opening ratio readable on its own, separate from the wall mass effect established in Strategy 1, so the two can be compared directly rather than assumed to scale in step.

3.10.3 Scenario 3: From Veranda Concept to Simulation Logic

The Jordanian house's front veranda is a better entry point into this variable than anything the Ottoman forecourt offers, for one simple reason: it puts a roofed element directly in front of the main façade, between the sun and the wall, rather than just opening onto the outside. That position is what makes it worth analyzing. A veranda roof intercepts direct solar radiation before it reaches the façade surface, so the wall absorbs less incident radiation and transfers less heat inward through conduction and re-radiation. Shading here isn't a passive side effect of the veranda's shape. It's the first step in a chain: less direct exposure lowers the façade's surface temperature, which reduces the driving force for heat gain into the room behind it, resulting in a measurable drop in cooling load and a steadier indoor operative temperature. But the veranda does more than block the sun. Because it's semi-enclosed rather than sealed, air moves through it, and that air isn't the same air arriving straight from an exposed exterior. It has already been shaded and cooled by the time it reaches the doorway or window behind it. The veranda pre-conditions incoming air before it enters the conditioned space, so whatever ventilation the interior gets starts from a lower baseline temperature than it would if the façade opened directly onto the outside, the way the

contemporary house does. Solar interception and air pre-conditioning together turn the veranda from a covered porch into a genuine thermal buffer zone: it doesn't just shade the wall; it actively moderates the thermal and airflow conditions of everything passing through it into the interior. This is the mechanism the strategy is built to test, isolating shading conditions as an independent variable so its contribution to solar heat gain, operative temperature, and cooling load can be measured separately from the wall mass and opening ratio effects already established.

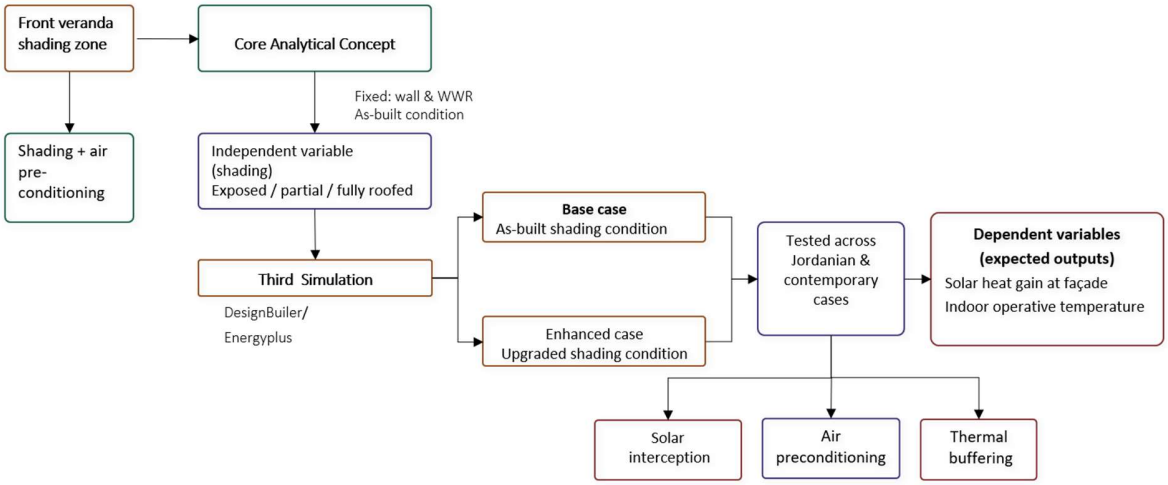


Figure 3-10: Impact of an External Transitional Space (Veranda) Connected to the Living Area

The outcomes of this phase provide an evaluation of the effectiveness of transitional spaces as climate-responsive design interventions in Mediterranean hot-summer residential environments.



Figure 3-11: the environmental mechanism chain in strategy 3

The veranda concept shows shading condition as the tested variable (base vs. enhanced) held against wall construction and WWR as fixed constants, traces the environmental mechanism chain (figure x) and closes on the three dependent-variable outputs the simulation is actually built to measure.

3.10.4 Scenario 4: Orientation as an Adaptive Environmental Strategy

Orientation is the one variable in this simulation framework that cannot be treated as a purely geometric decision, because in the Palestinian courtyard house it never was one. Hosh typology positioned its courtyard, its mass, and its façades in direct response to the sun's path and to the prevailing wind, and that response produced a building that shaded itself for a large part of the day without any mechanical intervention. A courtyard oriented to keep its enclosing walls in shadow through the peak summer hours, while still admitting low winter sun into the rooms that needed it, was not an incidental outcome of site constraints. It was the building doing thermal work through its geometry alone, long before the vocabulary of solar geometry or shading coefficients existed to describe it. Reading that logic back into a contemporary simulation framework means asking the same question the original builders were answering, just with instruments they didn't have: which orientation keeps a given façade out of direct radiation for the longest useful stretch of the day, and at what cost or benefit across the seasons.

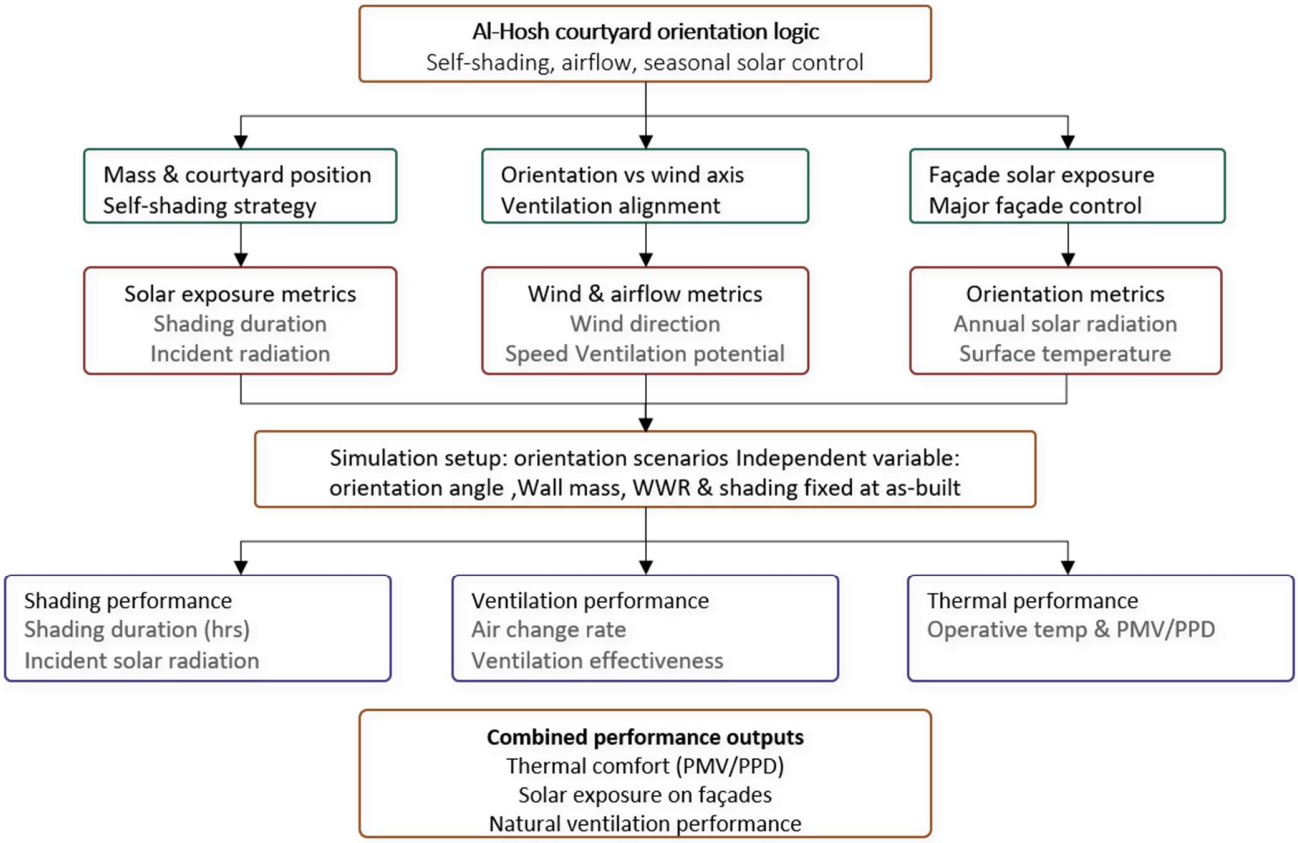


Figure 3-12: Orientation as an Adaptive Environmental Strategy

Translating this into a simulation strategy means converting each of those historical relationships into a parameter that can be varied and measured. The independent variable is building orientation, expressed as a set of rotation angles applied to a fixed building form, so that the same mass, the same courtyard relationship, and the same façade openings are tested under different exposures to the solar path and to the dominant wind direction rather than being redesigned for each case. Solar path and prevailing wind direction function as the external inputs against which each orientation is evaluated, while building mass configuration and courtyard position are held constant across the scenario set, in the same way that wall construction, window-to-wall ratio, and shading condition were held constant in the strategies that preceded this one. This keeps the analysis isolated: whatever difference in performance appears between orientation scenarios can be attributed to the rotation itself, not to some unrelated change in the building's form.

3.10.5 Strategy 5: Spatial Configuration and Environmental Performance

Strategy 5 tests a variable that earlier strategies hold fixed: the proportion of the habitable room itself. Roofing methods, structural spans, and plot economics pushed Ottoman, Jordanian, and contemporary rooms toward different length-to-width ratios, from the near-square plans that vaulted masonry favored to the elongated, single-aspect rooms that concrete slabs and corridor-access apartments made practical. This strategy sets that ratio aside from its historical origin and treats it as an independent variable in its own right, tested at fixed values from near-square to strongly elongated while the room's floor area, envelope construction, and window-to-wall ratio remain unchanged.

A second variable, degree of enclosure, is tested alongside it. A room with one external wall loses and gains heat through a smaller share of its perimeter than a room with two adjacent external walls of the same floor area, and this affects both winter heat retention and summer heat gain independently of how the room is proportioned. Ratio and enclosure are therefore varied one at a time rather than together, so that a change in indoor operative temperature or air velocity at the rear of the room can be attributed to one factor and not the other.

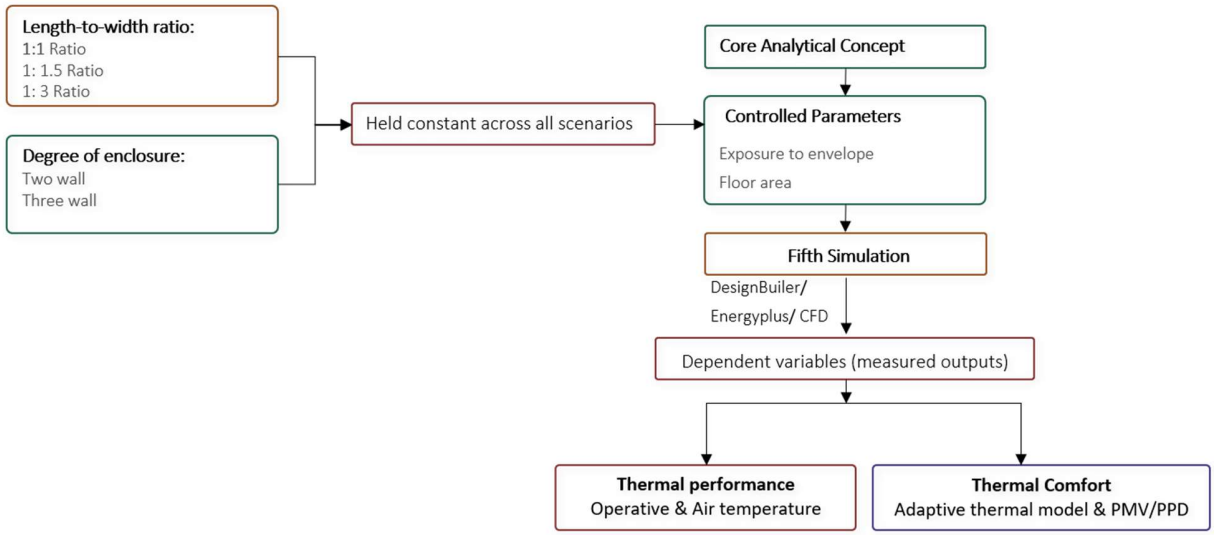


Figure 3-13: Spatial Configuration and Environmental Performance

The underlying logic is a near-square room places most of its floor area within the reach of a single opening, so that whatever ventilation or daylight enters through that opening extends across almost the entire space. In contrast, a deep and narrow room concentrates this effect at the front, leaving the rear comparatively less affected. Three scenarios were simulated using DesignBuilder/EnergyPlus, isolating this effect by keeping the floor area constant while varying only the room proportion. The result is a measure of the extent to which room geometry itself—independent of the period that produced it—governs the temperature gradient and the decay of ventilation between the front and rear of the space.

Chapter 4
Case Study

4.1 Preface (Study Area Overview: Abu Dis)

Abu Dis is a town in the eastern urban belt of Jerusalem, West Bank, situated at 31.76215° N, 35.26166° E, with an elevation of 600–700 m above sea level and a total area of approximately 27 km². Its urban expansion remains constrained by geopolitical and regulatory factors. Since the 1990s the town has undergone rapid demographic and urban growth, driven largely by its proximity to Jerusalem and the presence of major institutions such as Al-Quds University. The result is a heterogeneous urban fabric in which traditional and modern residential typologies coexist (ARIJ, 2012; PCBS, 2018).

Climatically, Abu Dis falls under the Csa category in the Köppen–Geiger classification, with long, hot, dry summers and mild to cool, wet winters. The town's stepped topography and street layout give rise to varied microclimatic conditions, shaping solar exposure, natural ventilation, and the thermal performance of living spaces. These conditions make Abu Dis a suitable case for examining how urban morphology relates to residential environmental performance (Juaidi et al., 2016; ARIJ, 2012).

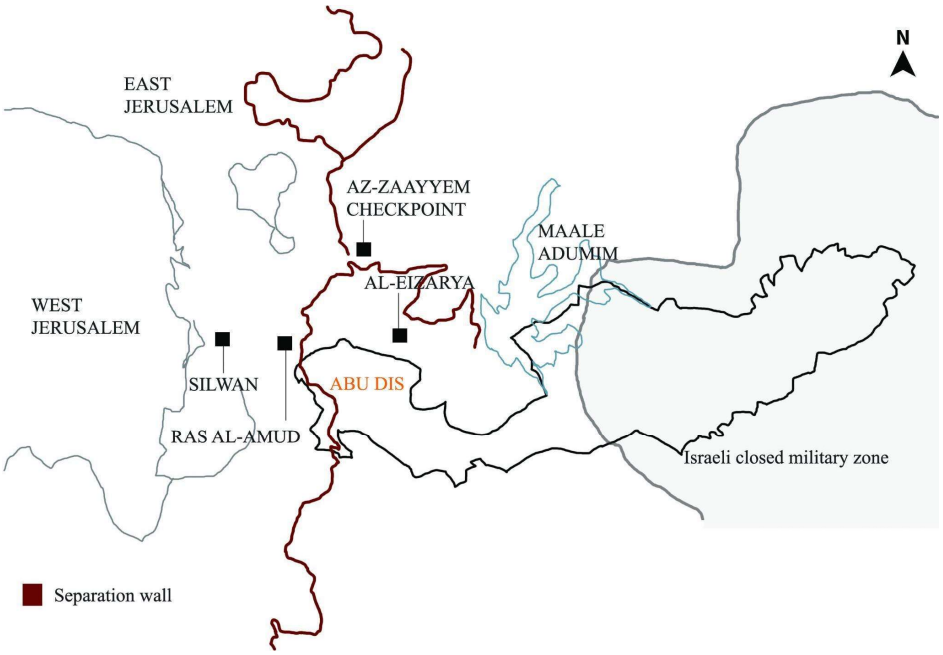


Figure 4-1: Abu Dis District map

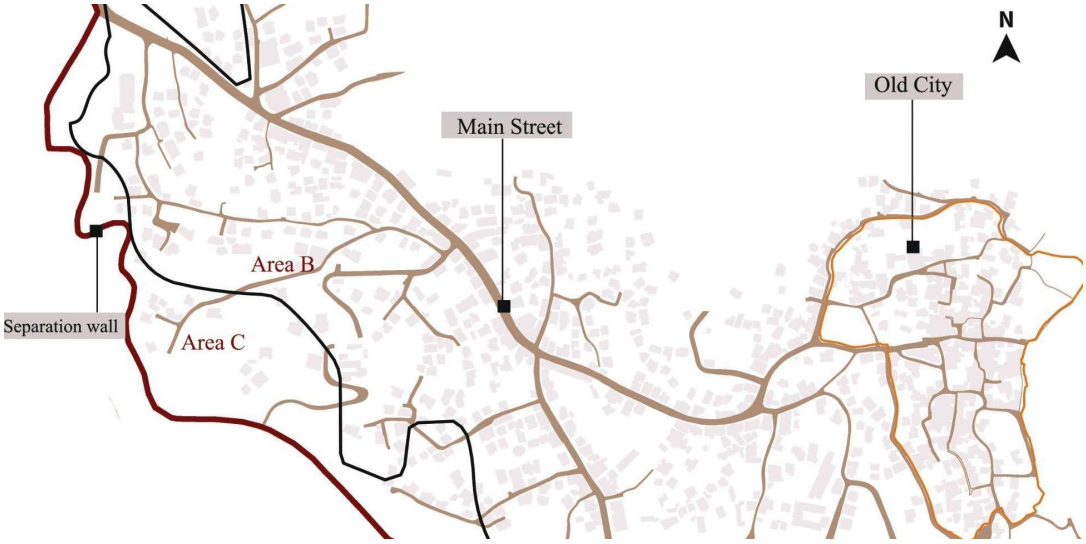


Figure 4-2: Street Selection map

4.2 Urban Morphological Analysis and Field Survey

The urban fabric of Abu Dis consists of two distinct morphological layers, each corresponding to a different stage in the town's development. The older layer developed as a compact, organic settlement: stone buildings sit close together and narrow streets wind through the town in response to its topography and social organization rather than any formal plan. Plots are small and irregular, and buildings are generally low-rise, one to two-story, with little intermediate space between them. What open space does exist is largely a by-product of how buildings happen to align, not the outcome of planned public space, and the overall pattern points to gradual, household-by-household expansion rather than centralized design.

A 1997 field survey by Riwaq documented 554 historic residential buildings in Abu Dis, most concentrated within the town core, which confirms the compactness of its urban structure and the limited extent of outward dispersion. Single-story dwellings predominated, particularly those with domed roofs, a hallmark of traditional Palestinian residential architecture. Most buildings were found to be structurally sound and still in use, suggesting continuity of habitation within the historic fabric. The variation in roof and ceiling types across the sample points to a diversity of construction techniques and local material adaptation, and lends the old town's urban form a certain architectural coherence.

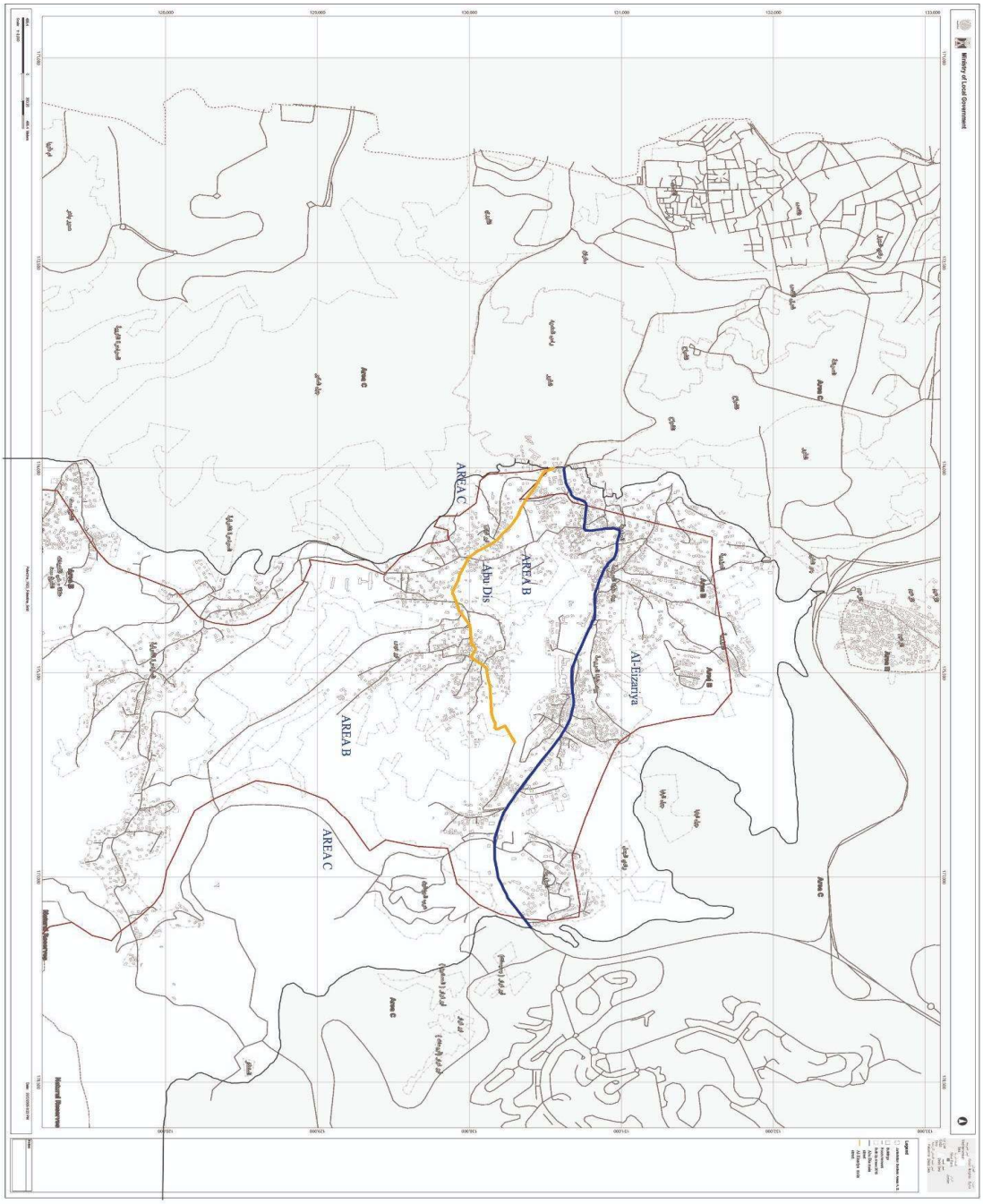


Figure 4-3: Master Map of Abu Dis with the surrounding

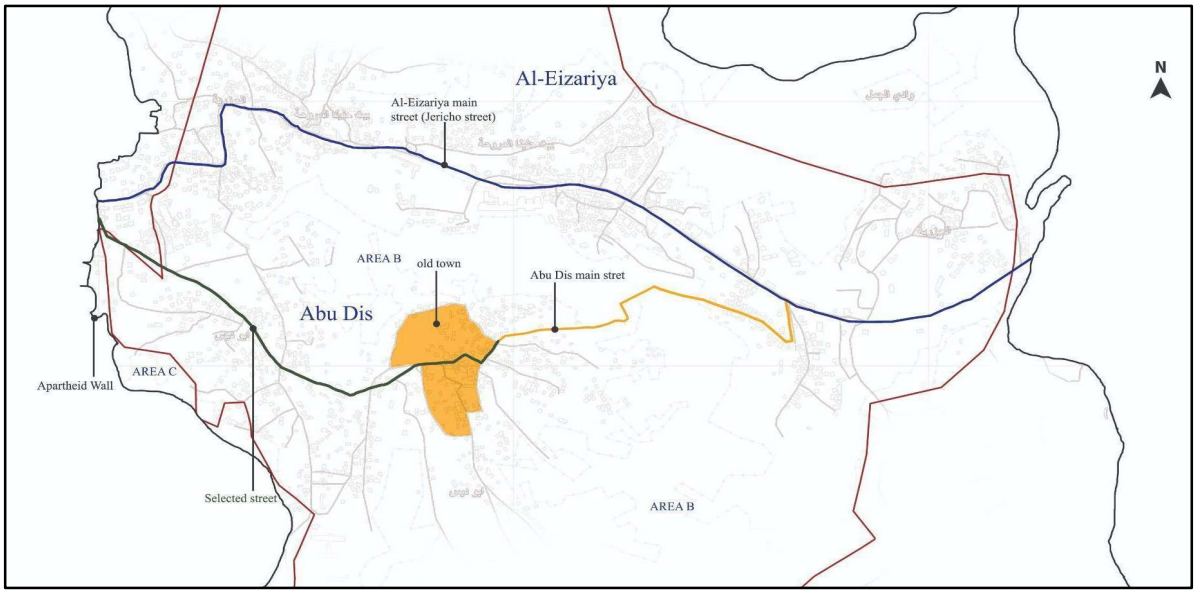


Figure 4-4: Master Map Showing the Boundaries from the Old Town to the Wall in Abu Dis

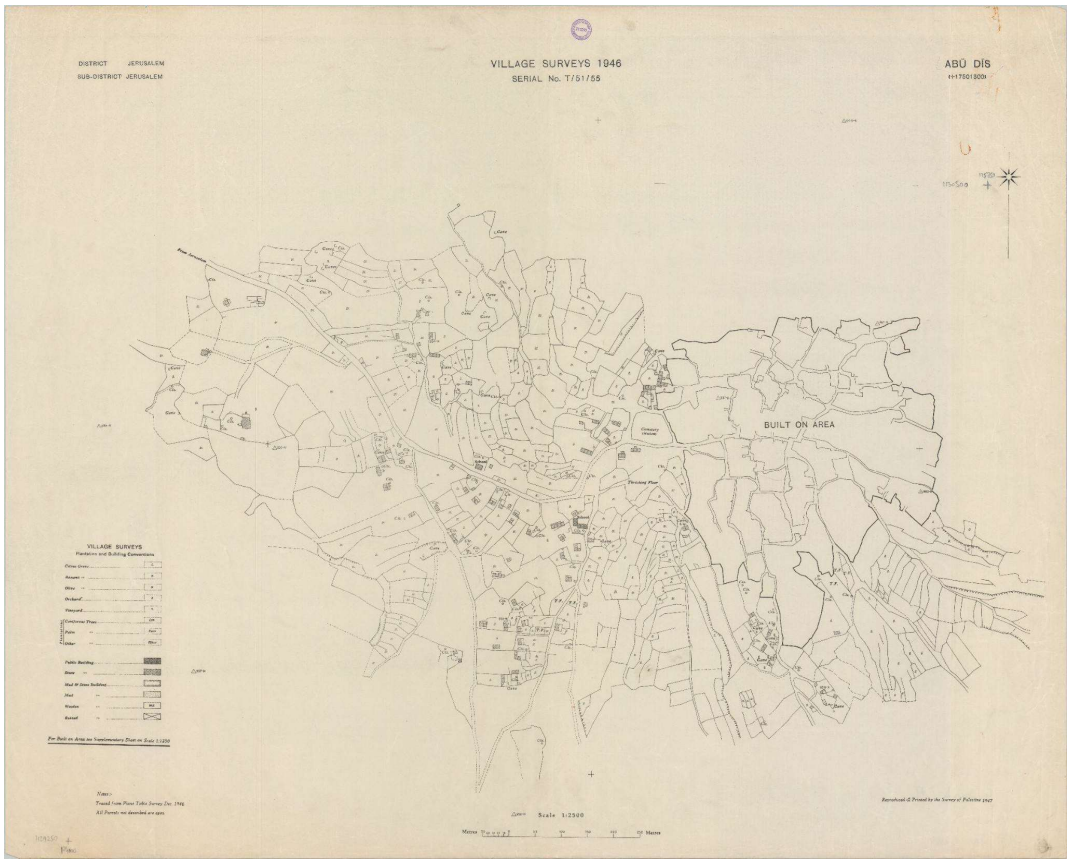


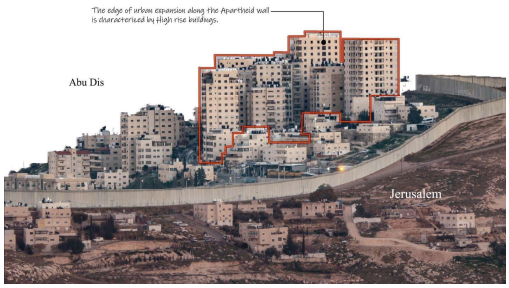
Figure 4-5: Historic Map of Abu Dis Village, Jerusalem Governorate, Survey of Palestine, 1946

In recent years, new additions have appeared within the boundaries of the old town, driven by growing household sizes and the lack of room for individual families to expand outward. These interventions have altered the visual character of the historic core, layering modern construction over the traditional fabric. The pattern is best read as an adaptive response to population pressure, worked out within the physical limits the old town imposes.

The second layer is the town's modern expansion, which took shape as the population grew and its functional ties to Jerusalem deepened. Land division here is comparatively regular, streets are wider, and buildings are multi-story concrete structures rather than stone. This expansion has been shaped by demographic pressure, scarce available land, and spatial and political constraints that closed off the town's natural room to grow horizontally. Construction has consequently concentrated within the existing built-up area, most intensively on land adjacent to the separation wall, where building densities and heights now reach their highest points. The resulting urban fabric combines the organic old town with this denser modern expansion, and traces the town's shift from a cohesive village into a semi-urban settlement shaped by constrained growth.



Extension of Modern Buildings alongside Historic Context



Picture of a high-rise building in Abu Dis in contemporary period

Figure 4-6: Transformations in Urban Morphology in Abu Dis

4.3 Analysis of the survey work

Based on the results of the field survey conducted on 40 houses in Abu Dis, extending from the Old Town to the wall along the main street in Abu Dis and its primary branches, and in conjunction with the questions posed to the residents of these homes, the following information was recorded:

4.3.1 Daily Dynamics of Living Space Usage: Behavior setting theory (Barker) and climate-responsive design

The living room is the dominant daily-use space in all three periods, but contemporary households show both the highest 'always in use' rate (62%) and the highest share of daily activity displaced to the kitchen (29%, against 0% in the Ottoman subgroup) — evidence of a coupled, high-intensity occupancy pattern. Barker's behavior setting theory holds that physical settings (a room, a threshold, a courtyard) structure and constrain the range of behaviors that occur within them; an open-plan setting, unlike a closed one, is a single behavior setting encompassing what were historically two or three separate settings (living, cooking, informal gathering). The contemporary open-plan layout therefore does not simply relocate activities; it merges behavior settings, which mechanically increases the internal-gains schedule of the monitored living zone (occupant metabolic load, cooking heat, appliance and lighting use) at exactly the same time as the fabric performance of that zone is weakest (see Section 4.3.4). This is a compounding, rather than an independent, relationship between behavior and fabric, and it is the clearest theoretical explanation in the dataset for why contemporary typology underperforms on both axes simultaneously, rather than trading one form of performance for another.

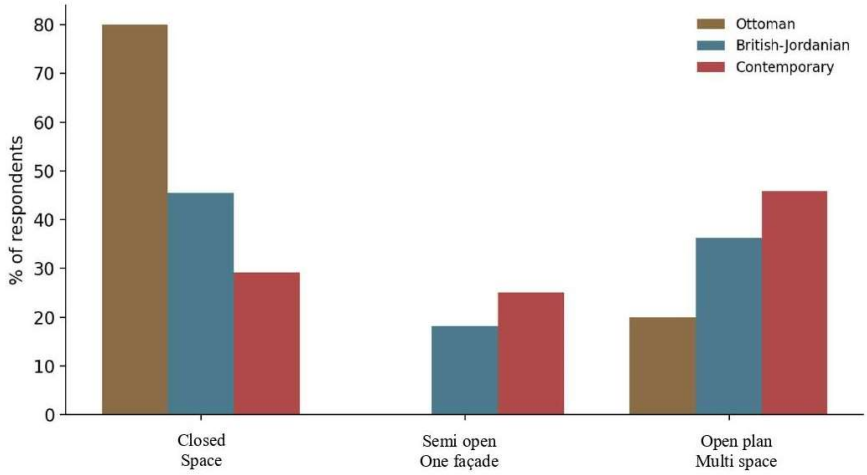


Figure 4-7: Row-normalized percentage of respondents per period reporting each natural ventilation rating

The decline in closed-space layouts from Ottoman (80%) to contemporary (29%) units, mirrored by the rise of open-plan layouts (Figure 4-8), is the behavior-setting evidence for the pattern described above: each shift toward open-plan merges what were previously separate behavior settings (living, cooking) into one, with the internal-gains consequences already discussed. Read alongside the privacy inversion, the

layout variable cannot be treated as a single one-dimensional ‘openness’ scale for simulation purposes — it needs to be decomposed into its thermal-coupling effect (internal gains sharing, addressed here) and its socio-spatial effect (privacy and threshold definition), since the two effects do not move together for the Ottoman case.

4.3.2 Residents’ Satisfaction with Natural Ventilation and Daylighting According to Spatial Layout: Environmental behavior/affordance theory, tested against passive design theory

Perceived ventilation quality rises monotonically with façade-opening count across the whole sample (0% ‘good’ with no openings, rising to 60% ‘good’ with openings on more than two façades) — a clean confirmation of affordance theory: openings are behavioral affordances that occupants read and use for airflow control, and more affordances produce more reported capability. But the same opening categories, tested against thermal comfort rather than ventilation perception, show the inverse relationship in winter: the ‘more than two façades’ category has the highest winter cold/very cold rate in the whole sample (90%), while the ‘two opposite façades’ category — offering genuine cross-ventilation without maximal envelope penetration — has the lowest (42%). This is the central theoretical tension in the dataset: affordance theory correctly predicts the behavioral/perceptual outcome (occupants successfully use more openings for ventilation) but is insufficient on its own to predict the environmental performance outcome, because it does not account for the heat-loss penalty of the same architectural feature. The two theories must be read together, with passive design theory setting the performance ceiling within which affordance-driven behavior operates.

Ventilation ratings remain relatively stable across periods (36–42% “good”), unlike thermal comfort, indicating they are driven by different variables. Ventilation perception aligns with opening count (affordance theory), while period reflects thermal mass and time lag affecting comfort. This supports treating opening ratio and thermal mass as separate variables rather than a single “period” factor in simulation.

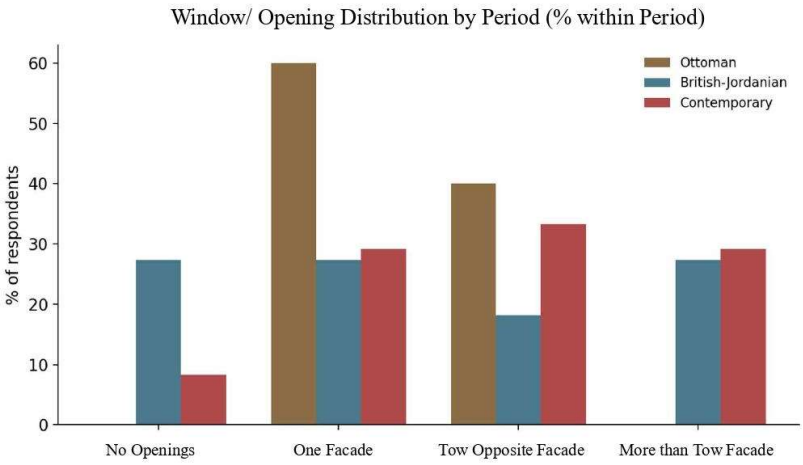


Figure 4-8: Row-normalized percentage of respondents per period reporting each façade-opening configuration

The (Figure 4-9) documents the affordance gradient against which (Figure 4-8) is read. Ottoman and British-Jordanian units cluster toward single- or two-façade configurations; contemporary units are the only group with a meaningful share (29%) of openings on more than two façades. Under affordance theory, this predicts — and Figure 2 confirms — higher perceived ventilation capability in contemporary units. The theoretical tension is that this same configuration also predicts, and Figure 4 confirms, the worst winter comfort outcome. The opening variable is therefore not unambiguously 'better' or 'worse' across theoretical lenses: it is a double-edged design variable whose net effect depends on which performance outcome and which season is being optimized for.

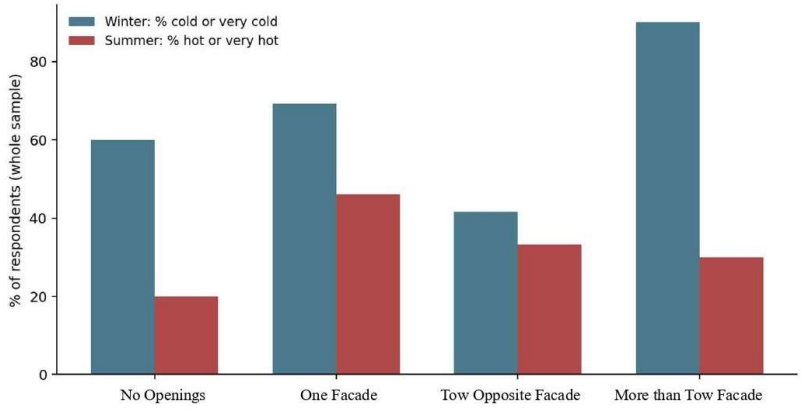


Figure 4-9: Percentage of the whole sample (independent of period) reporting hot/very hot summer conditions or cold/very cold winter conditions, by façade-opening configuration.

This figure isolates the affordance paradox described above from the period variable entirely, testing it at the level of the whole sample. Winter cold/very cold discomfort is highest (90%) at the maximum opening count and lowest (42%) at the two-opposite-façades configuration, which offers genuine cross-ventilation without the maximal envelope penetration of the four-plus-façade condition. Summer hot/very hot discomfort peaks instead at the single-façade configuration (46%), where limited cross-ventilation may trap solar and internal heat gains without adequate purge airflow. Together these two curves show that the relationship between opening count and thermal outcome is neither linear nor season-consistent, directly contradicting a simplified 'more openings equals better performance' design assumption and supporting a season-differentiated, mass-aware approach to opening ratio in the simulation matrix.

4.3.3 Spatial Enclosure, Privacy, and Long-Term Adaptation of Living Space by Building Period: Socio-spatial practice theory (Lefebvre) — spatial practice vs representational space

80% of Ottoman respondents describe their living-space layout as 'closed', the highest enclosure rate of the three periods, yet only 20% report high privacy and 40% report low privacy — the lowest reported privacy of any period despite the most enclosed layout. Read through Lefebvre's triad, the 'closed space' category as recorded in the questionnaire corresponds to representations of space: the conceived, categorical spatial layout as a planner or researcher would classify it from a plan. Reported privacy, by contrast, belongs to representational spaces: the lived, experienced meaning residents attach to that same layout in daily use. The mismatch between these two registers is evidence that enclosure at the level of built form (spatial practice — the physical rooms and walls) does not automatically produce the lived experience of privacy if the enclosed rooms open onto a shared, semi-public threshold rather than a private interior void. This directly supports treating the Ottoman case as a forecourt type: a forecourt is spatially open to a shared social threshold even where its constituent rooms are individually enclosed, which is exactly the combination of high enclosure and low privacy the data show. The finding operationalizes Lefebvre's theory as an empirical test rather than a purely interpretive frame: the conceived/lived gap is measurable as the divergence between the layout variable and the privacy variable.

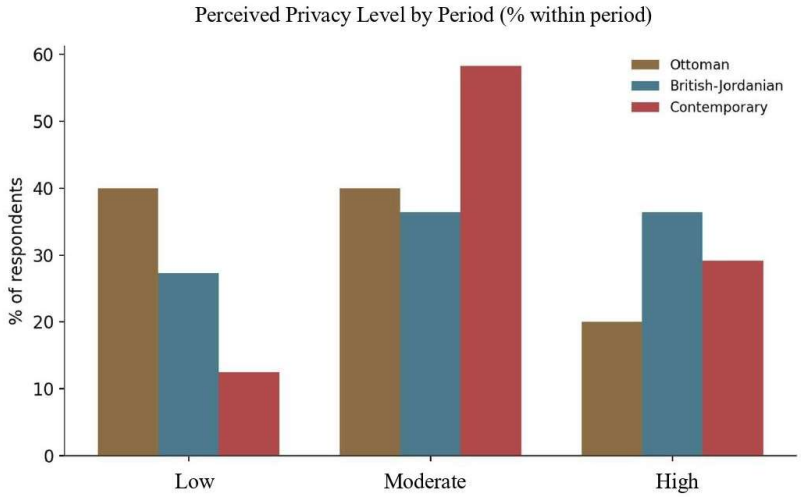


Figure 4-10: Row-normalized percentage of respondents per period reporting each privacy rating

- **Adaptive Hypothesis :**80% of Ottoman households and roughly half of the British-Jordanian and contemporary households added spaces after moving in. That addition tracks closely with a change in room function: 80% of cases with an addition also show a function change, against 50% where none occurred.

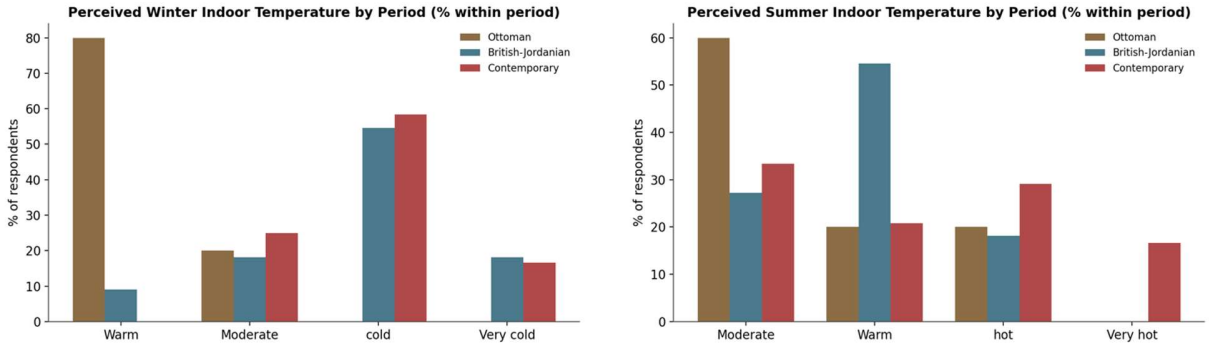
Occupants here are not just adjusting behavior inside a fixed room. They are changing the room itself, and that change reshapes how the rest of the house gets used, sometimes years later. So, space addition and functional change belong at the scale of the building and its history, not at the scale of a single occupant reacting to a fixed environment.

4.3.4 Comparative Analysis of Thermal Comfort by Building Era

0% of Ottoman respondents report cold or very cold winter conditions without heating (80% report 'warm'), against 75% of contemporary respondents reporting cold or very cold conditions. Adaptive comfort theory predicts that occupants with greater behavioral adaptive opportunity — more openings to close, more layers of movable shading, more control over their thermal environment — should report better tolerated, not worse, thermal outcomes. The data show the opposite: contemporary units have the highest opening counts (see Section 4.3.2) yet the worst winter outcomes. This is best explained by passive design theory: envelope thermal mass and time lag set an outer boundary on achievable indoor conditions that behavioral adaptation cannot compensate for once exceeded. The finding therefore does not simply support passive design theory in isolation — it extends adaptive comfort theory by showing that behavioral

adaptive opportunity has diminishing and even negative returns when it is not backed by adequate fabric performance: opening more façades in a low-mass envelope increases heat loss faster than it increases occupant control benefit.

Conceptually, this figure is the clearest evidence in the dataset that passive fabric performance, not occupant behavior, is the dominant explanatory variable for winter comfort. If adaptive comfort theory's behavioral-adjustment mechanism were sufficient on its own, the period with the most openings to close and the most immediate occupant control (contemporary) should show comparable or better outcomes to the period with the least control (Ottoman). It shows the opposite. This positions thermal mass and time lag as a precondition for adaptive behavior to be effective, not a parallel or substitutable factor — a distinction with direct design implication: retrofitting contemporary units with better user controls (for example, more adjustable shading) will not close this gap unless envelope mass is also addressed.



Winter Summer

Figure 4-11: Row-normalized percentage of respondents per period reporting each thermal sensation, without air conditioning

The smaller period gap in summer relative to winter is itself theoretically informative. In summer, shading behavior (a genuine behavioral adjustment mechanism under adaptive comfort theory) is active across all periods, partially equalizing outcomes; in winter, shading is largely irrelevant as a variable, allowing time lag and thermal mass to operate with less behavioral interference.

4.3.5 Limitation

This remains a descriptive, cross-tabulated analysis; the theoretical linkages above are interpretive readings of directional patterns in the data, not statistically tested associations. The Ottoman subgroup (n

= 5) precludes inferential statistics, and all theory-linked claims for that subgroup should be understood as corroborative of the qualitative and archival case built elsewhere in the thesis rather than as independently generalizable quantitative findings. Thermal sensation variables are self-reported perceptions, subject to adaptive expectation and recall effects consistent with the psychological-habituation mechanism in adaptive comfort theory itself — a reader should not treat 'perceived warm' as equivalent to a measured indoor temperature, but as evidence of the occupant's adapted comfort band, which is itself part of what adaptive comfort theory predicts should vary by dwelling type and behavioral history.

4.4 Analysis of the Selected Residential Case Studies

The following (Figure 4-12)illustrates the street selected for the study, from which the case studies were drawn. One representative case was chosen from each of the three historical periods to reflect the spatial and temporal transformations.



Figure 4-12: selected Case Study

- Case 1: Ottoman-style house (Beit Erekat – Abu Dis)

Beit Erekat is located in Abu Dis, outside the historic boundaries of the old town. The house was constructed in 1941 in the Ottoman construction tradition, characterized by load-bearing walls, semi-circular arches, and cross-vaulted roofing.

The property comprises two single-story buildings on a plot with a large garden. Architecturally, the selected house contains three cross-vaulted rooms, with a dome above one of the cross-vaults. The building reflects traditional craftsmanship through the use of local stone materials, embedded pottery vessels within the vaults, thick structural walls, and a locally derived spatial layout. Despite minor additions and modifications, it has largely preserved its original architectural character and material authenticity.

Although the building retains its historical and social significance due to its association with the Erekat family, changes in the surrounding context, loss of its original function, and current abandonment have weakened its intangible values, and the property is now at risk due to neglect and inappropriate use of the garden.

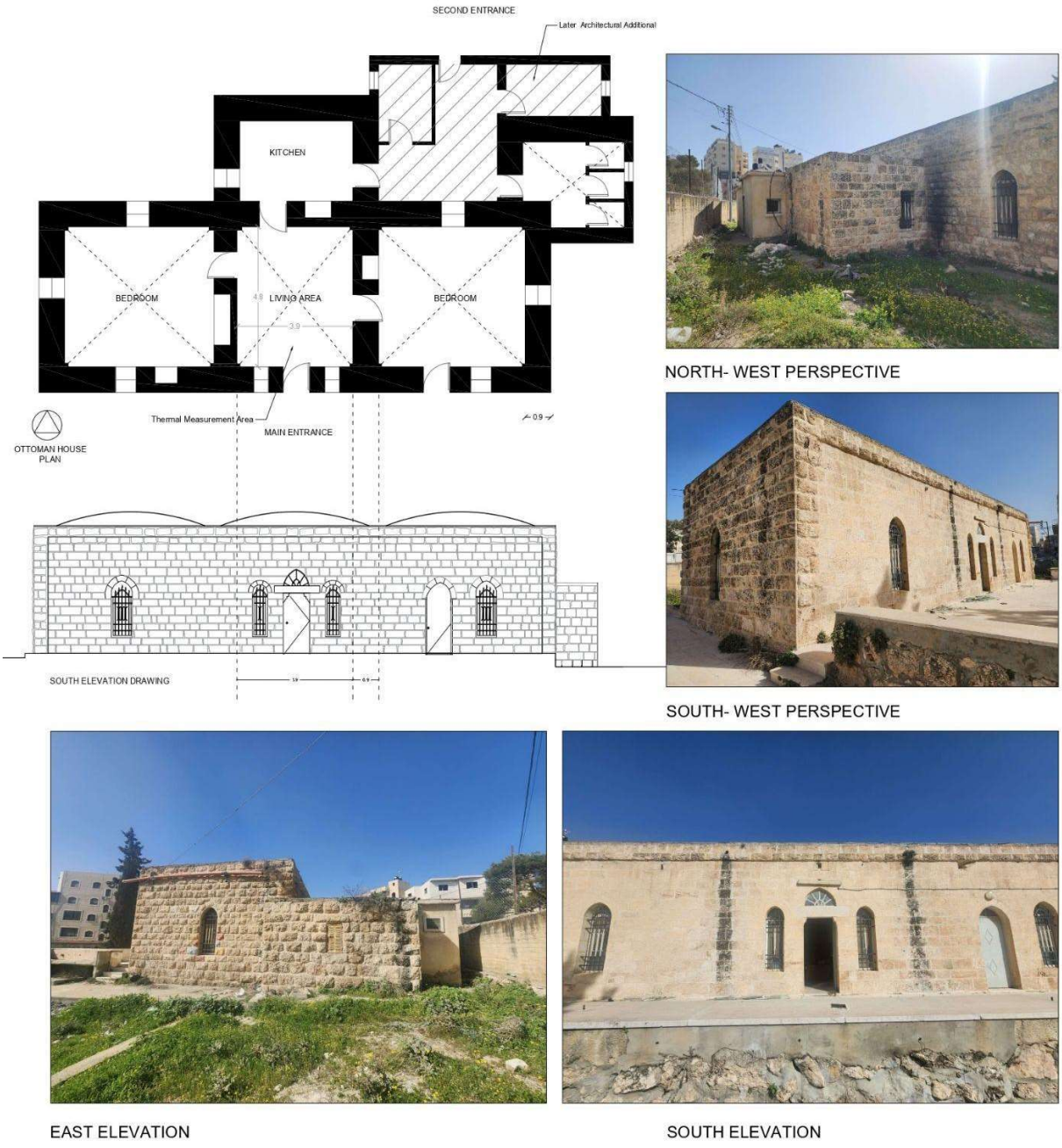


Figure 4-13: Architecture drawings & perspectives for Ottoman house sample

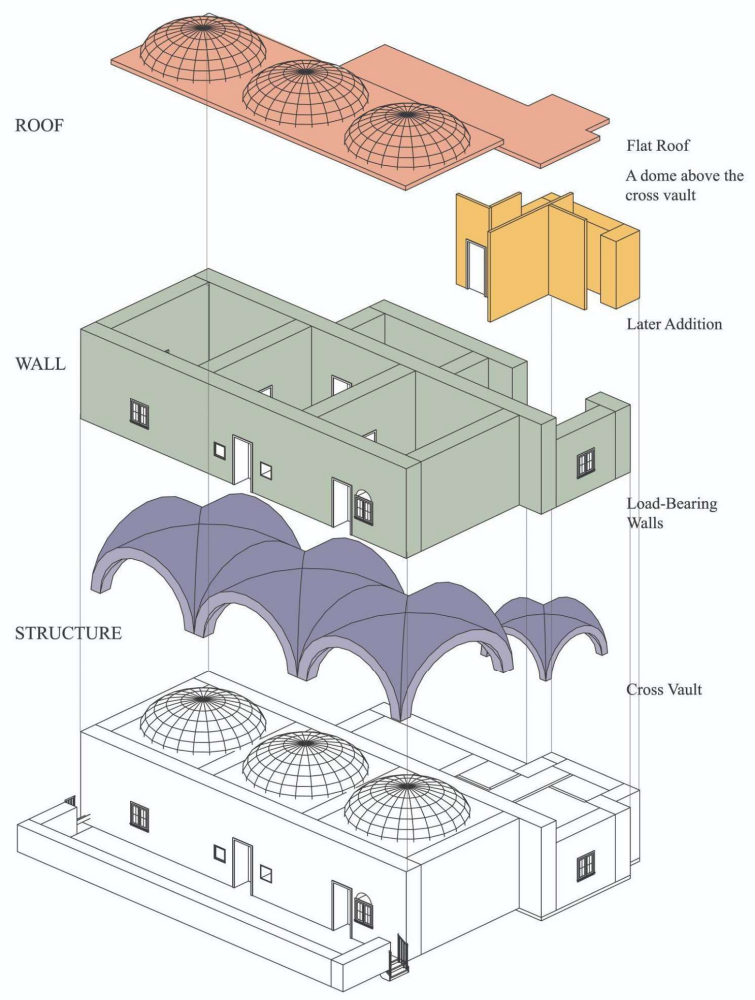


Figure 4-14: Exploded Axonometry for Ottoman house sample

- Case 2: Jordanian Style house

The house was built in 1964 during the Jordanian period and reflects the residential architectural characteristics common at that time, with a simple arrangement of openings and an exterior façade shaped from local stone. The house originally included an open front veranda that served as a transitional space between the interior and exterior and extended the living spaces. In 2004, the veranda was enclosed and incorporated into the building mass, which created a shift in the use of internal spaces. The enclosed veranda became the main living space, while the original interior living space was converted into a bedroom for one of the sons to meet changing family needs.

The use of clay roof tiles above the entrance veranda is among the architectural elements that emerged in residential buildings during the Jordanian period. In addition, the use of Qamat stone above door openings is visible, an element commonly used in residential architecture at that time.



Figure 4-15: Architecture drawings & perspectives for Ottoman house sample

4.4.3 Case 3: Contemporary Style house

Construction of the house commenced in 1997 but was subsequently halted in two separate phases. The first suspension lasted from 1997 until 2001 due to the absence of a building permit, while the second occurred in 2003 in conjunction with the construction of the Separation Wall on the adjacent land. A building permit was later obtained through Jerusalem-based lawyers. However, any horizontal expansion of the house was prohibited because the adjacent land was classified as the presence of the Wall restricted Area C, and vertical expansion was also prohibited.



Figure 4-16: Architecture drawings & perspectives for a contemporary house sample

4.5 Climate Analysis

The climatic analysis presented in this section was generated in Climate Consultant (UCLA Energy Design Tools Group) from an IWEC-format typical meteorological year file for the Jerusalem station (WMO Station Number 401840; 31.78° N, 35.22° E; elevation 782 m). No dedicated long-term meteorological record exists for Abu Dis itself, and the Jerusalem file, drawn from a station roughly 4 km to the west, is the nearest dataset with sufficient historical depth to support an ASHRAE 55 adaptive comfort analysis. This substitution deserves an explicit caveat rather than a silent assumption. Abu Dis sits on the eastern descending slope of the Judean highlands, at a somewhat lower elevation than central Jerusalem and closer to the climatic transition toward the Jordan Rift Valley. Actual conditions on site are therefore likely to run marginally warmer and drier than the Jerusalem file suggests, particularly in summer, owing to the partial rain-shadow effect and the loss of elevation moving east. The dataset used here should be read as a conservative proxy: defensible as a basis for climate characterization, but one that probably understates, rather than overstates, the cooling load and diurnal severity a building in Abu Dis actually experiences.

4.5.1 Annual Temperature Regime and Diurnal Behavior

The annual temperature range chart in Jerusalem- Abu Dis (Figure 4-17) shows a summer plateau of design highs around 30–33 °C from June through September, with a recorded maximum near 34 °C in August, against a comfort band (the ASHRAE 55 adaptive zone at 50% relative humidity) sitting at roughly 20–25 °C. Winter is markedly cooler: average lows fall to 3–5 °C in December and January, with a recorded low near –1 °C, indicating a genuine, if occasional, frost risk. The most diagnostic feature of the chart, however, is not the seasonal extremes but the diurnal amplitude, which is widest in the transitional months. April, for instance, records a low near 3 °C alongside a high near 28 °C — a swing approaching 25 °C within a single month's range — while the peak summer months show a narrower but still substantial daily amplitude of roughly 15–17 °C. This behavior is characteristic of a semi-arid highland climate, where low atmospheric moisture and largely clear skies allow rapid nocturnal radiative cooling once the sun sets, even during periods when daytime temperatures are high. Architecturally, this diurnal swing is not incidental; it is the physical resource that makes night ventilation and thermal-mass night-flushing viable cooling mechanisms in this climate.

The psychometric analysis indicates that Abu Dis has significant potential for passive climate adaptation. The identified percentages represent overlapping climatic opportunities rather than independent annual categories, and therefore describe theoretical potential rather than guaranteed building performance.

Passive solar gain is a major resource, accounting for approximately 35.7% of annual hours, while high thermal mass contributes 24.2% compared with 11.5% for low thermal mass, highlighting the importance of thermal storage in this climate. Internal heat gains also contribute significantly (31.4%). In contrast, cooling requirements remain limited, with cooling-related strategies accounting for 14.9% of hours and active cooling with dehumidification required for only 1.1%, while heating is needed for approximately 26.3% of annual hours.

These findings support prioritizing passive design strategies investigated later in this thesis, including thermal mass, window-to-wall ratio, shading, veranda configuration, and orientation.

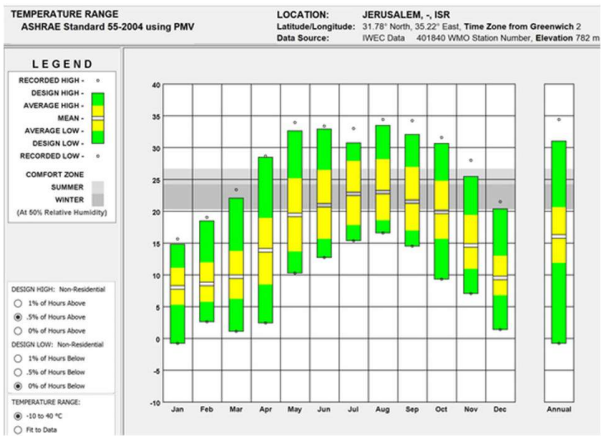


Figure ASHRAE 55 Temperature Range chart, Jerusalem IWEC data

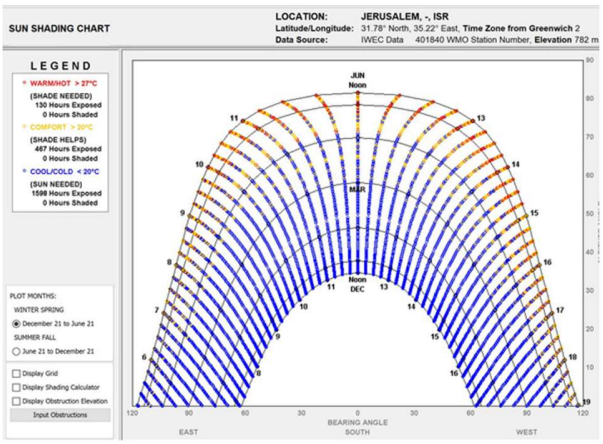


Figure Sun Shading chart, December 21–June 21

Figure 4-17: Jerusalem Climate Analysis using Climate Consultant (UCLA Energy Design Tools Group)-A

4.5.2 Solar Geometry, Shading Exposure and Window Control

The two sun-shading charts illustrate the annual balance between periods when solar exposure is beneficial and when it contributes to overheating. During the December–June period, only 5.9% of sun-hours require shading, while 72.8% occur under conditions where solar access is desirable.

During the June–December period, shading demand increases to 17.3%, with the remaining hours divided between comfort-assisting solar exposure and periods where solar gain is beneficial.

Across the full year, approximately 511 hours require solar protection against overheating, compared with around 2,247 hours where solar access is desirable for thermal gain. This indicates that Abu Dis has a strong seasonal dependence on solar availability: winter solar gain should be preserved, while summer overheating is limited to specific periods.

Both charts represent an unshaded baseline condition, identifying the solar exposure risk before any shading intervention is applied. The overheating periods are mainly concentrated around solar noon and afternoon hours on south- and west-facing surfaces during summer. Therefore, targeted shading devices, such as horizontal overhangs or transitional elements like the veranda/liwan discussed in this thesis, can effectively reduce unwanted solar gains by responding to the specific seasonal sun angles rather than shading the façade throughout the year.

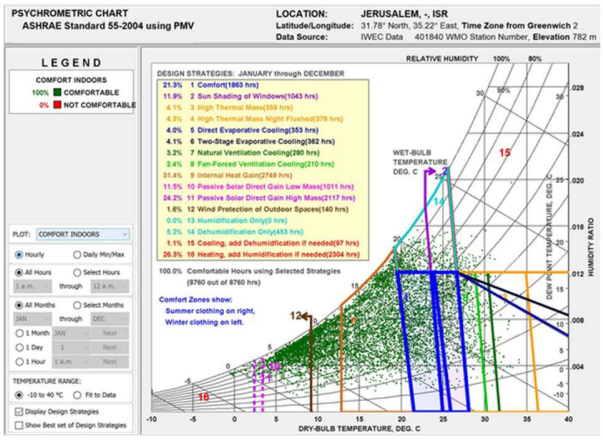


Figure Psychometric chart with ASHRAE 55 design strategy breakdown, January–December

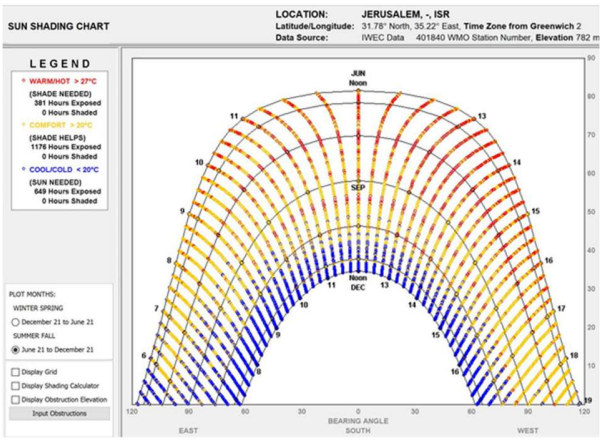


Figure Sun Shading chart, June 21–December 21

Figure 4-18: Jerusalem Climate Analysis using Climate Consultant (UCLA Energy Design Tools Group)-B

4.6 Summary

The analysis of the case study in Abu Dis reveals that the relationship between spatial configuration, building period, and urban morphology strongly influences residential environmental performance. The findings indicate that traditional residential structures exhibit a higher level of environmental responsiveness than more recent constructions. Historic houses were originally designed with passive

environmental considerations such as compact layouts, thick stone walls, and spatial connections that enhance natural ventilation and thermal stability. In contrast, many contemporary residential buildings exhibit a gradual decline in environmental efficiency due to increased reliance on modern construction materials and reduced integration of passive design strategies.

The results also highlight the importance of spatial connectivity in shaping the daily use and environmental quality of interior spaces. Living spaces that maintain a visual or physical connection with outdoor areas tend to perform better in terms of natural lighting, ventilation, and overall user comfort. Furthermore, façade orientation and the distribution of openings significantly affect indoor environmental conditions, emphasizing the role of building design in responding to local climatic characteristics.

Overall, the case study demonstrates that the transformation of the urban fabric in Abu Dis—from a compact traditional settlement to a denser contemporary environment—has altered the environmental behavior of residential spaces. These findings underscore the need to reconsider traditional design principles and adapt them to contemporary residential development to improve indoor environmental quality and enhance the sustainability of housing in the local context.

Chapter 5
Result and Discussion

5.1 Introduction

Field measurements were conducted on the three selected buildings that represent the three architectural typologies investigated in this thesis: Ottoman, Jordanian, and Contemporary. The monitoring campaign was conducted during both summer and winter to capture seasonal variations in thermal behavior. The summer campaign extended over seven consecutive days (20 Jun- 26 Jun), while the winter measurements covered a 30-hour period between 13 Feb and 15 Feb.

5.1.1 Analysis of Summer Measurement

The actual six-day raw in summer trace for each building, hour by hour, over the full monitored period. This shows day-to-day drift: The Contemporary house's night-time trough deepens noticeably on some days (e.g., around Day 6, dropping below 23°C), while the Ottoman trace stays comparatively flat night after night, confirming that the buffering effect isn't a one-day artifact but a consistent behavior across the whole campaign.

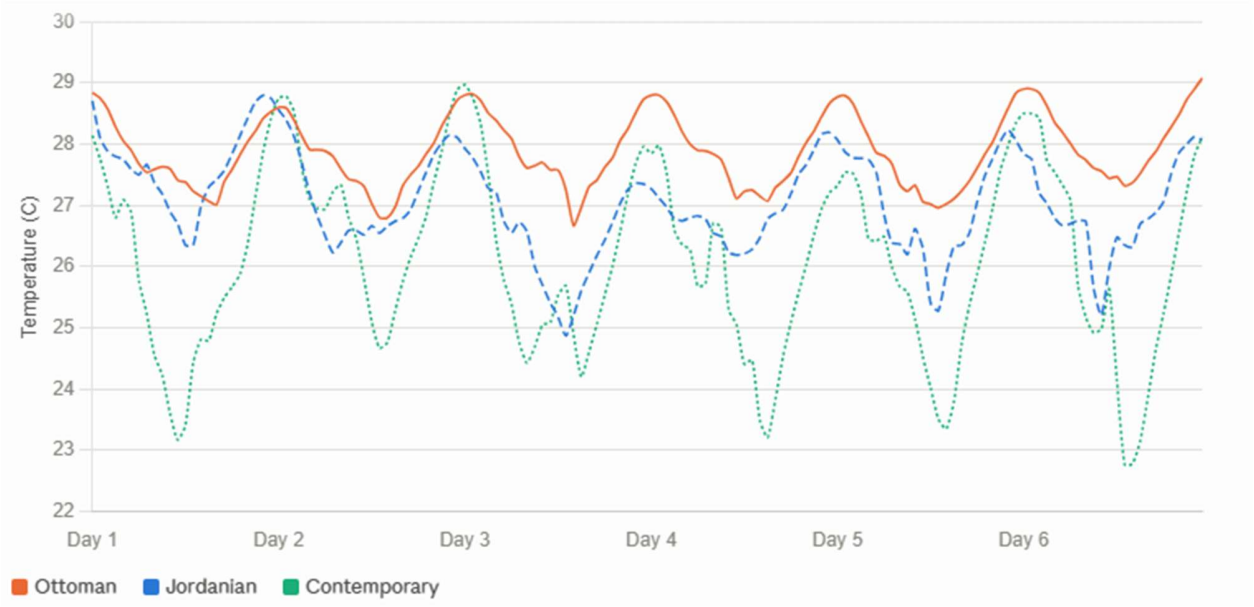


Figure 5-1: Continuous weekly indoor air temperature variation across the three typologies, summer monitoring period (20 Jun- 26 Jun)

Across the monitored summer week, the three buildings display markedly different diurnal curves. The Ottoman case maintains the narrowest and most stable profile, with a mean indoor air temperature of 27.9°C, oscillating gently between a night-time low of 27.0°C at 06:00 and a daytime high of 28.8°C at 16:00 — a diurnal swing of only 1.8°C, and an overall six-day range of 26.6–29.3°C. The Jordanian case behaves as an intermediate condition, with a mean of 27.0°C, a low of 26.0°C at 06:00, a high of 28.1°C at 16:00, and a wider swing of 2.2°C (overall range 24.8–31.1°C). The Contemporary case departs most sharply from the other two: its mean drops to 26.1°C, it cools to 23.9°C at 07:00 — well below either historical case — before rising steeply to a comparable afternoon peak of 28.2°C at 16:00, producing a diurnal swing of 4.4°C, more than double that of the Ottoman house (overall range 22.6–29.0°C).

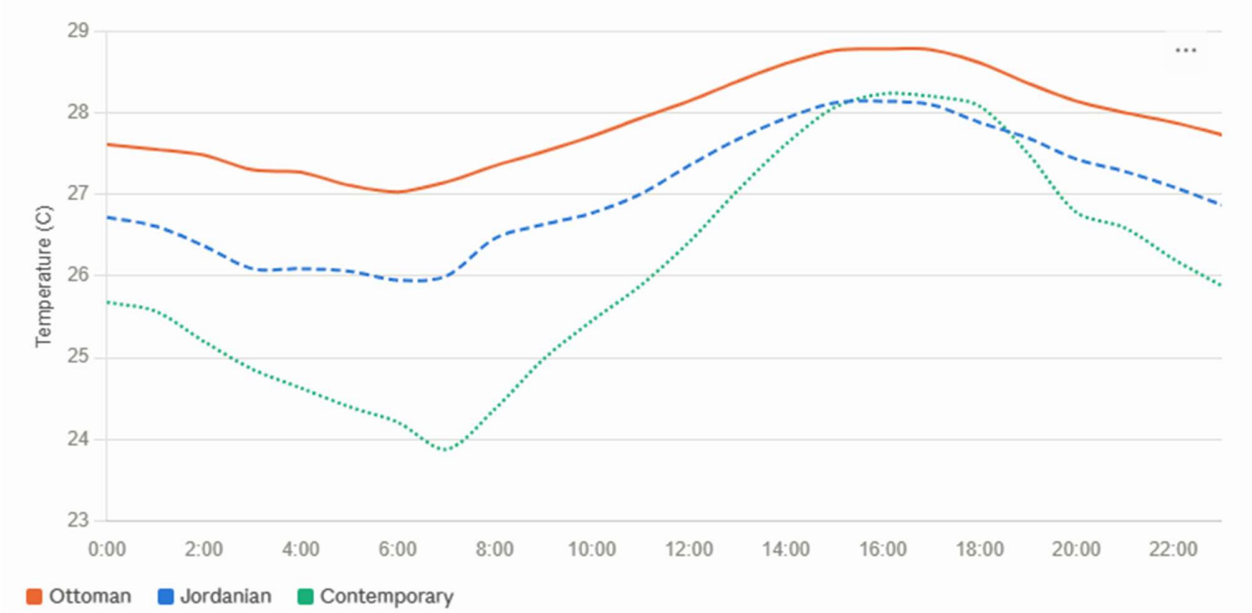


Figure 5-2: Comparative diurnal indoor air temperature profile of the Ottoman, Jordanian, and Contemporary case buildings during the summer day monitoring period

These differences are not incidental; they follow directly from the architectural characteristics that distinguish the three typologies. Building orientation governs the timing and intensity of solar heat gain through the envelope and openings; window-to-wall ratio determines how much of that gain is admitted directly as short-wave radiation versus resisted by opaque mass; thermal mass governs the amplitude and phase lag of the internal response to the external cycle; and spatial configuration and cellular in the Ottoman case, increasingly linear and open-plan by the Contemporary case — determines how heat and air move between rooms once admitted.

Read against these variables, the comparison becomes legible. The Ottoman house's narrow swing and delayed, damped peak is consistent with its thick stone construction and low window-to-wall ratio, which together impose a long-time lag and heavily attenuate the external signal before it reaches the interior. The Jordanian case, transitional in its construction — generally thinner masonry and larger openings than the Ottoman house, but still built with substantial mass relative to contemporary practice — sits between the two extremes on every indicator: swing, night-time minimum, and overall range all fall midway between Ottoman and Contemporary values. The Contemporary house, with lighter concrete/block construction, a markedly higher window-to-wall ratio, and a more open, linear spatial layout offering little internal buffering, shows the least resistance to the external cycle: it loses heat fastest overnight and gains it fastest by day, converging with the other two typologies only briefly at the afternoon peak before diverging sharply again after sunset.

- Reading the graph

The chart above makes this behavior visually explicit. All three curves converge tightly in the mid-afternoon, between roughly 15:00 and 17:00, when solar gain dominates regardless of construction type, and the three typologies briefly perform alike. Outside this window, however, the curves fan out in direct proportion to each building's thermal mass and envelope permeability: the Ottoman line sits consistently highest and flattest overnight, the Jordanian line tracks a shallower version of the same pattern, and the Contemporary line falls away most steeply after dark, reaching its trough roughly an hour later than the other two cases a lag consistent with a lighter envelope responding more directly to the diurnal radiative low rather than being damped by stored mass. The ordering of diurnal swing across the graph (Ottoman < Jordanian < Contemporary) is therefore not an isolated numerical finding but the direct visual signature of decreasing thermal mass, increasing window-to-wall ratio, and diminishing spatial configuration as the typology moves from Ottoman to Contemporary.

5.1.2 Analysis of Winter Measurement

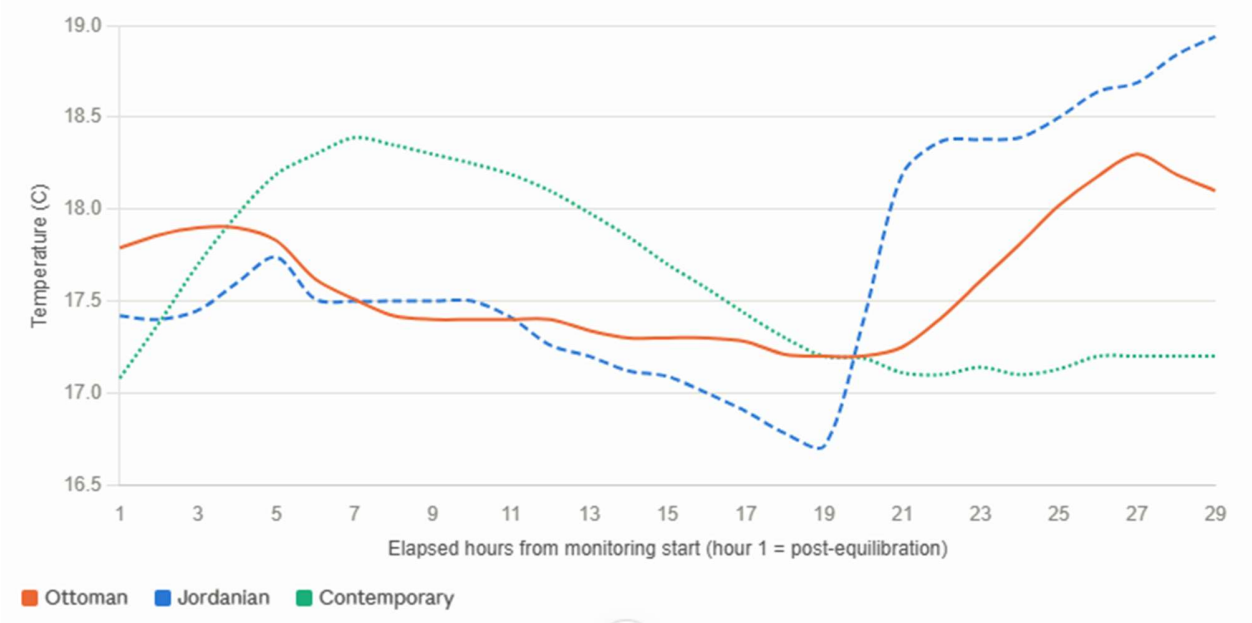


Figure 5-3: Comparative diurnal indoor air temperature profile of the Ottoman, Jordanian, and Contemporary case buildings during the winter day monitoring period

The winter pattern inverts, but does not simply mirror, the summer one. The Ottoman house again shows the flattest trace — a swing of just 1.1°C — consistent with its high thermal mass damping the diurnal cycle regardless of season; here, that same mass works to retain the modest daytime heat gain overnight rather than to exclude summer heat, giving it the most stable winter indoor climate of the three. The Contemporary house behaves differently to its summer profile: rather than showing the widest swing, it peaks earliest and settles into a comparatively narrow band (1.4°C) after a brief morning rise, consistent with a lighter fabric that responds quickly to whatever solar or internal gain reaches it before drifting with the ambient trend once that gain fades. The Jordanian case shows the widest winter swing of the three (2.3°C), with a marked rise toward the later part of the monitored window — a pattern consistent with its transitional envelope, where moderate thermal mass and larger window openings than the Ottoman case allow more of the available solar gain to register indoors over the course of the monitored period.

As this winter comparison is based on a single continuous 30-hour monitoring window per building, rather than the multi-day summer campaign, the analysis here centers on the diurnal behavior captured within that period — the relative damping, timing, and amplitude of each building's response — which is precisely the basis on which the three typologies are compared. Read this way, the winter results reinforce the same underlying ordering established in summer: the Ottoman envelope consistently damps the indoor

cycle most strongly, the Contemporary envelope responds fastest to available gain, and the Jordanian case continues to occupy an intermediate, transitional position — with thermal mass and window-to-wall ratio again standing out as the variables most clearly separating the three.

5.2 Validation of the Base Three Models

Model calibration assessed whether the simulated indoor air temperature reasonably reproduced the thermal behavior measured during the summer field campaign before the model was used for the subsequent parametric analysis. Agreement between the simulated and measured hourly indoor air temperature series was assessed using three indicators. The Normalized Mean Bias Error (NMBE) measures the systematic bias between the two series: it expresses the average signed deviation of the simulated values from the measured values as a percentage of the measured mean. A value close to zero indicates that the model neither consistently overestimates nor underestimates indoor temperature. The Root Mean Square Error (RMSE) quantifies the typical magnitude of the hourly deviation between simulated and measured values in absolute temperature units and penalizes larger individual deviations more heavily than an average would, yielding a direct, physically interpretable measure of hourly accuracy. The Coefficient of Variation of the Root Mean Square Error (CVRMSE) normalizes this same measure by the mean of the measured values, combining bias and hour-to-hour scatter into a single percentage.

5.2.1 Late Ottoman Period: Case 1

Ottoman house followed the sequence of physically motivated adjustments rather than direct numerical optimization of the indicators. The initial, uncelebrated model underestimated indoor air temperature systematically, with the error concentrated in the night-time hours relative to daytime. Because the monitoring campaign was conducted with windows closed throughout, natural ventilation was excluded from consideration, and attention turned instead to infiltration as the sole air-exchange pathway. The infiltration schedule was refined accordingly: the daytime rate was left unchanged, while the night-time multiplier was reduced to reflect the more limited stack-effect-driven air exchange expected under closed-window conditions, with a short transitional ramp introduced either side to avoid an artificial discontinuity at the day/night boundary. This adjustment reduced the night-time component of the bias without disturbing the already-acceptable daytime agreement.

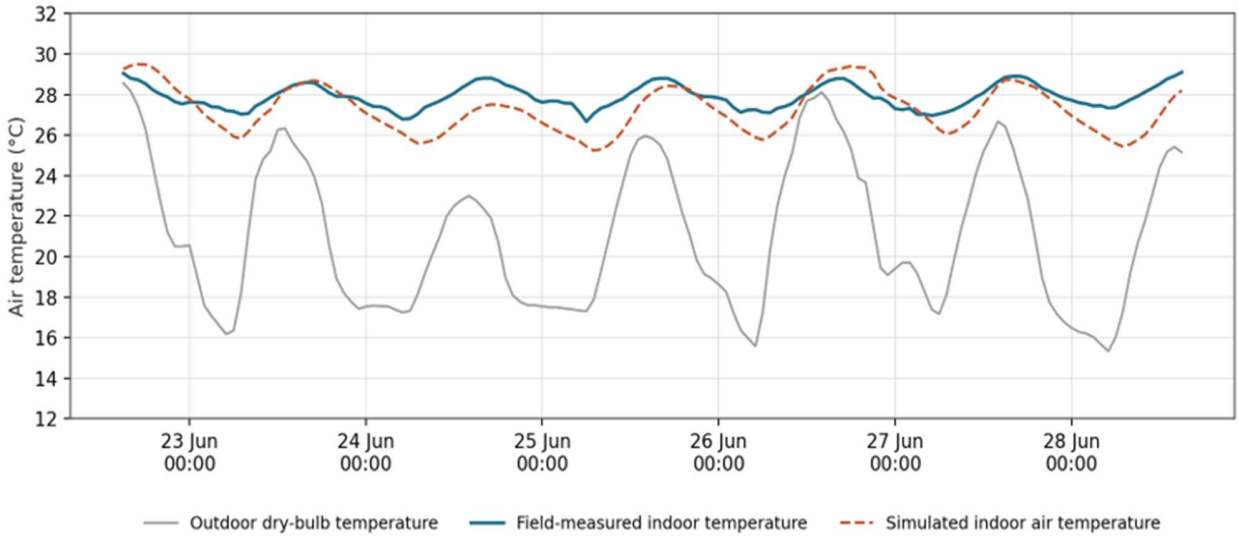


Figure 5-4: Simulated versus field-measured indoor air temperature for Ottoman case study

The residual deviation was found to be distributed evenly across day and night rather than concentrated at particular hours, a pattern consistent with a mechanism acting continuously on the building's heat balance. This directed attention to the external convection algorithm: the DOE-2 correlation used as Design Builder's default is derived in part from wind-exposed test conditions poorly matched to the sheltered, and replaced with the TARP algorithm, which is less sensitive to wind exposure and more representative of natural and wind-driven convection in an enclosed urban setting. Under the calibration criteria commonly used for hourly building energy models, an NMBE within ±10% and a CVRMSE within 30% are considered acceptable, and an RMSE of around 2°C or below is generally treated as good agreement for free-running residential buildings. The final calibrated model reached an NMBE of −2.33%, an RMSE of 0.98°C, and a CVRMSE of 3.53%, meeting all three thresholds.

5.2.2 Jordanian Period: Case 2

Figure 5-5 shows simulated indoor air temperature against field-measured indoor temperature across the full aligned period.

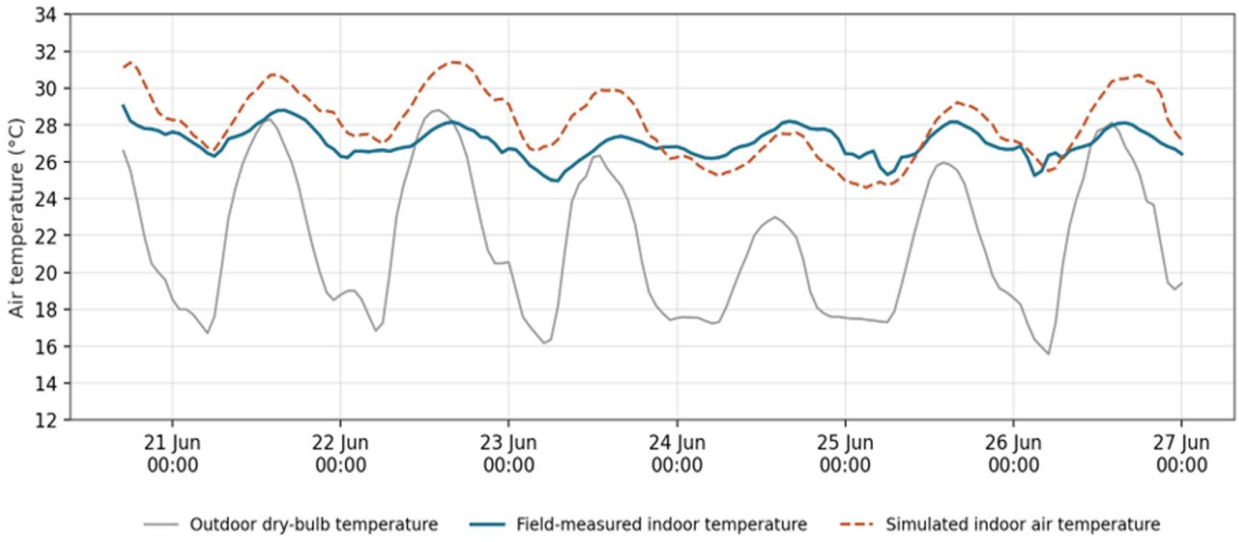


Figure 5-5: Simulated versus field-measured indoor air temperature for Jordanian-period case study

The calibration for the Jordanian-period case proceeded through a diagnosis-led sequence of adjustments rather than direct numerical optimization of the indicators. The initial model returned a combined ventilation and infiltration air change rate that remained nearly constant throughout the monitoring period, varying by less than 0.1 ac/h despite substantial diurnal swings in outdoor temperature and wind conditions. This behavior was physically implausible for a naturally ventilated stone dwelling and indicated that natural ventilation was not being actively driven by the model's airflow physics; airflow through the openings was instead governed by a fixed scheduled rate rather than by the stack- and wind-pressure equations appropriate to the building's operable window geometry. The natural ventilation method was therefore changed from a scheduled to a calculated formulation, allowing airflow to respond directly to the discharge coefficient, effective opening area, and hour-by-hour indoor-outdoor temperature and wind conditions. This produced a combined air change rate that varied realistically across the period (approximately 1.8 to 6.8 ac/h), consistent with the building's operable openings. The intent of this adjustment was to improve the model's physical representation of the building's ventilation behavior, not to optimize its statistics artificially. Under the calibration criteria commonly used for hourly building energy models, an NMBE within ±10% and a CVRMSE within 30% are considered acceptable, and an RMSE of around 2°C or below is generally treated as good agreement for free-running residential buildings. The final calibrated model reached an NMBE of 3.58%, an RMSE of 1.70°C, and a CVRMSE of 6.27%, meeting all three thresholds.

5.2.3 Contemporary Period: Case 3

The calibration for case 3: contemporary house proceeded through a sequence of physically motivated adjustments rather than direct numerical optimization of the indicators. The initial, uncelebrated model systematically overestimated indoor air temperature, with the error concentrated in the evening and night-time hours. This indicated that night-time air exchange was under-represented in the model. The natural ventilation parameters were refined accordingly: the operating schedule and ventilation rate were adjusted to allow greater air exchange at night, when occupants are expected to ventilate the space for cooling, and reduced air exchange during the day. This adjustment removed most of the bias associated with night-time heat retention. Once the airflow-related sources of error had been addressed, the remaining deviation was consistent with the model understating the wall's thermal storage capacity. The density and specific heat assigned to the concrete layer of the external wall were therefore adjusted within a physically realistic range. This step reflects the likely uncertainty between Design Builder's generic material database values and the properties of the actual building materials; the wall's layer composition, thicknesses, and overall geometry were left unchanged throughout. The intent of both adjustments was to improve the model's physical representation of the building, not to artificially optimize its statistics. Under the calibration criteria commonly used for hourly building energy models, an NMBE within ±10% and a CVRMSE within 30% are considered acceptable, and an RMSE of around 2°C or less is generally considered good agreement for free-running residential buildings. The final calibrated model reached an NMBE of 3.87%, an RMSE of 1.62°C, and a CVRMSE of 6.20%, meeting all three thresholds.

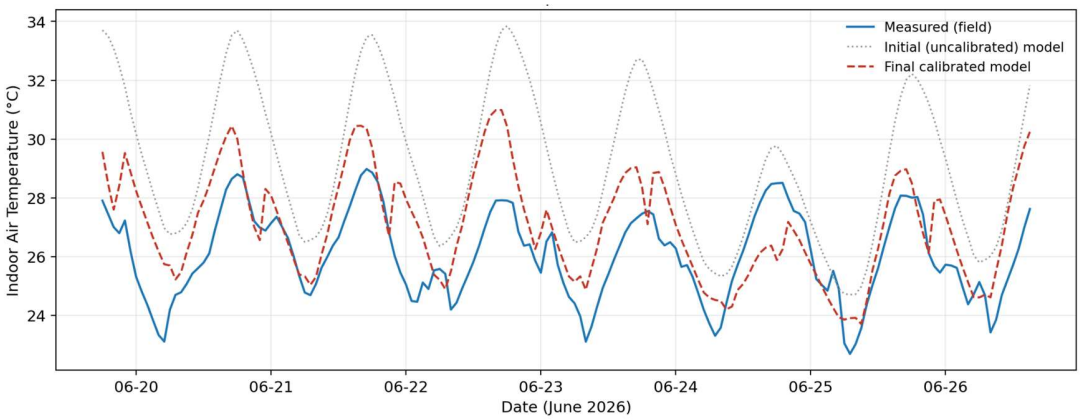


Figure 5-6: Simulated versus field-measured indoor air temperature for Contemporary case study

The improvement is evident in the comparison between the initial and final model in Table 5.Y and Figures 5.X and 5.Y. Bias and hourly deviation both fell substantially: NMBE dropped to 3.87%, RMSE to 1.62°C, and CVRMSE to 6.20% in the final model, so the calibrated model no longer systematically overestimates indoor conditions, and its hourly predictions now deviate from the measured values by a smaller and more consistent margin than before. The time-series comparison in Figure 5.X shows the calibrated model tracking the measured temperature profile far more closely than the initial model across the campaign period. The average daily thermal profile in Figure 5.Y shows a similar gain: the calibrated model reproduces the daily rise and fall of temperature, including the amplitude of the swing, much more closely than the initial model, which had overestimated it. Together, the statistical indicators and the graphical comparison support treating the final calibrated model as a reliable representation of the contemporary case's measured thermal behavior, and as the base model for the parametric simulations that follow in this chapter.

5.3 Base case Thermal Performance Across the Three Cases

The comparisons across the five proposed strategies in the thesis are based on two time periods: the summer design week and the winter design week. These periods are used to evaluate the impact of key design elements—thermal mass and time lag, window-to-wall ratio (WWR), orientation, veranda, and spatial configuration—on the thermal performance of the three houses, and are consistently applied across all simulations.

5.3.1 Case 1 Thermal Performance of the Ottoman house

The following analysis is based on hourly DesignBuilder/EnergyPlus simulation output for the Ottoman house base case, covering a typical summer week (1–7 August) and a typical winter week (15–21 January), each comprising 168 consecutive hourly records. The building is evaluated in free-running mode, without natural ventilation or mechanical heating or cooling, so that the results isolate the passive thermal behavior of the house's mass, envelope and openings.

- Typical Summer Week (1–7 August)

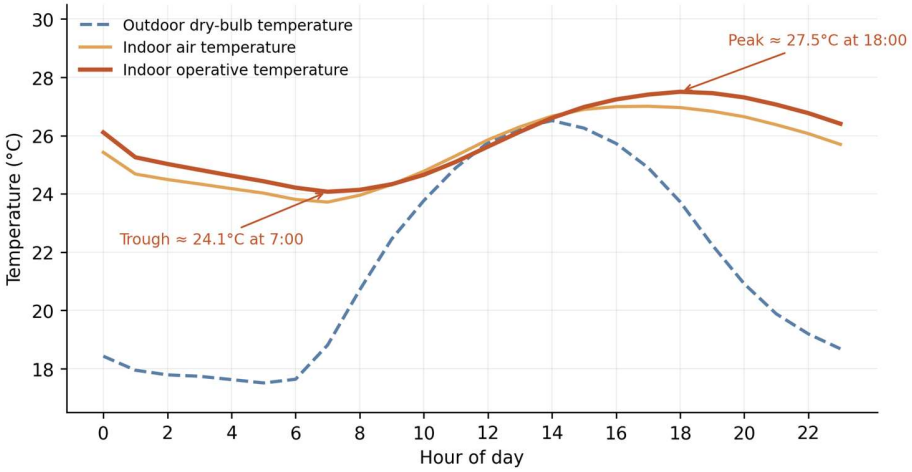


Figure 5-7: Operative temperature profile- Typical summer week for Ottoman case

Operative temperature: Over the simulated week, indoor air temperature ranged from 22.4°C to 28.8°C (mean 25.5°C), while operative temperature ranged from 22.6°C to 29.5°C (mean 25.8°C), against an outdoor dry-bulb range of 15.7–28.8°C (mean 21.5°C). The two indoor metrics track each other closely, with operative temperature exceeding air temperature by an average of only 0.33°C, rising to a maximum gap of 0.95°C during the hottest afternoon hours. This gap is driven almost entirely by the radiant component: mean radiant temperature sits 0.66°C above air temperature on average, reflecting the warming of internal wall and floor surfaces by absorbed solar and conductive heat. In a lightweight, low-mass building this radiant–air divergence would be negligible; its presence here is itself evidence that internal surfaces are behaving as active thermal storage elements rather than passive backdrops.

The diurnal pattern is markedly asymmetric. Outdoor temperature troughs at around 05:00 (mean 17.5°C) and peaks at approximately 14:00 (mean 26.5°C), giving a diurnal swing of roughly 9.0°C. Indoor operative temperature, by contrast, troughs at around 07:00 and does not peak until approximately 18:00, with a diurnal swing of only 3.4°C. This yields an apparent whole-building time lag of four hours between outdoor and indoor peaks, and a decrement factor of approximately 0.38 — meaning the house transmits only about 38 per cent of the outdoor diurnal amplitude into the occupied space. This is a whole-building (systems-level) figure that folds together envelope mass, opening behavior and internal air mixing; the material time lag of the thick stone masonry walls characteristic of Ottoman construction is typically longer still, but the building's openings, internal partitions and ventilation regime moderate the purely conductive signal.

The mechanism behind the four-hour lag is confirmed by the relationship between solar gains and indoor temperature. Solar gains through the exterior glazing peak at around 13:00, yet correlate very weakly with operative temperature at the same hour ($r \approx 0.06$). When solar gains are lagged by four hours, however, the correlation rises sharply to $r \approx 0.54$. In other words, the heat entering the building at midday is not felt immediately; it is first absorbed into the thermal mass of the walls, floors and internal partitions, stored, and only released into the space several hours later — precisely the delayed heat-release behavior that thick, high-capacity Ottoman construction is intended to produce. The consequence is that the hottest moment indoors coincides not with the sun's peak but with the early evening, after the outdoor air has already begun to cool. Occupants therefore experience a house that is coolest in the morning, when it is most useful for daytime activity, and warmest only in the evening, after peak outdoor heat has already passed.

This buffering is only partial, however, and its limits are visible across the week rather than only within a single day. Outdoor daily mean temperature rises steadily from 19.9°C (1 August) to 22.6°C (6–7 August), and indoor operative temperature rises in step, from a daily mean of 23.6°C to 27.6–27.9°C over the same period — a drift of roughly 4°C. Because thermal mass has no mechanism to discharge overnight when successive nights remain warm, each day's stored heat compounds with the next, so the house's advantage is strongest at the start of a hot spell and progressively erodes if the spell continues. This is an important qualification: thermal inertia is highly effective against single-day heat pulses but offers diminishing protection during a sustained multi-day heatwave, unless supported by strong night-time Ventilative purging.

- Adaptive Comfort Analysis and Discomfort Hours (ASHRAE Method)

Because occupancy heat gains in the model remain continuous (non-zero) through all 168 hours, consistent with a residential dwelling in which some occupant presence is assumed around the clock, the full week is treated as occupied for the purposes of this analysis.

The running mean outdoor temperature (Trm) was derived recursively from the week's own daily means, using the standard ASHRAE weighting $Trm(n) = 0.2 \cdot \bar{T}od(n-1) + 0.8 \cdot Trm(n-1)$, seeded from the first day's daily mean in the absence of an antecedent record. This produced a Trm rising from 19.9°C on 1 August to 21.2°C by 7 August, entirely within the 10–33.5°C range of validity for the ASHRAE 55

adaptive model. The corresponding neutral comfort temperature, Tcomf = 0.31·Trm + 17.8, therefore climbs modestly across the week, from 24.0°C to 24.4°C.

Table 5-1: Adaptive Comfort Performance: Comparison of 80% and 90% Acceptability Thresholds for Ottoman case (summer week)

Metric	80% acceptability (±3.5°C)	90% acceptability (±2.5°C)
Comfort hours	131 (78.4%)	110 (65.9%)
Discomfort hours	36 (21.6%)	57 (34.1%)

Set against the ASHRAE 80% criterion (the threshold conventionally used for naturally ventilated, non-air-conditioned buildings, and the more appropriate of the two bands for a passively operated house of this type), the Ottoman house achieves acceptable adaptive comfort for just over three-quarters of the summer week without any mechanical cooling. This is a creditable outcome for a free-running building and reflects the combined contribution of high thermal mass, modest window-to-wall ratios limiting direct solar penetration, and a spatial configuration (thick perimeter walls, small high-set openings, that historically evolved specifically to manage a semi-arid Mediterranean summer.

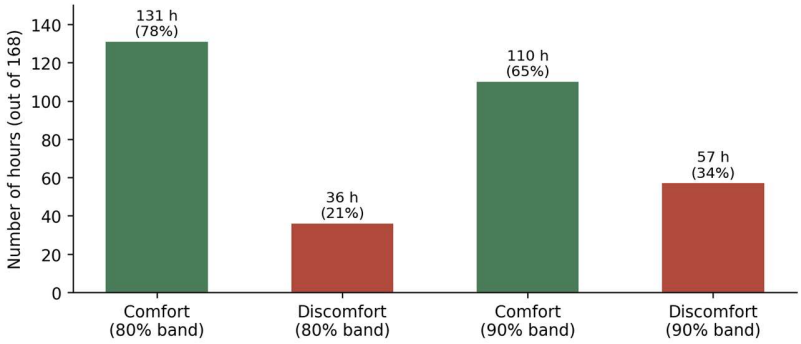


Figure 5-8: Discomfort Hours- Typical Summer Week (ASHRAE 55 Adaptive Comfort Model) for Ottoman base case

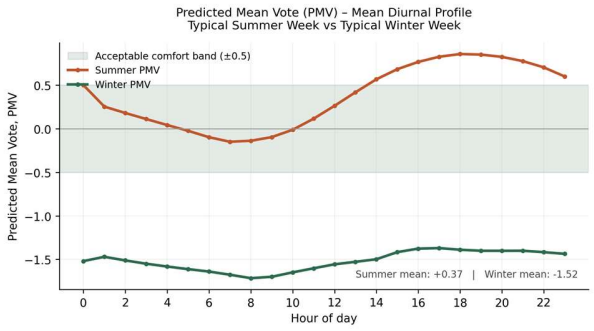
- PMV and PPD Analysis

Mean PMV across the summer week is +0.37, with a minimum of −0.52 and a maximum of +1.47. This places the average sensation between "neutral" and "slightly warm" on the Fanger seven-point scale, with excursions into the "warm" category during late-afternoon peaks. PMV follows the same diurnal shape as operative temperature: it is coolest at around 07:00 (mean −0.15) and warmest at around 18:00 (mean +0.86), again showing the four-to-five-hour delay behind the outdoor and solar peaks.

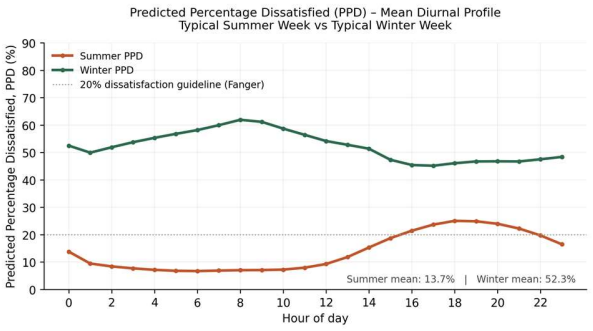
Of the 168 hours, 70 (41.7%) fall outside the ±0.5 acceptable PMV band; of these, 67 are on the warm side and only 3 on the cool side, confirming that summer discomfort in this building is overwhelmingly

an overheating phenomenon rather than a cold-stress one. Mean PPD is 13.7%, rising to a peak of 49.2% during the hottest evening hours — meaning that even at its worst, PMV-predicted dissatisfaction remains below half of occupants, and for most of the week remains in a range considered good-to-acceptable by Fanger's own classification (PPD < 20%).

The relationship between solar gains, thermal mass and PMV is the same delayed-release mechanism already established: solar gains absorbed near midday elevate internal surface temperatures, which in turn raise mean radiant temperature and, with it, PMV, but only after several hours of storage and re-radiation. The net effect is that the Ottoman house achieves acceptable thermal comfort without active cooling for the majority of the week, with dissatisfaction concentrated in a predictable evening window rather than distributed unpredictably across the day — a pattern that would, in occupied use, be amenable to simple behavioral adaptation (e.g. evening courtyard use, cross-ventilation, or evaporative measures) rather than requiring mechanical intervention.



PMV- Mean diurnal profile



PPD- Mean diurnal profile

Figure 5-9: PPD & PMV Graphs, typical summer week, Ottoman case

- Typical Winter Week

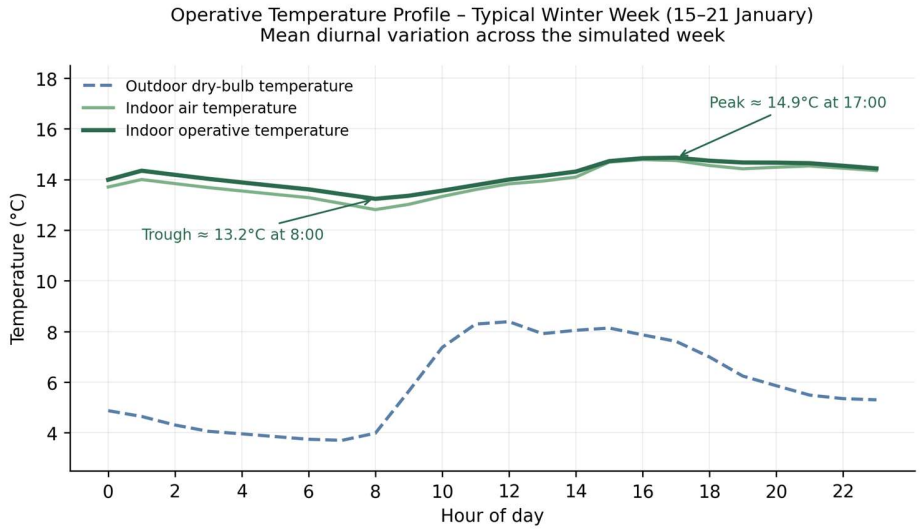


Figure 5-10: Operative temperature profile- Typical winter week for Ottoman case

Operative temperature: Over the winter week, indoor air temperature ranged from 10.9°C to 17.9°C (mean 13.9°C) and operative temperature from 11.2°C to 17.9°C (mean 14.2°C), against an outdoor dry-bulb range of 1.5–12.2°C (mean 5.9°C). As in summer, operative and air temperature track closely, with operative temperature averaging 0.23°C above air temperature — a smaller gap than in summer, since radiant surface temperatures are only modestly elevated (mean Trad–Tair = +0.46°C) in the absence of significant solar charging.

The diurnal pattern shows an outdoor trough at approximately 07:00 (mean 3.7°C) and an outdoor peak at approximately 12:00–13:00 (mean 8.4°C), a diurnal swing of about 4.7°C. Indoor operative temperature troughs at around 08:00 and peaks at around 17:00, an apparent time lag of roughly five hours and a diurnal swing of only 1.6°C — a decrement factor of approximately 0.35, closely comparable to the summer value. This consistency across two very different seasons is itself notable: it indicates that the damping and delaying behavior of the house is a structural property of its mass and envelope, largely independent of the direction or magnitude of the outdoor swing being damped.

The more consequential feature of the winter week, however, is not the diurnal cycle but the week-long synoptic trend. Outdoor daily mean temperature falls from 8.0°C on 15 January to a minimum of 3.2°C on 18 January, before recovering slightly to around 6°C by the week's end. Indoor operative temperature mirrors this trend with a lag of roughly one day, falling from a daily mean of 16.8°C to a minimum of

12.2°C on 19 January, before a partial, incomplete recovery to around 13.0°C. Two things follow from this. First, the house's thermal mass again buffers and delays the cold spell rather than transmitting it directly — the indoor minimum arrives a day after the outdoor minimum. Second, and less favorably, the same mass that buffers the cold spell also resists recovering from it: once the fabric has cooled through several consecutive cold days, it re-warms only slowly even as outdoor conditions improve, because there is no internal heat source in this free-running model to accelerate the process. This is the mirror image of the summer heatwave-accumulation effect: thermal mass smooths transients in both directions, but in a passive-only building it cannot manufacture heat that was never supplied, so a cold spell leaves a lingering thermal deficit that a compensating warm spell alone does not fully erase within the observed week.

- Adaptive Comfort Analysis and Discomfort Hours (ASHRAE Method)

Applying the same recursive method, running mean outdoor temperature for the winter week falls from 7.96°C to 6.18°C, with a corresponding Tcomf of 19.7–20.3°C. This Trm range sits below the 10°C lower bound of validity stipulated for the ASHRAE 55 adaptive model, which was developed and validated for naturally ventilated buildings under warm-to-temperate running-mean conditions. Strictly speaking, the adaptive model should not be applied to characterize winter comfort in this case, and the figures below are therefore reported only as a diagnostic comparison, not as the primary winter comfort verdict — that role is more properly filled by the static PMV/PPD (Fanger) model discussed in Section 3, which has no such lower-bound restriction.

Table 5-2: Adaptive Comfort Performance: Comparison of 80% and 90% Acceptability Thresholds for Ottoman case (winter) week)

Metric	**80% acceptability (±3.5°C)**	**90% acceptability (±2.5°C)**
Comfort hours	18 (10.8%)	2 (1.2%)
Discomfort hours	149 (89.2%)	165 (98.8%)

Read diagnostically, these figures simply confirm what is already evident from the raw temperatures: an unheated Ottoman house in mid-January, however well-buffered thermally, cannot on its own reach a neutral comfort temperature in the 20°C region purely through passive means — no vernacular envelope, however massive, generates heat; it can only conserve and redistribute what enters it. The genuine finding here is therefore not that adaptive comfort standards are "failed" in a numerical sense, but that winter

passive performance must be judged by how much thermal mass reduces the severity of cold discomfort relative to a lightweight, poorly buffered alternative, and by how it shapes the daily distribution of that discomfort (see Section 3) — not by whether it eliminates the need for supplementary heating altogether, which no unheated envelope could do in this climate.

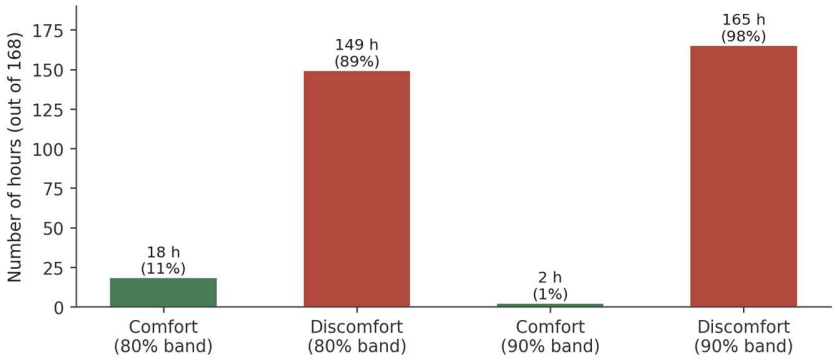


Figure 5-11: Discomfort Hours- Typical winter Week (ASHRAE 55 Adaptive Comfort Model) for Ottoman base case

- PMV and PPD Analysis

Mean PMV across the winter week is −1.52, with a minimum of −2.10 and a maximum of −0.78 — placing the entire week's sensation between "cool" and "cold" on the Fanger scale, and never once inside the ±0.5 neutral band. All 168 hours (100%) therefore register as cold-discomfort hours under the static PMV criterion. Mean PPD is 52.3%, ranging from 17.7% at its mildest to 81.1% at its most severe.

The diurnal pattern of PMV again lags the outdoor cycle: the coldest predicted sensation occurs at around 08:00 (mean PMV −1.72, PPD 61.9%), roughly one hour behind the outdoor temperature trough, while the least-cold sensation occurs at around 17:00 (mean PMV −1.37, PPD 45.1%), five hours behind the outdoor peak — the same lag structure identified in the temperature data, now expressed in comfort terms. Relative humidity over the week is comparatively stable (36–68%, mean 55.8%) relative to its summer counterpart, consistent with a more tightly closed winter ventilation regime that limits both heat loss and moisture exchange with the outdoor air.

These results should be read as characterizing a fully free-running, unheated building, and are consistent with the house's designed reliance in the historical Ottoman context on supplementary heating (braziers, hearths) during the coldest months rather than on envelope performance alone. The value of thermal mass in winter, on this evidence, lies not in eliminating the need for heating but in narrowing the range of indoor conditions (PMV spans only 1.3 units across the week, against an outdoor swing of over 10°C) and in

delaying and softening the arrival of the coldest hours, both of which would materially reduce the heating load and improve occupant experience relative to a lightweight structure exposed to the same climate.

5.3.2 Case 2 Indoor Thermal Performance of the Jordanian house

This section examines the indoor thermal performance of the Jordanian period house through operative temperature and the level of thermal satisfaction, based on Fanger's model (PPD& PMV) and the adaptive thermal comfort model (ASHRAE Method).

- Typical Summer Week (1–7 August)

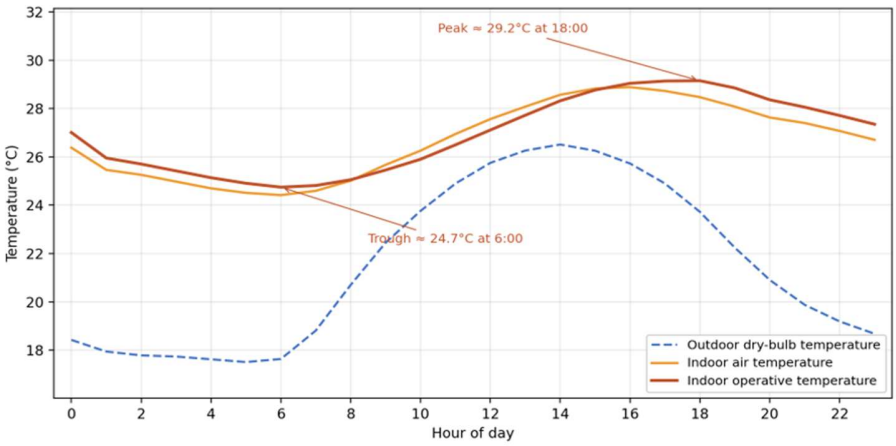


Figure 5-12: Operative temperature profile (Typical summer week), Mean diurnal variation

- Adaptive Comfort Analysis and Discomfort Hours (ASHRAE Method)

The ASHRAE 55 adaptive model can be applied to the summer week without qualification, since the running mean outdoor temperature of 19.8 to 21.3°C falls comfortably within the standard's valid range. Under this model, 103 of the 168 hours (61%) fall within the 80% acceptability band and 65 (39%) fall outside it; the narrower 90% band admits 79 hours (47%) and excludes 89 (53%). These figures sit close to, but somewhat more permissive than, the static PMV criterion, which places 104 hours (61.9%) outside the ±0.5 comfort range, of which 77 register as warm-side discomfort and 27 as cool-side. The two methods diverge in this direction because the adaptive model allows the comfort zone to shift upward with a warm outdoor running mean, so hours that Fanger's fixed-clothing assumption would flag as slightly warm can still register as acceptable once occupants are assumed to adapt their clothing and behavior to the season. Even so, the broad pattern holds across both methods: discomfort in the Jordanian house during summer is concentrated in the afternoon and early evening, when PPD rises toward its peak of 82.5% and

PMV moves furthest into the warm half of the scale, while the 20% dissatisfaction guideline is met for 107 of the 168 hours (64%). Read alongside the PMV and PPD results, the adaptive comfort figures do not describe a different thermal condition so much as a more forgiving standard applied to the same one, and the residual discomfort they still register in the late afternoon points to the same overheating mechanism identified in the static analysis rather than to any inconsistency between the two.

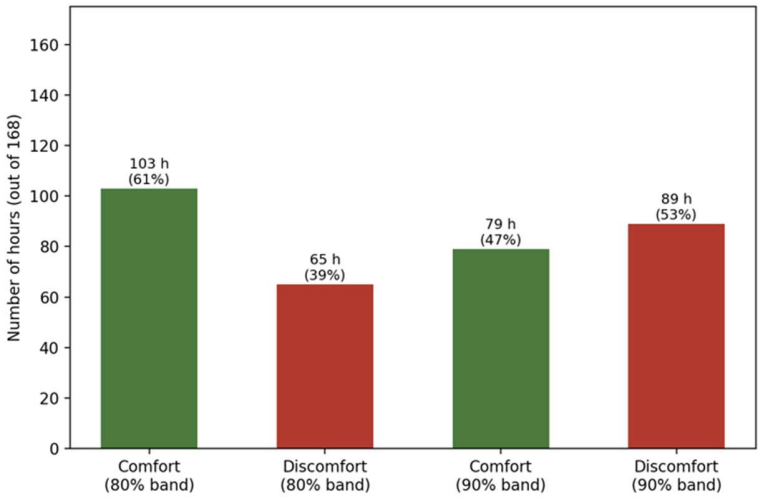


Figure 5-13: Discomfort Hours- Typical summer Week (ASHRAE 55 Adaptive Comfort Model) for Jordanian period base case

- PMV and PPD Analysis

Mean PMV across the summer week is +0.47, with a minimum of −0.94 and a maximum of +2.14. This places the average sensation between "neutral" and "slightly warm" on the Fanger seven-point scale, with excursions into the "warm" and "hot" categories during late-afternoon peaks. PMV follows the same diurnal shape as operative temperature: it is coolest at around 06:00 (mean −0.26) and warmest at around 18:00 (mean +1.19), again showing the four-to-five-hour delay behind the outdoor and solar peaks.

Of the 168 hours, 104 (61.9%) fall outside the ±0.5 acceptable PMV band; of these, 77 are on the warm side and 27 on the cool side, confirming that summer discomfort in this building is predominantly an overheating phenomenon, though with a more pronounced cool-morning tail than in the Ottoman case. Mean PPD is 22.8%, rising to a peak of 82.5% during the hottest afternoon hours — meaning that at its worst a large majority of occupants would be predicted dissatisfied, though for 107 of the 168 hours (64%) PPD remains below the 20% guideline considered good-to-acceptable by Fanger's own classification.

The relationship between solar gains, thermal mass and PMV follows the same delayed-release mechanism established for the Ottoman case: solar gains absorbed near midday elevate internal surface temperatures, which in turn raise mean radiant temperature and, with it, PMV, but only after several hours of storage and re-radiation. The net effect is that the Jordanian house shows a narrower comfortable margin than the Ottoman house over the same week, with a higher proportion of hours falling outside the acceptable PMV band and a markedly higher peak PPD, consistent with a lighter-mass envelope offering less buffering against the diurnal swing.

- Typical Winter Week (15-21 Jan)

Air temperature and Operative temperature: Over the winter week, indoor air temperature ranged from 8.8°C to 16.7°C (mean 12.2°C) and operative temperature from 8.4°C to 16.1°C (mean 11.7°C), against an outdoor dry-bulb range of 1.5–12.2°C (mean 5.9°C). As in summer, operative and air temperature track closely, with operative temperature lagging the outdoor trough by roughly two hours and running consistently colder than the Ottoman house's equivalent winter profile (mean 14.2°C), a pattern consistent with reduced thermal mass and a less airtight envelope. These figures simply confirm what is already evident from the raw temperatures: an unheated Jordanian house in mid-January, however well-buffered thermally, cannot on its own reach a neutral comfort temperature in the 20°C region purely through passive means — no vernacular or transitional envelope, however massive, generates heat; it can only conserve and redistribute what enters it. As with the Ottoman case, the genuine finding here is not that adaptive comfort standards are "failed" in a numerical sense, but that winter passive performance must be judged by how much thermal mass reduces the severity of cold discomfort relative to a lightweight, poorly buffered alternative, and by how it shapes the daily distribution of that discomfort — not by whether it eliminates the need for supplementary heating altogether, which no unheated envelope could do in this climate.

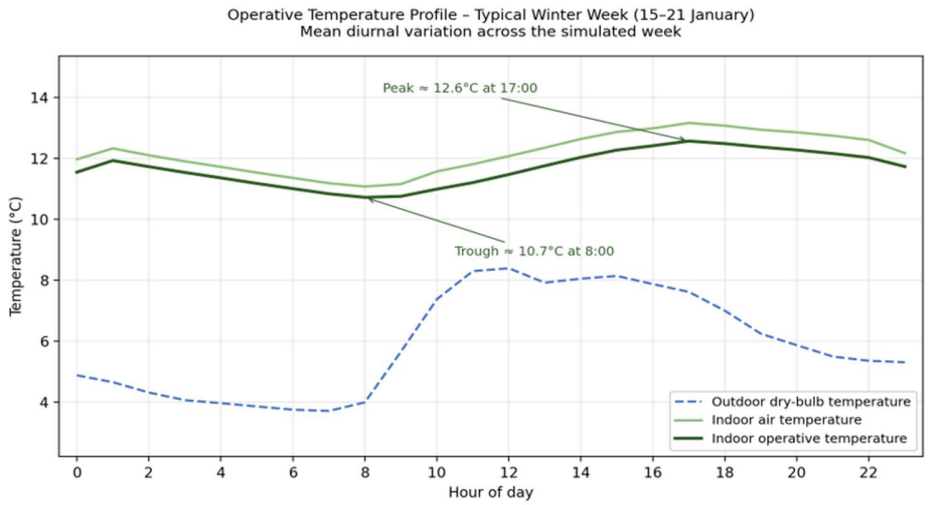


Figure 5-14: Operative temperature Profile- Typical winter week, Mean diurnal variation across the simulated week

- Adaptive Comfort Analysis and Discomfort Hours (ASHRAE Method)

Applying the ASHRAE 55 adaptive model to the winter week produces a result that agrees with the static PMV and PPD findings rather than adding a separate line of evidence. The running mean outdoor temperature for the period is 5.7 to 7.9°C, below the standard's 10°C lower limit of applicability, so the adaptive bands calculated here function as a diagnostic check rather than a formal acceptability test. Under those bands, all 168 hours of the week fall outside both the 80% and 90% comfort limits, giving zero comfort hours by either criterion. This outcome is consistent with the Fanger analysis: mean PMV for the week is −2.49 and never rises above −1.54, and mean PPD is 88.6%, so a building already classified as uniformly cold under the static model has no real chance of falling inside an adaptive band set several degrees above its actual operative temperature range of 8.4 to 16.1°C. The coincidence of these two results is expected rather than incidental, since both methods are reading the same underlying condition: an unheated house whose winter operative temperature sits too far below neutral for behavioral adjustments, such as clothing changes or activity levels, to close the gap. Taken together with the discomfort-hours count, the adaptive comfort results should be read as confirmation of the severity already established by PMV and PPD, not as an independent finding, and they should not be used on their own to argue that the passive envelope has failed some absolute test of adaptive comfort, given that the model was never intended to be applied at these outdoor temperatures in the first place.

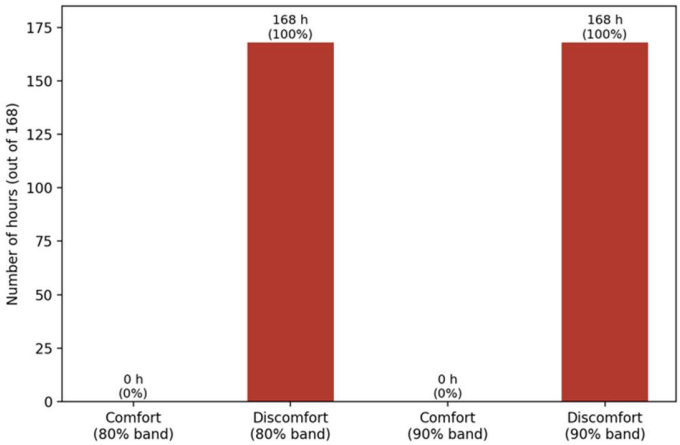


Figure 5-15: Discomfort Hours- Typical winter Week (ASHRAE 55 Adaptive Comfort Model) for Jordanian period base case

- PMV and PPD Analysis

Mean PMV across the winter week is −2.49, with a minimum of −3.22 and a maximum of −1.54 — placing the entire week's sensation between "cold" and "cool" on the Fanger scale, and never once inside the ±0.5 neutral band. All 168 hours (100%) therefore register as cold-discomfort hours under the static PMV criterion, a colder distribution than the Ottoman house's equivalent winter week (mean PMV −1.52). Mean PPD is 88.6%, ranging from 53.1% at its mildest to 99.7% at its most severe.

The diurnal pattern of PMV again lags the outdoor cycle: the coldest predicted sensation occurs at around 08:00 (mean PMV −2.72, PPD 93.7%), roughly consistent with the outdoor temperature trough, while the least-cold sensation occurs at around 17:00 (mean PMV −2.30, PPD 83.4%), reflecting the same delayed thermal response seen in the Ottoman case but shifted toward more severe and more consistently high dissatisfaction throughout the day — evidence of a building that stores and re-releases comparatively less solar and internal heat than the Ottoman house across the winter week

5.3.3 Case 3: Indoor Thermal Performance of the Contemporary house

This section examines the indoor thermal performance of the Jordanian period house through operative temperature and the level of thermal satisfaction, based on Fanger's model (PPD& PMV) and the adaptive thermal comfort model (ASHRAE Method).

- Typical Summer Week (1–7 August)

Operative Temperature: The simulated indoor operative temperature for the contemporary base case, evaluated over the representative summer week (1–7 August), ranged from a minimum of 24.65°C to a maximum of 32.72°C, giving an overall diurnal-to-weekly range of 8.07°C and a weekly mean of 28.26°C. This range confirms that the free-running zone tracks the outdoor thermal cycle closely in amplitude, since the outdoor dry-bulb temperature over the same period varied between 18.52°C and 28.59°C (mean 23.10°C) — the indoor operative swing is, in fact, wider than the outdoor swing, indicating that solar and internal gains, rather than outdoor air temperature alone, are driving much of the indoor thermal profile.

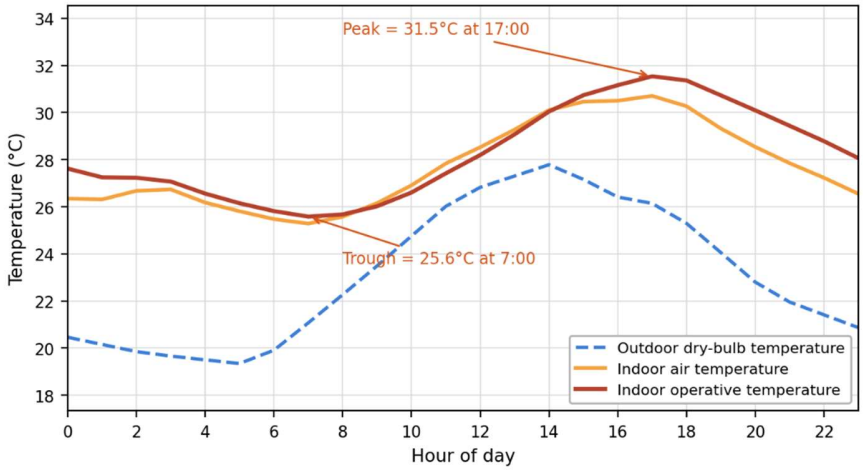


Figure 5-16: Operative temperature profile -Typical summer week, Mean diurnal variation across the simulated week

The daily behavior is highly repeatable. The hourly-averaged profile across the week shows the operative temperature reaching its minimum consistently between 06:00 and 08:00 (around 25.6–25.8°C), then rising steadily through the morning, crossing 28°C by roughly midday, and peaking in the late afternoon at 17:00 on six of the seven days (reaching 18:00 on one day), with values in the 30.6–32.7°C range at the daily maximum. Seasonally — in the sense of week-to-week drift within the campaign — the daily peak also trends upward over the week, from 30.73°C on 1 August to 32.72°C on 6 August, tracking a corresponding rise in outdoor conditions rather than representing a change in building behavior.

Assessed against ASHRAE 55, two comfort frameworks are relevant here. Under the adaptive comfort model (ASHRAE 55 / EN 16798-1), appropriate for this free-running, naturally ventilated residential building, the 80% acceptability band can be estimated from the prevailing mean outdoor temperature of 23.10°C as approximately 21.5–28.5°C (using Tcomf = 0.31 Trm + 17.8 ± 3.5°C; this is a simplified

single-week proxy for the running mean rather than a full 30-day antecedent record, and should be read as indicative). Against this band, the early morning and mid-morning hours (06:00–12:00, operative temperatures of 24.7–28.2°C) sit comfortably within the acceptable range, but the afternoon and evening block — roughly 14:00 to 21:00, when operative temperatures exceed 29°C and reach as high as 32.7°C — pushes well above the upper adaptive comfort limit on every day of the simulated week. In practical terms, this means the contemporary base case, left to free-run under summer conditions, is only comfortable for roughly half of each 24-hour cycle; the remainder, concentrated in the afternoon-to-evening period when occupants are typically most active in a residential setting, constitutes a sustained overheating condition rather than an occasional exceedance.

- PMV and PPD Analysis

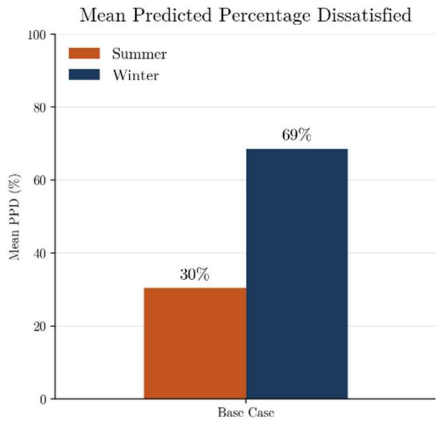


Figure 5-17: PPD Graph, case 3

The corresponding PPD values, calculated from PMV using the standard Fanger relationship, range from 5.0% (at the single hour where PMV was closest to neutral) to 88.6% (coinciding with the PMV peak of +2.31), with a weekly mean PPD of 30.5%. This mean value is three times the 10% threshold that ISO 7730 Category II (and the equivalent ASHRAE 55 PMV-PPD comfort criterion) specifies for an acceptable general thermal environment, and it exceeds even the more permissive Category III threshold of 15%. The hours of peak dissatisfaction (PPD approaching 89%) occur during the same late-afternoon window (broadly 15:00–19:00) identified as the operative temperature peak period, confirming that the discomfort is being driven by elevated radiant and air temperatures during peak solar and internal gain hours rather than by any humidity or air-movement effect isolated from the temperature signal. It is worth noting, however, that the PMV-PPD index itself assumes fixed clothing and metabolic rate inputs

consistent with a mechanically conditioned environment; in a real free-running dwelling, occupants retain some adaptive capacity (clothing adjustment, activity pacing, shading, window operation) that the static PMV-PPD calculation cannot capture, so the reported dissatisfaction levels should be read as an upper-bound, standardized indicator of thermal stress rather than a literal prediction of occupant complaint rates.

- Discomfort Hours

Using the ISO 7730 / ASHRAE 55 PMV-PPD comfort threshold of $|PMV| \leq 0.5$ (equivalent to the 10% PPD boundary for Category II) as the criterion for acceptable thermal conditions, 116 of the 167 simulated hours — 69.5% of the analyzed week — fall outside this comfort band and are classified as discomfort hours. Every one of these 116 hours falls on the warm side of the scale ($PMV > +0.5$); there are zero hours of cold-side discomfort ($PMV < -0.5$) anywhere in the dataset. This is an unambiguous, single-direction result: whatever thermal performance problem the contemporary base case exhibits in summer, it is entirely an overheating problem, with no offsetting cold-discomfort periods to average against it.

The scale of this figure is significant for evaluating the contemporary base case's summer performance. A discomfort incidence of nearly 70% of occupied hours indicates that, under the conditions represented by the field-calibrated summer week, the building spends more time outside the acceptable comfort band than within it, and that the free-running strategy alone — without supplementary cooling, shading intervention, or ventilation optimization — is insufficient to maintain acceptable conditions through a typical Abu Dis summer day. Given that discomfort concentrates specifically in the afternoon-to-evening hours when residential occupancy and activity levels are typically highest, the practical consequence for occupants is that the period of greatest use coincides almost exactly with the period of greatest thermal stress. This establishes the contemporary base case's comfort baseline against which the parametric strategies examined elsewhere in this chapter are subsequently evaluated, with any reduction in the 69.5% discomfort-hour figure or in mean PPD serving as a direct, quantifiable measure of a given strategy's contribution to summer comfort performance.

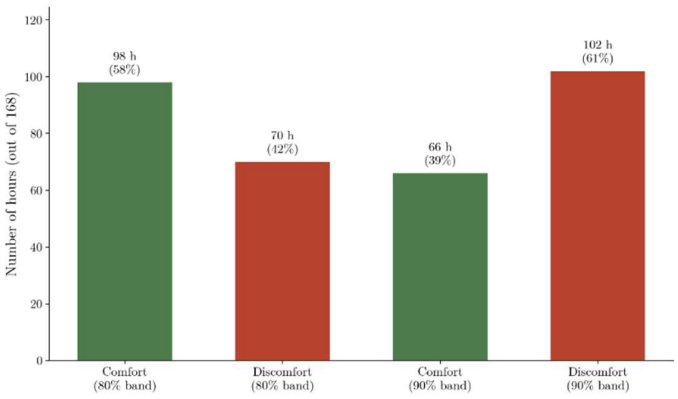


Figure 5-18: Discomfort hour, Typical summer week, contemporary case

- Typical winter week

Operative Temperature: Over the 15–21 January simulated week, indoor operative temperature ranged from a minimum of 11.09°C (21 January, 08:00) to a maximum of 17.93°C (17 January, 16:00), giving a weekly mean of 14.55°C and a range of 6.84°C — narrower than the corresponding summer swing (8.07°C), and, critically, sitting entirely below any recognized winter comfort threshold rather than straddling one. The daily pattern is the mirror image of the summer profile: operative temperature reaches its daily minimum consistently in the mid-morning, between 08:00 and 09:00 on six of the seven days, rather than at dawn as might be assumed, reflecting the time needed for the building to lose the last of the previous evening's accumulated heat before solar gain begins to reverse the decline; it then climbs through the day to a daily maximum concentrated between 16:00 and 17:00 on five of the seven days, coinciding with the point of maximum solar gain through the glazing before outdoor temperatures begin their evening fall.

Against the ASHRAE 55 adaptive comfort model, using the week's mean outdoor dry-bulb temperature of 8.53°C as the running-mean proxy, the estimated 80% acceptability band sits at approximately 16.9–23.9°C. Measured against this band, 146 of the 167 simulated hours (87.4%) fall below the lower comfort limit, and using the stricter 90% acceptability band (17.9–22.9°C), every single simulated hour (167/167, 100%) falls below the lower limit. Even the warmest hour of the entire week, 17.93°C, only just clears the 80% band's lower boundary and remains well short of the adaptive comfort center point of 20.4°C. This stands in direct contrast to the summer result, where the building spent roughly 30% of hours within the comfort band; in winter, under free-running conditions, the base case effectively spends none of the week within an acceptable thermal range by any adaptive comfort measure.

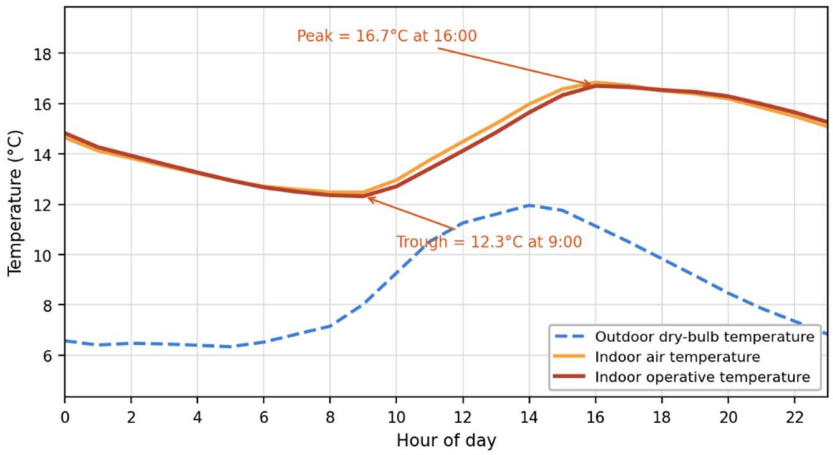


Figure 5-19: Operative Temperature Profile- Typical winter week, Mean diurnal variation across the simulated week

- PMV& PPD Analysis

The winter PMV record shows a thermal sensation profile that is the mirror image of summer in direction but more severe in magnitude. PMV ranges from −2.63 to −1.13 across the week, with a mean of −1.87 — placing the average winter sensation firmly in the "cool" band of the seven-point scale, and at no point during the entire 167-hour period does the value rise even into the "slightly cool" category, let alone neutral. Categorizing the hours: 126 (75.4%) register as cool (−1.5 to −2.5), 35 (21.0%) as slightly cool (−0.5 to −1.5), and 6 (3.6%) — the seven daily minima — cross into the cold band (below −2.5). Not a single hour of the week registers neutral, slightly warm, warm, or hot sensation.

The daily pattern is tightly repeatable: PMV reaches its coldest point between 08:00 and 09:00 on every one of the seven days (the same window already identified as the operative temperature minimum), with values as low as −2.63 (21 January, 08:00), and its least-cold point in the late afternoon, between 16:00 and 18:00, where PMV recovers only as far as roughly −1.13 to −1.5 — still solidly in the "cool" range even at its daily best. This confirms that solar gain through the afternoon is enough to pull the sensation back from "cold" toward "cool," but never far enough to reach a neutral or acceptable sensation at any hour of the free-running week.

The corresponding PPD values are correspondingly severe: they range from 32.0% at the mildest hour of the week to 95.8% at the coldest, with a weekly mean of 68.7%. This mean is nearly seven times the 10% ISO 7730 Category II acceptability threshold, and even the single best hour of the entire week — the absolute minimum PPD recorded — still sits more than three times above that threshold. Framed against the summer result (mean PPD 30.5%), the winter condition is markedly more severe: not only is winter

discomfort universal rather than partial, the average predicted dissatisfaction rate in winter (68.7%) is more than double the summer average, indicating that the cold-season failure mode is a harsher one for occupants than the warm-season failure mode, at least as captured by the static PMV-PPD index.

- Discomfort Hours

Applying the same |PMV| > 0.5 threshold used for the summer analysis, all 167 simulated hours (100%) register as discomfort hours, and every one of them is cold-side discomfort (PMV < −0.5); there are zero hours of warm-side discomfort anywhere in the week. This is an even more one-sided result than the summer case, where 69.5% of hours were uncomfortable with the remaining 30.5% falling within the neutral band — in winter, the free-running contemporary base case provides no comfortable hours at all, at any time of day, on any day of the simulated week.

The significance of this result is considerable when set against the summer benchmark. Where the summer base case oscillated between an acceptable morning and an overheated afternoon, the winter base case never crosses into acceptability at any point in its daily cycle — the building's passive heat balance narrows the gap to outdoor conditions (as shown by the indoor-outdoor offset discussed previously) but never closes it far enough to register even a single neutral hour. This establishes that, of the two seasonal extremes evaluated for the contemporary base case, winter under-heating is the more severe and more uniformly distributed comfort failure, and it is this 100% cold-discomfort, zero-neutral-hour baseline that any winter-oriented design strategy examined later in this chapter must be judged against.

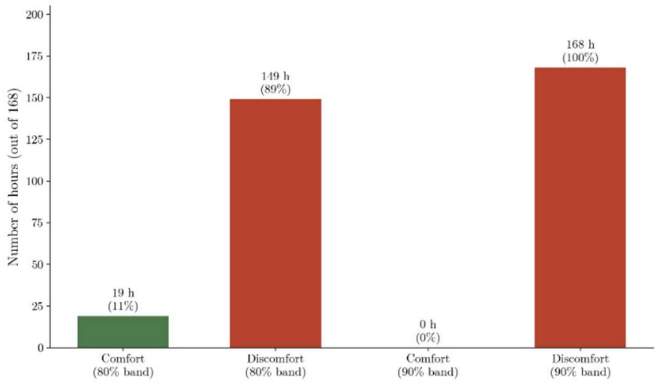


Figure 5-20: Discomfort hour, Typical winter week, contemporary case

5.4 Results of the Parametric Simulation Strategies

5.4.1 Strategy 1 — Wall Thermal Mass and Time Lag

The use of hourly surface-temperature output from a dynamic simulation tool to determine time lag is well established in the building physics literature. Kontoleon and Bikas (2007) demonstrated that the phase shift between outdoor and indoor wall-surface temperatures under realistic, non-sinusoidal periodic boundary conditions can be extracted directly from a dynamic thermal-network simulation, and used this approach to quantify how wall composition and surface absorptivity govern time lag and decrement factor. This validates the general principle applied here: that time lag is not solely a property to be derived from closed-form analytical equations under idealized sinusoidal assumptions, but is equally, and often more reliably, obtained from the transient surface-temperature response generated by a validated dynamic simulation.

This is directly applicable to the EnergyPlus environment used in the present study, since EnergyPlus solves transient conduction through multilayer constructions using Conduction Transfer Functions (CTFs), a numerical method that reproduces the same delayed, damped surface-temperature response captured by dynamic thermal-network models (Crawley et al., 2001). Because the CTF algorithm accounts for the coupled sequence of dense and lightweight layers within the wall section, rather than treating each layer as an isolated, the resulting Surface Outside Face Temperature and Surface Inside Face Temperature outputs already embed the full phase-shift behavior of the wall as built. Extracting time lag as the peak-to-peak difference between these two outputs is therefore a physically sound and literature-supported method, not a simplification of the underlying physics.

- Case 1: Ottoman Period House

The time lag and the decrement factor are the two principal indicators used to characterize the dynamic thermal performance of an opaque building element under a diurnal temperature cycle. For the Ottoman case wall — a 900 mm solid limestone leaf with a 30 mm internal lime-plaster finish — this report compares two independent routes to these parameters: an analytical solution following the periodic heat-transfer matrix method of ISO 13786, and an empirical determination taken directly from the paired Inside Surface Temperature and External Surface Temperature outputs of the calibrated

DesignBuilder/EnergyPlus model. The purpose is to establish which method is the more appropriate basis for characterizing this wall, and to situate the discrepancy between the two against established literature.

The analytical method treats the wall as an isolated heat-transfer element by applying a sinusoidal 24-hour temperature wave to its external surface and solving the one-dimensional transient conduction problem using the complex-admittance (transfer-matrix) formulation. The calculation is based on the thermal diffusivity of each layer, the periodic penetration depth, and the thickness ratio ξ=d/δ\xi = d/\deltaξ=d/δ. For the composite wall, the complex matrices of the individual layers were multiplied in their actual physical sequence, starting with the limestone layer followed by the internal plaster layer.

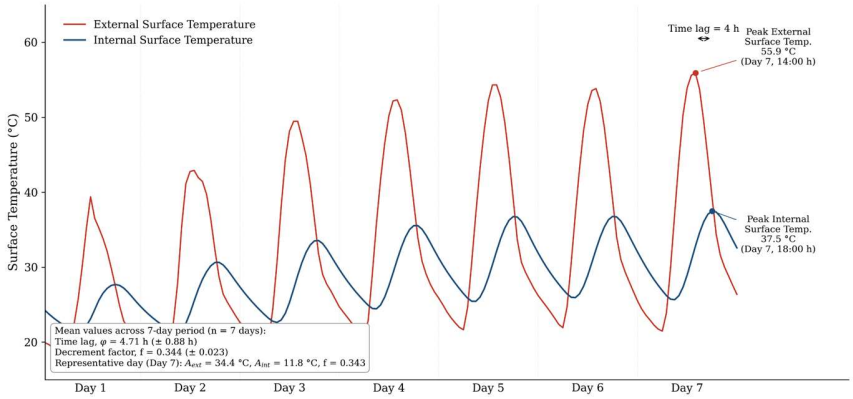


Figure 5-21: Thermal Response of the Ottoman Case wall Assembly (External vs Internal Surface temperature, 1-7 Aug simulation Period)

First, thermal diffusivity is found from thermal conductivity, density, and specific heat capacity — it shows how fast heat moves through the material. From thermal diffusivity, the periodic penetration depth is derived: how far a daily heat wave travels before losing most of its strength. Dividing the wall thickness by the penetration depth gives a ratio: a low ratio means little resistance to the wave; a high ratio means the wall far exceeds the wave's reach. For the 900 mm Ottoman limestone wall, this ratio is roughly 9.4, so attenuation is very strong.

Next, a complex parameter is calculated to capture the wall's full dynamic response — both amplitude reduction and phase shift. From this parameter come two indicators: the decrement factor, obtained as one divided by the magnitude of that complex parameter, which is the fraction of the outdoor swing still felt indoors; and the time lag, the delay in hours between outdoor and indoor peaks.

Finally, the areal heat capacity, obtained by multiplying density, specific heat capacity, and wall thickness together, measures how much heat the wall can store — the physical basis for its ability to delay and dampen the fluctuation.

In contrast, the empirical method derives time lag and decrement factor directly from the actual surface temperature time series generated by the full building simulation. The calculation is based on the measured peak-to-peak time interval and amplitude ratio between the external and internal surface temperatures, averaged over seven simulated August days. Unlike the analytical approach, this method includes the effects of solar radiation, longwave radiant exchange, and convective interactions within the occupied zone, therefore representing the wall's effective in-situ thermal behavior under realistic operating conditions.

Table 5-3: Comparison of Dynamic Thermal Properties between ISO 13786 Analytical Calculations and DesignBuilder Simulation Results

Parameter	**Analytical (ISO 13786)**	**Empirical (DesignBuilder output)**
Decrement factor, f	0.000138	0.344 (± 0.023)
Time lag, φ	12.66 h (mod 24h); 36.66 h true delay	4.71 h (± 0.88 h)
U-value	0.7505 W/m²K	0.727 W/m²K
Areal heat capacity, κ	2200.3 kJ/m²K	

The analytical result is consistent with the classical numerical basis established by Asan and Sancaktar (1998) and Asan (2000), who solved the transient conduction equation for composite walls under idealized periodic convective boundary conditions and showed that decrement factor falls approximately exponentially, while time lag rises near-linearly, with increasing thermal mass thickness. Ulgen (2002) confirmed similar trends experimentally for a range of masonry thicknesses under comparable idealized conditions. Both studies support the analytically derived near-total damping (f = 0.000138) obtained for a wall this thick relative to its periodic penetration depth.

The scale of the discrepancy with the empirical result, however, is well documented rather than anomalous. Gasparella et al. (2011) directly compared analytical periodic solutions against dynamic whole-building simulation and found systematic divergence once solar radiation and the full surface heat

balance are included — precisely the pattern observed here. Mazzeo, Oliveti and Arcuri (2016) quantified this further, showing that solar radiation incident on both outer and inner faces, together with radiative and convective coupling to the room, substantially raises the effective decrement factor and shortens the effective time lag relative to the idealized analytical case — again in the same direction as the present results. Ruivo, Ferreira and Vaz (2013) explicitly caution against using a single constant decrement factor/time-lag pair to predict wall heat gains, since real walls operate under non-sinusoidal, radiation-influenced conditions rather than the idealized periodic-convective case assumed analytically; the Ottoman wall's results closely match this caution. Evola, Margani and Marletta (2017), studying a comparably massive traditional stone wall in Mediterranean Sicily, similarly concluded that heavyweight masonry of this kind is best characterized through coupled dynamic simulation validated against field measurement, since closed-form periodic solutions cannot capture the coupled radiative environment of an occupied room.

On this evidence, the simulation-derived (empirical) time lag and decrement factor are judged the more appropriate values for characterizing the Ottoman case wall's actual in-situ thermal behavior, since they capture the radiative and convective coupling that the literature identifies as dominant for massive, solar-exposed masonry. The analytical ISO 13786 result nonetheless retains value as a bounding case: it isolates the wall's pure conductive contribution and demonstrates that, absent any solar or radiative coupling, this assembly's thermal mass alone would be sufficient to almost fully decouple the interior face from the outdoor diurnal cycle. Reporting both figures together, rather than either in isolation, follows the position taken by Gasparella et al. (2011) and Ruivo et al. (2013), and gives a more complete characterization than either method alone.

- Case 2: Jordanian Period House

Across the full summer design week (1–7 August), indoor operative temperature ranged from a weekly minimum of 25.59°C to a weekly maximum of 34.74°C. On the peak diurnal cycle (7 August) considered in isolation, the daily operative range was 30.79–34.74°C, an amplitude of 3.95°C, against an outdoor dry-bulb range of 17.62–28.75°C, an amplitude of 11.12°C — a reduction in daily swing of roughly 65 per cent. Figure 5.4.1a illustrates this diurnal response, plotting outdoor air, external surface, internal surface, and operative temperature together and showing clearly both the delayed, flattened internal response and the mismatch between the external surface's solar-driven peak and the outdoor air's later peak.

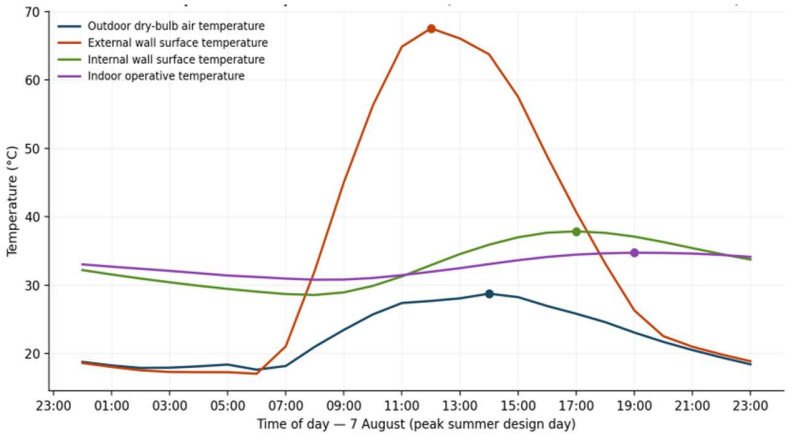


Figure 5-22: Diurnal temperature response, Case 2 Wall, 7 August (peak summer design day)

A second pattern emerges when the full week is examined rather than a single day. Figure 5.4.1b shows that both outdoor and indoor operative temperatures rise progressively across the seven simulated days: the daily operative range climbs from (25.59–27.32°C) on 1 August to (30.79–34.74°C) on 7 August, tracking a comparable rise in outdoor conditions from (17.68–22.73°C) to (17.62–28.75°C) over the same period. This upward drift across a sustained warm spell is a meaningful finding in its own right. It indicates that the thermal mass of Case 2 Wall, while effective at damping the swing within any single day, is also accumulating heat across successive hot days faster than it is able to shed it overnight — a form of progressive thermal charging. Under a short-lived hot spell, this mass would be expected to discharge fully overnight and the building would return to a stable baseline; under a sustained multi-day heatwave, as simulated here, the wall's stored heat appears to compound day-on-day, gradually eroding the short-term buffering advantage that thermal mass otherwise provides. This has a direct bearing on the vernacular argument developed later in this section: thick masonry construction is best suited to climates and building-use patterns — such as traditional occupancy with night-time cross-ventilation and thick-walled courtyard cooling — that allow the stored heat to be actively purged each night, rather than to fully sealed, mechanically ventilated modern occupancy patterns where that nightly discharge does not occur.

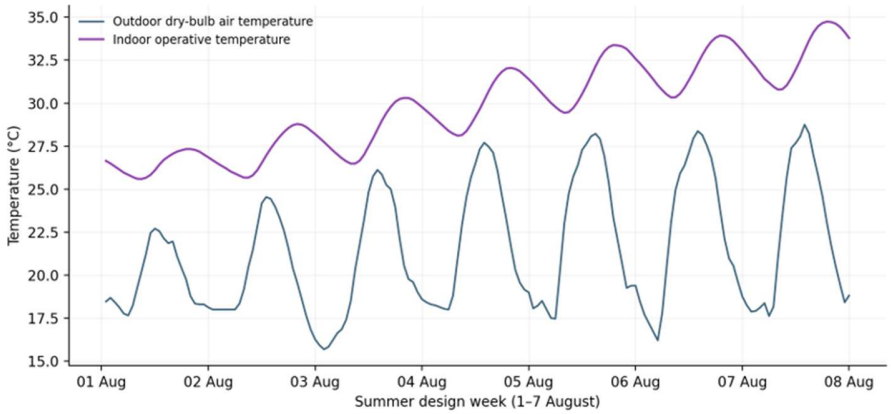


Figure 5-23 Weekly indoor–outdoor temperature trend, Case 2 Wall, summer design week (1–7 August)

- Time Lag & Decrement Factor

The results give quantitative substance to a construction logic that long precedes the language of decrement factors and time lags. The Jordanian-period wall assembly examined here — a locally quarried limestone outer leaf, a concrete block inner leaf, and an internal gypsum mortar finish — reflects a broader Mediterranean and Levantine building tradition in which thick, dense stone envelopes function as thermal moderators rather than thermal barriers. This is a materially and economically different logic from that of contemporary insulation-led construction: rather than resisting heat flow through a low-conductivity layer, the traditional wall accepts that heat will pass through it, and instead manages when and at what intensity it arrives indoors.

Table 5-4: Peak temperatures and their timing, Case 2 Wall, 7 August (peak summer design day)

Parameter	**Peak Value (°C)**	**Time of Peak**
Outdoor dry-bulb air temperature	28.75	14:00
External wall surface temperature	67.57	12:00
Internal wall surface temperature	37.87	17:00
Indoor operative temperature	34.74	19:00

The Mediterranean semi-arid climate of the Palestinian highlands, characterized by pronounced diurnal temperature swings — hot, high-solar-gain days followed by markedly cooler nights, even within the summer season — is precisely the climatic condition under which this strategy is most effective. A five-hour time lag and a surface-to-surface decrement factor of 0.18 mean that the sharpest heat of the early

afternoon does not reach the occupied interior until the early evening, and arrives there substantially flattened; by the time the delayed peak has passed, outdoor night-time temperatures have typically fallen enough to allow effective natural ventilation, permitting the stored heat in the wall mass to be purged before the next solar cycle begins. This diurnal charge-and-discharge cycle — heat absorbed by day, released and flushed by night — is the operative principle behind traditional thick-walled construction across arid and semi-arid Mediterranean building cultures, and it is a genuinely passive cooling strategy: it requires no mechanical input, relying instead on the coupling of a high-heat-capacity envelope with an occupant behavior of night-time ventilation that the traditional built form and, historically, the traditional pattern of domestic life supported.

At the same time, the weekly heat-accumulation trend identified in (Figure 5-23) is a caution against romanticizing thermal mass as an unconditional solution. The same property that allows the wall to store and delay heat also allows it to accumulate heat across a sustained hot spell if the nightly discharge is incomplete — whether because of insufficient night ventilation, elevated night-time outdoor temperatures, or changes in occupant behavior and building sealing that are themselves part of the contemporary transformation this thesis traces. The vernacular wall's effectiveness, in other words, is not an intrinsic material property alone but the outcome of a coupled system of thick construction and active nocturnal ventilation behavior; where one half of that coupling is present without the other, as increasingly appears to be the case in contemporary occupancy patterns, the thermal-mass benefit demonstrated here is only partially realized. This coupling — and its erosion across the Ottoman-to-contemporary transformation of Palestinian domestic space — is returned to in the cross-strategy discussion later in this chapter.

Table 5-5: Time lag summary, Case 2 Jordanian Wall

Wall Type	**External Surface Peak**	**Internal Surface Peak**	**Operative Temp Peak**	**Time Lag (surface-to-surface)**	**Time Lag (outdoor air-to-operative)**
Case 2 Wall	12:00	17:00	19:00	5 h	5 h

A notable feature of the peak-day data is that the external surface temperature peaks two hours before the outdoor dry-bulb air temperature (12:00 against 14:00). This is physically consistent with the two variables having different drivers: the external surface temperature responds directly to incident solar radiation, which peaks near solar noon, whereas the outdoor dry-bulb temperature is a lagged response of the

atmosphere as a whole and continues to rise into the early afternoon. The external surface, absorbing direct solar gain, therefore behaves as an effective sol-air temperature rather than tracking shaded air temperature, which explains its markedly higher amplitude (an external surface swing of over 50°C against an outdoor air swing of just over 11°C on the same day).

- Case 3: Contemporary Period House

Time lag for the contemporary house with contemporary wall was determined directly from the DesignBuilder/EnergyPlus simulation output, since the coupled solar, convective and conductive boundary conditions applied by the software provide a representative estimate of the wall's actual dynamic response, Two hourly surface-temperature outputs were requested for the external wall construction: Surface Outside Face Temperature, reporting the temperature of the outermost limestone face as it responds to solar radiation, convection and the outdoor air temperature; and Surface Inside Face Temperature, reporting the temperature of the innermost lightweight block face as it exchanges heat with the zone air and internal surfaces. Both outputs were generated at hourly resolution for a representative summer week for post-processing. The time lag was then calculated simply as the difference between these two peak occurrences:

$$\text{Time lag} = (\text{time of peak inside face temperature}) - (\text{time of peak outside face temperature})$$

- Contemporary wall section:

Applied consistently across all seven days of the simulated week, the outside face temperature peaked at 14:00 on every single day, while the inside face temperature peaked at 18:00 on every single day, giving an identical result across the full week with no day-to-day variation. This consistency indicates that the wall had reached a stable, repeatable periodic response to the diurnal temperature cycle.

$$\text{Resulting time lag} = 3 \text{ hours}$$

- Physical Interpretation of the Four-Hour Time Lag

The diagram above illustrates the mechanism underlying this result. The wall's outer limestone face absorbs the peak solar and ambient heat load at 14:00, in the early afternoon, when outdoor conditions are at their most severe. Rather than transmitting this peak instantaneously to the interior, the wall's thermal

mass — principally the 100 mm cast concrete layer, which holds over half of the wall's total heat capacity — absorbs and temporarily stores a substantial share of that heat before releasing it toward the interior face. By the time this stored heat reaches the innermost lightweight block face and raises its temperature to its own daily maximum, four hours have elapsed, placing the peak of the interior surface at 18:00.

This four-hour delay has a direct thermal comfort implication. It shifts the moment of maximum wall heat gain out of the hottest part of the afternoon and into the early evening, meaning the wall's contribution to indoor heat gain no longer coincides directly with the period of peak outdoor solar exposure. In a free-running or naturally ventilated dwelling, this separation is beneficial: it reduces the overlap between the wall's heat release and the period when solar and ambient loads are simultaneously at their highest, and it moves part of the thermal load toward a time of day when outdoor temperatures have already begun to fall and natural ventilation becomes more effective at removing the accumulated heat.

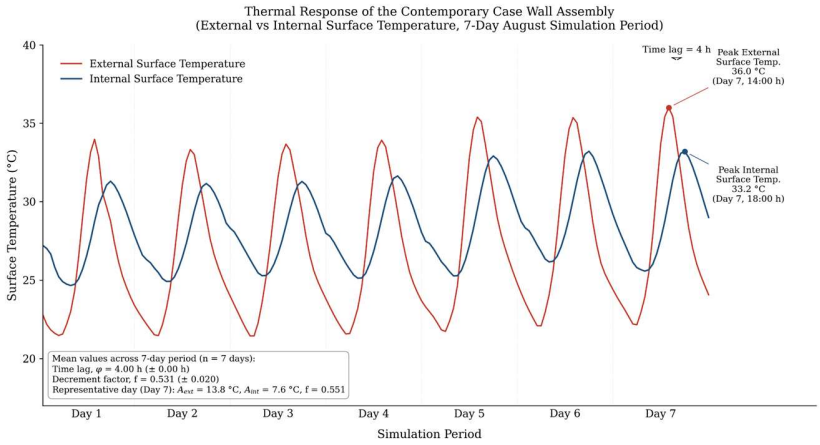


Figure 5-24: Thermal Response of the Contemporary Case wall Assembly (External vs Internal Surface temperature, 1-7 Aug simulation Period)

This behavior is a direct expression of the wall's thermal mass and heat storage capacity. A wall with negligible mass would transmit the outdoor temperature signal to the interior with little delay, so that indoor surface temperatures would closely track outdoor peaks in time. The four-hour lag observed here confirms that, even in a comparatively lightweight contemporary assembly, the combined limestone-concrete-block construction retains enough heat capacity to meaningfully decouple the timing of indoor and outdoor thermal peaks — a property that becomes directly comparable, in the cross-case analysis that follows, against the markedly greater mass and correspondingly longer time lags expected of the Ottoman and Jordanian wall constructions.

Mean decrement factor ≈ 0.53 across the week — meaning the internal surface swings through only about 53% of the amplitude seen on the external surface, with the wall damping the rest. Combined with the 4.0-hour lag, this gives you both figures needed to complete the time-lag/decrement-factor pair for this wall, as referenced in the earlier calibration discussion but never finished numerically.

5.4.2 Strategy 2 — Opening Ratio and Natural Ventilation

This strategy investigates the role of opening ratio and natural ventilation in regulating indoor thermal conditions. It evaluates how variations in window-to-wall ratio influence air movement, solar gains, and overall thermal comfort across the studied cases.

- Case 1: Ottoman house

The analysis was conducted using four window-to-wall ratio (WWR) scenarios, ranging from the surveyed Ottoman base case to higher opening ratios representing ventilation thresholds, peak air change performance, and the ASHRAE 90.1 prescriptive limit. The selected values (WWR1–WWR4) were used to evaluate the relationship between opening ratio, natural ventilation potential, and thermal performance.

- Indoor air temperature and operative temperature

  The clearest pattern in the summer results is a divergence between mean and peak conditions. Mean indoor air temperature is almost unchanged across the four scenarios, ranging from 24.8°C to 25.2°C, while peak air temperature rises consistently with WWR, from 28.6°C at the base case to 29.4°C at 40% WWR. If additional glazing were simply adding heat uniformly through the day, the mean would be expected to rise by a similar margin; instead, the added heat is concentrated in the hours when solar gain is already at its highest, superimposing a sharper afternoon peak onto an average that ventilation is still able to moderate. Operative temperature follows the same shape as air temperature at a consistently higher level, which indicates that the added heat is entering through direct solar gain and re-radiated surface heat in broadly similar proportion, rather than one mechanism dominating the other.

Table 5-6: Parametric Window-to-Wall Ratio (WWR) Scenarios and Their Thermal Implications for case study 1

Case	Value	Description
WWR1	9.3%	The surveyed Ottoman base case
WWR2	20.4%	marks the threshold where cross-ventilation becomes meaningfully effective
WWR3	30.9%	the point of peak realized ACH before ventilation returns diminish
WWR4	44.4%	the ASHRAE 90.1 prescriptive ceiling, included deliberately to test whether code compliance and thermal performance actually coincide.

Winter behaves differently, and in a direction that a simple heat-loss argument would not predict. Both mean and peak indoor temperatures rise with WWR rather than falling: mean air temperature increases from 13.0°C at the base case to 14.0°C at 40% WWR, and mean PPD falls from around 60% to around 51% over the same range. Because winter ACH is essentially constant across all four scenarios (see below), this improvement cannot be attributed to ventilation; it follows from solar gain through the enlarged glazed area, which for a south-oriented masonry building under a Mediterranean winter sun evidently outweighs the additional conductive loss through the same glazing. The improvement is real but partial: even at 40% WWR the building remains in a state of near-continuous winter discomfort, so the result should be read as a modest passive-solar contribution rather than as a route to acceptable winter comfort on its own.

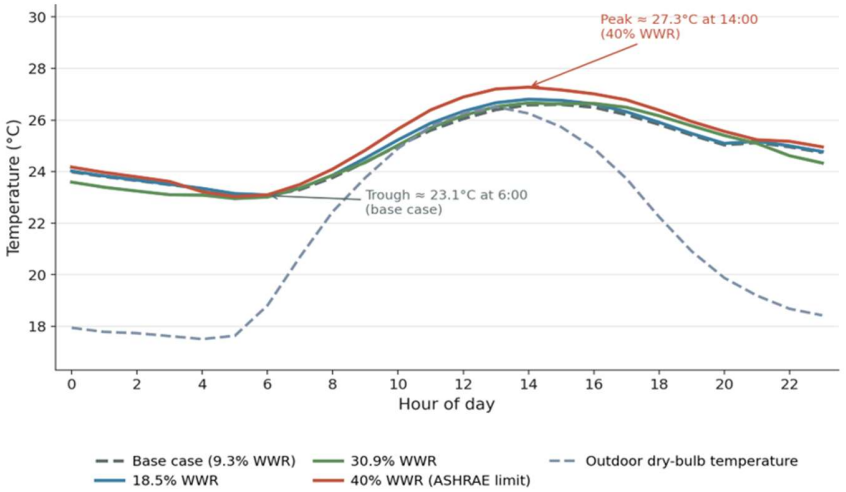


Figure 5-25: Indoor air temperature, mean diurnal profile, typical summer week, by WWR scenario.

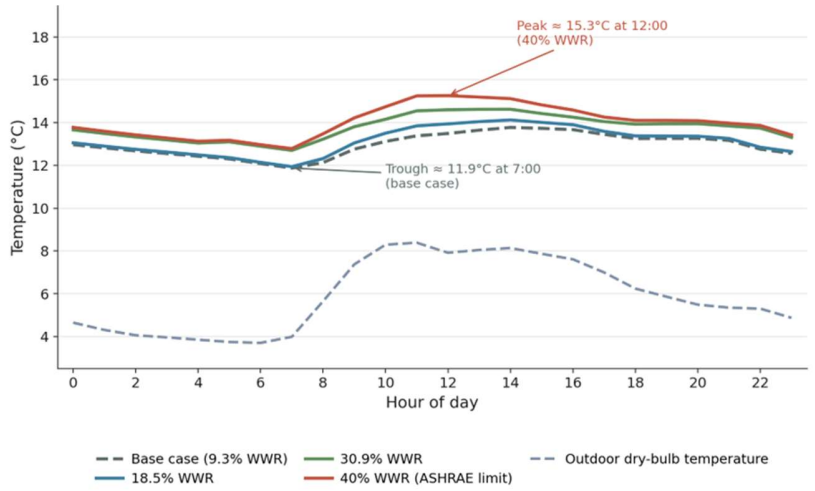


Figure 5-26: Indoor air temperature, mean diurnal profile, typical winter week, by WWR scenario.

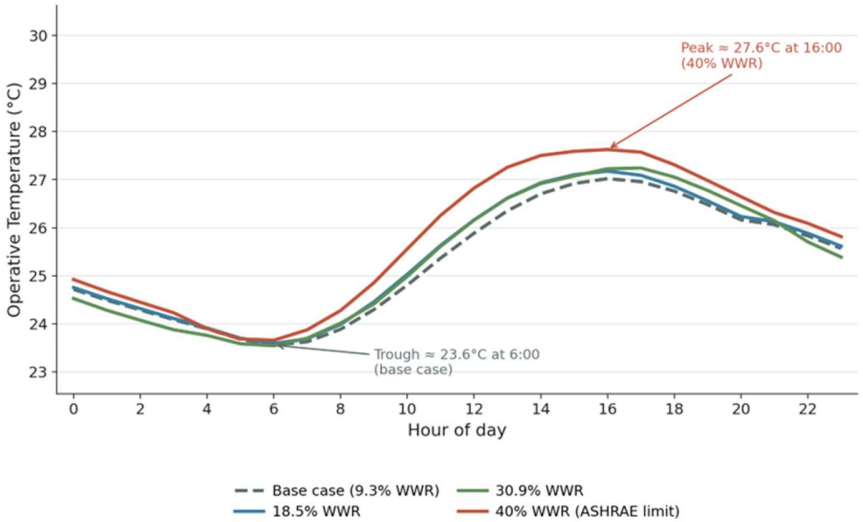


Figure 5-27 Operative temperature, mean diurnal profile, typical summer week, by WWR scenario.

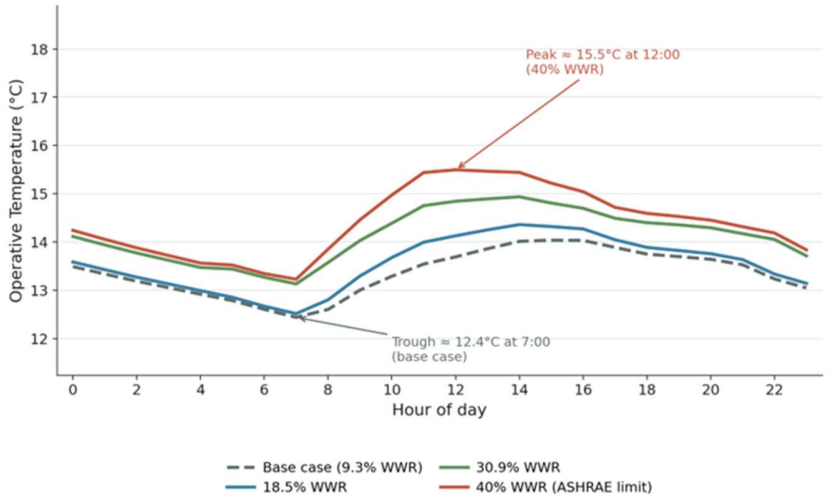


Figure 5-28: Operative temperature, mean diurnal profile, typical winter week, by WWR scenario.

- Discomfort Hour

Summer discomfort hours increase with WWR, from 24 hours at the base case to 40 hours at 40% WWR, but the increase is not proportional to the change in opening ratio. The step from 30.9% to 40% WWR adds 10 discomfort hours on its own, nearly double the combined increase across the three preceding steps. Winter discomfort hours fall from 168 to 148 out of a possible 168, consistent with the passive-solar improvement described above, though the building remains uncomfortable for the great majority of the winter week regardless of WWR.

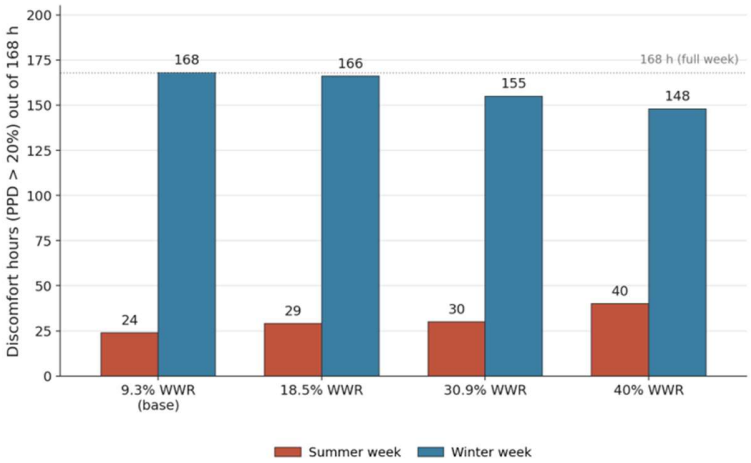
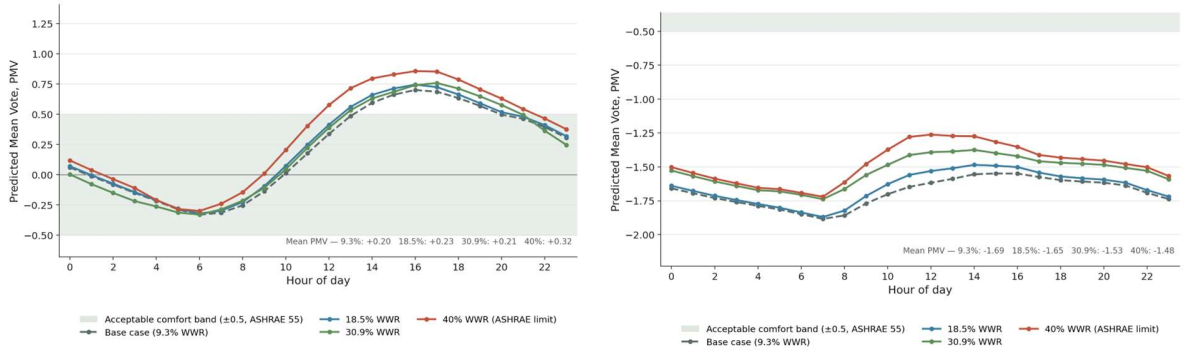


Figure 5-29: Discomfort hours (Fanger PPD > 20%) by season and WWR scenario

- Thermal comfort analysis: PMV and PPD

The discomfort-hour count above is a threshold applied to the Fanger Predicted Percentage Dissatisfied (PPD) output; reading the underlying Predicted Mean Vote (PMV) and PPD values directly, rather than only the threshold derived from them, shows how the combined effect of air temperature, operative temperature, solar exposure and ventilation shifts the thermal sensation of the space as WWR increases, and in which direction.

In summer, mean PMV rises only slightly with WWR, from 0.20 at the base case to 0.23 at 18.5% and 0.21 at 30.9%, before increasing more noticeably to 0.32 at 40% WWR. All four-summer means fall within the ISO 7730 Category II band ($|PMV| \leq 0.5$), and the mean alone understates how the distribution changes: the proportion of hours with PMV above 0.5, indicating a warm sensation beyond the Category II boundary, rises from 32.1% of the week at the base case to 38.1% at 40% WWR, while mean PPD rises from 11.7% to 14.0%. The base, 18.5% and 30.9% cases behave similarly to one another on this measure, which is consistent with the earlier finding that ACH keeps pace with the added glazing area up to 30.9%; ventilation is offsetting most of the additional solar gain across that range. At 40% WWR, where ACH falls back below the 30.9% and even the 18.5% cases, ventilation is no longer offsetting the added solar gain to the same degree, and the shift in thermal sensation becomes visible in the PMV distribution rather than only in the mean.

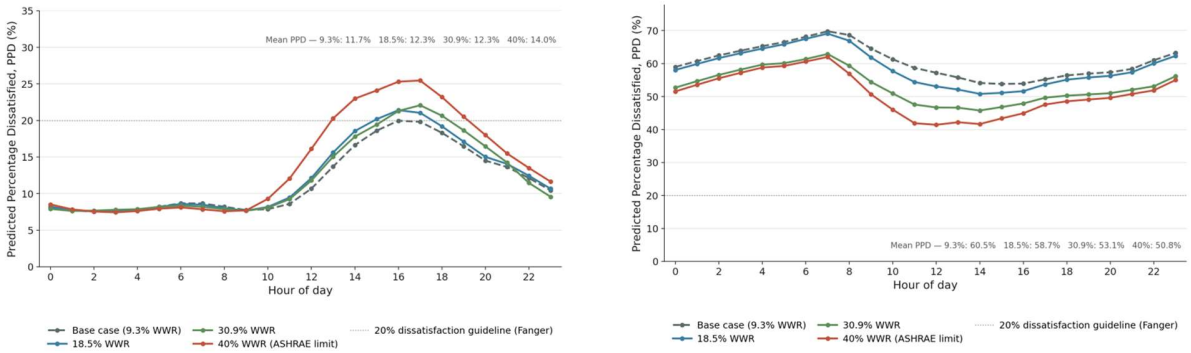


Typical summer week Typical winter week

Figure 5-30: Predicted Mean Vote (PMV), mean diurnal profile, typical winter week, by WWR scenario

In winter, PMV tells a story the discomfort-hour count alone does not fully convey. Mean PMV is strongly negative at every WWR, from −1.69 at the base case to −1.48 at 40% WWR, corresponding to a sensation

between ‘cool’ and ‘cold’ on the seven-point ASHRAE thermal sensation scale, and every scenario keeps at least 98.8% of the week outside the ISO 7730 Category III band (|PMV| ≤ 0.7) in the cold direction. Increasing WWR moves the mean PMV toward neutral, from −1.69 to −1.48, and mean PPD falls accordingly, from 60.5% to 50.8%. This is a measurable improvement in the same direction across all three indicators, air temperature, operative temperature and PPD, but the improvement is a shift within an already severe cold-discomfort condition rather than an approach to an acceptable comfort category. None of the four winter scenarios reach ISO 7730 Category II, and the practical reading is that additional glazing area provides a genuine but bounded passive-solar contribution to winter comfort, not a substitute for supplementary heating or improved insulation.



Typical summer week Typical winter week

Figure 5-31: Predicted Percentage Dissatisfied (PPD), mean diurnal profile, by WWR scenario.

Reading air temperature, operative temperature, solar gain and ACH together against the PMV/PPD results clarifies why the two seasons respond in opposite directions to the same variable. Increasing WWR raises solar gain in both seasons; the sign of its effect on PMV depends on whether that added heat is being removed by ventilation (summer, where ACH rises with WWR up to 30.9%) or retained by thermal mass against an already cold background (winter, where ACH does not respond to WWR at all). PMV and PPD, being combined indices of air temperature, radiant temperature and the resulting sensation, capture this interaction more directly than air or operative temperature alone; the summer PMV distribution only shifts materially once the ventilation response to added WWR itself weakens at 40%, and the winter PMV shift is attributable to solar and radiant effects alone, since ACH is constant across all four winter scenarios.

Set against the applicable standards, the summer results sit close to acceptable performance and the winter results do not. ASHRAE 55 treats a PMV range of −0.5 to +0.5 as generally acceptable, corresponding to roughly 90% satisfaction, and the summer mean PMV values for all four WWR scenarios fall inside that range, even though a growing share of individual hours exceeds it as WWR increases. The winter mean PMV values, by contrast, sit far outside both the ASHRAE 55 acceptable range and the ISO 7730 Category III boundary at every tested WWR, which means that no opening ratio examined in this strategy resolves winter thermal comfort on its own. For the Ottoman case, this places a limit on what Strategy 2 can be expected to achieve: WWR adjustment is a genuinely useful lever for summer comfort and ventilation performance within the 18.5–30.9% range identified earlier, but winter comfort in this typology depends on measures outside the scope of opening ratio.

- Air Change Rate

The air change rate results are the most informative for interpreting the other indicators. Summer ACH does not increase monotonically with WWR: it rises from 1.18 ac/h at the base case to 1.31 ac/h at 30.9% WWR, then falls to 1.12 ac/h at 40% WWR, a value below both the 30.9% and 18.5% cases. Reviewing the hourly profile at 40% WWR shows a coherent daily control cycle rather than a data artefact, in which openings are held closer to an infiltration-only condition for longer stretches of the day than at 30.9%. This is consistent with a ventilation control regime that curtails opening once indoor conditions approach the upper edge of an acceptable range, rather than one that simply scales airflow with available aperture. Winter ACH is effectively flat across all four scenarios, at approximately 0.91 ac/h, which indicates that the ventilation control logic is not responsive to WWR in cold conditions; the winter results are therefore governed by conduction and solar gain rather than by airflow.

- Optimal WWR Range and Critical Transition Point

The results place the practically useful range for this typology between approximately 18.5% and 30.9% WWR. Within this range, each increase in opening ratio is met by a corresponding increase in realized ACH, and the discomfort-hour cost of that ventilation gain remains small, five additional summer hours at 18.5% and six at 30.9%, relative to the base case. The 30.9% scenario represents the point of maximum ventilation return in the tested range, combining the highest mean ACH of any scenario with a discomfort-hour cost close to that of the more conservative 18.5% case.

The transition between 30.9% and 40% WWR marks the point at which increasing the opening ratio stops providing a net thermal benefit. Ventilation benefit, measured as ACH gain over the base case, falls from 10.4% at 30.9% WWR to −5.8% at 40% WWR, while the overheating penalty, measured as additional discomfort hours over the base case, rises sharply from six hours to sixteen. This is the critical transition identified by the methodology: beyond it, further increases in opening ratio no longer buy additional ventilation and instead add solar-driven overheating without compensation. Because 40% WWR is also the ASHRAE 90.1 prescriptive ceiling, the simulation results indicate that code compliance and thermal performance diverge for this particular typology; the code maximum performs worse than a mid-range opening ratio on every indicator examined, which is a materially different conclusion from assuming that the code-permitted range is thermally appropriate by default.

- Case 2: Jordanian house

This section presents the simulated thermal performance of the Jordanian-period case under three window-to-wall ratio (WWR) configurations, evaluated on the following criteria: operative and air temperature, natural ventilation rate (ACH), EN 16798-1 adaptive thermal comfort, and Fanger PMV/PPD. The three scenarios are summarized in Table 5-7

Table 5-7: Parametric Window-to-Wall Ratio (WWR) Scenarios and Their Thermal Implications for case study 2

Scenario	**WWR**	**Description**
WWR2	10%	Ottoman vernacular baseline, small-opening configuration
WWR1	22%	Existing Jordanian-house condition (survey-based)
WWR3	30%	Empirically derived optimum (peak realized ventilation gain before ACH returns diminish)

- Operative Temperature and Air Temperature

The modified façade faces north. This is material to how the results should be read: on a north elevation, direct-beam solar exposure is minimal for most of the year — including throughout the August design week — and admitted solar radiation is dominated by the diffuse sky component rather than direct beam gain. Enlarging the window area on this orientation therefore does not carry the same overheating risk it would on a south- or west-facing wall; the principal physical pathway through which WWR affects

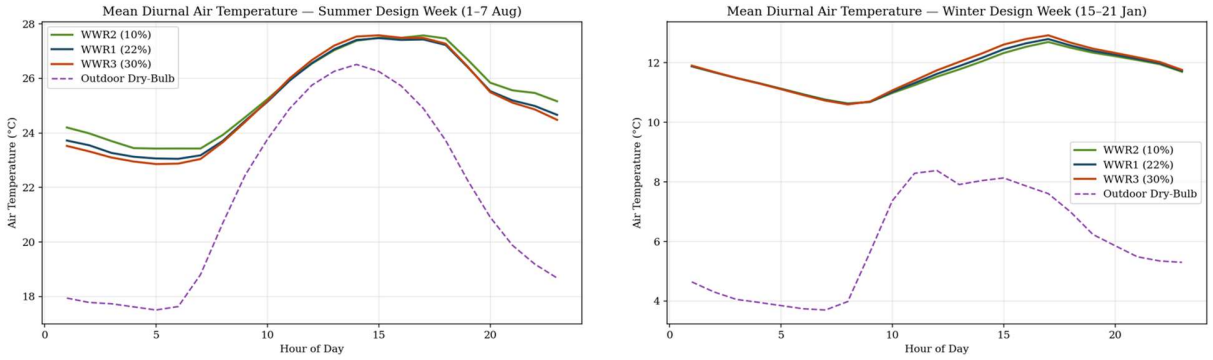
performance here is airflow and glazing conductance rather than solar control. This orientation effect is visible directly in the data and is discussed at each metric below.

Table 5-8: Summer and winter temperature statistics by scenario (°C)

Scenario / Season	Air T max	Air T min	Air T mean	Diurnal range	Op. T mean
WWR2 (10%) — Summer	30.1	21.4	25.4	8.7	25.7
WWR1 (22%) — Summer	29.0	21.0	25.0	8.4	25.6
WWR3 (30%) — Summer	30.0	21.6	25.2	8.5	25.6
WWR2 (10%) — Winter	16.7	7.3	11.7	8.9	11.2
WWR1 (22%) — Winter	16.8	7.5	11.7	9.1	11.2
WWR3 (30%) — Winter	17.0	7.7	11.8	9.3	11.3

The summer temperature results are essentially flat with respect to WWR: mean air temperature varies by only 0.28°C across the full 10%–30% range (25.44°C, 25.20°C, 25.15°C), and peak air temperature stays within 0.2°C of 30.0°C in all three cases. This is a materially different picture from a south-facing façade, where a comparable window-area increase would be expected to raise both figures more clearly. The explanation is orientation: mean solar gain through the glazing does rise with WWR (0.24 kW at 10%, 0.29 kW at 22%, 0.36 kW at 30%), but the absolute magnitude stays modest throughout because the façade receives diffuse rather than direct-beam radiation for nearly the entire design week, so the added glazed area is not admitting a large additional heat load for ventilation to offset.

Winter behaves the same way: mean air and operative temperature are effectively invariant across the three scenarios (11.67°C, 11.72°C, 11.78°C), and diurnal range differs by less than half a degree. On a south-facing wall, a larger WWR would normally be expected to deliver a clearer passive-solar benefit in the cold season; here that benefit is small because the orientation limits direct solar access regardless of how much glazing is provided. In effect, the north orientation of this façade decouples WWR from solar performance in both directions — larger openings neither overheat the space in summer nor meaningfully warm it in winter — which shifts the entire practical argument for this façade's WWR onto ventilation performance, examined next.



summer design week. winter design week.

Figure 5-32: Mean diurnal air temperature profile

- Natural Ventilation Performance (ACH)

WWR shows a clear effect on ventilation rate (ACH), but this effect diminishes sharply beyond a certain point. Mean ACH increases from 4.72 at 10% WWR to 5.66 at 22%, representing a strong gain of 0.078 per percentage point. Beyond this, the improvement slows significantly, reaching only 5.94 at 30%, equivalent to 0.035 per point—indicating that each additional increase past 22% delivers minimal benefit. This plateau is more pronounced at night, where ACH effectively stops improving (3.27 at 22% vs. 3.21 at 30%), while daytime values continue to rise only marginally. Overall, increasing WWR beyond the low-twenties provides limited ventilation gains, particularly for night flushing—the more critical cooling mechanism—suggesting that performance reaches a practical saturation point near this range.

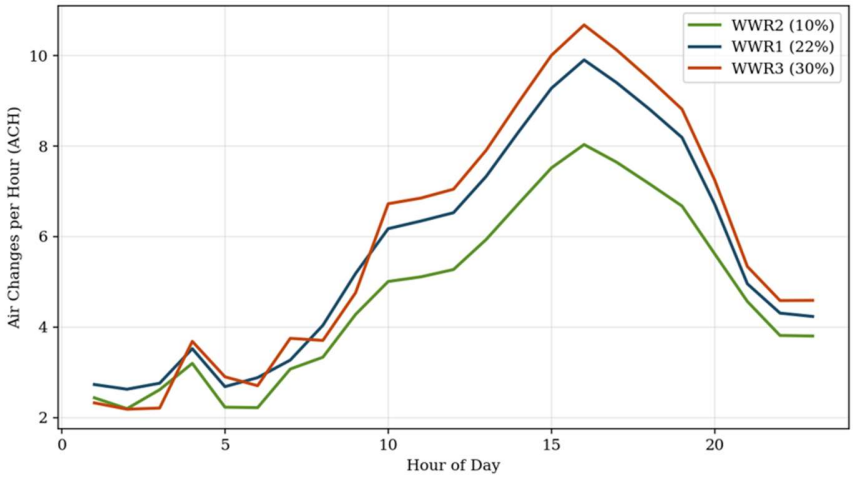


Figure 5-33: Mean diurnal ACH profile, summer design week.

- Adaptive Thermal Comfort (EN 16798-1)

The adaptive model was applied to the summer week only, since winter Trm (≈5.9°C) falls outside the standard's 10–30°C validity range for naturally ventilated buildings. Summer Trm (≈20.5°C, common to all scenarios) sits within range, giving a Category I band of roughly 21.6–25.6°C and a Category II band of roughly 20.6–26.6°C.

Table 5-9: Adaptive comfort compliance, summer design week

Scenario	Category I (±2K)	Category II (±3K)
WWR2 (10%)	49.1%	72.0%
WWR1 (22%)	49.7%	72.0%
WWR3 (30%)	49.7%	70.2%

Adaptive comfort compliance is essentially flat across the WWR range on Category I (49.1–49.7%) and only marginally lower at 30% on Category II (70.2% against 72.0% at both 10% and 22%). This mirrors the temperature results directly: because operative temperature itself barely moves with WWR on this orientation, the comfort classification built on it does not move much either. The small Category II dip at 30% is consistent with the slightly wider variability that comes with the higher ventilation-driven airflow at that scenario, rather than with any solar-driven heat gain.

- PMV and PPD Analysis

PMV, PPD, and discomfort-hours are all effectively insensitive to WWR in both seasons — summer PMV stays within 0.04 of neutral across all three scenarios, and winter discomfort hours are identical (56.5%) regardless of window size. This closes out the discrepancy noted in the previous version of this section, where the existing-condition file appeared to diverge sharply from the two parametric variants; that divergence has not persisted once all three scenarios were run with matching ventilation control and internal-gains settings, which confirms it was a data-consistency artefact rather than a genuine WWR effect. The one measurable, physically coherent gradient in this entire dataset is the ACH result in the previous section; everything else responds to WWR only marginally on this façade, which is itself the finding worth stating plainly rather than a null result to explain away.

Table 5-10: Fanger PMV/PPD summary and discomfort hours

Scenario / Season	Mean PMV	Mean PPD	Discomfort hrs. (%)
WWR2 (10%) — Summer	+0.07	18.1%	42.3%
WWR1 (22%) — Summer	+0.03	17.9%	42.2%
WWR3 (30%) — Summer	+0.04	18.5%	42.8%
WWR2 (10%) — Winter	−2.61	89.8%	56.5%
WWR1 (22%) — Winter	−2.60	89.5%	56.5%
WWR3 (30%) — Winter	−2.59	89.1%	56.5%

Discussion: Vernacular Precedent, Existing Condition, and Empirical Optimum:

Framed this way, the vernacular 10% baseline is not thermally penalized on this façade so much as under-ventilated relative to what the opening could provide without cost; the existing 22% condition already captures most of the available night-flushing benefit; and the 30% empirical optimum adds a further, smaller daytime ventilation gain at negligible thermal cost given the orientation

- Case 3: contemporary house

This section evaluates the impact of Window-to-Wall Ratio (WWR) on the indoor thermal performance of the contemporary residential case study, following the same evaluation framework applied in the preceding Ottoman- and Jordanian-period analyses. Three WWR scenarios were simulated on the East-South (E-S) oriented façade (external wall area 9.4 m²): WWR 10% (0.94 m² glazed area), WWR 20% (1.88 m²), and WWR 30% (2.82 m²). Each scenario was simulated for a representative summer week (1–7 August) and winter week (15–21 January) at hourly resolution (168 hours per season), using DesignBuilder/EnergyPlus exports of Air Temperature, Radiant Temperature, Operative Temperature, and Outside Dry-Bulb Temperature.

- Operative temperature

Table 5-11 summarizes the hourly operative temperature statistics for each WWR scenario across the summer and winter simulation weeks.

Table 5-11: Operative temperature summary statistics by WWR scenario and season

Scenario	Season	Mean Top (°C)	Max Top (°C)	Min Top (°C)	Diurnal Range (°C)	Peak Hour
WWR 10%	Summer	32.40	34.31	30.77	3.54	15:00
WWR 20%	Summer	28.28	32.51	24.64	7.86	17:00
WWR 30%	Summer	32.09	34.87	29.74	5.14	10:00
WWR 10%	Winter	19.32	20.65	17.86	2.79	21:00
WWR 20%	Winter	14.53	17.80	11.26	6.54	18:00
WWR 30%	Winter	18.15	19.65	16.34	3.31	15:00

WWR 10% and WWR 30% both remain well above summer comfort limits throughout the week (means 32.40°C and 32.09°C), with WWR 30% reaching the highest peak of the three scenarios (34.87°C, at 10:00) and the lowest minimum (29.74°C), giving it the largest diurnal range between these two ventilation-inactive cases (5.14°C vs 3.54°C) — consistent with its larger glazed area admitting more solar gain during the day and losing more heat overnight through the higher-conductance glazing. WWR 20%, with active natural ventilation, shows a substantially lower mean (28.28°C) and the widest diurnal range of all three (7.86°C), with its peak delayed to 17:00; this reflects the combined effect of window area and active ventilation rather than window area in isolation.

In winter, the same ordering holds: WWR 10% (19.32°C mean) and WWR 30% (18.15°C mean) remain closer to the heating comfort band than WWR 20% (14.53°C mean, minimum 11.26°C), whose active ventilation exchanges indoor heat with the cold outdoor air far more rapidly, producing both a lower mean and a wider diurnal swing (6.54°C vs 2.79–3.31°C).

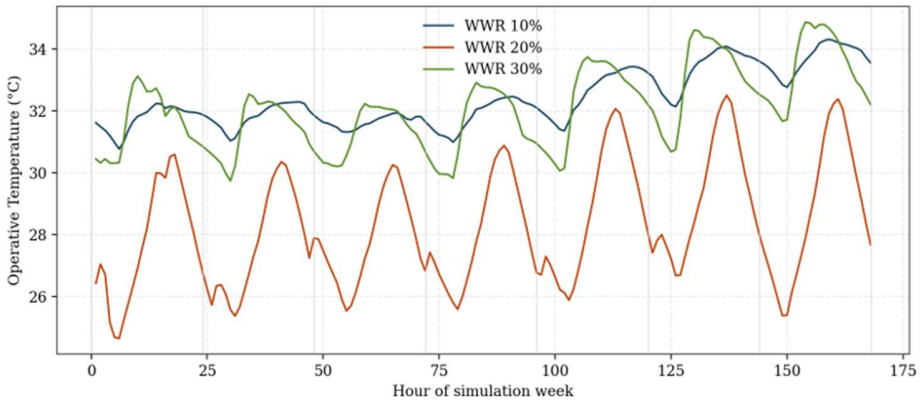


Figure 5-34: Weekly hourly operative temperature profile — summer (1–7 August)

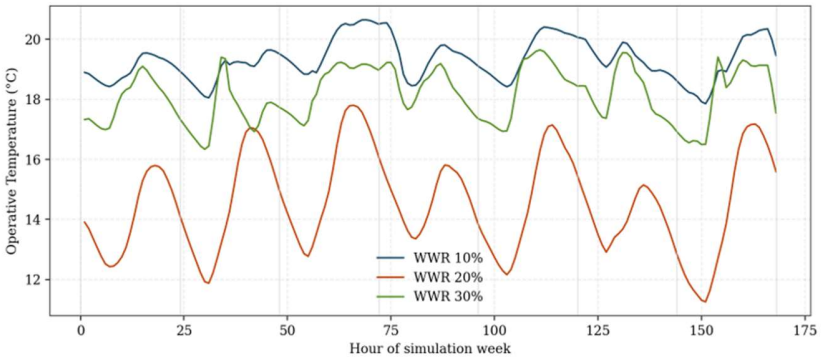


Figure 5-35: Weekly hourly operative temperature profile — winter (15–21 January)

- Thermal Comfort (PMV and PPD)

Table 5-12: Fanger PMV/PPD summary by WWR scenario and season.

Scenario	Season	Mean PMV	PPD range (%)	Mean PPD (%)	Thermal Sensation
WWR 10%	Summer	+2.36	67.7 – 99.1	87.7	Hot
WWR 20%	Summer	+0.76	5.0 – 86.8	25.2	Neutral/slightly warm
WWR 30%	Summer	+2.24	48.1 – 99.6	82.0	Hot
WWR 10%	Winter	−0.59	6.8 – 22.3	12.7	Slightly cool
WWR 20%	Winter	−1.96	34.5 – 96.8	72.4	Cool
WWR 30%	Winter	−0.87	10.9 – 38.4	21.6	Slightly cool

WWR 10% and WWR 30% both produce a mean summer PMV in the 'hot' range (+2.24 to +2.36) and severe mean PPD (82.0–87.7%), indicating unacceptable summer comfort for both. WWR 20% is markedly milder (PMV +0.76, 'neutral to slightly warm') and records the lowest summer PPD of the three (25.2%), reflecting the cooling benefit of its active natural ventilation during the summer week. Between the two ventilation-inactive scenarios, WWR 30% shows a marginally lower PPD than WWR 10% (82.0% vs 87.7%), a modest improvement attributable to its lower minimum night-time temperatures pulling its mean PMV down slightly, though both remain firmly in the 'hot' category.

In winter, WWR 10% achieves the mildest sensation ('slightly cool', PMV −0.59, PPD 12.7%), followed by WWR 30% (PMV −0.87, PPD 21.6%); WWR 20% is markedly colder and less comfortable ('cool', PMV −1.96, PPD 72.4%), the ventilation that assists summer cooling becoming a significant winter heat-loss penalty. This is the central trade-off of Strategy 2 in this dataset: the

same natural ventilation that meaningfully improves WWR 20%'s summer comfort substantially worsens its winter comfort relative to the sealed 10% and 30% cases.

- Adaptive Thermal Comfort (EN 16798-1, Summer)

Table 5-13: Percentage of summer hours within each EN 16798-1 adaptive comfort category

Scenario	Category I (%)	Category II (%)	Category III (%)	Outside all categories (%)
WWR 10%	0.0	0.0	0.0	100.0
WWR 20%	56.5	12.5	14.9	16.1
WWR 30%	0.0	0.0	12.5	87.5

WWR 10% fails to achieve adaptive comfort for the entire summer week (100% of hours outside all categories). WWR 30% performs marginally better, with 12.5% of hours reaching Category III, likely reflecting its lower night-time minimums bringing a portion of the week closer to the adaptive comfort band, though the great majority of hours (87.5%) still fall outside it. WWR 20% is the clear outlier on this indicator: the majority of its summer hours (56.5%) fall within Category I, and a further 27.4% within Categories II and III combined, leaving only 16.1% of hours outside the adaptive range — a direct result of active natural ventilation moderating daytime overheating, consistent with the adaptive comfort model's underlying assumption that occupants in naturally ventilated buildings can achieve comfort at higher indoor temperatures when supported by airflow and behavioral adaptation.

5.4.3 Strategy 3 — Veranda Shading concept as Thermal Buffer: base vs. enhanced shading conditions (Applied for case 2& 3)

This strategy examines the thermal comparison between the 0.6 m shading fin and the (2m) veranda, inspired from Jordanian period case for the contemporary period case. Results are drawn from paired summer (1–7 August) and winter (15–21 January) weeks, each run for three configurations: the unshaded base case, the shading fin, and the veranda.

The aim is to produce a physically defensible differentiation between the two shading strategies, and to interpret why the magnitude of that differentiation differs between summer and winter.

- Case 2: Jordanian house

As noted in the case study chapter, the Jordanian-period house was not static: it accumulated additions and modifications as the needs of its occupants changed. The veranda, a defining feature of domestic architecture in that period, was eventually enclosed to meet growing demands for interior space, and in doing so became what is now the living area. The liwan underwent a comparable shift, evolving over time into a bedroom.

This strategy's simulation examines three scenarios built around that transformation. The first reflects the space as it stands today, with the veranda fully enclosed. The second reverses this process, restoring the veranda to its original open, transitional role between indoors and outdoors. The third goes further still, removing the veranda altogether so that the living space is left directly exposed to solar radiation and the surrounding outdoor conditions.

Three configurations of the same living space are tested against matched summer (1–7 August) and winter (15–21 January) weeks: Scenario 1 (S1), the veranda closed and folded into the conditioned interior, as the house exists today; Scenario 2 (S2), the veranda reopened as a semi-outdoor transitional buffer, restoring the historical layout; and Scenario 3 (S3), the veranda removed entirely, exposing the living space directly to the outdoor environment. The three represent a spectrum rather than three independent options — full enclosure at one end, full exposure at the other, and a mediating buffer in between — and the results, read in sequence across temperature, adaptive comfort, and PMV/PPD, converge on the same conclusion from three independent directions: the mediating position is not a compromise between two better alternatives, but the best-performing configuration in its own right.

- Operative Temperature and Air Temperature

The clearest way to see what the veranda is doing thermally is to look first at what happens in its absence, in both directions. Enclosure (S1) produces the highest and latest summer peak of the three scenarios — 34.7°C at 18:00 — reached from the highest overnight minimum (25.5°C) and sustained across a diurnal amplitude compressed to just 3.5°C. A narrow amplitude sounds like stability, but the outdoor-correlation analysis shows what it actually is: S1 lags outdoor dry-bulb temperature by six hours with a comparatively weak correlation ($r = 0.70$), meaning the space is only loosely coupled to the daily cycle that would otherwise let it recover overnight. Heat enters and simply accumulates. Full exposure (S3) shows the opposite failure. Its correlation with outdoor conditions is far tighter (3-hour lag, $r = 0.90$) and its overnight

minimum correspondingly lower (22.3°C), but that same tight coupling means it inherits nearly the full outdoor swing: its amplitude widens to 6.7°C and its peak (33.0°C) sits barely 1.7°C below the enclosed case, arrived at from a much lower base rather than avoided.

Scenario 2 occupies neither failure mode. It shares S3's tight outdoor coupling (3-hour lag, r = 0.89) and consequently a comparably low overnight minimum (22.1°C), so it does not inherit S1's stagnation — but its daytime peak (31.6°C) is the lowest of all three scenarios, roughly a full degree below S3 and three degrees below S1. In other words, the open veranda achieves the Ventilative recovery that enclosure forfeits, while damping the peak that unmediated exposure fails to control. This is precisely what a transitional buffer space is supposed to do: it does not simply average the outcomes of full enclosure and full exposure; it improves on both, cutting the peak more effectively than removal alone while avoiding the heat retention that enclosure introduces. The winter data reinforces the same reading by showing where the mechanism runs out of runway: with much smaller day–night temperature differentials to exploit in January, S2 tracks S3 almost exactly (11.5°C versus 11.6°C mean), while S1 remains elevated by roughly two degrees — the same trapped-heat behavior that inflated its summer peak now register as a mild, and for reasons developed below, largely illusory winter advantage.

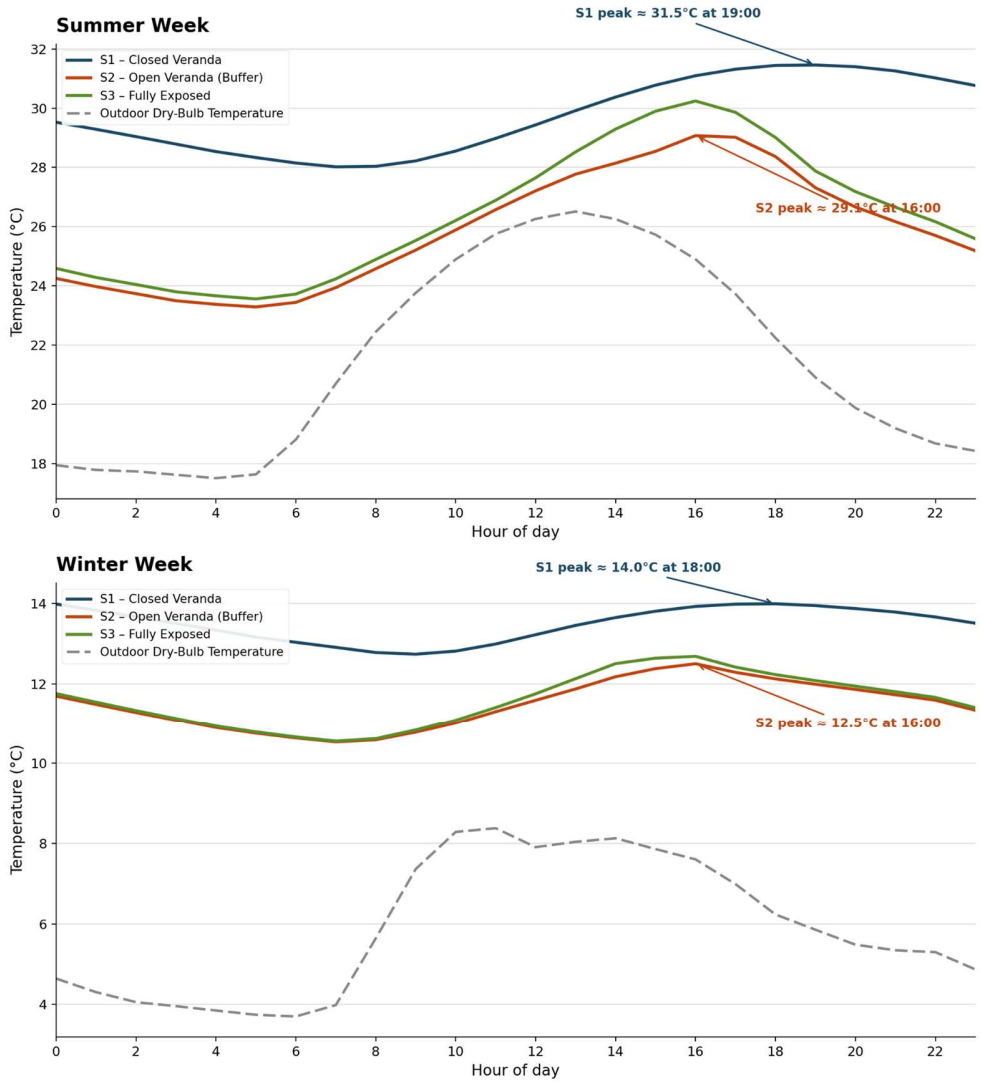


Figure 5-36: Operative Temperature Profile (Veranda scenarios)

If the temperature data suggests the veranda is moderating rather than merely shifting the thermal problem, the adaptive comfort results confirm it in the metric that matters for occupants rather than for the fabric. Applying the EN 16798-1 running-mean model to the summer week (winter Trm falls to 5.6–6.8°C, below the standard's 10°C validity threshold, so the model is not applied there), Scenario 2 places 69.0% of summer hours within Category II and 49.4% within the stricter Category I — the highest of the three scenarios on both counts, and by a wide margin over S1 (39.3% and 29.2%). What is more telling for the argument being built here is that S2 also edges out S3 (66.1% and 47.6%), despite the two sharing an almost identical Ventilative regime. The difference is concentrated exactly where the temperature data predicts it would be: in the afternoon peak hours, where S2's buffered daytime maximum keeps more hours inside the comfort envelope than S3's higher, less-mediated peak allows.

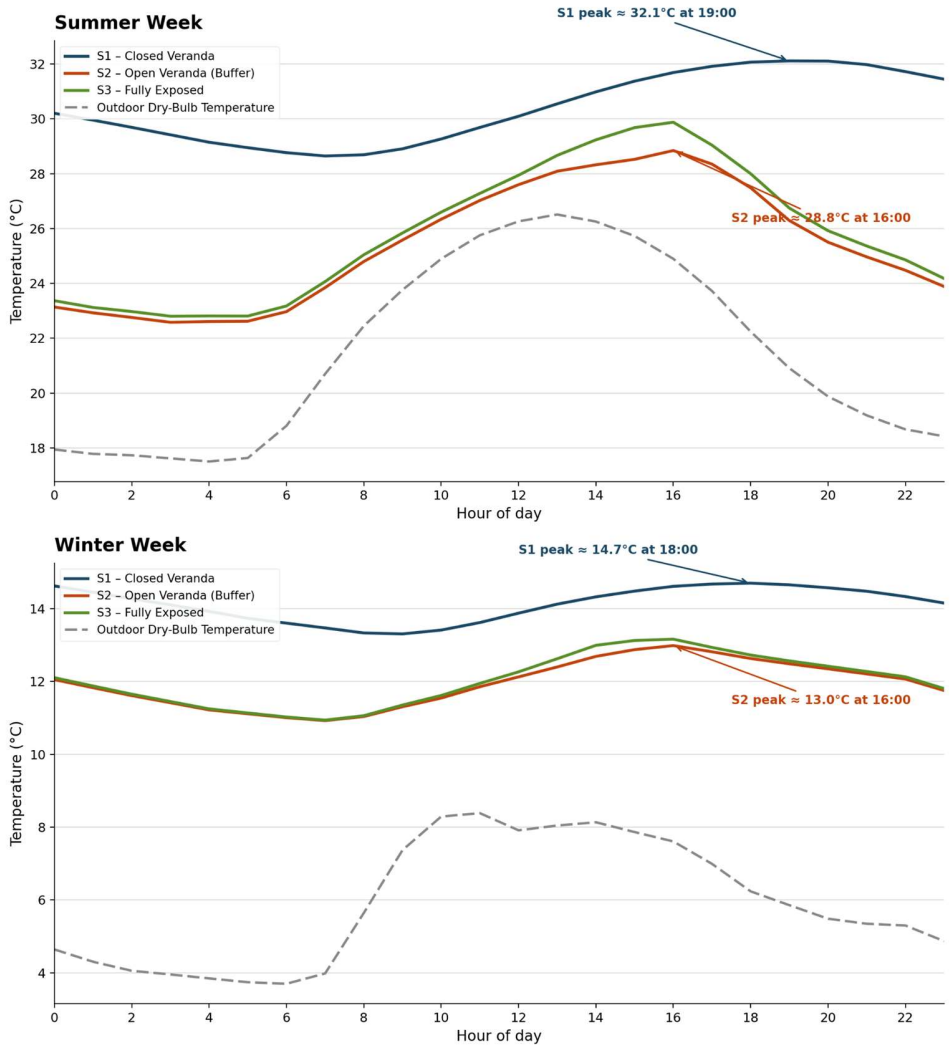


Figure 5-37: Air temperature profile (three veranda scenario)

This is the sense in which the veranda should be read as a climatic mediator rather than a simple shading device. A shading device only ever reduces gain; it has no mechanism for improving on a fully exposed condition's night-time performance, and no benefit to offer once its shading effect is stripped out of the analysis. What the adaptive comfort results show instead is a scenario that reduces the duration and severity of overheating relative to both alternatives simultaneously — narrowing the exceedance period that afflicts S1 around the clock, and lowering the peak severity that affects S3 during the hottest hours — which is a buffering function, operating on both the timing and the magnitude of thermal exchange with the outdoor environment, not a filtering function that only ever removes gain.

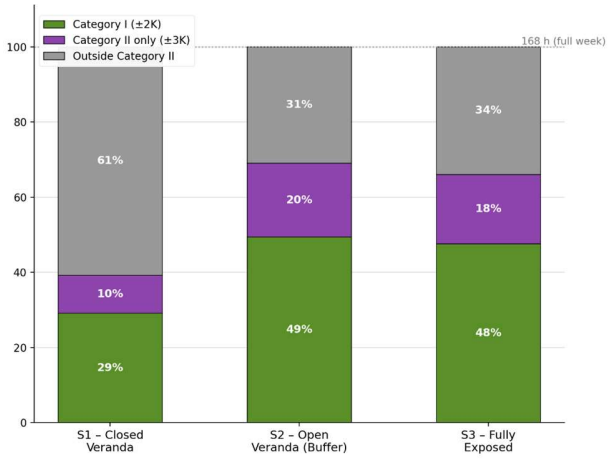


Figure 5-38: hours within thermal comfort range

In summer. The static comfort model removes any remaining ambiguity about which scenario performs best under present-day conditions. Mean summer PMV falls from 1.42 in S1 — solidly in the "warm" range for over four-fifths of the week — to 0.28 in S3 and 0.12 in S2, the only scenario whose weekly mean sits within half a scale-point of true neutrality. The proportion of hours with |PMV| exceeding 0.5 drops from 81.5% in S1 to roughly 61% in both S2 and S3, but mean PPD separates the two more decisively than PMV alone suggests: 19.2% in S2 against 22.7% in S3, the only one of the three scenarios to fall under the 20% dissatisfaction rate conventionally treated as the threshold of acceptable indoor comfort. Given that S2 and S3 share nearly identical ventilative coupling, this gap is attributable almost entirely to the lower peak the veranda buffer sustains during the hours that drive the week's PPD average upward — the same afternoon window identified in the adaptive comfort results above.

In winter, the veranda configuration shows a measurable reduction in thermal retention compared with the fully enclosed case, and this effect should be acknowledged rather than overlooked. Mean winter PMV in S2 (−2.55) is slightly more negative than in S1 (−2.09), with a corresponding increase in mean PPD (88.4% versus 76.5%). Considered in isolation, this suggests that reopening the veranda reduces the indoor heat storage provided by the enclosed configuration.

However, comparison with S3 reveals that this behavior is not specific to the veranda buffer itself. S3 records an almost identical winter response, with a PMV of −2.53 and PPD of 87.8%, confirming that the lower winter performance is primarily associated with the loss of full enclosure and its heat-retention effect rather than with the transitional nature of S2.

More importantly, none of the three configurations achieves acceptable winter comfort conditions: all scenarios maintain PMV values below −1.2 throughout the entire week, indicating that S1's relative advantage represents only a reduction in the severity of cold conditions rather than a complete comfort solution. Therefore, the more balanced interpretation is that S2 does not introduce a distinct winter disadvantage compared with the exposed alternative (S3), while the improvement it provides during summer represents a more significant climatic benefit. In a Mediterranean semi-arid climate, where overheating is the more persistent and more effectively addressable challenge through spatial configuration, the ability of the veranda to reduce summer heat stress becomes the more consequential performance outcome.

- Case 3: contemporary house

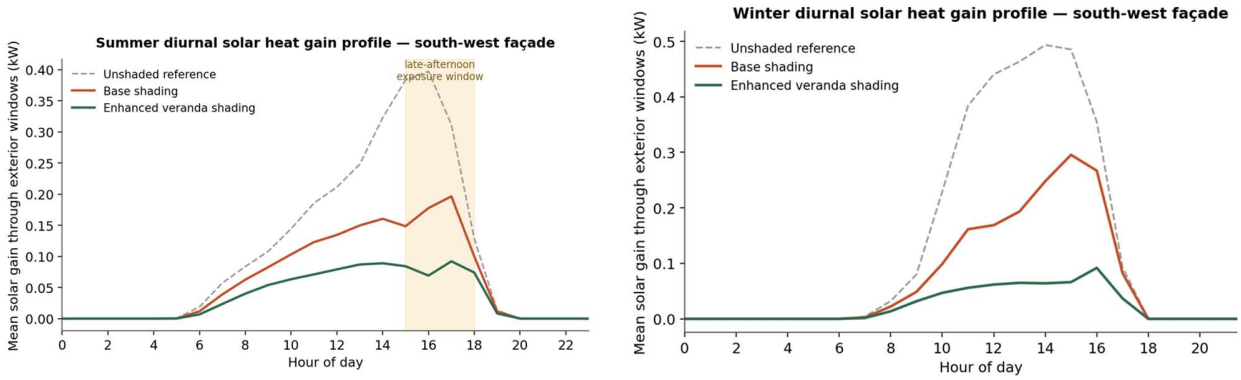
Veranda Shading Concept as a Thermal Buffer

This section examines the simulated thermal performance of the veranda shading strategy against the base unshading condition established earlier in this chapter. The studied living space faces south-west, an orientation that, within the semi-arid Mediterranean climate of Abu Dis, exposes the façade to sustained direct radiation through the mid-afternoon and into the early evening, when solar altitude drops and the incidence angle on the façade approaches normal. The enhanced scenario introduces a projecting, roofed veranda in front of the south-west openings. Rather than treating this as a shading device alone, the analysis considers the veranda as a transitional climatic space: a covered zone ahead of the window that absorbs and moderates solar exposure before it reaches the interior, in the same manner as the covered porches and liwan spaces of traditional Palestinian houses. Two simulation periods, each a representative seven-day sequence (1–7 August and 15–21 January), capture the cooling-dominated and heating-dominated regimes of the annual cycle. An unshaded reference case sits alongside the two shaded scenarios, giving the veranda's incremental contribution a fuller range of comparison than the base condition alone would allow.

- Solar Heat Gain

Cumulative solar gains through the south-west glazing fall further under the veranda than under base shading alone, in both seasons. Over the summer week, cumulative gains drop from 10.50 kWh under base shading to 5.89 kWh under the veranda, a further reduction of 43.9 percent on top of what base

shading already removes relative to the unshaded reference (18.30 kWh). In winter the gap widens: cumulative gains fall from 11.12 kWh to 3.75 kWh, a reduction of 66.3 percent. The difference between seasons follows from solar geometry rather than any change in the device itself. The veranda's roof plane sits between the sun and the window, and because the winter sun travels at a lower altitude, more of its path falls within the veranda's shadow. The summer sun, already partly cut by the base shading device before the veranda's added depth comes into play, simply has less left to lose.



Summer week (1-7) August

Winter Repeatable Week (51-21) Jan

Figure 5-39: Mean diurnal solar heat gain profile through the south-west glazing, for the unshaded reference, base shading, and enhanced veranda scenarios.

The diurnal solar gain profile (Figure 5-39) carries the signature of the south-west orientation in all three scenarios. Instead of a single midday peak, which a south-facing aperture would show, the curve leans toward late afternoon: the unshaded reference peaks at 16:00 (0.397 kW on average), and both shaded cases hold a plateau, or even a small secondary rise, between 16:00 and 17:00 before gains collapse toward sunset. Under base shading, the highest hourly gain (0.196 kW) falls at 17:00, later than the unshaded peak; the veranda case shows the same late lean, with gains at 17:00 (0.092 kW) slightly above those at 15:00 and 16:00. Low solar altitude explains this. A projecting horizontal roof such as the veranda's works best against high sun, roughly overhead through late morning and midday, and loses depth as the sun drops toward the horizon and swings around to face the façade more directly. Some late-afternoon gain, therefore, still reaches the window even with the veranda in place, not through any failure of the device, but because a horizontal overhang was never suited to blocking low, raking light on a west-facing wall. Orientation, in other words, sets a limit that shading depth alone cannot fully close.

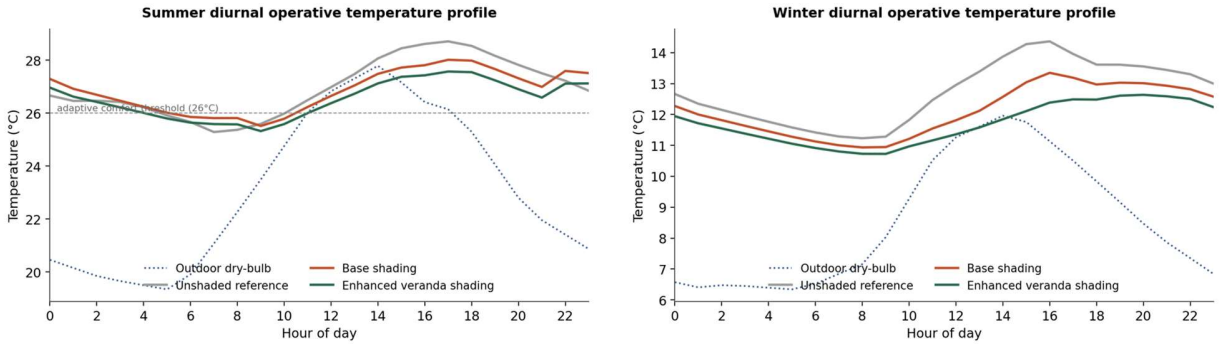
The winter profile follows the same afternoon-leaning shape but starts from a much higher base: unshaded gains peak at 0.494 kW around 14:00–15:00, since the low winter sun angle lets radiation reach further into the room. Here the veranda's effect is to flatten the entire midday-to-afternoon curve into a low band that rarely exceeds 0.09 kW. Acting as a transitional climatic buffer, the veranda intercepts this radiation in the air layer between the roof overhang and the window, where it can be re-radiated rather than transmitted directly through the glazing. In summer this interception is unambiguously beneficial. In winter it removes solar heat that would otherwise offset heating demand, a trade-off returned to in the discussion below.

Table 5-14: Summary of solar heat gain indicators, base shading vs. enhanced veranda scenarios

Indicator	**Unshaded reference**	**Base shading**	**Enhanced veranda**	**Veranda vs base (%)**
Cumulative solar gain – summer (kWh/wk)	18.30	10.50	5.89	43.9%
Cumulative solar gain – winter (kWh/wk)	21.43	11.12	3.75	66.3%
Peak hourly solar gain (avg.) – summer, 17:00	0.397 kW	0.196 kW	0.092 kW	53.1%

- Operative Temperature Assessment

The reduced solar admission carries through to a measurable cooling of the indoor environment, though the shift in mean and peak conditions is modest against the size of the seasonal drop in solar gain. Mean operative temperature falls from 26.85 °C under base shading to 26.53 °C under the veranda, a difference of 0.32 °C, while the peak, reached at 17:00 in both cases and coinciding with the late-afternoon solar peak described above, falls from 28.01 °C to 27.57 °C, a difference of 0.44 °C. The peak sits at the same hour in both shaded scenarios, so the veranda's effect in summer is one of amplitude rather than timing: it narrows the swing without shifting when it happens. Diurnal amplitude falls from 3.42 °C in the unshaded case to 2.50 °C under base shading and 2.25 °C under the veranda, a combined narrowing of roughly a third against the unshaded reference. This fits the veranda's role as a buffer positioned ahead of the building's thermal mass rather than at the window plane itself: because it removes radiation before it reaches the glazing and internal surfaces, it dampens the size of the daily swing without changing the pace at which the room responds to outdoor conditions, a pace still set by the unchanged fabric and mass of the dwelling.



Summer week (1-7) August

Winter Repeatable Week (51-21) Jan

Figure 5-40: Mean diurnal operative temperature profile, compared with outdoor dry-bulb temperature, for the unshaded reference, base shading, and enhanced veranda scenarios.

The winter profile (Figure 5-40) shows a similar drop in mean operative temperature, from 12.11 °C under base shading to 11.71 °C under the veranda, but the change in the shape of the curve matters more than the change in its level. Where the base shading and unshaded profiles both peak sharply at 16:00, the veranda profile flattens into a plateau running roughly from 16:00 to 20:00, with no single clear maximum. Once the direct solar component is largely removed, what remains of the daily swing owes less to when the sun strikes the window and more to the slower thermal response of the fabric itself, the kind of decrement delay usually associated with thermal mass rather than instantaneous solar gain. The veranda, in effect, pushes the room's behavior further from a solar-driven pattern toward a mass-driven one, and the daily cycle lags and flattens as a result. That shift is welcome in summer. In winter it comes at the cost of a solar contribution that would otherwise help offset heating demand, a point taken up further below.

5.4.4 Strategy 4 — Orientation: rotation-angle scenario results against solar exposure

This section examines how the orientation of the contemporary case-study house affects indoor thermal comfort. Four rotation scenarios were simulated in DesignBuilder/EnergyPlus using the calibrated model for the base contemporary house: South-West (the as-built orientation of the case study and therefore the reference scenario), South-East, North-East, and West-North. Each scenario was run for one representative summer week (1–7 August) and one representative winter week (15–21 January), with hourly output for operative temperature, air temperature, Fanger PMV, Fanger PPD, and outdoor dry-bulb temperature. All four scenarios share an identical envelope, internal gains, and occupancy schedule, so any differences in indoor conditions arise solely from the orientation of the glazed and opaque facades relative to the sun path.

- Adaptive Thermal Comfort Calculation (EN 16798-1)

The comfort temperature is calculated using the adaptive comfort method of EN 16798-1 (the successor to EN 15251), which sets a comfort temperature that tracks the outdoor running mean rather than a fixed value. As

$$Tcomf = 0.33 \times Trm + 18.8$$

Where (Trm) is the exponentially weighted running mean of daily outdoor temperature over the preceding days. Because the simulated period covers a single representative week without a longer prior weather record, Trm was calculated using the standard five-day weighted formula (yesterday weighted 1.0, two days prior 0.8, and so on, normalized by the sum of the weights actually available), with the first day of the week treated as a steady-state continuation of itself in the absence of prior history; this is a standard simplification when only a short representative period is simulated. Three acceptability categories were then evaluated around Tcomf: Category I (±2°C, high expectation), Category II (±3°C, normal expectation, the category typically applied to existing and standard residential buildings), and Category III (±4°C, low expectation).

- Case 1: Ottoman house

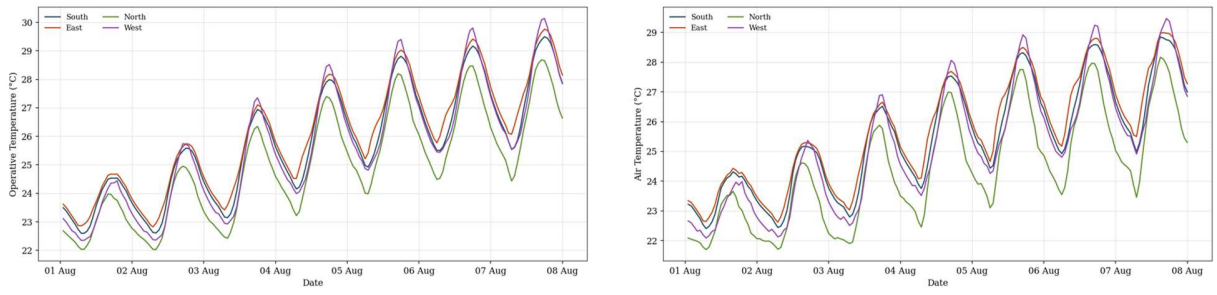
  This strategy examines the effect of orientation changes on the Ottoman house by comparing rotation-angle scenarios with variations in solar exposure and their impact on thermal performance.

- Weekly Operative and Air Temperature Comparison — Summer Week

Figure 5-41 shows that orientation does not simply shift the indoor temperature curve up or down uniformly; it reshapes it, and the shape carries the diagnostic information. West separates from the other three orientations specifically in amplitude rather than level: its weekly mean (25.67 °C) sits below both South (25.80 °C) and East (26.06 °C), yet it produces the single highest operative temperature recorded across the entire study (30.14 °C, 7 August) and by far the widest diurnal range (7.79 °C, versus 6.66–6.94 °C for the other three). This pattern is the signature of a concentrated, single-window solar event: a due-west wall receives no useful direct gain until the sun's azimuth swings past due south in the early afternoon, at which point the entire facade is struck at a steep, near-normal angle simultaneously — and, critically, this exposure coincides with the point in the diurnal cycle when outdoor air temperature is itself

at or near its own maximum. Solar and convective loading therefore peak together rather than at different times of day, and the two effects compound multiplicatively in the operative temperature trace rather than simply adding.

East, by contrast, records the highest weekly mean of any orientation (26.06 °C) despite a diurnal range essentially identical to South and North (6.94 °C). This combination — the highest average without the widest swing — points to a different mechanism from West's single sharp peak: an east-facing wall is struck by the sun during the cooler morning hours, when outdoor temperature is still climbing from its overnight minimum. Because the fabric absorbs this gain while the space is still relatively cool, less of it is lost to the still-modest temperature differential with the outdoors, and the stored heat is carried forward through the remainder of the day rather than being released against an already-hot exterior. The result is a sustained elevation of the whole diurnal trace rather than a single dramatic spike — East raises the floor of the daily cycle, West raises the ceiling. North, receiving neither of these direct-gain events, returns the lowest mean (24.99 °C) and lowest peak (28.68 °C) of the four by a consistent margin, confirming that in a free-running masonry space with no direct solar access, indoor conditions default toward the damped, delayed envelope response set by convective and conductive exchange alone.



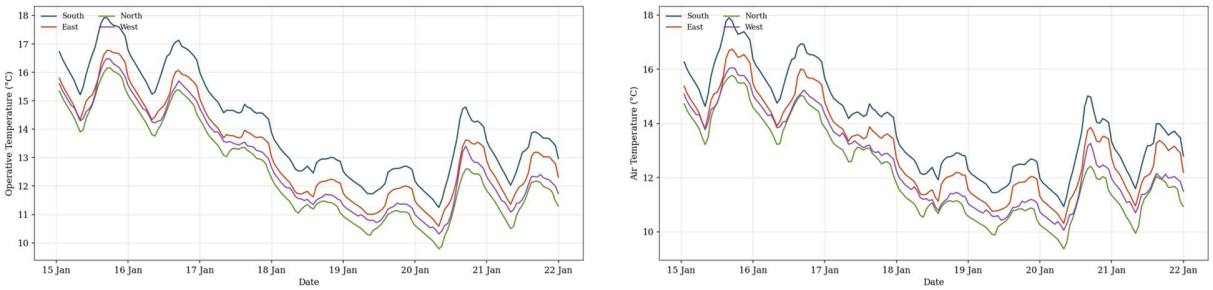
Operative temperature Air temperature

Figure 5-41: Weekly air temperature & operative temperature comparison across the four orientations, summer week (1–7 August)

- Weekly Temperature Comparison — Design Winter Week

Figure 5-42 shows the same physical mechanism operating in reverse. South records the highest weekly mean operative temperature (14.15 °C) and the highest peak (17.92 °C) of the four orientations, because a due-south wall intercepts the winter sun — which tracks a low arc close to the southern horizon at this latitude — for the longest single continuous exposure of any orientation, and does so through the middle of the day when the differential with the cold outdoor air is at its most exploitable. North again returns the

lowest performance (mean 12.56 °C, minimum 9.79 °C), and here the absence of direct gain is a straightforward liability rather than a mixed outcome: without a compensating summer benefit to offset it, North is the coldest orientation in both seasons examined. East and West converge to within 0.3 °C of one another in winter (13.28 °C and 12.89 °C respectively), because the asymmetry that separates them in summer — East's cool-morning charging versus West's hot-afternoon spike — collapses once the outdoor temperature itself is low and uniform across the day; neither orientation's timing advantage has an elevated ambient temperature left to compound against.



Operative temperature Air temperature

Figure 5-42: Weekly air temperature & operative temperature comparison across the four orientations, Winter week (15–21 Jan)

The operative-minus-air differential corroborates this reading: South is the only orientation where operative temperature exceeds air temperature by a material margin in winter (0.23 °C on average), a radiant surplus generated by direct solar charging of the internal wall and floor surfaces that the other three orientations, lacking equivalent direct exposure, cannot reproduce. Winter therefore does not introduce a new mechanism — it simply removes the compounding effect that made West and East diverge from one another in summer, leaving orientation differentiated almost solely by cumulative solar access, for which South is unambiguously best positioned and north unambiguously worst.

- Adaptive Thermal Comfort Analysis (EN 16798-1)

The EN 16798-1 adaptive model was applied to the summer week using the running mean outdoor temperature (Trm, $\alpha = 0.8$) to derive the dynamic comfort temperature $T_{comf} = 0.33 \times T_{rm} + 18.8$ °C, and the Category I (±2 °C), II (±3 °C), and III (±4 °C) acceptability bands. Because Trm is a function of outdoor climate alone, it is identical across all four orientations (19.9–21.5 °C, within the standard's 10–30 °C range of applicability), which means Figure 7 and Table 4 isolate the orientation effect against a

genuinely constant benchmark rather than one that shifts with the scenario being tested. The winter week (Trm approximately 5–9 °C) falls outside this range and is therefore assessed only under the fixed-threshold and PMV/PPD metrics.

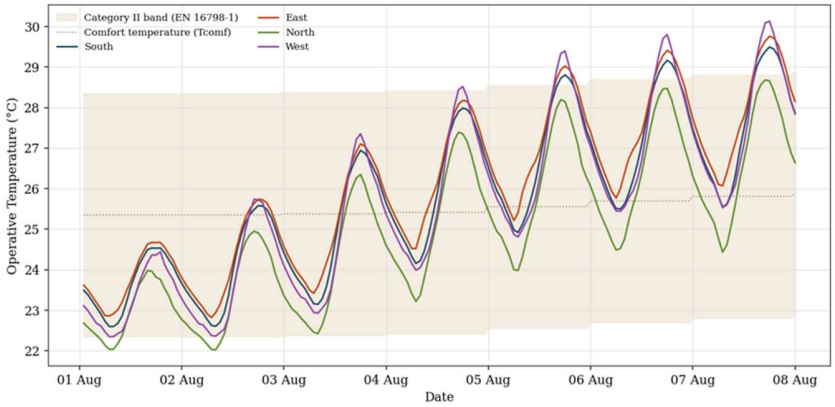


Figure 5-43: Weekly operative temperature plotted against the Category II adaptive comfort band (summer week)

Figure 5-43 shows West as the first, and only, orientation to breach the upper Category II boundary, and it does so from 6 August onward — precisely the point in the week where the rising running mean has pushed the comfort band's absolute level high enough that West's already-wide swing is what finally pushes it outside rather than any change in West's own behavior. This timing is itself diagnostic: an orientation whose discomfort is driven by amplitude rather than by mean, as West's is, will characteristically breach an adaptive band later in a warming sequence than one whose discomfort is driven by a persistently high mean, since the band's climb absorbs the mean level for longer before the swing outpaces it. North and South track nearest the center of the band, consistent with their comparatively narrow summer ranges, though for different underlying reasons — North because it receives the least gain of any kind, South because its single-aspect midday exposure is moderate rather than concentrated.

Table 5-15 makes this legible in hours rather than degrees, North's advantage looks substantial and categorical (78 of 168 hours, 46.4 per cent, against 60–66 per cent for the other three); recast against the adaptive bands, the same advantage persists but the gap compresses, because the adaptive benchmark is itself already responding to the same warm week that is driving the exceedances. What does not compress, and is arguably the more analytically important finding, is which orientation is the outlier: West is the only orientation whose Category I compliance (100 hours) is actually lower than its Category II compliance would suggest it should be relative to the other three — evidence that West's exceedances are

not marginal overshoots just outside a tight band but genuine excursions driven by the concentrated peak, which no adaptive relaxation of the benchmark can fully absorb.

Table 5-15: Adaptive Thermal Comfort Performance of the Ottoman House under Different Orientation Scenarios

Orientation	Adaptive Cat. I (±2 °C)	Adaptive Cat. II (±3 °C)
South	110 (65.5%)	153 (91.1%)
East	112 (66.7%)	148 (88.1%)
North	108 (64.3%)	158 (94.0%)
West	100 (59.5%)	146 (86.9%)

- PMV and PPD Analysis

Figure 5-44 translates the temperature findings into predicted thermal sensation in summer. North returns both the lowest mean PMV (+0.11) and the only mean PPD within the 10 per cent Category B threshold (10.80 per cent) — a direct consequence of its lack of direct solar loading rather than of any difference in the space's underlying ventilation or occupancy conditions, which are identical across all four scenarios. East's higher mean PMV (+0.44) than West's (+0.30), despite West producing the week's single highest instantaneous PMV (1.63, against East's 1.54), is the PMV/PPD-domain expression of the same mean-versus-peak asymmetry established in Section 1.1: East's morning-charged, sustained warmth elevates the whole week's average sensation, while West's afternoon spike elevates only the extremes.

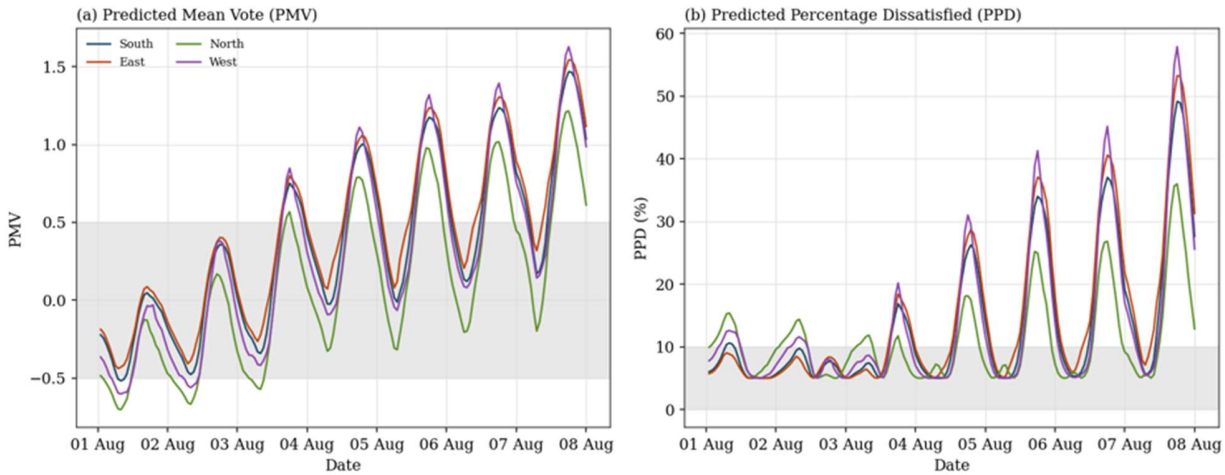


Figure 5-44: Weekly PMV (a) and PPD (b) trends by orientation, summer week

Table 5-16 represent the comfort-hour count ($-0.5 \leq PMV \leq +0.5$) which is narrower across orientations (94–101 of 168 hours) than the spread in mean PMV would suggest, and this compression is itself

informative: it shows that the ISO 7730 comfort band is wide enough to absorb most of the mean-level differences between orientations, so that what actually pushes an orientation's hours outside the band is not a modestly elevated average but the tails of its distribution. East's comparatively low comfort-hour count (94, the lowest of the four) despite not having the widest range is explained by its elevated mean sitting closer to the band's upper edge for more of the week, so that ordinary diurnal fluctuation around that mean crosses the boundary more often than West's lower mean does, even though West's fluctuation is larger in absolute terms.

Figure 5-45 shows all four orientations entirely below the ISO 7730 comfort band throughout the winter week, with zero comfort hours recorded for any orientation the expected outcome for a free-running masonry space with no direct solar gain sufficient to offset a 5.9 °C mean outdoor temperature. Within this uniformly cold result, the ranking still carries interpretive value: South's least-severe mean PMV (−1.52) and PPD (52.3 per cent) is the direct winter counterpart of its summer disadvantage relative to North — the same midday solar exposure that is moderate rather than harmful in summer becomes the space's only meaningful heat source in winter. North's mean PMV (−1.84) and PPD (67.9 per cent) are the most severe of any orientation in either season, confirming that its summer advantage is not a neutral trade-off but is bought at the single largest seasonal comfort cost measured in this study.

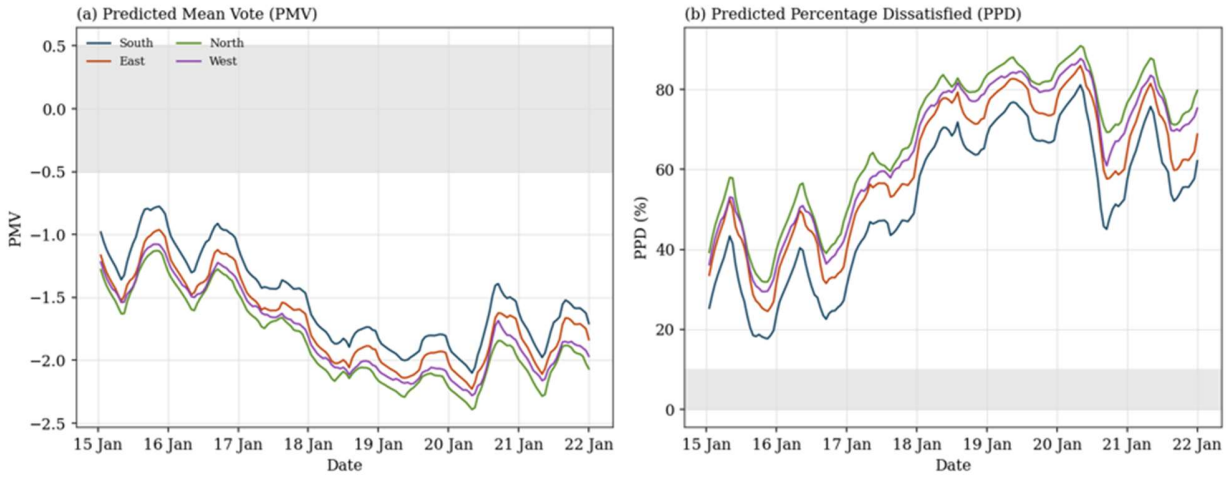


Figure 5-45: Weekly PMV (a) and PPD (b) trends by orientation, winter week.

- Diurnal PMV and PPD — Peak Summer Day (7 August)

Figure 5-46 shows North as the only orientation to register a negative (cool-side) PMV at any point in the diurnal cycle, at 07:00 (−0.20), immediately before the onset of solar charging — a residual signature of its lack of any stored gain from the previous day to keep the space from cooling fully overnight, in contrast

to the other three orientations, which retain enough residual mass heating to stay marginally on the warm side even at their coolest hour. West's peak (PMV 1.63, PPD 57.9 per cent) and North's (PMV 1.21, PPD 36.0 per cent) both occur within the same 17:00–18:00 window identified as the fabric's fixed response delay in Section 1.3, reinforcing that thermal sensation in this space is governed almost entirely by the same lagged solar-plus-mass mechanism rather than by any orientation-dependent difference in humidity or air movement, which the model holds constant across scenarios.

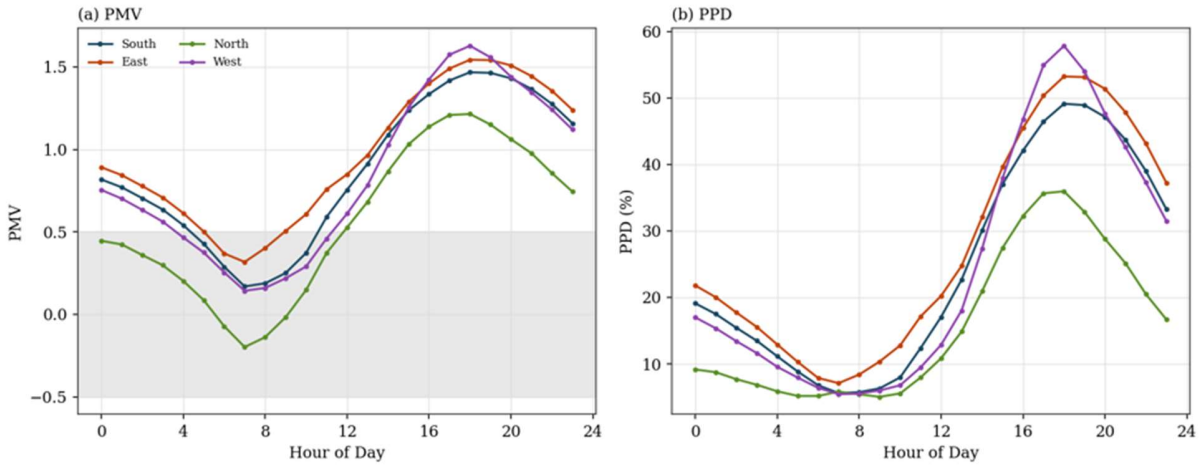


Figure 5-46: Diurnal PMV (a) and PPD (b) for peak summer day (7 August).

The PMV/PPD evidence therefore does not merely restate the temperature findings in a different unit; it isolates which of the two orientation mechanisms identified in this chapter — East's mean elevation and West's peak amplitude — dominates occupant-perceived discomfort, and shows that the two are not equivalent in comfort terms even when their underlying temperature ranges overlap. North's summer advantage and winter penalty are two faces of a single fact about this envelope and this latitude: an orientation is not comfortable or uncomfortable in the abstract, but only relative to which season's solar geometry it is being asked to manage, and no single-aspect cardinal orientation in this dataset manages both seasons well. South, as the as-surveyed reference orientation, comes closest to a balanced compromise — second-best in summer PPD, best in winter PPD — which is consistent with a historical building tradition in which orientation was chosen empirically to minimize the worse of the two seasonal extremes rather than to optimize either one in isolation.

Table 5-16: Weekly mean PMV, mean PPD, and ISO 7730 comfort-band hours by orientation and season.

Season	Orientation	Mean PMV	Mean PPD (%)	Comfort Hours (|PMV|≤0.5)
Summer	South	+0.37	13.68	98 (58.3%)
Summer	East	+0.44	14.85	94 (56.0%)
Summer	North	+0.11	10.80	101 (60.1%)
Summer	West	+0.30	13.94	97 (57.7%)
Winter	South	−1.52	52.27	0 (0.0%)
Winter	East	−1.69	60.64	0 (0.0%)
Winter	North	−1.84	67.91	0 (0.0%)
Winter	West	−1.77	64.74	0 (0.0%)

- Case 2: Jordanian house

The implementation of the orientation strategy was studied after restoring the house to its original condition by reopening the veranda as it was previously. This allowed for evaluating the performance of the strategy within the authentic spatial configuration, free from the effects of later enclosures.

- Operative and Air Temperature Analysis

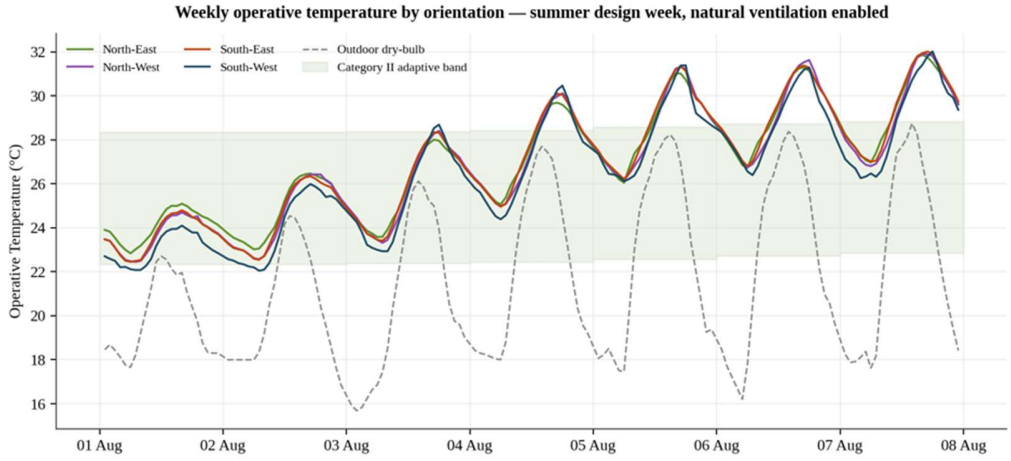


Figure 5-47: Weekly operative temperature by orientation, summer design week, natural ventilation enabled, with the EN 16798-1 Category II adaptive comfort band (shared across orientations, shaded)

Table 5-17: Summer design-week adaptive comfort compliance by orientation and adaptive category, with and without natural ventilation (EN 16798-1, n = 161 occupied hours)

Orientation	**With natural ventilation — hrs. (%) of 161**			**Without ventilation — hrs. (%) of 161**		
	Cat I (±2°C)	Cat II (±3°C)	Cat III (±4°C)	Cat I (±2°C)	Cat II (±3°C)	Cat III (±4°C)
North-East	82 (50.9%)	114 (70.8%)	130 (80.7%)	63 (39.1%)	86 (53.4%)	110 (68.3%)
North-West	79 (49.1%)	115 (71.4%)	129 (80.1%)	62 (38.5%)	90 (55.9%)	110 (68.3%)
South-East	77 (47.8%)	112 (69.6%)	127 (78.9%)	58 (36.0%)	81 (50.3%)	103 (64.0%)
South-West	70 (43.5%)	105 (65.2%)	134 (83.2%)	61 (37.9%)	93 (57.8%)	109 (67.7%)

Under natural ventilation, north-west and north-east are the strongest performers against the Category II band, with 71.4% and 70.8% of occupied hours falling inside the ±3°C envelope respectively, followed by south-east (69.6%) and, some way behind, south-west (65.2%). This ranking does not simply track cumulative solar exposure: south-west receives the largest cumulative solar gain through its exterior glazing of the four orientations (29.9 kWh across the week, against 20.7 kWh for north-east), yet it is south-west that falls outside the adaptive band most often. The explanation lies in the shape rather than the level of the temperature response. South-west's late-afternoon and early-evening solar exposure — receiving direct low-angle sun for longer into the evening as the sun moves round the west-facing façade — produces the widest diurnal swing of the four orientations (9.97°C, against 9.02°C for north-east), so that although its weekly mean operative temperature is in fact the lowest of the four (26.54°C), its excursions above the neutral band are proportionally larger and more frequent. Category II, being a relatively narrow band tied to the running mean, penalizes this amplitude far more than a fixed-threshold or mean-based metric would. North-west, by contrast, receives the second-largest solar gain (25.6 kWh) but converts a substantial share of it into useful early-to-mid-afternoon warming that decays before the neutral band is next breached, producing the best adaptive compliance of the set despite not having the lowest solar load.

Removing natural ventilation collapses adaptive compliance across all four orientations — Category II compliance falls to 53.4% (north-east), 55.9% (north-west), 50.3% (south-east) and 57.8% (south-west) — confirming that, under passive operation, ventilation is doing a substantial share of the comfort-delivering work for every orientation, not simply compensating for the worst-exposed one. What is notable

is that the size of this collapse is itself orientation-dependent: north-east and south-east lose roughly 17–19 percentage points of Category II compliance when ventilation is removed, while south-west loses only about 7 points. This is consistent with south-west's discomfort being driven predominantly by direct and delayed radiant solar gain rather than by convective heat accumulation — a mechanism that natural ventilation, which primarily removes internal air-borne heat and moisture, addresses only partially. For north-east and north-west, where solar gain is lower and more evenly distributed through the day, ventilation is proportionally more effective at holding the indoor condition inside the adaptive band, so its removal costs those orientations more. Natural ventilation therefore reduces, but does not eliminate, the orientation-driven disadvantage of the more solar-exposed façades, and its effectiveness as a compensating mechanism is itself a function of orientation.

- Design summer week

Table 5-18: Weekly summer operative temperature statistics and cumulative solar gain by orientation, (7-day design week, peak day 7 August).

Orientation	Mean (°C)	Max (°C)	Min (°C)	Amplitude (°C)	Peak time	Solar gain (kWh)
North-East	27.08	31.86	22.84	9.02	16:00	20.7
North-West	26.92	31.91	22.45	9.46	16:00	25.6
South-East	27.02	32.01	22.45	9.56	17:00	22.8
South-West	26.54	32.02	22.05	9.97	18:00	29.9

The summer results illustrate directly why cumulative solar gain and overheating risk are not interchangeable measures. South-west receives 44% more cumulative solar gain across the week than north-east (29.9 kWh versus 20.7 kWh), yet it records the lowest weekly mean operative temperature among the four orientations (26.54°C), and a maximum temperature (32.02°C) that is within 0.16°C of the highest value. Three mechanisms explain this apparent paradox. First, solar angle: south-west exposure is concentrated in the lower-angle, longer-path late afternoon sun, which, following the cosine law of incidence, delivers energy less efficiently per unit of direct-normal irradiance than the more perpendicular mid-morning sun received by north-east and north-west (Duffie and Beckman, 2013); a larger solar total therefore does not translate proportionally into a higher peak heat flux. Second, thermal mass buffering: with identical wall construction across all orientations, the thermal mass absorbs and delays the release of the additional solar energy received by the south-west, distributing its effect over a longer period into the

evening rather than concentrating it into a sharper daytime peak — a time-lag and decrement-factor response well established for orientation-differentiated walls in Mediterranean-adjacent climates (Balaras, 1996; Kontoleon and Eumorfopoulou, 2008; Verbeke and Audenaert, 2018) — and this is consistent with the south-west's having the widest diurnal temperature range (9.97°C) despite having the lowest mean. Third, diurnal timing mismatch: because the indoor peak in the south-west occurs later (around 18:00), it coincides with the period when outdoor temperatures have already begun to fall, reducing the available time for the space to dissipate heat to a cooling exterior, and thus favoring a wider temperature swing rather than a higher average — the same delayed-release mechanism documented for west-oriented and high-mass envelopes generally (Kontoleon and Eumorfopoulou, 2008; Karimi et al., 2024).

Comparing ventilated and unventilated summer cases quantifies the cooling contribution of ventilation. Removing ventilation increases the weekly mean operative temperature by 0.90–1.42°C depending on orientation (lowest in the south-west and highest in the south-east), and increases the weekly maximum temperature by 1.30–2.76°C (lowest in the south-east and north-east, highest in the north-west and south-west). This indicates that ventilation is not a uniform or orientation-independent cooling effect; rather, its effectiveness depends on how the solar load is distributed throughout the day, since buoyancy- and wind-driven natural ventilation is itself a function of the indoor–outdoor and diurnal temperature differential and is consistently reported as least effective when that differential is smallest — typically the late afternoon and early evening (Ahmed, Kumar and Mottet, 2021). In the south-west case, where solar gains are concentrated in exactly this period, ventilation removes a smaller proportion of peak heat, consistent with the unventilated south-west case showing the largest increase in diurnal temperature range (from 9.97°C to 10.96°C). Accordingly, the naturally ventilated scenario should be considered the realistic operating condition; however, comparison with the unventilated case shows that orientation-driven overheating risk is not eliminated but remains latent — ventilation mitigates, but does not resolve, the underlying disadvantage associated with solar geometry in west-facing orientations.

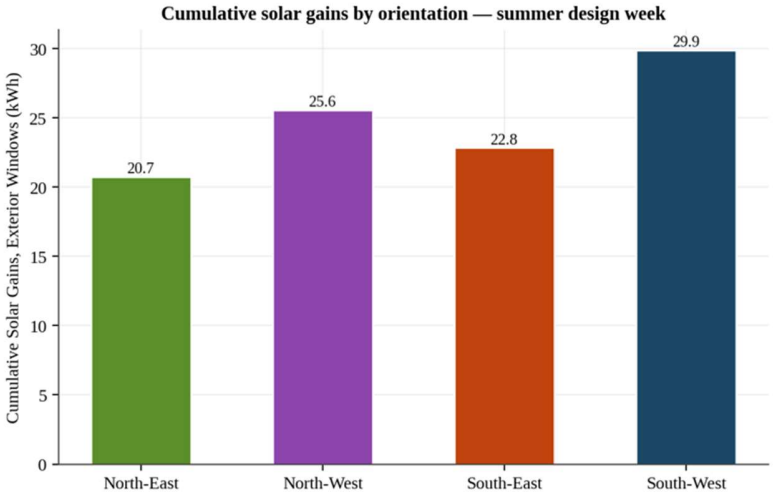


Figure 5-48: Cumulative solar gain through exterior windows by orientation, summer design week

- Design winter week

Table 5-19: Weekly winter operative temperature statistics and cumulative solar gain by orientation.

Orientation	**Mean (°C)**	**Max (°C)**	**Min (°C)**	**Amplitude (°C)**	**Solar gain (kWh)**
North-East	12.13	16.62	8.57	8.05	10.3
North-West	11.68	16.11	8.37	7.74	6.6
South-East	12.83	18.42	8.66	9.76	20.1
South-West	12.21	18.30	8.08	10.22	15.8

Winter performance inverts the summer ranking in a way that is characteristic of passive solar design trade-offs. South-east receives the largest winter solar gain of the four orientations (20.1 kWh, more than three times north-west's 6.6 kWh) and records both the highest weekly mean operative temperature (12.83°C) and the highest maximum (18.42°C), confirming that its exposure to the lower winter sun path is genuinely useful heating rather than incidental gain. South-west, despite having the largest solar gain of all four orientations in summer, receives markedly less in winter (15.8 kWh) because its dominant exposure window — the late-afternoon, low-angle west sun — is foreshortened in the shorter winter day, so it under-performs south-east for passive heating even though both are broadly "south-facing" in general terms. North-west is the weakest winter performer on every measure (lowest mean, lowest maximum, lowest solar gain), consistent with its orientation receiving the least direct low-angle winter sun of the four. North-east sits between the two extremes, gaining more solar than north-west but less than the south-

facing pair, and recording the narrowest diurnal amplitude of the week (8.05°C) — a product of its more evenly distributed, lower-intensity exposure rather than of any difference in envelope heat loss, since construction is held constant across orientations.

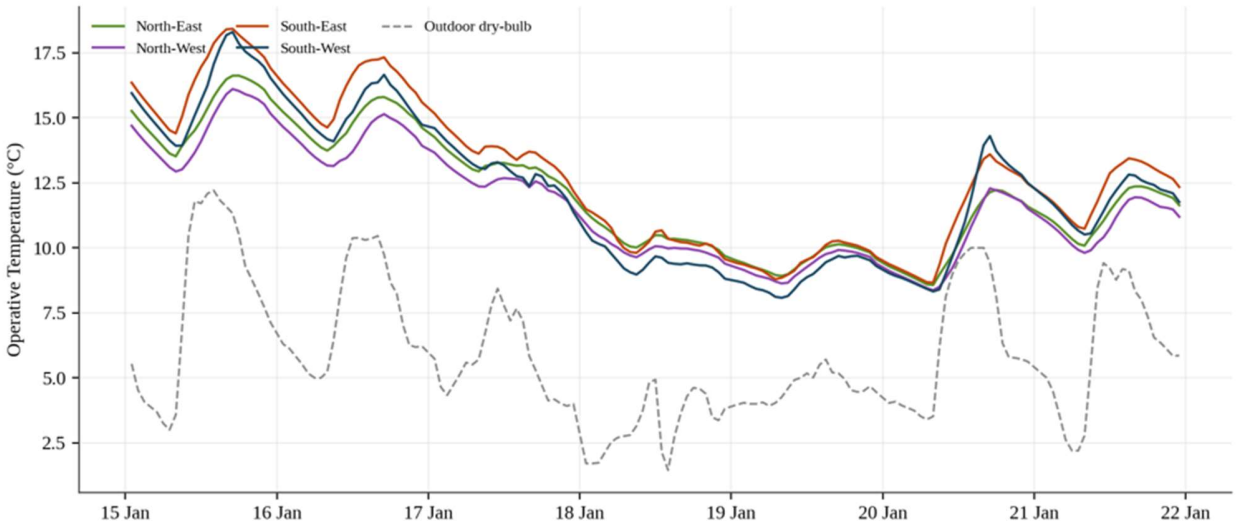


Figure 5-49: Weekly operative temperature by orientation, winter design week, against outdoor dry-bulb temperature

- PMV and PPD Analysis

Table 5-20: Mean Fanger PMV, mean PPD, and percentage of occupied hours within the ±0.5 PMV acceptable range, by orientation and simulation condition, typical summer week

Orientation	Mean PMV	Mean PPD	Hours within ±0.5 PMV	Hours exceeding limit
North-East	+0.52	22.4%	39.1%	98 / 161
North-West	+0.46	23.0%	38.5%	99 / 161
South-East	+0.50	23.8%	34.2%	106 / 161
South-West	+0.34	22.4%	36.6%	102 / 161

Table 5-21: Mean Fanger PMV, mean PPD, and percentage of occupied hours within the ±0.5 PMV acceptable range, by orientation and simulation condition, typical winter week

Orientation	Mean PMV	Mean PPD	Hours within ±0.5 PMV	Hours exceeding limit
North-East	−2.39	85.4%	0.0%	161 / 161
North-West	−2.49	88.5%	0.0%	161 / 161
South-East	−2.24	79.1%	0.0%	161 / 161
South-West	−2.38	82.9%	0.0%	161 / 161

In the ventilated summer case, PMV is uniformly positive (a mild-to-moderate warm sensation) across all four orientations, with south-west returning the lowest mean PMV (+0.34) and south-east the highest (+0.50) — a ranking that broadly mirrors mean operative temperature rather than amplitude, since PMV is evaluated instantaneously at each hour and, unlike the adaptive Category II count, is not directly sensitive to the shape of the diurnal swing, only to the momentary combination of temperature and (implicitly, through the model's air-speed input) ventilation-driven air movement. This is why south-west can simultaneously show the lowest mean PMV and the worst adaptive Category II compliance in Section 1: the two metrics are measuring different things, mean thermal sensation against a fixed physiological baseline in one case, and time spent outside a running-mean-referenced comfort band in the other.

- Diurnal PMV and PPD — Peak Summer Day (7 August)

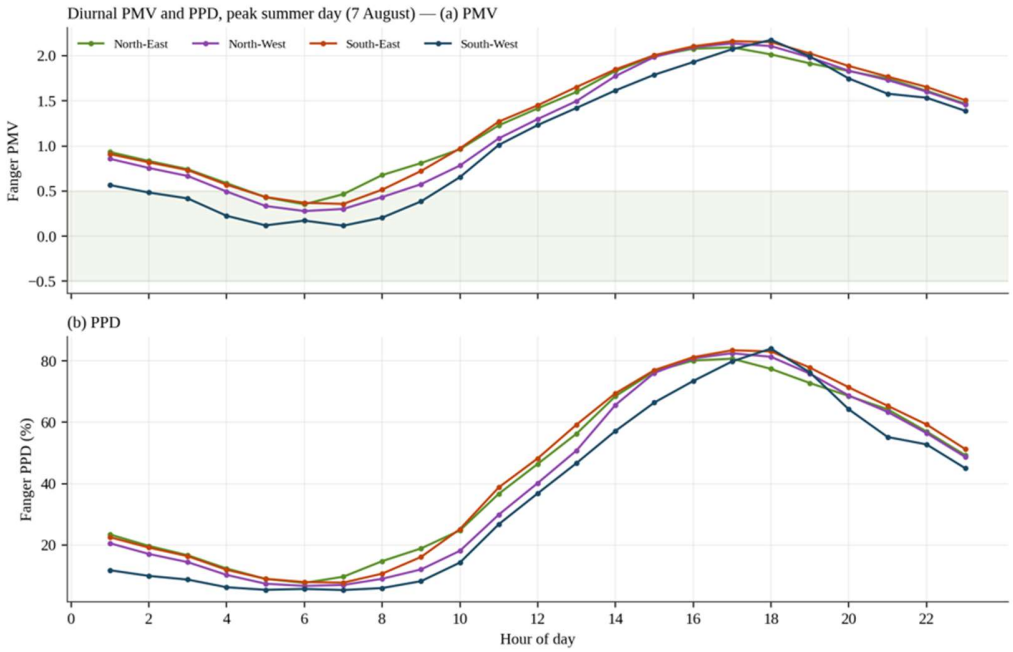


Figure 5-50: Diurnal PMV (a) and PPD (b) on the peak summer day (7 August), by orientation, natural ventilation enabled

7 August, the hottest day of the week, shows orientation shifting the *timing* of discomfort as much as its severity. Through the morning all four orientations track together, since solar exposure differs little between the rotated façades at that hour and outdoor warming is still the main driver. Divergence starts in early afternoon: the sun swings round to favour south-west's west-facing surfaces, and south-east's to a lesser degree, while north-east and north-west — whose main exposure has already passed — level off and start to fall. The result is a clear order to the operative temperature peak: north-east and north-west at

16:00, south-east at 17:00, south-west at 18:00, a two-hour spread caused entirely by the angle of afternoon sun, since all four orientations share the same outdoor conditions and the same 14:00 outdoor peak.

PMV and PPD peak in the same hour as operative temperature for each orientation (17:00 for north-east, north-west and south-east; 18:00 for south-west), so temperature is driving thermal sensation on this day, not humidity or air movement. Peak discomfort grows with the delay too: south-west hits the highest PPD of the four (84.0%, against 80.7% for north-east).

Evening recovery is slower where solar exposure ran heaviest. By 22:00, north-east and north-west have dropped back near the outdoor curve, but south-west stays visibly warmer, carrying heat stored in the mass during its later, stronger afternoon exposure. This is the mechanism from Section 2 again: the mass that delays and dampens the daytime peak also delays its release, so the orientations with the latest sun carry a longer discomfort tail into the evening — when ventilation (the gap between the solid and dotted lines in Figure 5-49) becomes the main way stored heat leaves the space.

- Case 3: contemporary house

This strategy examines the effect of orientation changes on the contemporary house by comparing rotation-angle scenarios with variations in solar exposure and their impact on thermal performance.

- Operative and Air Temperature Analysis

Figure 5-51 and Figure 5-52 compare weekly operative and air temperature profiles across the four orientations during the summer week, alongside the outdoor dry-bulb temperature. All orientations track the diurnal rhythm of the outdoor climate, rising through the morning and early afternoon and falling overnight, but the amplitude and the base level of the indoor curves differ noticeably by orientation. The North-East scenario is consistently the coolest and the flattest of the four curves, remaining below the other three orientations on every day of the week, while South-West produces the warmest and most peaked profile. South-East and West-North occupy an intermediate position, tracking each other closely for most of the week with West-North running marginally warmer during the later afternoon hours.

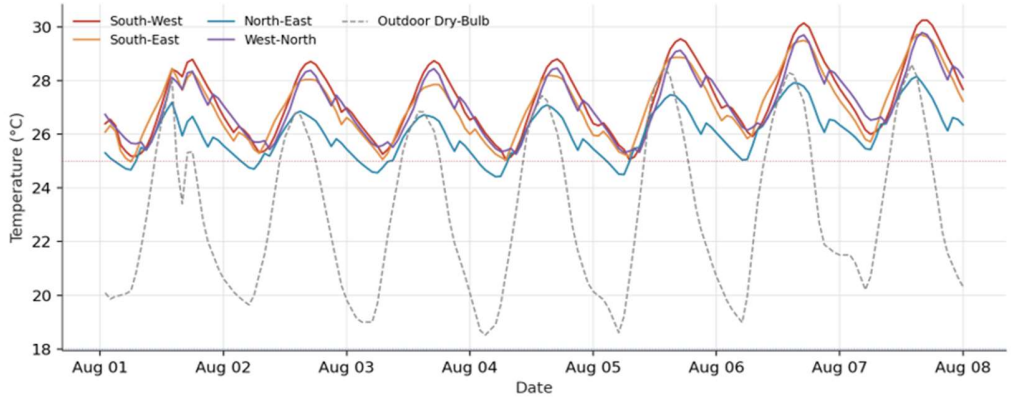


Figure 5-51: Weekly operative temperature comparison across the four orientations, summer week (1–7 August)

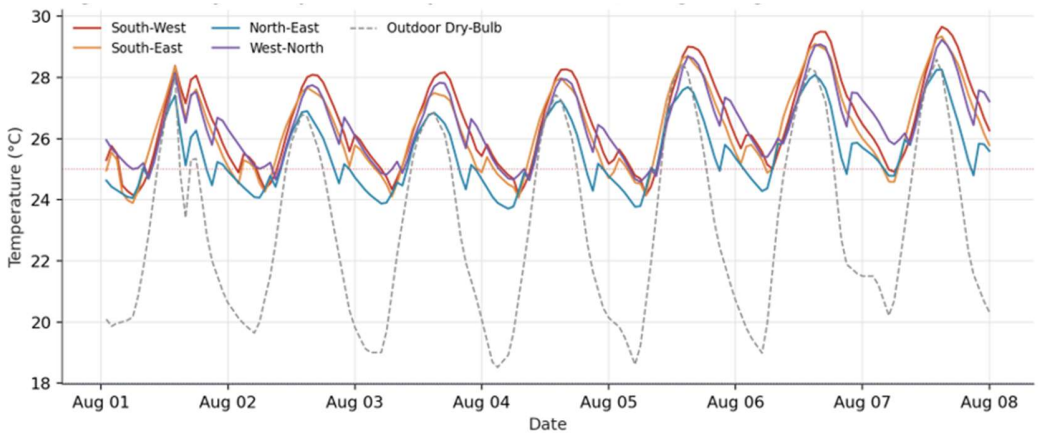


Figure 5-52: Weekly air temperature comparison across the four orientations, summer week (1–7 August)

Table 5-22 summarizes the mean, peak, minimum and mean diurnal range of operative and air temperature for both seasons. In summer, mean operative temperature ranges from 26.0°C in the North-East scenario to 27.3°C in South-West, a difference of 1.3°C driven almost entirely by the timing and intensity of solar gain through the differently oriented glazing. The gap widens at the peak: South-West reaches an operative peak of 30.2°C over the week, 2.1°C above the North-East peak of 28.2°C. Air temperature follows the same ranking and a similar magnitude of separation, though air temperature peaks are consistently 0.3–0.6°C below the corresponding operative temperature peaks, reflecting the added contribution of radiant surface temperature once the walls and glazing have absorbed solar energy.

During winter, the pattern of orientation ranking is preserved but compressed at a much lower base temperature. Mean operative temperature falls to 11.6°C for North-East and West-North against 13.0–13.1°C for South-West and South-East. In other words, the two orientations that stay coolest in summer are also the coolest in winter, because both outcomes stem from the same underlying cause: reduced

exposure of glazed area to direct, low-angle winter sun and reduced exposure of the dominant facade to the high summer sun.

Table 5-22: Weekly operative and air temperature statistics (°C) by orientation and season

Orientation	Summer Operative (Mean / Peak / Min / Range)	Summer Air (Mean / Peak / Min / Range)	Winter Operative (Mean / Peak / Min / Range)	Winter Air (Mean / Peak / Min / Range)
South-West	27.3 / 30.2 / 25.0 / 3.9	26.5 / 29.7 / 24.1 / 4.3	13.0 / 15.7 / 10.6 / 3.5	12.6 / 15.6 / 10.1 / 3.8
South-East	27.1 / 29.7 / 25.0 / 3.4	26.3 / 29.3 / 23.9 / 4.1	13.1 / 15.4 / 10.7 / 3.1	12.7 / 15.3 / 10.1 / 3.5
North-East	26.0 / 28.2 / 24.4 / 2.6	25.5 / 28.3 / 23.7 / 3.4	11.6 / 12.7 / 10.1 / 1.8	11.3 / 12.9 / 9.6 / 2.4
West-North	27.1 / 29.8 / 25.3 / 3.2	26.5 / 29.2 / 24.6 / 3.4	11.7 / 13.1 / 10.0 / 2.1	11.3 / 13.0 / 9.6 / 2.4

The winter week (Figures 53 and 54) shows the same orientation ordering as summer but with far smaller day-to-day fluctuation, because the mid-January outdoor temperature swings less than the early-August outdoor temperature over the simulated week. North-East and West-North remain the two coolest orientations throughout, sitting 1.3–1.5°C below South-West and South-East on average, which in winter works against comfort rather than for it.

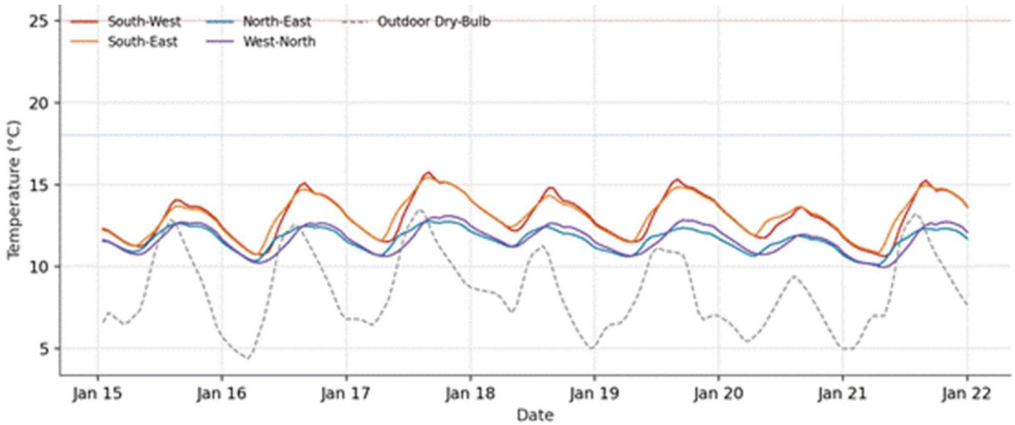


Figure 5-53: Weekly operative temperature comparison across the four orientations, winter week (15–21 January)

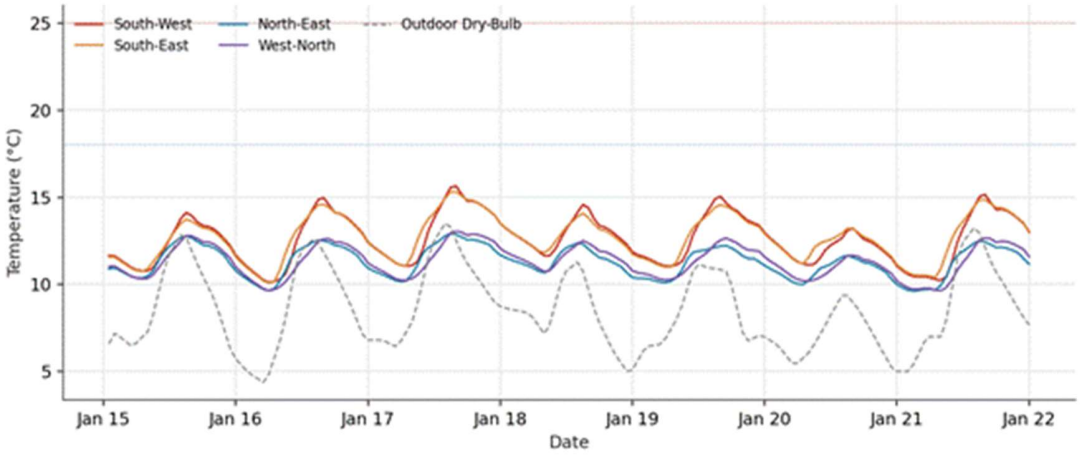


Figure 5-54: Weekly air temperature comparison across the four orientations, winter week (15–21 January)

To examine diurnal behavior at higher resolution, 7 August was selected as the representative peak summer day, since it records the highest outdoor peak of the week (28.6°C) among the seven simulated days. Figure 5 plots the diurnal operative and air temperature curves for that day, with peak and minimum values labelled for each orientation and the outdoor dry-bulb curve superimposed for reference.

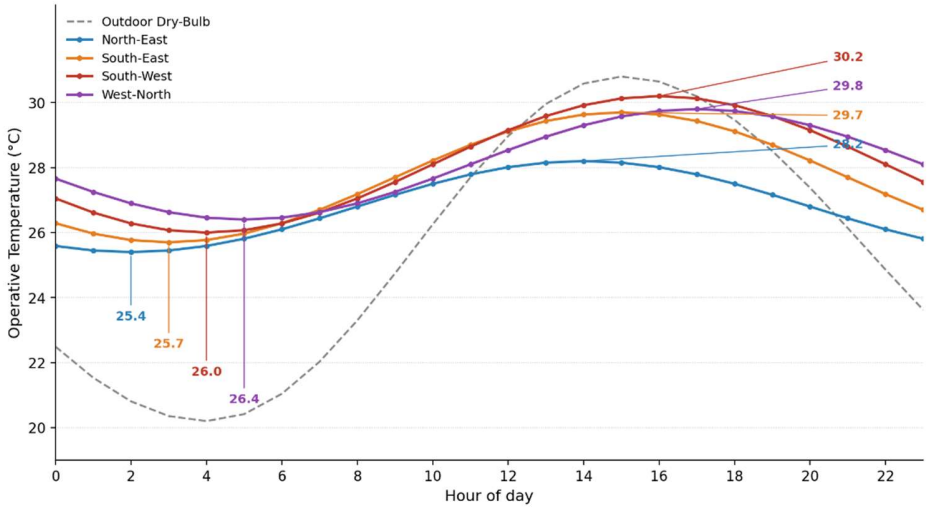


Figure 5-55: Diurnal operative temperature profiles for the representative peak summer day, 7 August, with peak and minimum values annotated

The diurnal range (the difference between the daily maximum and minimum) is itself a useful comfort indicator, since a flatter curve implies a more stable indoor environment and a smaller number of hours spent at the temperature extremes. North-East again produces the flattest curve of the four, with a mean diurnal range of 2.6°C for operative temperature against 3.9°C for South-West, a reduction of roughly one-third. This damping is consistent with reduced direct-beam solar gain reaching the North-East facade

during the hours of highest solar altitude, which in the Palestinian summer occur when the sun is close to due south.

- Adaptive Thermal Comfort Calculation (EN 16798-1)

The method carries an explicit validity constraint: EN 16798-1 restricts the adaptive model to conditions where the outdoor running mean temperature falls between 10°C and 30°C, on the basis that adaptive behavior cannot be assumed to compensate for very cold conditions. The summer week satisfies this condition comfortably, with Trm ranging from 22.8°C to 23.2°C across the seven days. The winter week does not: Trm ranges from 8.1°C to 9.0°C, below the 10°C floor, so the adaptive model is not formally applicable in winter.

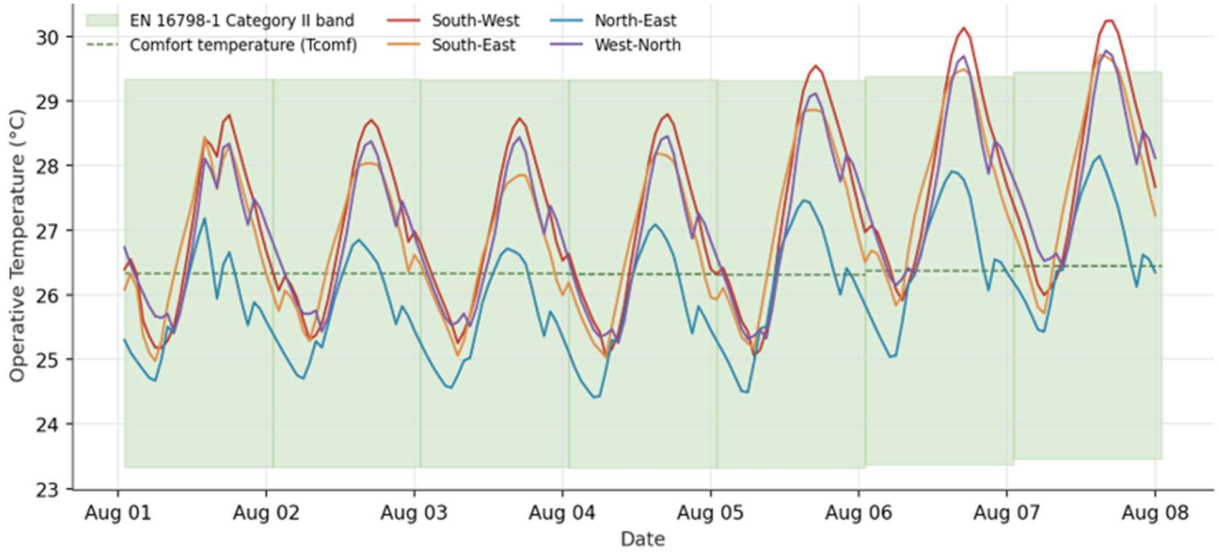


Figure 5-56: Weekly operative temperature against the EN 16798-1 Category II adaptive comfort band, summer week

Figure 5-56 plots the same weekly operative temperature curves against the Category II adaptive band, which sits at roughly 23.3–29.4°C across the week. (Table 5-23) quantify this: under Category II, South-West falls outside the band for only 14 of the 168 hours (8.3%), South-East for 8 hours (4.8%), West-North for 6 hours (3.6%), and North-East for zero hours, meaning the North-East scenario remains within adaptive comfort for the entire simulated summer week. Category I, the stricter band, still shows South-West exceeding the limit for 43 hours (25.6%) against zero for North-East, while under the most permissive Category III band no orientation records a single hour of overheating.

Table 5-23: Summer overheating hours (of 168) under the fixed threshold versus EN 16798-1 adaptive comfort categories I–II. summer week

Orientation	**Adaptive Cat. I Overheating (>Tcomf+2)**	**Adaptive Cat. II Overheating (>Tcomf+3)**
South-West	43 (25.6%)	14 (8.3%)
South-East	24 (14.3%)	8 (4.8%)
North-East	0 (0%)	0 (0%)
West-North	24 (14.3%)	6 (3.6%)

- PMV and PPD Analysis

The Fanger PMV and PPD outputs provide a comfort assessment that accounts for humidity, radiant temperature, clothing and metabolic rate together, rather than air or operative temperature alone, and allow the fixed-threshold discomfort-hour analysis above to be cross-checked against a recognized comfort index. Figure 5-57 plots the weekly PMV and PPD trends for the summer week; Figure 5-58 shows the equivalent winter trends; Figure 5-59 gives the high-resolution diurnal PMV and PPD curves for the representative peak summer day.

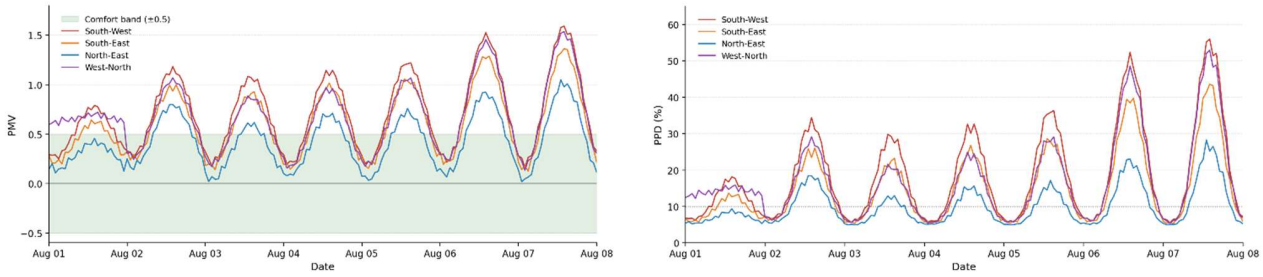


Figure 5-57: Weekly PMV (a) and PPD (b) trends by orientation, summer week

In summer, PMV rises above the upper comfort boundary of +0.5 on every orientation during the afternoon peak, but the height and duration of that excursion differ sharply. North-East holds the lowest mean PMV of the week at 0.45, close to the neutral–slightly-warm boundary, and spends 99 of the 168 hours within the ±0.5 comfort band (59% of the week). South-West, South-East and West-North each average a mean PMV between 0.74 and 0.80 and remain within the comfort band for only 46–48 hours (27–29% of the week). The PPD curves in Figure 5-57 b mirror this pattern: North-East peaks at a maximum PPD of

27.2%, whereas South-West peaks at 58.1%, more than double, meaning that at the hottest moment of the week over half of a notional occupant population would be predicted dissatisfied under the South-West orientation against roughly a quarter under North-East.

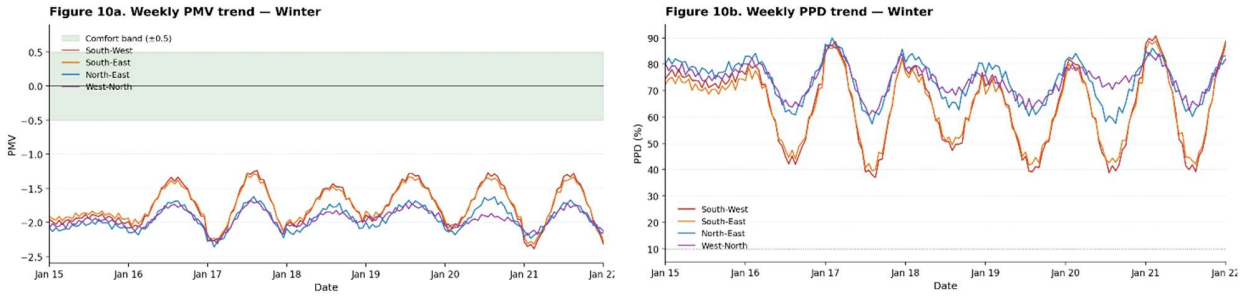


Figure 5-58: Weekly PMV (a) and PPD (b) trends by orientation, winter week

The winter PMV trends in Figure 5-58 invert the summer ranking. Every orientation records a negative mean PMV throughout the week, and none achieves a single hour inside the ±0.5 comfort band, but North-East and West-North are now the least favorable orientations, with mean PMV of −2.01 in both cases and PPD averaging 76.5–76.8%, against −1.72 to −1.74 and 62.6–63.2% PPD for South-East and South-West. The same reduction in solar gain that damps North-East's summer overheating removes a source of passive winter heating that the south-facing orientations continue to receive, even though it is insufficient on its own to reach comfort in any scenario.

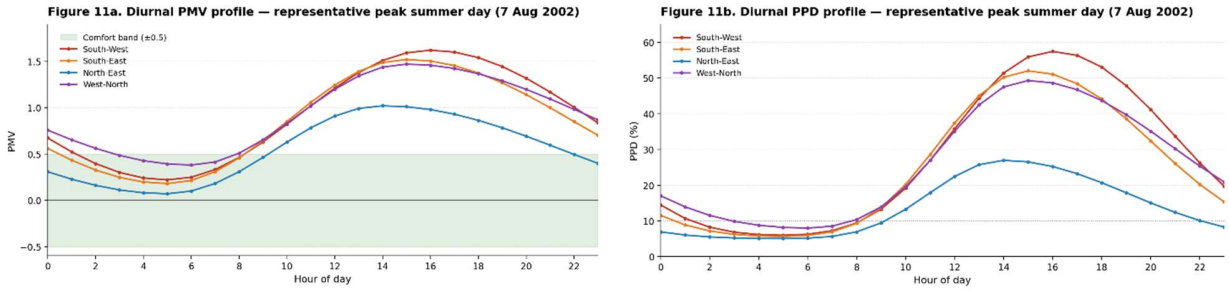


Figure 5-59: Diurnal PMV (a) and PPD (b) profiles for the representative peak summer day, 7 August

On the peak summer day itself (Figure 11), all four orientations cross into the uncomfortably warm zone (PMV > 0.5) by mid-morning and remain there until early evening, but North-East is the only orientation whose PMV curve dips back toward the comfort band overnight and in the early morning, briefly touching zero around 04:00–05:00, while the south- and west-facing orientations stay in slightly-warm territory for almost the entire 24-hour cycle.

Table 5-24: Weekly mean PMV, mean PPD and comfort-band hours by orientation and season

Orientation	Summer Mean PMV	Summer Mean PPD (%)	Summer Comfort Hours (of 168)	Winter Mean PMV	Winter Mean PPD (%)
South-West	0.80	21.5	46 (27%)	−1.74	63.2
South-East	0.74	19.1	48 (29%)	−1.72	62.6
North-East	0.45	10.5	99 (59%)	−2.01	76.8
West-North	0.76	19.3	47 (28%)	−2.01	76.5

Discussion: Orientation, Solar Gain, and Thermal Response:

The relationship between operative and air temperature is itself diagnostic of the underlying mechanism. Operative temperature combines air temperature with mean radiant temperature, weighting the two according to air speed and the radiant exchange between the body and surrounding surfaces (ISO 7730, 2005; Olesen, 2002). An orientation that limits direct solar exposure of internal surfaces therefore narrows the gap between the two variables, since less incident radiation is available to raise surface temperatures above air temperature and drive the radiant component upward. This is precisely the pattern observed in North-East, where the operative–air temperature gap at the summer peak is smaller than in the other three orientations. The result is consistent with Olesen's (2002) account of operative temperature as a composite index sensitive to radiant asymmetry, and it indicates that North-East's internal surfaces absorb and re-radiate comparatively little solar energy over the course of the day.

Overheating patterns track solar exposure closely, a finding well supported in the orientation literature (Givoni, 1998; Santamouris, 2016). South-West and West-North both include a west-facing component and consequently receive strong late-afternoon direct-beam solar gain, at precisely the hour when outdoor air temperature is already close to its daily maximum. Givoni (1998) identifies this coincidence of peak solar incidence and peak outdoor temperature on west-facing facades as one of the most severe overheating risks in hot and semi-arid climates, since neither the building fabric nor the occupant has any thermal "buffer" left to absorb the additional load. The combination of already-warm outdoor air and intense low-angle solar gain on a large glazed or exposed facade produces the highest and latest operative temperature peaks of the four scenarios, occurring at 16:00 in South-West. South-East, which faces the morning and midday sun rather than the afternoon sun, peaks earlier, at 14:00, and reaches a slightly lower

maximum, reflecting a solar exposure profile that front-loads gain earlier in the diurnal cycle before ambient temperatures reach their daily high. North-East, which minimizes exposure to the high-intensity midday and afternoon sun altogether, produces both the lowest peak and the earliest-arriving one among the three non-reference orientations. Taken together, these results align with Santamouris's (2016) broader argument that facade orientation, rather than fabric specification alone, is frequently the dominant control on peak indoor temperature in climates with strong seasonal solar geometry. The most critical hours of discomfort across all orientations fall between approximately 12:00 and 18:00 in summer, when solar gain, outdoor temperature, and accumulated envelope heat coincide, and between 03:00 and 07:00 in winter, when outdoor temperature reaches its overnight minimum, and the envelope has had the longest interval since the previous day's solar input to lose heat through radiation and conduction.

These findings also bear on adaptive comfort assessment. Nicol and Humphreys (2002) and de Dear and Brager (1998) argue that acceptable indoor temperature ranges shift with the running mean of outdoor temperature, and EN 16798-1 formalizes this relationship through its Category I–III comfort bands. Because the timing and magnitude of an orientation's peak operative temperature determine how far it departs from the adaptive comfort band at any given hour, the earlier, lower peak recorded for North-East implies a materially better fit with adaptive comfort criteria during the critical summer afternoon window than either South-West or West-North, independent of any change to occupant behavior or clothing.

In terms of stability, North-East is also the most stable of the four orientations, shown by its comparatively small diurnal range and its short lag relative to the outdoor cycle. South-West, by contrast, combines the largest diurnal range with the strongest and most direct outdoor coupling. This is consistent with a facade that absorbs heat over an extended period through direct exposure and releases it with a corresponding four-hour delay, the classic signature of a solar-gain-dominated facade response rather than of the building fabric alone, since the fabric specification is identical across all four scenarios. This distinction matters for how the lag itself should be interpreted: Givoni (1998) treats thermal lag primarily as a fabric property, governed by wall mass and conductivity, but the present results show that orientation can produce comparable lag effects on an otherwise-identical envelope purely through the timing of solar incidence.

5.4.5 Strategy 5 — Room Geometry and Enclosure: results of the Three ratio/enclosure scenarios on temperature gradient and ventilation decay.

- Case 1: Ottoman house

The Ottoman-period house is characterized by a close-to-square principal room, a proportion inherited from load-bearing stone construction and vaulted or flat-roofed spans that discouraged deep, elongated plans. Later transformations of the domestic plan, driven by the shift to reinforced concrete framing, permitted rooms to be extended well beyond this proportion without a structural penalty. This strategy isolates that single change in plan geometry, independent of window area, orientation, or construction, to test whether departing from the historical near-square enclosure carries a measurable thermal or ventilation consequence.

Three plan ratios were simulated for the Ottoman case room, holding floor area constant at 36.4 m² (the surveyed dimensions of 6.5 × 5.6 m, treated here as the near-square reference) so that only the length-to-width proportion, and with it the distance between opposing surfaces, changes between scenarios.

Table 5-25: Room geometry scenarios, Ottoman case, floor area held constant

Scenario	**Ratio (L: W)**	**Dimensions**	**Floor area**
Case 1 (Compact)	1: 1	6.03 × 6.03 m	36.4 m²
Case 2	2: 1	8.53 × 4.27 m	36.4 m²
Case 3	3: 1	10.45 × 3.48 m	36.4 m²

- Operative temperature

The temperature response to plan elongation is non-monotonic. Case 2 (2:1) is the warmest scenario in both seasons, running 0.4°C above Case 1 in summer and 0.9°C above it in winter. Case 3 (3:1) then reverses this, falling back below Case 1 in summer and dropping a further 1°C below it in winter — the coldest winter mean and the widest diurnal range of the three scenarios. Rather than tracking plan proportion directly, this pattern tracks the ventilation behavior reported in the next section: temperature moves with how much outdoor air each geometry admits, not with elongation as such.

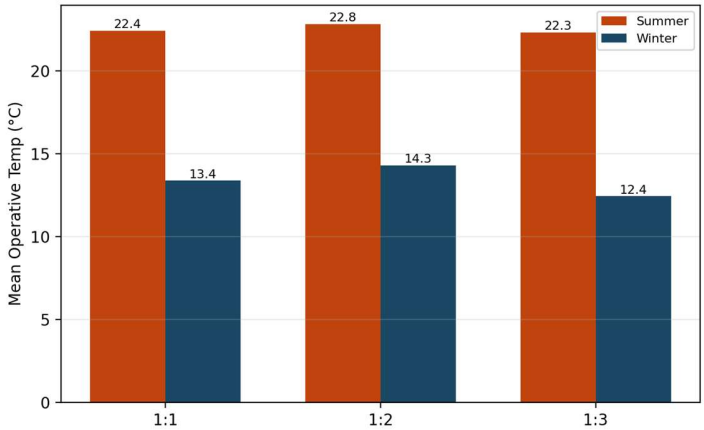


Figure 5-60: Mean operative temperature by scenario

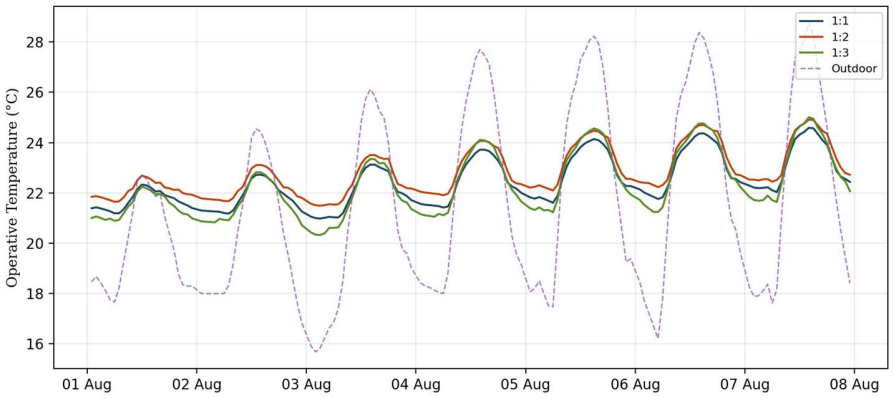


Figure 5-61: Weekly operative temperature profiles, summer week, by plan ratio

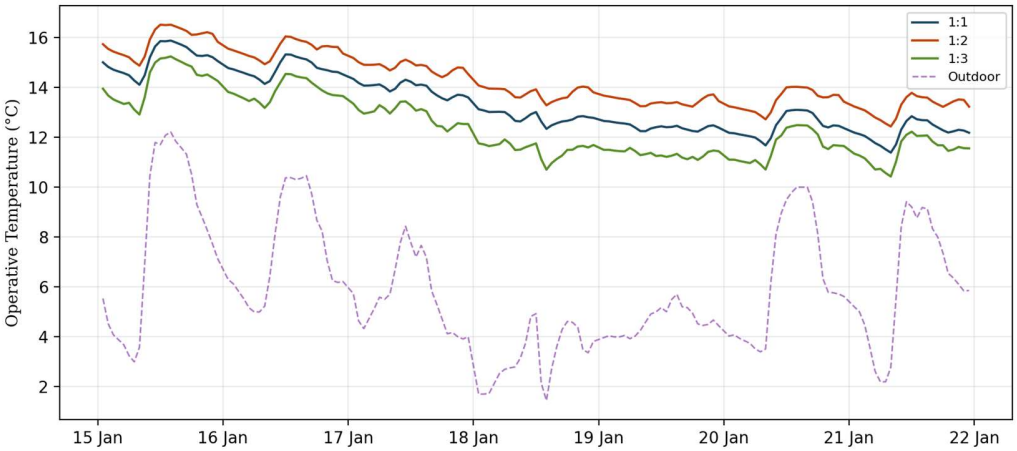


Figure 5-62: Weekly operative temperature profiles, winter week, by plan ratio

- Ventilation Rate

Ventilation rate, unlike temperature, follows plan proportion in a clear and near-monotonic way. Mean ACH rises from 2.33 in Case 1 to 2.69 in Case 2 and then sharply to 4.62 in Case 3 during

summer — very nearly doubling from the compact to the most elongated plan. The winter pattern is more striking still: Case 1 and Case 2 sit close together around 1.8 ac/h with a narrow, sharply-defined daily on/off cycle, while Case 3 runs a permanently elevated ventilation floor of roughly 3.8 ac/h even during its 'off' hours, cycling up to about 5.1 ac/h rather than down to the 1.5 ac/h baseline of the other two scenarios. The most elongated plan is therefore not simply achieving marginally more airflow; it is operating under a qualitatively different ventilation regime, with a much higher sustained air change rate across both seasons.

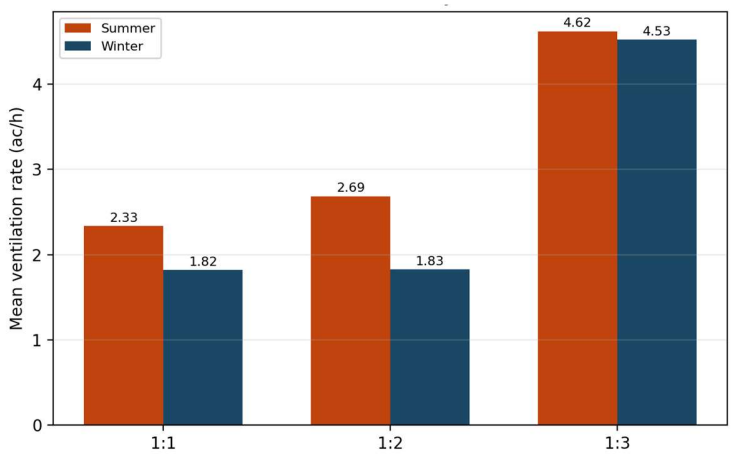


Figure 5-63: Mean ventilation rate by scenario

- Case 2: Jordanian house

This strategy evaluates the impact of room geometry and enclosure proportions by analyzing the thermal performance across three aspect-ratio scenarios.

Table 5-26: Room geometry scenarios, Jordanian case, floor area held constant

Scenario	Ratio (L: W)	Dimensions	Floor area
Case 1 (Compact)	1: 1	5.04 × 5.04 m	25.4 m²
Case 2	2: 1	7.13 × 3.56 m	25.4 m²
Case 3	3: 1	8.73 × 2.91 m	25.4 m²

- Operative Temperature

Temperature responds to plan elongation consistently in both seasons: mean operative temperature falls steadily as the room elongates, from 26.43°C (Case 1) to 25.99°C (Case 2) to 25.55°C (Case 3) in summer, and from 11.59°C to 11.46°C to 11.23°C in winter. The diurnal range narrows in step with this, from 10.69°C to 8.76°C in summer and from 9.33°C to 8.76°C in winter. The room's diurnal

swings are wide in both seasons (9–11°C), consistent with the lighter concrete-block construction responding closely to the outdoor cycle rather than damping it, as the heavier Ottoman stone construction does.

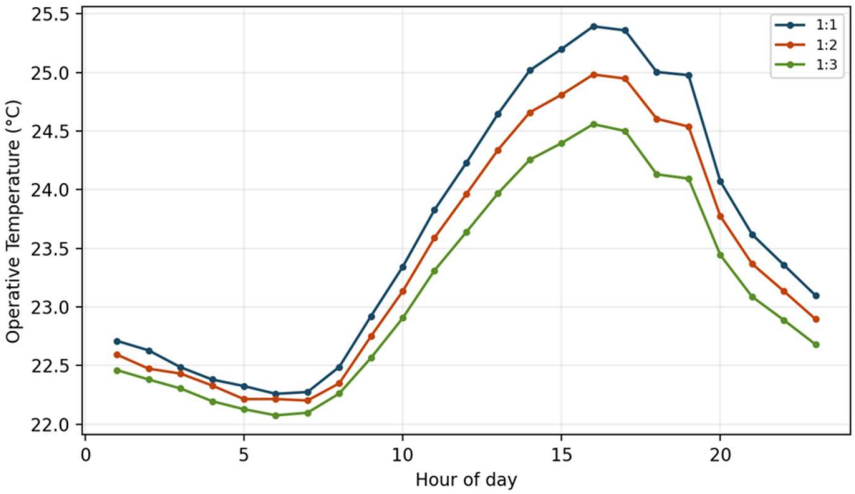


Figure 5-64: Diurnal operative temperature profile, peak summer day (1 Aug)

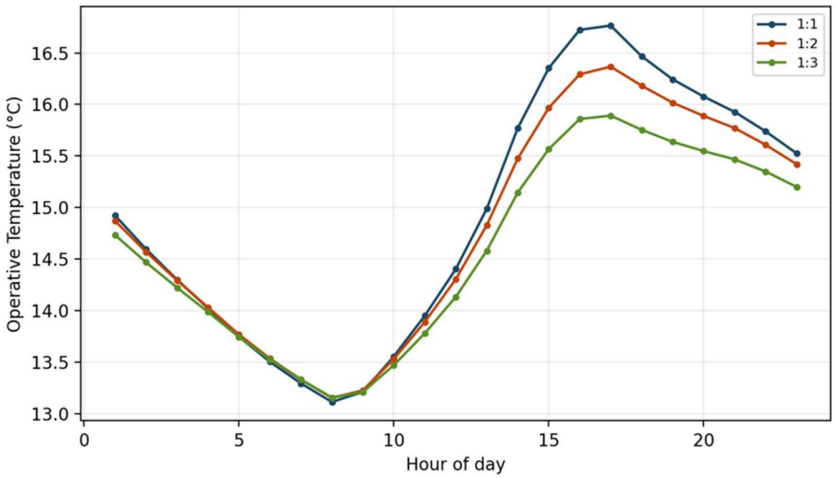


Figure 5-65: Diurnal operative temperature profile, peak winter day (15 Jan)

- Ventilation Rate

Winter ventilation is effectively flat across all three scenarios, sitting at 0.714–0.715 ac/h regardless of plan ratio — this is infiltration-only behavior, consistent with ventilation openings remaining closed throughout the winter week, and it explains why the winter temperature differences between scenarios are small and gradual rather than ventilation-driven.

Summer ventilation is very similar across all three plan ratios: 3.978 ac/h (Case 1), 3.949 ac/h (Case 2), and 3.896 ac/h (Case 3) — a gentle, near-linear decline of only about 2% from the most compact to the most elongated plan.

Table 5-27: Combined mechanical, natural, and infiltration air change rate by scenario and season

Scenario	Season	Mean ACH	Max ACH	Min ACH
1:1	Summer	3.978	5.831	2.860
1:1	Winter	0.715	0.727	0.700
1:2	Summer	3.949	5.826	2.615
1:2	Winter	0.715	0.727	0.700
1:3	Summer	3.896	5.826	1.776
1:3	Winter	0.714	0.727	0.699

- Discussion

The Jordanian-case results only make sense once ventilation rate and envelope geometry are read as two largely independent pathways rather than a single causal chain, and separating them is what explains why the scenario-to-scenario differences are modest. Because the window opening was held at a fixed absolute size and position across all three plan ratios, the mean air change rate barely moved (3.978, 3.949, and 3.896 ac/h for the 1:1, 2:1, and 3:1 cases respectively, a change of under two per cent): in a single-sided, single-opening configuration, bulk airflow through an orifice is governed primarily by the pressure differential across that opening — wind pressure coefficient and buoyancy-driven stack effect — and by the opening's own geometry, not by the internal proportions of the room behind it (Awbi, 2003; Etheridge, 2011); the room's aspect ratio can reshape how that incoming air distributes and mixes internally, but it does very little to the volume of air crossing the opening in the first place. Since ventilation is therefore effectively a constant across the three scenarios, it cannot be doing the work of explaining the steady, monotonic decline in operative temperature that plan elongation actually produces (26.43 → 25.99 → 25.55 °C in summer; 11.59 → 11.46 → 11.23 °C in winter) — that trend has to be traced instead to the envelope itself. At fixed floor area, elongating a rectangular plan from 1:1 toward 3:1 necessarily increases its perimeter and therefore its total external wall area relative to the enclosed volume, raising the surface-to-volume ratio; a higher S/V ratio increases the fabric's conductive and convective coupling with outdoor conditions per unit of conditioned space (Givoni, 1994; Santamouris, 2013), which in a lightweight, low-thermal-mass concrete-block assembly — already evidenced here by diurnal swings of 9–11 °C, several times wider than the heavier Ottoman stone construction — translates directly into a faster, more complete response to the outdoor cycle, including greater nocturnal heat rejection during the Mediterranean semi-arid summer, which is consistent with the narrowing diurnal range observed alongside the falling mean. The comparatively small magnitude of these shifts (under 1 °C in summer, well under half a degree in

winter) is itself the expected outcome once geometry is understood as a second-order variable: building-shape studies consistently find that massing changes alone, absent a compensating change to glazing ratio, shading, or fabric insulation, yield only marginal thermal or energy differences relative to those levers (Depecker et al., 2001; AlAnzi et al., 2009), which is precisely why Strategies 1 and 2 in this thesis — wall construction and window-to-wall ratio — registered larger effects than geometry does here; room shape modulates the envelope's exposure to the climate, but with the opening fixed, it cannot touch the ventilation term, and it is this decoupling of the two mechanisms that keeps the Jordanian case's inter-scenario differences limited rather than dramatic.

- Case 3: contemporary case

Three plan configurations of equal floor area (24.8 m²) were tested under identical envelope, opening, and boundary conditions to isolate the effect of length-to-width ratio on internal thermal and ventilation behavior. Because floor area was held constant, changing the proportion redistributes the room's perimeter and, by extension, the ratio of external wall exposed per unit depth: the elongated case (8.0 × 3.5 m) carries roughly 15% more external wall length than the base or square cases (23.0 m against 20.4 m and 20.0 m respectively), while the base and square cases are nearly equivalent in this respect. This distinction matters for interpreting the results, since it means the elongated room's thermal response is shaped by two compounding factors — reduced ventilation penetration and increased envelope exposure — rather than geometry acting through airflow alone.

- Operative Temperature

The three configurations, sharing an identical floor area of 24.8 m² and an identical envelope, produce measurably different operative temperature profiles once proportion is varied. Over the summer week, the square room (5.0 × 5.0 m) records the highest mean operative temperature at 28.53 °C and the highest peak at 31.39 °C, the base case (6.2 × 4.0 m) follows closely at 28.32 °C mean and 31.28 °C peak, while the elongated room (8.0 × 3.5 m) registers the lowest figures at 28.18 °C mean and 30.96 °C peak. The same ordering holds in winter, with the elongated case again the coolest (14.30 °C mean, 16.15 °C peak) against the square case's 14.64 °C mean and 16.52 °C peak. Read at the whole-zone level, this would suggest the elongated proportion performs best thermally in both seasons, yet the zone-average figure is precisely the metric that a stretched plan is least able to represent faithfully. Operative temperature in a single well-mixed simulation node reports a spatial mean; it does not distinguish between a room that is

uniformly moderate and one in which a well-conditioned zone near the opening is averaged against a stagnant, thermally decoupled zone at depth. The elongated room's lower bulk figure is therefore better read as evidence of a wider front-to-back differential than as an indicator of superior comfort throughout the space, since the portion of floor area lying beyond the opening's effective zone of influence grows in direct proportion to the room's depth.

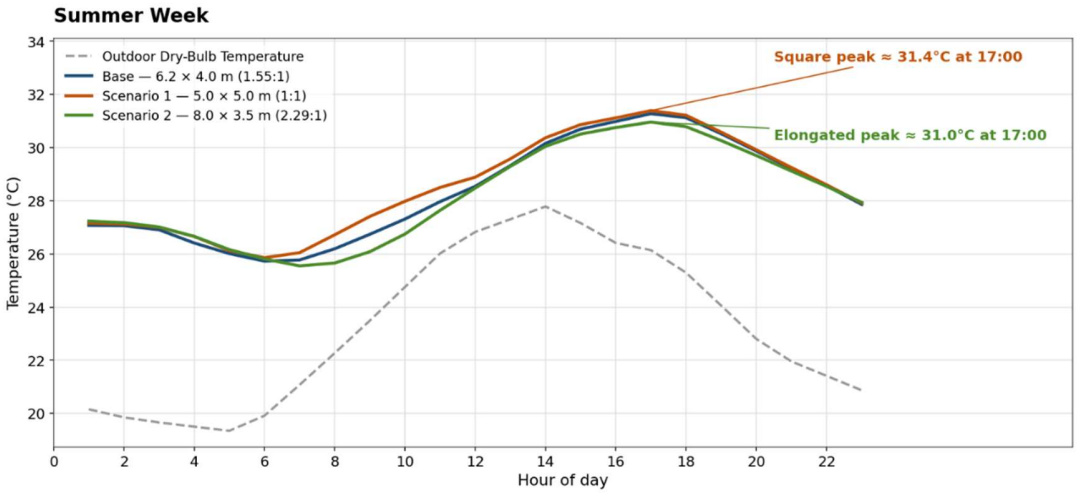


Figure 5-66: Operative temperature Profile across three proportion scenarios

This distinction is reinforced by the diurnal swing. The elongated case shows the narrowest swing in both seasons (5.41 °C in summer, 3.77 °C in winter), while the base and square cases swing more widely and almost identically to one another (5.54–5.55 °C in summer, 4.03–4.08 °C in winter). A narrower swing at the zone average is consistent with a room in which the near-opening zone is actively exchanging heat with the outdoor environment while the rear zone, buffered from that exchange by depth and by the additional external wall area the elongated plan carries per unit floor area, lags behind and damps the average. In other words, the elongated proportion does not achieve thermal stability by mixing more effectively; it achieves a smaller apparent swing by averaging two increasingly divergent thermal conditions. The base and square cases, by contrast, allow a larger share of the room to remain within reach of the opening's mixing influence, so their zone average tracks the near-opening condition more closely and swings more visibly with outdoor and solar drivers, which is the more physically honest signature of a room behaving as a single thermal volume rather than two loosely coupled ones.

On this reasoning, the base case offers the more defensible claim to spatial uniformity among the three. Its proportion, at 1.55:1, keeps the room shallow enough that convective mixing driven by the opening can plausibly reach most of the floor area, while its perimeter-to-area ratio is close to that of the square

case rather than inflated as in the elongated plan. The square configuration achieves a comparable swing but at a consistently higher temperature baseline in both seasons, indicating that compactness alone does not guarantee comfort; a 1:1 proportion reduces the maximum distance from the opening to the room's far corner, which supports uniformity, but its geometry does not reduce heat accumulation, since it retains the same envelope area within a shorter, more exposed perimeter relative to internal depth. The elongated case, despite its favorable zone-average figures, is the configuration most likely to conceal a significant front-to-back gradient, and should be treated in the thesis as the least homogeneous of the three rather than the most efficient.

- Ventilation Rate

Peak ac/h (~6.8) converges across all three, as expected — cross-ventilation's maximum flow is set by opening area and pressure difference, not room shape. The difference shows up overnight, when driving pressure weakens: the base case has the shallowest, shortest ac/h dip (2.67, 1 hr.), while both the square and elongated cases dip further and longer (2.55, 2 hrs.) — the elongated room from frictional losses over its longer path, the square room from lateral dispersion reducing effective throughflow.

Overall: The base case (6.2×4.0 m) remains the best performer under cross-ventilation, balancing enough elongation to channel airflow against not so much that path losses or fabric heat loss dominate — an optimum between the square's recirculation penalty and the elongated case's path-length penalty.

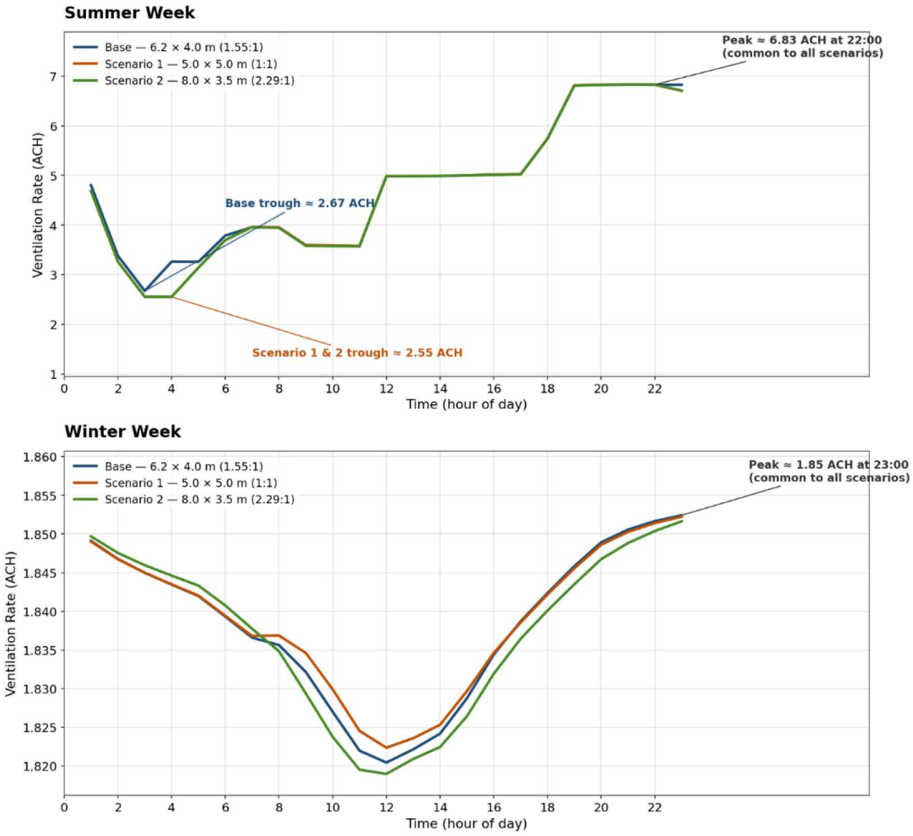


Figure 5-67: Ventilation Rate Profile across three proportion scenarios

5.6 Summary

Chapter 5 opens by validating the three DesignBuilder/EnergyPlus models against field-measured data (all three cases meet ASHRAE Guideline 14 thresholds for NMBE and CVRMSE), before comparing baseline thermal performance across the Ottoman, Jordanian, and contemporary houses. The pattern that emerges is stark: the Ottoman house holds a summer diurnal swing of just 1.8°C, the Jordanian house sits at an intermediate 2.2°C, and the contemporary house swings by 4.4°C and falls outside the Fanger comfort range for 69.5% of summer hours. This ordering tracks directly with construction: thick stone walls and a low window-to-wall ratio in the Ottoman case impose a long-time lag and heavily damp the external temperature signal, while the contemporary house's lighter concrete envelope, larger glazing, and open-plan layout offer little buffering against outdoor swings.

The chapter's second half tests five design strategies drawn from historical precedent against this baseline. Window-to-wall ratio proved to have an optimal range of roughly 18.5–30.9%, balancing ventilation gains against a modest rise in discomfort hours beyond that point. Reintroducing a veranda as a transitional

buffer was the strongest single intervention tested, cutting solar heat gain by 43.9% in summer and 66.3% in winter and reducing the Predicted Percentage of Dissatisfied to 19.2%. Wall thermal mass and time lag, building orientation, and room geometry were also tested parametrically; orientation and geometry showed real but case-dependent effects; on room geometry specifically, elongation increased ventilation in the Jordanian case but produced a more complex, non-monotonic temperature response, cautioning against treating any single geometric ratio as universally optimal.

Read together, the chapter's findings support the thesis's central argument: thermal comfort in Palestinian housing tracks the loss of specific historical spatial and constructional strategies (thick mass, moderate openings, transitional buffer spaces) rather than any single factor in isolation, and selectively reintroducing those strategies, particularly the veranda, offers a measurable and passive route to improving comfort in contemporary housing without wholesale reconstruction.

Chapter 6
Conclusion and Recommendations

This study set out to answer a question that the existing literature on Palestinian domestic architecture had left largely unaddressed: whether the successive reorganization of the Palestinian dwelling's living space, from the Ottoman courtyard house through the Jordanian-period liwan dwelling to the compartmentalized contemporary apartment, could be traced not only in descriptive or typological terms but in measurable thermal performance. Chapters One and Two established that the documentary record of this transformation was extensive but fragmented, treating each period's spatial form as a matter of architectural history and rarely connecting formal change to its environmental consequences. Chapters Three to Five built and tested a framework capable of closing that gap: three case studies in Abu Dis, surveyed, measured, modelled and calibrated against field data, and a set of five parametric strategies derived directly from the spatial logic of the historical houses rather than imported from unrelated precedent. This concluding chapter draws the findings of that framework together, considers what they mean individually and cumulatively, and sets out the study's contribution, its limits, and the questions it leaves open for further work.

6.1 Synthesis of Findings

The central finding of the study is that the social and environmental decline documented across the three periods are not parallel but coupled outcomes of the same spatial decisions. The Ottoman house's hosh, its high-thermal-mass envelope, and its narrow window-to-wall ratio worked as a single regulatory system: the courtyard mediated ventilation and shade, the 900 mm limestone wall absorbed and delayed the diurnal heat wave, and the modest window area limited direct solar admission, together producing a summer diurnal swing of only 1.8°C and a mean indoor air temperature of 27.9°C that varied by less than three degrees across the whole monitored week. That same courtyard-mass-opening arrangement also organized the household's social life, providing the shared, graduated space in which family gathering, privacy management and daily domestic activity took place. The measured environmental performance and the documented social function were, in other words, two readings of the same architectural decision rather than two separate ones.

The Jordanian period did not abandon this logic outright, but began to substitute one of its elements. The liwan preserved the mediating, semi-enclosed function of the courtyard while opening on one side rather than four, and the composite limestone-and-concrete-block wall of this period, thinner and lighter than its Ottoman predecessor, produced a shorter time lag (around four hours, against the far greater thickness of the Ottoman wall) and a substantially larger decrement factor of approximately 0.53, letting through roughly half of the external swing rather than damping nearly all of it. The measured consequence is a wider diurnal amplitude of 2.2°C and, under the sustained multi-day heat examined in Chapter Five, a tendency for the wall to accumulate heat faster than it could shed it overnight, a form of progressive thermal charging largely absent from the far more massive Ottoman assembly. The Jordanian house, in short, retained the architectural intention of thermal buffering while losing a meaningful share of its physical capacity to deliver it.

The contemporary house completes this trajectory rather than departing from it. With the courtyard and the liwan both abandoned in favor of a fully enclosed, corridor-organized layout, the case-study envelope produced a diurnal swing of 4.4°C, more than double the Ottoman figure, and left the building outside the Fanger comfort band for 69.5% of the simulated summer week, entirely on the overheating side of the scale. In winter, the same base case recorded no comfortable hours at all across the monitored period under the static PMV criterion. These figures are not an isolated technical shortfall; they are the numerical expression of the same uncoupling identified in Chapter Two, where the progressive removal of shared, climatically active space also removed the spatial precondition for the collective domestic life the earlier typologies supported. The historical narrative and the simulation results converge on the same conclusion from two independent methods: as the passive envelope was progressively dismantled across the three periods, thermal performance and social function deteriorated together, not because one caused the other directly, but because both were casualties of the same spatial decisions.

Read against this trajectory, the parametric strategies tested in Chapter Five function as a controlled dissection of what the historical envelope was actually doing, isolating variables that operated jointly in the vernacular house so that each could be assessed on its own evidentiary basis before being reassembled into design guidance. Three findings stand out for their bearing on contemporary application. The reopened veranda, tested as a semi-outdoor buffer ahead of the living space in both the Ottoman and contemporary cases, produced the strongest single result in the study: in the Ottoman

case, restoring the veranda brought mean summer PMV from 1.42, solidly in the warm range, to 0.12, and cut PPD to 19.2%, the only one of the tested scenarios to fall under the 20% dissatisfaction threshold conventionally treated as the boundary of acceptable comfort; in the contemporary case, the same principle applied to a south-west-facing façade cut cumulative solar gain by 43.9% in summer and 66.3% in winter relative to base shading alone. The mechanism in both cases was the same: a buffer positioned ahead of the glazing intercepts radiation before it reaches the room's thermal mass, moderating the peak without sacrificing the night-time ventilative recovery that full enclosure forfeits. Window-to-wall ratio behaved less as a single optimum and more as a range within which ventilation gain and solar penalty stay in balance: for the Ottoman-derived typology, that range sat between approximately 18.5% and 30.9%, beyond which the realized air change rate itself fell, discomfort hours rose sharply, and the ASHRAE 90.1 prescriptive ceiling of 40% performed worse on every indicator examined than a mid-range opening ratio, separating code compliance from thermal performance for this typology rather than assuming the two coincide. Orientation, tested on the contemporary envelope alone, produced the widest spread of any single strategy: rotating the same building to face north-east rather than its as-built south-west orientation nearly doubled the number of comfortable hours in the simulated summer week, from 46 (27%) to 99 (59%), simply by moving the façade's principal exposure away from the coincidence of late-afternoon direct-beam radiation and the day's peak outdoor temperature that afflicts south- and west-facing elevations in this climate.

The remaining two strategies were more qualified in their contribution, and that qualification is itself informative. Wall thermal mass, examined through the analytical-empirical comparison of the Ottoman and Jordanian wall assemblies, confirmed that mass alone produces a large and reliable damping effect, but also that its benefit depends on a use pattern, night-time ventilative discharge, which historical occupancy provided and sealed contemporary living does not; mass without a corresponding ventilation regime risks the progressive heat accumulation observed in the Jordanian case rather than delivering the stability of the Ottoman one. Room geometry, tested by elongating the plan at fixed floor area, produced the smallest and most case-dependent effect of the five: in the Jordanian case, air change rate remained close to flat across all three plan ratios while operative temperature fell modestly and monotonically with elongation, a result attributable to the rising surface-to-volume ratio of an elongated plan rather than to any change in ventilation. Geometry, in other words, is real but second-order: it reshapes the envelope's exposure to outdoor conditions

without materially altering airflow through a fixed opening, and its measured effect in this study was consistently smaller than that of the wall assembly, the opening ratio, the shading configuration, or the orientation.

The significance of these findings rests on the methodology that produced them, and that methodology's contribution deserves to be stated in its own right rather than treated only as a means to an end. Chapter Two established that the existing literature on Palestinian residential transformation is descriptive rather than measured; the gap this thesis set out to close was therefore not one of missing historical documentation but of missing quantification. Closing it required building three separate DesignBuilder/EnergyPlus models grounded in field survey and household questionnaire data, then calibrating each against summer field-measured indoor air temperature using the criteria commonly applied to hourly building energy models: an NMBE within ±10%, a CVRMSE within 30%, and an RMSE close to or below 2°C. All three case-study models met these thresholds, with the Ottoman case achieving an NMBE of −2.33% and a CVRMSE of 3.53%, the Jordanian case an NMBE of 3.58% and a CVRMSE of 6.27%, and the contemporary case an NMBE of 3.87% and a CVRMSE of 6.20%. This calibration exercise was not a procedural formality; it is what allowed the historical narrative developed in Chapter Two to be tested against physically grounded, field-anchored simulation rather than generic material assumptions, and it distinguishes the parametric results reported here from a purely typological or literature-based comparison. Evaluating thermal comfort through both the static Fanger PMV/PPD model and the EN 16798-1 adaptive comfort model, rather than either alone, served a comparable function: the two methods repeatedly agreed on the direction of a given result while differing in the precise number of comfortable hours they attributed to it, and reading them together, as in the veranda and orientation analyses, made it possible to distinguish a genuine change in occupant comfort from an artefact of a single, fixed-clothing assumption. This dual evaluation, together with the analytical-empirical comparison used for wall time lag and decrement factor, gave the study a degree of internal cross-checking that a single method could not have provided on its own.

6.2 Contribution of the Study

Taken together, these findings make three contributions to the study of sustainable and climate-responsive residential design in the Palestinian context. First, they establish a causal and quantified link between the historical spatial transformation of the Palestinian dwelling and its measurable

thermal consequences, replacing a descriptive account of formal change with an evidentiary one grounded in field-calibrated simulation, an approach the literature reviewed in Chapter One had not previously applied across all three periods within a single analytical framework. Second, they identify which specific historical spatial elements, thermal mass calibrated to a night-time ventilation regime, an opening ratio held within a defined range, a transitional buffer space positioned ahead of the glazing, and an orientation that avoids the coincidence of west-facing exposure with peak outdoor temperature, carry measurable and design-actionable performance value under present-day climatic conditions, rather than treating historical precedent as a single undifferentiated source of inspiration. Third, and most directly applicable to practice, the study translates these findings into evidence-based ranges and configurations, an 18.5–30.9% window-to-wall ratio, a reintroduced transitional veranda, a north-east-oriented principal façade where site conditions allow, that a designer working in Abu Dis or a comparable Mediterranean semi-arid setting could apply directly, rather than as generic passive-design advice disconnected from the specific building stock and climate under study.

6.3 Limitations of the Study

These contributions should be read within the boundaries the study set for itself. The analysis is confined to the living space as the core unit of investigation rather than the building envelope or structure as a whole, a scope decision that kept the comparison analytically consistent across three very different construction periods but that leaves the performance of adjoining rooms, roofs and foundations outside the present account. The three case studies are drawn from a single locality, Abu Dis, and from single-story typologies; while the climatic and constructional conditions examined are broadly representative of the central West Bank, the findings are best treated as most directly applicable to comparable climatic and cultural settings rather than generalized without qualification to Palestinian housing as a whole. The simulation results, however carefully calibrated, remain dependent on the assumptions, boundary conditions and material inputs used in DesignBuilder and EnergyPlus, and where field measurement could not resolve a discrepancy directly, as with the divergence between the analytical and empirical wall time-lag figures for the Ottoman case, the study has reported both routes rather than presenting a single unqualified value. Finally, the historical reconstruction of the Ottoman and Jordanian-period houses draws on the available documentary and case-study record, which cannot fully capture the range of variation that existed across these periods;

the specific wall assemblies, window ratios and courtyard proportions examined here should be understood as representative rather than universal instances of their respective typologies.

6.4 Recommendations for Future Research

Several extensions follow directly from where this study's scope ends. The parametric strategies were tested individually against a fixed baseline; a logical next step is to test them in combination, an optimized opening ratio, a reintroduced veranda and a corrected orientation applied together to the same case, to establish whether their measured effects are additive or whether they interact, positively or negatively, once combined. The present analysis is confined to single-story typologies; extending the same framework to the multi-story apartment buildings that now dominate Palestinian residential construction would test whether the same passive strategies retain their measured value once shared party walls, stacked floors and communal circulation are introduced. The thermal comfort evaluation in this study did not extend to energy demand or mechanical cooling and heating load, since only microclimatic rather than energy data was available from the field campaign; coupling the calibrated models developed here to an energy analysis would allow the passive strategies identified to be assessed in terms of the mechanical energy they displace, not only the comfort hours they recover. Finally, the social dimension of spatial transformation, addressed in this study primarily through the historical and questionnaire evidence reviewed in Chapters Two and Four, would benefit from a dedicated occupant study of a retrofitted or newly built house incorporating the veranda and orientation principles identified here, to establish whether the measured thermal improvement is matched by a corresponding change in how residents actually use and value the reintroduced space.

6.5 Concluding Remarks

The evidence assembled across this thesis does not support a case for restoring the Palestinian courtyard house as a literal contemporary model. The household structures, construction economics and urban densities that made the Ottoman hosh viable no longer hold, and the study's own findings show that isolated elements of that historical envelope, mass without ventilation, opening without shading, perform inconsistently once removed from the integrated system in which they originally operated. What the evidence does support, and what this study has attempted to demonstrate through field-calibrated simulation rather than typological argument alone, is a more selective proposition: that specific, measurable components of the historical envelope, a transitional buffer space ahead of

the glazing, an opening ratio held within a defined performance range, an orientation that avoids the worst of the local solar geometry, and a thermal mass matched to a genuine night-time discharge regime, continue to deliver quantifiable comfort benefits under present-day conditions, and can be reintegrated into contemporary Palestinian housing as tested design parameters rather than as historical reference alone. The task facing Palestinian residential design, on this evidence, is not to choose between the vernacular past and the compartmentalized present, but to recover, deliberately and selectively, the specific mechanisms by which the historical house achieved a level of passive thermal performance that the contemporary house has not yet regained

References

Abdelkader, R. and Park, J.-H. (2018) 'Spatial principles of traditional Cairene courtyard houses in Cairo', Journal of Asian Architecture and Building Engineering, 17(2), pp. 223–230. doi: 10.3130/jaabe.17.223.

Abu-Hilal, A. (2009) *The changing architectural style realized in the Palestinian domestic vernacular architecture during the end of 19th/beginning of 20th centuries: case study from Hebron.* PhD thesis. Middle East Technical University. Available at: https://etd.lib.metu.edu.tr/upload/3/12610355/index.pdf (Accessed: 5 August 2026).

Abuarkub, M. and Al-Zwainy, F.M. (2018) 'Architectural and historical development in Palestine', International Journal of Civil Engineering and Technology, 9(9), pp. 1217–1233.

Abuarkub, M. and Al-Zwainy, F.M.S. (2022) 'House with central hall (liwan) as an important element in the Palestinian cities' houses', International Journal of Advanced Research in Engineering and Technology, 13(3), pp. 18–32.

Ahmed, T., Kumar, P. and Mottet, L. (2021) 'Natural ventilation in warm climates: the challenges of thermal comfort, heatwave resilience and indoor air quality', Renewable and Sustainable Energy Reviews, 138, 110669.

Aktemur, C., Bilgin, F. and Tunçkol, S. (2021) 'Optimisation on the thermal insulation layer thickness in buildings with environmental analysis: an updated comprehensive study for Turkey's all provinces', Journal of Thermal Engineering, 7(5), pp. 1239–1256. doi: 10.18186/thermal.978057.

Al-Houdalieh, S. (2010) 'Traditional urban fabric of Palestinian historic towns: typology and transformation', International Journal of Architectural Heritage, 4(1), pp. 1–23.

Al-Ja'beh, N. and Bishara, K. (2002) Ramallah: Architecture and History. Ramallah: RIWAQ – Centre for Architectural Conservation.

Al Qadi, S., Sodagar, B. and Elnokaly, A. (2018) 'Estimating the heating energy consumption of the residential buildings in Hebron, Palestine', Journal of Cleaner Production, 196, pp. 1292–1305.

Al Tawayha, F., Bragança, L. and Mateus, R. (2019) 'Contribution of the vernacular architecture to the sustainability: a comparative study between the contemporary areas and the old quarter of a Mediterranean city', Sustainability, 11(3), 896. doi: 10.3390/su11030896.

Allweil, Y. (2016) 'Plantation: modern-vernacular housing and settlement in Ottoman Palestine, 1858–1918', ABE Journal. Architecture beyond Europe, (9–10).

Almhafdy, A., Ibrahim, N., Ahmad, S.S. and Yahya, J. (2013) 'Thermal performance of courtyard housing in a hot–humid climate', Journal of Building Performance Simulation, 6(6), pp. 463–475. doi: 10.1080/19401493.2012.718792.

Almhafdy, A., Ibrahim, N., Ahmad, S.S. and Yahya, J. (2013) 'Courtyard design variants and microclimate performance', Procedia – Social and Behavioral Sciences, 101, pp. 170–180.

Amad, E.M.A. (2012) Architecture and Society in Ottoman Palestine. Jerusalem: Institute for Palestinian Studies.

Amiry, S. (2018) The Peasant Architecture in Palestine. Ramallah: Riwaq. Available at: https://www.riwaq.org/book/95379 (Accessed: 5 August 2026).

Amiry, S. and Tamari, V. (1989) The Palestinian Village Home. London: British Museum Publications.

ARIJ (2012) Abu Dis Town Profile. Bethlehem: Applied Research Institute–Jerusalem.

ASHRAE (2020) ANSI/ASHRAE Standard 55-2020: Thermal Environmental Conditions for Human Occupancy. Atlanta: American Society of Heating, Refrigerating and Air-Conditioning Engineers.

ASHRAE (2022) ANSI/ASHRAE/IES Standard 90.1-2022: Energy Standard for Buildings Except Low-Rise Residential Buildings. Atlanta: American Society of Heating, Refrigerating and Air-Conditioning Engineers.

Asan, H. and Sancaktar, Y.S. (1998) 'Effects of wall's thermophysical properties on time lag and decrement factor', Energy and Buildings, 28(2), pp. 159–166. doi: 10.1016/S0378-7788(98)00007-3.

Asan, H. (2000) 'Investigation of wall's optimum insulation position from maximum time lag and minimum decrement factor point of view', Energy and Buildings, 32(2), pp. 197–203.

Asan, H. (2006) 'Numerical computation of time lags and decrement factors for different building materials', Building and Environment, 41(5), pp. 615–620.

Atran, S. (1986) 'Hamula organization and masha'a tenure in Palestine', Man, 21(2), pp. 271–295. doi: 10.2307/2803027.

BADIL Resource Center for Palestinian Residency and Refugee Rights (2004) From the 1948 Nakba to the 1967 Naksa. BADIL Occasional Bulletin No. 18. Bethlehem: BADIL Resource Center. Available at: https://badil.org/phocadownloadpap/Badil_docs/bulletins-and-briefs/Bulletin-18.pdf (Accessed: 5 August 2026).

Bagasi, A.A., Calautit, J.K. and Karban, A.S. (2021) 'Mashrabiya and its impact on thermal comfort and ventilation', Energies, 14(3), 530.

Balaras, C.A. (1996) 'The role of thermal mass on the cooling load of buildings: an overview of computational methods', Energy and Buildings, 24(1), pp. 1–10.

Bianca, S. (2000) Urban Form in the Arab World. London: Thames & Hudson.

Carabelli, G. (2021) 'Vertical living and spatial reconfiguration in Palestinian housing', Urban Studies, 58(4), pp. 675–693. doi: 10.1177/0042098020919234.

CIBSE (2013) TM52: The Limits of Thermal Comfort: Avoiding Overheating in European Buildings. London: Chartered Institution of Building Services Engineers.

Crawley, D.B., Lawrie, L.K., Winkelmann, F.C., Buhl, W.F., Huang, Y.J., Pedersen, C.O., Strand, R.K., Liesen, R.J., Fisher, D.E., Witte, M.J. and Glazer, J. (2001) 'EnergyPlus: creating a new-generation building energy simulation program', Energy and Buildings, 33(4), pp. 319–331.

de Dear, R.J. and Brager, G.S. (1998) 'Developing an adaptive model of thermal comfort and preference', ASHRAE Transactions, 104(1), pp. 145–167.

Duffie, J.A. and Beckman, W.A. (2013) Solar Engineering of Thermal Processes. 4th edn. Hoboken, NJ: John Wiley & Sons.

El Zein, R. (2017) 'Developing a Palestinian resistance economy through agricultural labor', Journal of Palestine Studies, 46(3), pp. 7–26. doi: 10.1525/jps.2017.46.3.7.

EN 16798-1:2019. Energy Performance of Buildings — Ventilation for Buildings — Part 1: Indoor Environmental Input Parameters for Design and Assessment of Energy Performance of Buildings Addressing Indoor Air Quality, Thermal Environment, Lighting and Acoustics. Brussels: European Committee for Standardization.

Evola, G., Margani, G. and Marletta, L. (2017) 'Thermal inertia of heavyweight traditional buildings: experimental analysis of a building in Catania', Energy Procedia, 133, pp. 42–52.

Fanger, P.O. (1970) Thermal Comfort: Analysis and Applications in Environmental Engineering. Copenhagen: Danish Technical Press.

Fathy, H. (1986) Natural Energy and Vernacular Architecture: Principles and Examples with Reference to Hot Arid Climates. Chicago: University of Chicago Press.

Femenías, P. and Geromel, F. (2019) 'Adaptable housing? A quantitative study of contemporary apartment layouts that have been rearranged by end-users', Building Research and Information, 47(8), pp. 908–922. doi: 10.1080/09613218.2018.1515635.

Freewan, A. (2019) 'Advances in passive cooling design: an integrated design approach', in Hailu, G. (ed.) Zero and Net Zero Energy. London: IntechOpen. doi: 10.5772/intechopen.87123.

Gasparella, A., Pernigotto, G., Baratieri, M. and Baggio, P. (2011) 'Thermal dynamic transfer properties of the opaque envelope: analytical and numerical tools for the assessment of the response to summer outdoor conditions', Energy and Buildings, 43(9), pp. 2509–2517.

Gerber, H. (1987) The Social Origins of the Modern Middle East. Boulder, CO: Lynne Rienner Publishers.

Givoni, B. (1976) Man, Climate and Architecture. 2nd edn. London: Applied Science Publishers.

Givoni, B. (1994) Passive and Low Energy Cooling of Buildings. New York: Van Nostrand Reinhold.

Givoni, B. (1998) Climate Considerations in Building and Urban Design. New York: Van Nostrand Reinhold.

Haj Hussein, M., Barlet, A. and Semidor, C. (2010) 'Socio-environmental dimensions of private outdoor spaces in contemporary Palestinian housing', Open House International, 35(2), pp. 67–76.

Haj Hussein, M., Monna, S., Abdallah, R., Juaidi, A. and Albatayneh, A. (2022) 'Improving the thermal performance of building envelopes: an approach to enhancing the building energy efficiency code', Sustainability, 14(23), 16264.

Hanaishy, R. and Khader, A. (2024) 'Reducing carbon footprint by using thermal insulation materials in Palestinian buildings', An-Najah University Journal for Research – A (Natural Sciences), 39(1), pp. 55–62. doi: 10.35552/anujr.a.39.1.2267.

International Organization for Standardization (2005) ISO 7730:2005 Ergonomics of the Thermal Environment — Analytical Determination and Interpretation of Thermal Comfort Using Calculation of the PMV and PPD Indices and Local Thermal Comfort Criteria. Geneva: ISO.

International Organization for Standardization (2017) ISO 13786:2017 Thermal Performance of Building Components — Dynamic Thermal Characteristics — Calculation Methods. Geneva: ISO.

Itma, M. and Monna, S. (2022) 'The role of collective spaces in achieving social sustainability: a comparative approach to enhance urban design', Sustainability, 14(14), 8756. doi: 10.3390/su14148756.

Jawabrah, M.Q. (2005) Courtyard Housing in Palestine: Typological Analysis and Development. Master's thesis. Birzeit University. Available at: http://hdl.handle.net/20.500.11889/4806 (Accessed: 5 August 2026).

Jóźwik, M. (2024) 'Architectural and urban changes in a residential environment: implications for design science', Buildings, 14(3), 631. doi: 10.3390/buildings14030631.

Juaidi, A. et al. (2016) 'Renewable energy in Palestine', Renewable and Sustainable Energy Reviews, 65, pp. 943–960.

Karimi, M., Chikamoto, T., Lee, M. and Tanaka, T. (2024) 'Impact of building orientation on energy performance of residential buildings in various cities across Afghanistan', Sustainability, 16(24), 11076.

Khamaisi, R. (1997) 'Israeli use of the British Mandate planning legacy as a tool for the control of Palestinians in the West Bank', Planning Perspectives, 12(3), pp. 321–340. doi: 10.1080/026654397364672.

Kontoleon, K.J. and Bikas, D.K. (2007) 'The effect of south wall's outdoor absorption coefficient on time lag, decrement factor and temperature variations', Energy and Buildings, 39(9), pp. 1011–1018.

Kontoleon, K.J. and Eumorfopoulou, E.A. (2008) 'The influence of wall orientation and exterior surface solar absorptivity on time lag and decrement factor in the Greek region', Renewable Energy, 33(7), pp. 1652–1664.

Magdziak, M. (2019) 'Flexibility and adaptability of the living space to the changing needs of residents', World of Real Estate Journal, 107, pp. 55–68. doi: 10.14659/WOREJ.2019.107.05.

Mallah, D., Haj Hussein, M. and Ardda, N. (2025) 'Windows: socio-environmental dimensions in Palestinian residential buildings', An-Najah University Journal for Research – A (Natural Sciences), 39(1), pp. 15–30. doi: 10.35552/anujr.a.39.1.2253.

Mazzeo, D., Oliveti, G. and Arcuri, N. (2016) 'Influence of internal and external boundary conditions on the decrement factor and time lag heat flux of building walls in steady periodic regime', Applied Energy, 164, pp. 509–531.

meteoblue (2025) Technical Documentation. Available at: https://docs.meteoblue.com/en (Accessed: 11 July 2026).

Muhaisen, A.S. (2006) 'Shading simulation of the courtyard form in different climatic regions', Building and Environment, 41(12), pp. 1731–1741.

Nasereddin, H. (2022) The Control of Thermal Comfort and Energy Saving Through External Walls in Apartment Buildings in Palestine. Master's thesis. Palestine Polytechnic University. Available at: https://scholar.ppu.edu/handle/123456789/9001 (Accessed: 5 August 2026).

Nicol, J.F. and Humphreys, M.A. (2002) 'Adaptive thermal comfort and sustainable thermal standards for buildings', Energy and Buildings, 34(6), pp. 563–572.

Nimlyat, P.S., Audu, H.O. and Kandar, M.Z. (2021) 'Assessment of indoor environment quality and occupant satisfaction in residential buildings', Journal of Building Engineering, 38, 102200. doi: 10.1016/j.jobe.2021.102200.

Olesen, B.W. (2002) 'Comparative study of European and American thermal comfort standards', Building Research & Information, 30(6), pp. 428–436.

PCBS (2010) Refugee Status and Demographic Conditions. Ramallah: Palestinian Central Bureau of Statistics.

PCBS (2018) Population Census 2017 Final Results. Ramallah: Palestinian Central Bureau of Statistics.

Pelsmakers, S. and Warwick, E. (2022) 'Housing adaptability: new research, emerging practices and challenges', Buildings and Cities, 3(1), pp. 1–10. doi: 10.5334/bc.166.

Quagraine, K.A., Ramde, E.W., Fiagbe, Y.A.K. and Quansah, D.A. (2020) 'Evaluation of time lag and decrement factor of walls in a hot humid tropical climate', Thermal Science and Engineering Progress, 20, 100758. doi: 10.1016/j.tsep.2020.100758.

Ratti, C., Raydan, D. and Steemers, K. (2003) 'Building form and environmental performance: archetypes, analysis and an arid climate', Energy and Buildings, 35(1), pp. 49–59.

RehabiMed (2015) Bethlehem Rehabilitation Guide. Available at: https://www.archnet.org (Accessed: 5 August 2026).

Rochma, N. (2023) 'The presence of memory through materiality, spatial configuration, and collective as a system for sustainable high-rise residence', IOP Conference Series: Earth and Environmental Science, 1195, 012017. doi: 10.1088/1755-1315/1195/1/012017.

Ruivo, C.R., Ferreira, P.M. and Vaz, D.C. (2013) 'On the error of calculation of heat gains through walls by methods using constant decrement factor and time lag values', Energy and Buildings, 60, pp. 252–261.

Saifi, Y. (2023) 'An analysis into East Jerusalem's housing environment: from social and climatic perspective', Journal of Asian Architecture and Building Engineering, pp. 19–42. doi: 10.1080/13467581.2023.2229393.

Saifudeen, A. and Mani, M. (2024) 'Adaptation of buildings to climate change: an overview', Energy and Buildings, 302, 113764. doi: 10.1016/j.enbuild.2023.113764.

Samman, M. and Saifi, Y. (2021) 'Adapting modernity: designing with modern architecture in East Jerusalem, 1948–1967', Journal of Design History, 34(2), pp. 129–148.

Santamouris, M. (2016) 'Cooling the buildings – past, present and future', Energy and Buildings, 128, pp. 617–638.

Shemesh, M. (2004) 'The Palestinian society in the wake of the 1948 War: from social fragmentation to consolidation', Israel Studies, 9(1), pp. 86–100. doi: 10.1353/is.2004.0020.

Soflaei, F., Shokouhian, M. and Mofidi Shemirani, S.M. (2016) 'Investigation of Iranian traditional courtyard as passive cooling strategy: a field study on BS climate', International Journal of Sustainable Built Environment, 5(1), pp. 99–113. doi: 10.1016/j.ijsbe.2015.12.001.

Sylejmani, M. (2020) 'Transformation of living spaces', Journal of Contemporary Urban Affairs, 4(2), pp. 1–12. doi: 10.25034/ijcua.2020.v4n2-1.

Tokazhanov, G., Tleuken, A., Guney, M., Turkyilmaz, A. and Karaca, F. (2020) 'How is COVID-19 experience transforming sustainability requirements of residential buildings? A review', Sustainability, 12(20), 8732. doi: 10.3390/su12208732.

UCLA Energy Design Tools Group (2024) Climate Consultant 6.0: A Graphic-Based Computer Program for Building Design Analysis. Los Angeles, CA: University of California, Los Angeles.

Ulgen, K. (2002) 'Experimental and theoretical investigation of effects of wall's thermophysical properties on time lag and decrement factor', Energy and Buildings, 34(3), pp. 273–278.

Verbeke, S. and Audenaert, A. (2018) 'Thermal inertia in buildings: a review of impacts across climate and building use', Renewable and Sustainable Energy Reviews, 82, pp. 2300–2318.

Yasmin, T. and Nilufar, F. (2023) 'Adaptability in interior space: public housing for lower-middle income group in Dhaka', Frontiers of Architectural Research, 12(1), pp. 76–91. doi: 10.1016/j.foar.2022.06.003.